Imperial College London

Cellular and Viral Determinants for Hepatitis C Virus Replication

PhD Thesis

Andrew James Baillie
2010

Abstract

The recent discovery of an HCV isolate which replicates in cell culture has opened up opportunities to study the full viral life cycle *in vitro*. This genotype 2a isolate (JFH-1) and its derivatives are the only ones known to replicate efficiently in cell culture, and recent work has indicated that viral determinants for efficient replication may lie in the non-structural protein coding region of the genome. In this thesis chimaeric JFH-1 virus containing full length NS3, NS3 helicase and NS3 protease sequences from genotype 1a and 1b were constructed. The replication efficiencies of chimaeric viruses were tested in cell culture, and were shown not to replicate, indicating that vital viral determinants for JFH-1 replication exist in NS3. The JFH-1 model also provides the opportunity to study the effect of the full viral life cycle on the host cell. Microarray analyses were performed to identify gene expression changes in Huh7 and Huh7.5 cells that had been infected with JFH-1 for 6, 12, 18, 24 and 48 hours. A large number of host genes were found to be regulated during JFH-1 infection, including those involved in lipid metabolism, oxidative stress, apoptosis and intracellular transport. The microarray data were validated by quantitative PCR analyses of separate infection experiments. A selection of the most highly regulated genes was assessed for their necessity to HCV replication by RNA interference studies. The knockdown by siRNA of genes ABLIM3, SPTLC3 and CYP1A1 resulted in significant impairment of HCV replication. The knockdown by siRNA of gene TXNIP (thioredoxin interacting protein) resulted in up to 90% reduction in HCV replication. This is a novel finding which may be of importance to the study of HCV as TXNIP plays roles in oxidative stress, lipid metabolism and glucose metabolism, all of which have potential to influence the HCV lifecycle. Magnetic resonance spectroscopy indicated a change in levels of choline metabolites in JFH-1 infected cells, which has implications for the aspects of the HCV lifecycle associated with lipid membranes and other lipid structures.

Acknowledgements

I would like to thank my supervisor Michael McGarvey for his tutelage.

I would like to thank my supervisors Helen Bright and Pia Thommes at GSK for their assistance in making the microarray studies possible, and particularly Robert Hamatake for giving me the opportunity to perform my studies at the GSK facility in North Carolina.

I would like to thank my colleagues at GSK for their assistance during my time there. I would like to thank Shihyun You for her valuable assistance and creating Jc1p7Fluc2A used in this work. I would like to thank Katja Remlinger for performing microarray analyses and teaching me how to perform microarray analyses. I would like to thank Cindy, JJ, Amy, Jill, Jeff, Christian, Neil, Mike, Chris, Vanessa, Margaret, and my friends at GSK for their welcoming of me and allowing me to get so much done in my time with them.

I would like to thank the members of Dr McGarvey's lab with whom I have worked closely, Sam and Fadel. I would like to thank Jane Cox for the use of and some training in her magnetic resonance spectroscopy facility. I would like to thank my colleagues at Imperial from whom I have learnt and by whom I have been assisted, including Simon, Anna and Essam, and all my friends at Imperial.

I would finally like to thank my family for their support during my studies.

Publications

Work described in this thesis has been presented at:

14th International Symposium on Hepatitis C Virus and Related Viruses, September 2007, Glasgow
Baillie, A., Al-Hababi, F., Mong, L., McGarvey, M., The Inhibition of Intracellular dsRNA Receptors by HCV. Poster presentation.

18th British Chapter ISMRM Annual Symposium, March 2009, London
Baillie, A., Blackham, S., Cox, J., Thommes, P., Murray, D., McGarvey, M., Changes in Liver Cell Gene Expression and Metabolism during Hepatitis C Virus Replication. Poster presentation.

16th International Symposium on Hepatitis C Virus and Related Viruses, October 2009, Nice
Blackham, S., Baillie, A., Al-Hababi, F., Remlinger, S., Hamatake, R., McGarvey, M. J. Changes in Host Cell Gene Expression during HCV Infection. Poster presentation.

Blackham, S., Baillie, A., Al-Hababi, F., Remlinger, S., You, S., Hamatake, R., McGarvey, M. J. Gene Expression Profiling Indicates The Role of Host Oxidative Stress, Apoptosis, Lipid Metabolism and Intracellular Transport Genes in the Replication of Hepatitis C Virus, *Journal of Virology* **84** 5404-5414 (2010)

Contents

Abstract 2
Acknowledgements 3
Publications 4
Contents 5
Abbreviations 9
List of Figures 12
List of Tables 14
Introduction 15
1.1 HCV Epidemiology 16
1.2 HCV Taxonomy 17
1.3 HCV Disease 19
1.4 HCV Treatment 21
1.5 HCV Particle Structure 23
1.6 HCV Genome 24
1.7 HCV Lifecycle 30
1.8 HCV Entry to the Cell 31
1.9 HCV Replication Complex 32
1.10 HCV Assembly and Release 34
1.11 Immune Response to Infection and Viral Evasion 38
1.12 HCV Animal Models of Replication 42
1.13 HCV Replicon Cell Culture Models 43
1.14 HCV Infectious Cell Culture Models 45
1.15 Chimaeric HCV Genomes 47
1.16 Mutation in the HCV Genome 49
1.17 Cell Lines Capable of Supporting Replication of Infectious HCV 51
1.19 Aims and Hypotheses 59
Methods 60
2.1 Cell Culture 61
2.2 HCV Constructs 61
2.3 JFH-1 Infectious Virus Cell Culture System 61
2.3.1 Plasmid Preparation 61
2.3.2 *In Vitro* RNA Transcription 62
2.3.3 RNA Transfection of Huh7.5 Cells 62

2.3.4 Harvest of Infectious JFH-1 Virus 63
2.3.5 Titration of JFH-1 Virus Stocks 63
2.3.6 Staining for HCV Core Protein 63
2.3.7 JFH-1 Virus Production by Media Passage 64
2.4 Jc1 Infectious Virus Production 65
2.4.1 Plasmid Preparation 65
2.4.2 *In Vitro* RNA Transcription 65
2.4.3 RNA Electroporation of Huh7.5 Cells 65
2.4.4 Harvest of Infectious Jc1 Virus 65
2.4.5 Titration of JFH-1 Virus Stocks (TCID50) 65
2.5 Microarray Studies 66
2.5.1 Titration Assay 66
2.5.2 Infection of Huh7.5 Cells (Initial Method) 66
2.5.3 Infection of Huh7.5 (Revised Method) 66
2.5.4 Infection of Huh7 Cells and Addition of Protease or Polymerase Inhibitors 66
2.5.5 RNA Extraction 67
2.5.6 Microarray Data Aquisition 67
2.5.7 Microarray Data Processing 67
2.6 Validation of Microarray Data by Quantitative PCR 69
2.6.1 Infection and RNA Extraction 69
2.6.2 Synthesis of cDNA 69
2.6.3 Quantitative PCR 69
2.7 The Effect of Host Gene Knockdown by RNA Interference on HCV Replication 71
2.7.1 Jc1 Infectious Virus Model System 71
2.7.2 JFH-1 Infectious Virus Model System 71
2.8 Protein Level Analysis of Genes of Interest 73
2.8.1 Protein Preparation 73
2.8.2 SDS-PAGE and Western Blotting 73
2.9 Sequencing of JFH-1 74
2.9.1 RNA Transfection of Huh7.5 Cells 74
2.9.2 Passage of Transfected Huh7.5 Cells 74
2.9.3 Reverse Transcription 74
2.9.4 PCR and Sequence Analysis 74
2.10 Chimaeric JFH-1 Construction and Replication 75

2.10.1 Cloning of Chimaeric JFH-1 Constructs 75
2.10.2 RNA Transfection of Huh7.5 Cells 76
2.10.3 Passage of Transfected Huh7.5 Cells 77
2.10.4 Quantification of Intracellular JFH-1 77
2.11 Magnetic Resonance Spectroscopy 78
Results and Discussion 79
3.1 Viral Determinants for JFH-1 Replication 80
3.1.1 Role of NS3 Sequence Determinants in JFH-1 Replication 80
3.1.2 Construction of Chimaeric JFH-1 81
3.1.3 Replicative Ability of Chimaeric JFH-1 86
3.1.4 NS3 Sequence Determinants for JFH-1 Replication 88
3.2 Mutation in the JFH-1 Genome during Cell Culture 91
3.2.1 Testing of Primers for PCR of Regions of JFH-1 to be Sequenced 91
3.2.2 Identification of Mutations in Cell Cultured JFH-1 92
3.2.3 Mutation in the JFH-1 Genome during Cell Culture 93
3.3 Identification of Host Genes Regulated During HCV Infection 97
3.3.1 Initial Timecourse 98
3.3.2 Identification of Host Genes Regulated During HCV Infection of Huh7.5 Cells 101
3.3.3 Identification of Host Genes Regulated During HCV Infection of Huh7 Cells 110
3.3.4 Host Cell Biological Processes Altered during HCV Infection 123
3.3.4.1 Immune Modulation 125
3.3.4.2 Lipid Metabolism 126
3.3.4.2.1 Micro RNA 122 (miR122) 128
3.3.4.3 Oxidative Stress 130
3.3.4.3.1 Metallothionein (MT) 130
3.3.4.4 Protein Synthesis 132
3.3.4.5 Intracellular Transport 132
3.3.4.6 Apoptosis and Cell Proliferation 133
3.4 Inhibition of JFH-1 Replication by Anti-Viral Inhibitors 134
3.5 Host Genes with a Role in HCV Replication 138
3.5.1 Identification of Host Genes with a Role in HCV Replication 138
3.5.2 Genes Identified as Required for HCV Replication 147
3.5.2.1 Actin binding LIM protein family, member 3 (ABLIM3) 148
3.5.2.2 Cytochrome P450, family 1, subfamily A, polypeptide 1 (CYP1A1) 149

3.5.2.3 Serine palmitoyltransferase long chain base subunit 3 (SPTLC3) 151
3.5.2.4 Thioredoxin-interacting protein (TXNIP) 152
3.6 Cellular Metabolites in JFH-1 Infected Cells 156
3.6.1 Spectroscopic Profiling of Cellular Metabolites 156
3.6.2 Choline Metabolites 160
Summary 161
4. Summary 162
Further Work 166
5.1 Viral Determinants of HCV Replication 167
5.2 Metabolic Changes during HCV Replication 167
5.3 Host Gene Expression Changes during HCV Replication 168
References 171
Appendix 224
A1 Primer Sequences 224
A1.1 Primers used in the construction of chimaeric JFH-1 224
A1.2Primer used for reverse transcription of JFH-1 RNA 224
A1.3 Primers used in the sequencing of JFH-1 224
A1.4 Primers used in JFH-1 quantitative PCR 225
A1.5 Primers used in qRT-PCR and qPCR of host genes 225
A2 siRNA Sequences 227
A3 SDS-PAGE and Western Blotting Solutions 228
A4 Immunofluorescence microscopy reagents 229
A5 DNA Ladders 229
A6 Characterisation of JFH-1 Cell Culture 230
A7 Microarray Data Quality Control 235
A8 Metallothionein proteins levels 241

Abbreviations

18S	18S ribosomal RNA
2'-5' OAS	2'-5' oligoadenylate synthase
ABLIM3	actin binding LIM protein family, member 3
ACSL3	acyl-CoA synthetase long-chain family member 3
ALDOA	aldolase A
ALT	serum alanine aminotransferase
ANOVA	analysis of variance
apoB	apolipoprotein B
apoE	apolipoprotein E
ASK1	mitogen-activated protein kinase kinase kinase 5 (MAP3K5)
ATP	adenosine triphosphate
bp	base pairs
BVDV	bovine viral diarrhoea virus
CCNG1	cyclin G1
ChoRE	carbohydrate response element
CLDN1	claudin 1
CT	threshold cycle
CYP1A1	cytochrome P450, family 1, subfamily A, polypeptide 1
DAPI	4',6-diamidino-2-phenylindole
DC-SIGN	dendritic cell-specific intercellular adhesion molecule-3-grabbing integrin
DDX3X	DEAD (Asp-Glu-Ala-Asp) box polypeptide 3, X-linked
DMEM	Dulbecco's modified Eagles Medium
DMSO	dimethyl sulphoxide
DNA	deoxyribonucleic acid
EMCV	encephalomyocarditis virus
ER	endoplasmic reticulum
FBL2	F-box and leucine rich repeat protein 2
FBS	foetal bovine serum
FMDV	foot and mouth disease virus
FOXO	forkhead box O
GBV	GB virus
GFP	green flluorescent protein
GPC	glycerophosphocholine
HCC	hepatocellular carcinoma
HCV	hepatitis C virus
HDAC	histone deacetylase
HDL	high density lipoprotein
Huh7	Human hepatoma 7 (cell line)
IFN	interferon
IRES	internal ribosomal entry site
IRF7	interferon regulatory factor 7
ISDR	interferon sensitivity determining region
JFH-1	Japanese fulminant hepatitis-1 (an HCV genotype 2a isolate)
JNK	c-Jun N-terminal kinase

LB	Luria Bertani
LDL	low density lipoprotein
L-SIGN	liver/lymph node-specific intercellular adhesion molecule-3-grabbing non-integrin
LSMean	least squares mean
MAD	median absolute deviation
MAS MRS	magic angle spinning magnetic resonance spectroscopy
MAT1A	methionine adenosyltransferase I, alpha
MAVS	mitochondrial antiviral signalling protein
MBN	mung bean nuclease
Mda5	melanoma differentiation-associated gene-5
MeV	MultiExperiment Viewer
miR122	microRNA 122
miRNA	micro ribonucleic acid
M-MLV RT	Moloney murine leukaemia virus reverse transcriptase
MOI	multiplicity of infection
mRNA	messenger ribonucleic acid
MRS	magnetic resonance spectroscopy
MT	metallothionein
NAFLD	non-alcoholic fatty liver disease
NDRG	N-myc downstream regulated
NLRP3	NLR family, pyrin domain containing 3
NMR	nuclear magnetic resonance
NOXA	see PMAIP1
NS	non-structural
NTR	non-translated RNA
OCCLN	occludin
ORF	open reading frame
PBS	phosphate buffered saline
PC	phosphocholine
PCA	principal component analysis
PCR	polymerase chain reaction
PIK4, PI4K	phosphatidylinositol 4-kinase
PKR	protein kinase R
PMAIP1	phorbol-12-myristate-13-acetate-induced protein 1
PPAR	peroxisome proliferator activated receptor
PtdC	phosphatidylcholine
QC	quality control
qPCR	quantitative polymerase chain reaction
qRT-PCR	quantitative reverse transcrition polymerase chain reaction
Rb	retinoblastoma
RIG-I	retinoic acid inducible gene I
RNA	ribonucleic acid
ROS	reactive oxygen species
RT-PCR	reverse transcrition polymerase chain reaction
SCID	severe combined immunodeficiency
SDS-PAGE	sodium dodecylsulphate polyacrylamide gel electrophoresis

SH3	Src homology 3
siRNA	short interfering ribonucleic acid
SLC7A1	solute carrier family 7 (cationic amino acid transporter, y+ system), member 1
SPTLC3	serine palmitoyltransferase, long chain base subunit 3
SR-BI	scavenger receptor class B type I
SVR	sustained virological response
TBE	Tick-Borne Encephalitis
TCID50	50% tissue culture infectious dose
TGF-β	transforming growth factor beta
TLR3	toll-like receptor 3
TRIF	TIR-domain-containing adapter-inducing interferon-β
TRX	thioredoxin
TXNIP	thioredoxin interacting protein
uPA	urokinase type plasminogen activator
VAP-A	vesicle-associated membrane protein-associated protein A
VAP-B	vesicle-associated membrane protein-associated protein B
VLDL	very low density lipoprotein
WNV	West Nile virus
YFV	Yellow Fever virus

List of Figures

Figure 1: Phylogenetic trees of the *Flaviviridae* and HCV genotypes. 18
Figure 2: The structure of the HCV genome. 24
Figure 3: Structures, membrane association and processing of HCV proteins[101]. 26
Figure 4: A schematic representation of the lifecycle of hepatitis C virus. 30
Figure 5: Membranous structures created by HCV during viral replication. 33
Figure 6: Density profiles of HCV particles. 37
Figure 7: Structures of HCV replicons[341] 44
Figure 8: Structure of JFH-1 derived genomes[341]. 46
Figure 9: NS3 sequence similarity between different HCV genotypes. 50
Figure 10: Mutations observed in replicon cell clones[86]. 51
Figure 11: Major steps in the cloning of chimaeric JFH-1 viruses. 82
Figure 12: Agarose gel electrophoreses as confirmation of site directed mutagenesis insertion of BlpI restriction site in pTANS32a. 83
Figure 13: Agarose gel electrophoreses as confirmations of successful PCR of NS3 coding sequences. 84
Figure 14: Agarose gel electrophoresis of AflII/NsiI digests of constructs prior to final cloning step. 84
Figure 15: Agarose gel electrophoresis of final chimaeric constructs. 85
Figure 16: Agarose gel electrophoresis of JFH-1 constructs digested with AflII and NsiI. 85
Figure 17: Replication of chimaeric JFH-1. 87
Figure 18: Amplification of targets for sequencing of JFH-1 genome. 91
Figure 19: Number of genes changing in expression level at multiple time points in the initial microarray analysis of JFH-1 infected Huh7.5 cells. 100
Figure 20: Fold change in expression of Metallothioneins during JFH-1 infection of Huh7.5 cells. .. 106
Figure 21: Host biological processes regulated during JFH-1 infection of Huh7.5 cells. 107
Figure 22: Validation by PCR of gene expression levels in Huh7.5 cells infected with JFH-1. 108
Figure 23: Validation by PCR of metallothionein gene expression levels in Huh7.5 cells infected with JFH-1. 109
Figure 24: Fold change in expression of Metallothioneins during JFH-1 infection of Huh7 cells. 116
Figure 25: Host biological processes regulated during JFH-1 infection of Huh7 cells (apoptosis and cell cycle). 117
Figure 26: Host biological processes regulated during JFH-1 infection of Huh7 cells (protein synthesis). 118
Figure 27: Host biological processes regulated during JFH-1 infection of Huh7 cells (cytoskeleton and transport). 119
Figure 28: Host biological processes regulated during JFH-1 infection of Huh7 cells (immunity). 119
Figure 29: Host biological processes regulated during JFH-1 infection of Huh7 cells (lipid metabolism). 120
Figure 30: Host biological processes regulated during JFH-1 infection of Huh7 cells (oxidative stress and detoxification). 120
Figure 31: Validation by PCR of gene expression levels in Huh7 cells infected with JFH-1. 122
Figure 32: Induction and action of PMAIP1[462] 133
Figure 33: Structures of anti-viral molecules. 134
Figure 34: JFH-1 dose responses to anti-viral treatment. 135

Figure 35: Cellular toxicity of anti-viral compounds..... 136
Figure 36: HCV constructs used to identify host genes with a role in HCV replication. 138
Figure 37: Efficiency of siRNA delivery. 140
Figure 38: Knockdown efficiency of siRNAs targeted to the 15 host genes selected for study by RNA interference. 141
Figure 39: Effect of host gene knockdown on HCV replication using pooled siRNAs. 142
Figure 40: Effect of host gene knockdown on HCV replication using deconvoluted siRNAs. 143
Figure 41: Cellular toxicity of siRNAs..... 145
Figure 42: Relative expression of genes observed to change in microarray studies in Huh7.5 cells harbouring subgenomic replicons compared to Huh7.5 cells. 146
Figure 43: The cytochrome P450 catalytic cycle. 150
Figure 44: Biosynthetic pathway of sphingolipids in mammalian cells[500]. 151
Figure 45: An example proton MAS MRS profile with the major metabolite peaks identified. 157
Figure 46: Magnetic resonance spectra of mock infected and JFH-1 infected Huh7.5 cells. 158
Figure 47: Relative areas of magnetic resonance spectra peaks for mock infected and JFH-1 infected Huh7.5 cells. 159
Figure 48: DNA Ladders. 229
Figure 49: Preparation of RNA transcripts of JFH-1 and its derivatives..... 230
Figure 50: Immunofluorescent staining for HCV core protein. 231
Figure 51: Image of a JFH-1 infected Huh7.5 cell stained for HCV core protein. 232
Figure 52: Production of infectious JFH-1 virus titres by cell culture. 233
Figure 53: Intracellular JFH-1 RNA levels after infection with a range of MOI. 234
Figure 54: Quality control of arrays used in Huh7.5 microarray experiment, performed using Array Studio..... 237
Figure 55: Quality control of arrays used in Huh7 microarray experiment, performed using Array Studio..... 240
Figure 56: Metallothionein protein levels in JFH-1 infected and Mock infected Huh7.5 cells. 241

List of Tables

Table 1: Mutations identified in cell cultured JFH-1..... 92
Table 2: Host genes most highly regulated during JFH-1 infection of Huh7.5 cells identified by the initial microarray experiment. 99
Table 3: Number of probe sets significantly regulated between JHF-1 infected and mock infected Huh7.5 cells. 101
Table 4: Host genes most highly regulated at 48 hours post-infection of Huh7.5 cells. 103
Table 5: Probe Sets regulated during infection of Huh7.5 cells by a greater than 2-fold change at all timepoints..... 104
Table 6: Host cellular biological processes identified to be affected by transcriptional regulation during JFH-1 infection of Huh7.5 cells. 105
Table 7: Number of probe sets significantly regulated between JHF-1 infected and mock infected Huh7 cells. 110
Table 8: Host genes most highly regulated at 48 hours post-infection of Huh7 cells. 112
Table 9: Probe Sets regulated during infection of Huh7 cells by a greater than 2-fold change at all timepoints..... 113
Table 10: Host cellular biological processes affected during JFH-1 infection of Huh7 cells. 114
Table 11: Effect of BILN2061 treatment on gene expression in JFH-1 infected Huh7 cells. 137
Table 12: Expression level changes, during JFH-1 infection of Huh7 and Huh7.5 cells, of genes selected for RNA interference studies. 139
Table 13: Transfection optimisation of Huh7.5 cells with JFH-1. 231

Introduction

1.1 HCV Epidemiology

Hepatitis C Virus (HCV) is estimated to have infected 170 million people around the world[1], resulting in a serious global health problem.

There are estimated to be 200, 000 people chronically infected with HCV in England[2], based on a seroprevalence of 0.5% calculated from specimens collected from 1995 to 1996, and chronicity rate of 80%. In the USA an estimated 4.1 million people have anti-HCV antibodies, and 3.2 million have a chronic infection[3]. HCV is epidemic In Egypt, where according to the recent demographic and health survey, 15% of individuals aged 15-59 had anti-HCV antibodies indicating exposure, and 10% had an active infection[4].

The major route of infection in the UK and around the world is through use of contaminated needles. In the UK, intravenous drug use is the primary cause of infections, accounting for 80% of cases. The remainder of cases are accounted for by previous infection through contaminated blood transfusions or other blood products. Since testing for presence of the virus was introduced, the number of new infections by this route has fallen greatly. However, there are still many people living with the disease, having contracted it though one of these routes. In Ireland, between 1977 and 1978, 704 women were infected when administered with anti-D immune globulin that was contaminated with HCV[5]. Similar events have occurred all over the world, for example an outbreak in Germany from the same source. In Egypt, the high prevalence of infection was caused by a programme of immunisation against schistosomiasis[6]. The goals of the programme required the fast delivery of vaccines to a large population, and the medical practices involved resulted in needles being shared before they were properly sterilised. A high level of HCV in the population can also make the transfer of HCV by blood transfusion a significant risk[7], unless screening is carried out on all blood donations. HCV can also be transmitted through sexual contact and vertically from mother to child during childbirth.

The incidence of infection with HCV is declining due to testing of blood products and when proper precautions are taken in medical situations involving needles. However infections will still occur among intravenous drug users who share non-sterile needles.

1.2 HCV Taxonomy

HCV is a member of the family *Flaviviridae,* which consists of three genera, the Flaviviruses, Pestiviruses and Hepaciviruses. Phylogenetic trees indicating the genetic relationships between viruses of this family are shown in Figure 1[8-10]. The Flavivirus genus includes the pathogens of humans Yellow Fever virus (YFV) and Dengue virus, as well as West Nile virus (WNV) and Tick-Borne Encephalitis virus (TBE), and are transmitted by arthropod vectors. The Pestivirus genus is comprised of animal pathogens such as Bovine Viral Diarrhoea virus (BVDV). The Hepacivirus genus consists of the GB viruses (GBV-A, GBV-B and GBV-C) and Hepatitis C virus (HCV). Since HCV is likely to have evolved before the use of needles for injection, it is not clear how the virus was originally transmitted. The six genotypes of HCV (Figure 1C) appear to have evolved more recently (within the last 200 years[11]) which may coincide with an increase in transmission as the use of needles became more common.

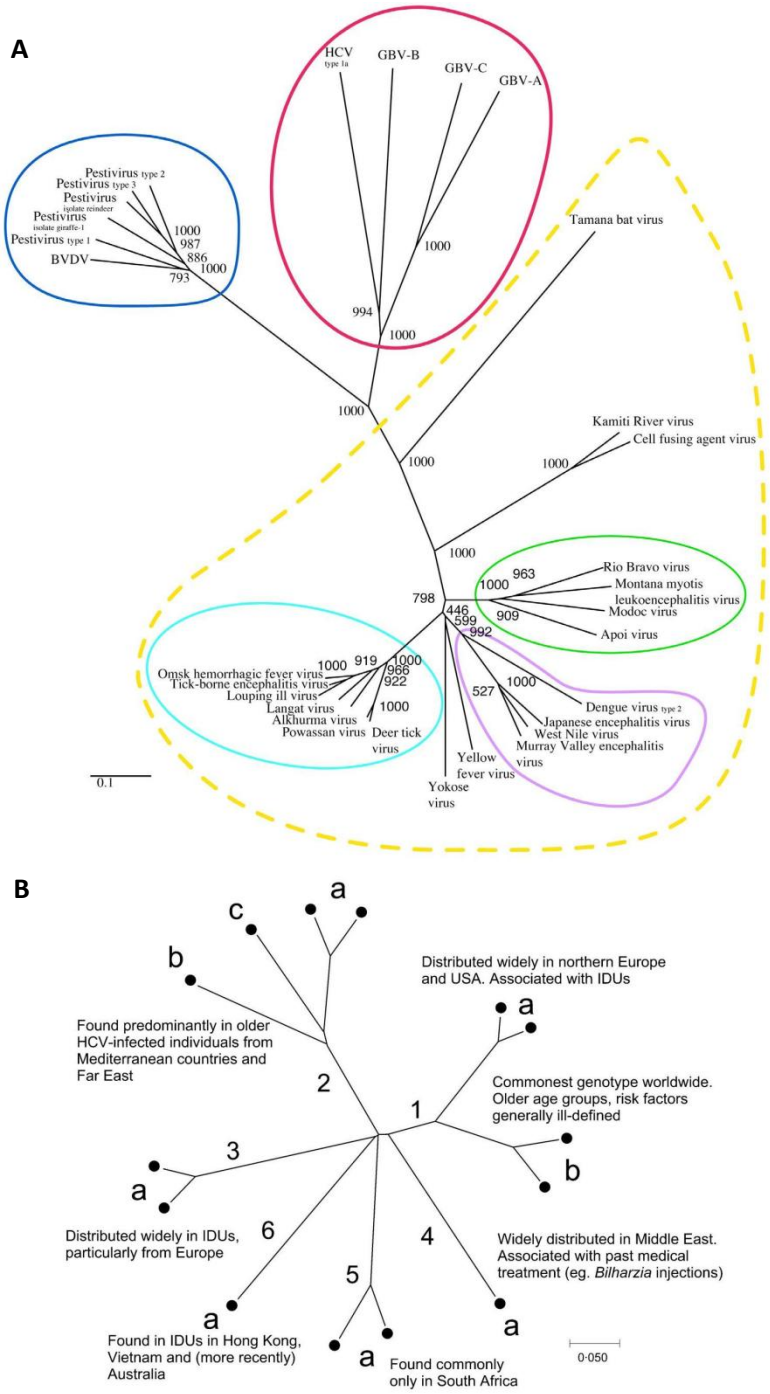


Figure 1: Phylogenetic trees of the *Flaviviridae* and HCV genotypes.

A Phylogeny of *Flaviviridae* based on polymerase sequences[8]. Numbers at nodes indicate the statistical support of the branching order by bootstrap criteria. The bar at the bottom of the phylogram indicates the evolutionary distance, to which the branch lengths are scaled based on the estimated divergence. **B** Evolutionary tree of available complete open-reading frame sequences for each HCV genotype. The main identified risk groups and the world regions where they are found are indicated for each genotype[10]

1.3 HCV Disease

The acute phase of HCV infection is largely asymptomatic. The lack of symptoms is the major reason that HCV infections are often not diagnosed until many years after initial exposure. Some infections will spontaneously resolve, leaving HCV RNA undetectable, and anti-HCV antibodies present in the patient. However, most cases (around 80%) will progress to chronic infection, characterised by continuing disease for more than six months. The virus persists in the liver and eventually causes damage resulting in fibrosis (20% of cases), cirrhosis and hepatocellular carcinoma (4% of cases). The incidence of liver failure coupled with the number of cases of HCV, mean that HCV infection is one of the major reasons why patients require a liver transplant.

The damage which occurs to the liver impairs the liver functions, resulting in further pathologies of disease. This damage can allow measurement of the progression of disease as, for example, levels of the enzyme alanine aminotransferase (ALT) in blood increase with damage to liver cells, although histopathology grade is not directly related to ALT levels. A major cause of fibrosis and liver damage during HCV infection is the host inflammatory response to the virus. An important feature in the development of fibrosis is the activation of hepatic stellate cells (HSC), which produce the extracellular collagen matrix[12]. Natural killer (NK) cells may aid the process by production of inflammatory and profibrogenic cytokines[13-14]. HSC also express high levels of CD81, to which HCV protein E2 can bind, inducing production of a matrix metalloproteinase which degrades the extracellular matrix[15]. HCV infection is linked to progression to cancer, and it is likely that the effects of long term inflammation, cirrhosis, oxidative stress and subsequent DNA damage are partly responsible for development of cancer[16]. There is also evidence for more direct carcinogenic effects of HCV proteins, for example mice expressing core protein have been shown to develop hepatocellular carcinoma[17-18].

Steatosis is the accumulation of lipid in hepatocytes, and occurs with varying severity in around 50% of patients with chronic HCV infection[19-20]. Steatosis associated with HCV can be induced directly by the virus, or as a result of metabolic factors. Virally induced steatosis is associated with genotype 3 HCV infections[21-22], and there is a correlation between viral load and severity of steatosis (not observed in other genotypes[23]). Expression of genotype 3a core protein alone has been shown to induce steatosis in transgenic mice[17]. HCV core protein has been shown to localise to intracellular membranes and lipid droplets in hepatocytes[24]. Steatosis induced by genotype 3 HCV has been shown to resolve in patients after achieving a sustained virological response to treatment[25].

Steatosis is more common in patients with HCV than in patients with other viral infections of the liver such as HBV, further indicating that HCV replication itself is a cause of fatty liver[26-27], and HCV has been shown to cause steatosis in the absence of other risk factors such as obesity, alcoholism and diabetes[20]. Metabolic factors contributing to steatosis can include dysfunctional oxidation of fatty acids[28], alcohol abuse, and non-alcoholic fatty liver disease (NAFLD) which occurs due to obesity, hyperlipidaemia and diabetes[29]. Insulin resistance is a major mechanism for development of steatosis[30-31], and it has been shown that the use of insulin sensitising therapy can improve steatosis in patients[32]. Chronic HCV infection is associated with insulin resistance[33], and several mechanisms for HCV induced insulin resistance have been proposed. Core protein has been shown to cause interferon resistance by reducing levels of signalling molecules IRS-1 and IRS-2[34-35], and by reducing association of IRS-1 with its downstream effector phosphoinositide 3-kinase (PI3K)[36]. Increases in levels of SOCS3 (suppressor of cytokine signalling 3)[35] and SOCS7[37] have also been associated with expression of HCV core protein, leading to reduced levels of IRS-1. An inducer of late proteasome activity, PA28γ, has been shown to be required for the development of interferon resistance in mice expressing HCV core protein[38]. Protein phosphatase 2A (PP2A) has been shown to be upregulated in HCV infection and by expression of HCV protein NS5A[39]. PP2A can dephosphorylate and therefore inactivate Akt, potentially leading to HCV associated interferon resistance[40]. HCV biopsies have shown reduced levels of peroxisome proliferator activated receptor α (PPARα) and PPARγ. These are modulators of lipid and glucose metabolism[41]. PPARα is required for HCV core induced steatosis in mice[42], and treatment of cells expressing HCV core with a PPARγ agonist resulted in improved insulin signalling[37]. Oxidative stress in expression of HCV protein (*in vitro*[16] and in mouse models[16,43]) and in HCV infected patients has been associated with steatosis and insulin resistance. HCV infection is therefore a risk factor for development of diabetes and steatosis.

Symptoms of HCV infection can also be displayed outside of the liver. These include fatigue[44], minor mental problems such as mild depression and minor cognitive inhibition[45-46]. Patients may experience cryoglobulinemia necrotizing vasculitis of the skin and glomerulonephritis[47], for which the precise mechanisms of pathology are not known. Some pathologies observed in HCV infected patients may be due to autoimmune diseases. HCV can induce autoreactive cytotoxic T lymphocytes by molecular mimicry, as for example in the case of some cytochrome p450 molecules which have regions of amino acid sequence homology with HCV core protein[48-49].

HCV can be a major burden on the individuals who have the disease, and on the healthcare systems. In the USA alone, the estimated annual cost of HCV (1998), including medical care and work loss was over US$1 billion[50].

1.4 HCV Treatment

There is no vaccine available for prevention of HCV infection. Primary infection does not prevent a secondary infection, so a vaccine based on a killed virus would be unlikely to be effective. HCV also displays variation in the sequence of its envelope proteins, so the antigens presented to the immune system are different across HCV subtypes, and can change inside one infected individual[51-54]. This presents difficulty in designing vaccines, although similar situations have been overcome, for example in the case of influenza.

The current treatment for HCV is pegylated interferon alpha plus ribavirin. Interferon alpha induces the host to initiate innate immune responses which may have otherwise been suppressed or not activated by the actions of the virus. Ribavirin is a guanosine analogue, which has anti-viral activity against a number of DNA and RNA viruses[55-57]. The exact mechanism of its action against HCV is unknown but several mechanisms have been proposed. Ribavirin may directly inhibit the viral polymerase as it is taken up as a substrate, or it may cause mutations to occur after it is incorporated into the genome and then errors are made in copying the genome, however it is unlikely that this is the mechanism of inhibition. As in the case of yellow fever virus, ribavirin may inhibit inosine monophosphate dehydrogenase leading to depletion of GTP[58] (this may not be the mode of action in chronic HCV). Ribavirin may enhance production of T-helper cells, interleukin-2 and interferon gamma (although the L-enantiomer which shares these properties, but not anti-viral activity, did not inhibit HCV as ribavirin does)[59]. The regimen advised by NICE (National Institute for Health and Clinical Excellence) in 2006 for patients with genotype 1 or 4 was 180µg pegylated interferon alpha 2a (Roferon, Roche) per week plus 1000-1200mg ribavirin per day for 48 weeks. Patients with genotype 2 or 3 were recommended to have 180µg pegylated interferon alpha 2a per week plus 800mg ribavirin per day for 24 weeks. The strict regimen must be adhered to and can only be undertaken by willing patients. Treatment with interferon can also have unpleasant side effects, primarily flu-like symptoms, depression and nausea. The combination of a strict regimen and side-effects mean that not all patients are suitable for treatment. Of the patients who are

treated, a sustained virological response (SVR) will be achieved in 40-50% of those with genotype 1 or 4 and in 80% of those with genotype 2 or 3[60]. The lack of an effective treatment for genotype 1 HCV is of concern as this is the most common genotype in Europe and the USA, and genotype 4 is the most prevalent in Egypt. The development of new and effective treatments for HCV is a major healthcare priority.

A number of avenues of research are being examined to find possible new treatments for HCV. These include small molecule inhibitors of viral protease and polymerase, RNA interference based methods, and improvements to the current forms of interferon and ribavirin. Many drugs are currently in the early stages of development and early clinical trials. Treatments in development that are based on modifications of the current regimen include Taribivirin[61] (or Viramidine, Valeant Pharmaceuticals), and Albumin-IFN-α_{2b} (produced by Human Genome Sciences as under the name Zalbin) which is designed to last longer in the body than standard interferon, and is currently in phase III trials[62-63].

The NS3/4 protease is a popular candidate for targeting with antiviral drugs, and the only specifically anti-HCV targeted drugs currently at phase III trials are protease inhibitors. BILN2061 (also known as Ciluprevir, produced by Boehringer-Manheim)[64] was shown to give reductions in HCV viral load of 2-3 $\log_{10}$ copies/ml after two days of treatment during phase I trials[65]. However, histology on rhesus monkeys treated with BILN2061 showed cardiotoxicity, stopping the development of the drug. BILN2061 is also a powerful inhibitor of HCV replicons in cell culture, and is often used for *in vitro* studies. Resistance mutations can occur, primarily around the binding site of the drug[66]. Efficacy of BILN2061 is greater against genotype 1 than genotypes 2 or 3, which corresponds to the greater affinity for BILN2061 displayed by the genotype 1 protease[67]. Telaprevir (VX-950, Vertex)[68] also showed positive results in phase I trials, achieving a 4 $\log_{10}$ drop in HCV RNA in those patients receiving a 750mg dose[69]. Resistance mutations also occur in patients and replicons, but this can be partly overcome by combination therapy[70]. Telaprevir has also shown the highest response of any drug so far in a trial of patients (50% in Prove 3 trial) who failed to respond to standard treatment. A rash is a common side effect, but is rarely severe (less than 10% of cases). Telaprevir is currently undergoing phase III trials. Boceprevir (also known as SCH503034, Schering-Plough/Merck)[71], is also currently in phase III trials. Results of phase II trials on patients who did not respond to standard treatment showed a 55% sustained virological response rate after 48 weeks of treatment[72].

Polymerase enzymes are the other classical targets for anti-virals, and a number of HCV polymerase inhibitors are in early development or have been stopped after clinical trials. NM107 (Idenix/Novartis) is the nucleoside 2'-*C*-methylcytidine. This molecule was found to inhibit the replication of bovine viral diarrhoea virus (BVDV) in cell culture. NM107 has been shown to have strong activity against HCV replicons with an EC_{50} of around 0.5 μM[73]. The 3'-*O*-valinyl ester of NM107 was synthesised as a prodrug (NM283 or valopictabine) for better oral bioavailability[74], but trials with this drug have been stopped. Drugs targeting other HCV proteins, particularly NS5A and NS4B, are also in development and early clinical trials. An entry inhibitor, ITX5061[75] (iTherx) is currently in phase Ib trials.

Given the difficulty in producing anti-virals targeted to HCV proteins, a number of treatments are in development targeting the host factors that HCV requires for replication. These include the cyclophilin inhibitors SCY-635[76] (Scynexis) and DEBIO-25[77] (Debio) which is currently in phase II trials. Better understanding of the host factors involved in HCV replication could lead to identification of additional potential targets for therapy.

1.5 HCV Particle Structure

The HCV particle consists of the positive strand RNA genome encapsulated by an icosahedron made up of core protein capsomers. The capsid is surrounded by a lipid bi-layer envelope, in which are embedded viral envelope glycoproteins E1 and E2 as heterodimers. HCV particles produced in cell culture have been observed using immune-electron microscopy. In these studies two sizes of particles were observed. Those measuring 30-35nm in diameter were thought to be viral capsids, and those measuring 50-60nm were infectious virions[78-80]. In the host, HCV can be associated with lipoproteins ApoB and ApoE, low-density lipoproteins (LDL), and very low-density lipoproteins (VLDL)[81-85].

1.6 HCV Genome

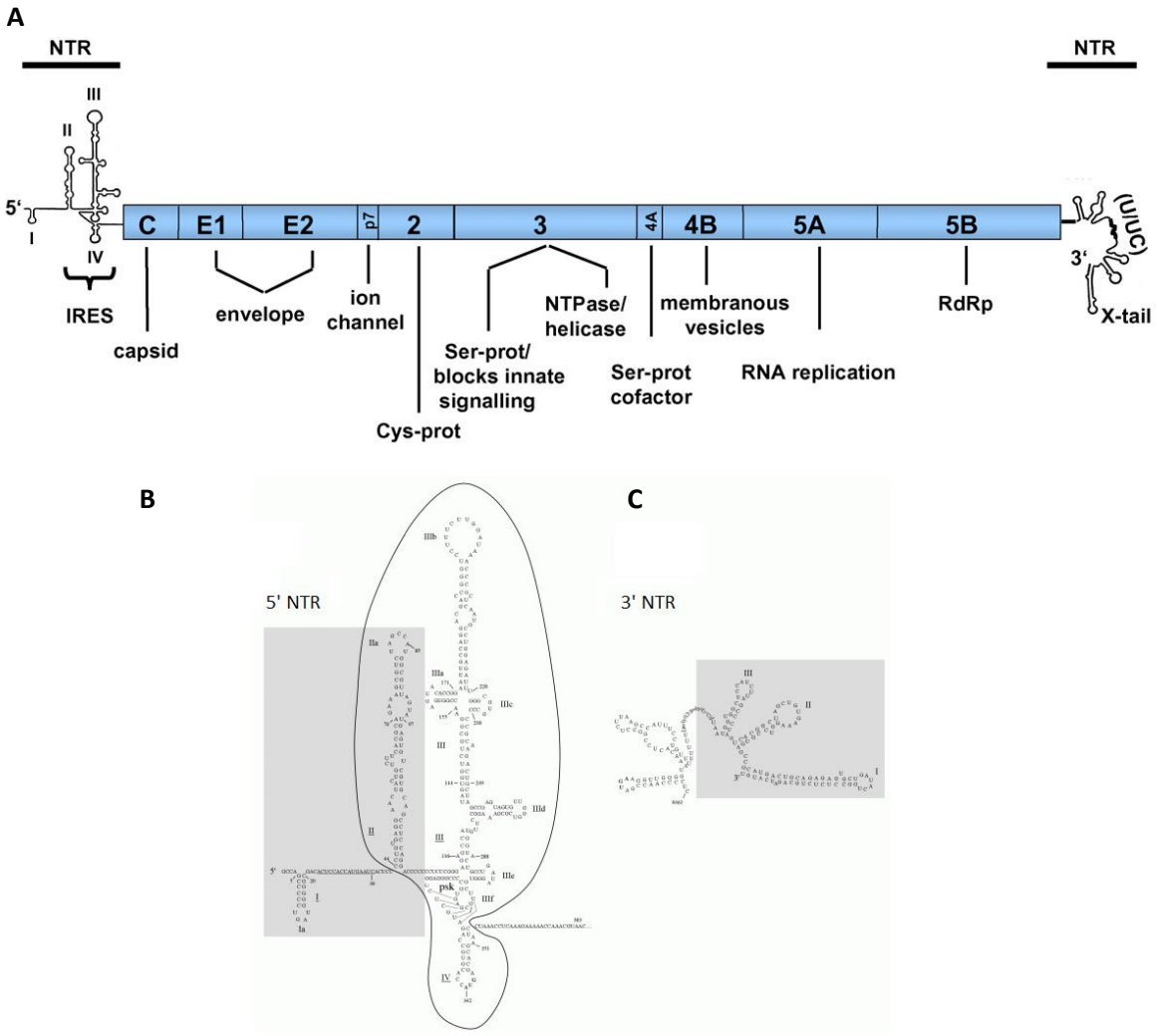


Figure 2: The structure of the HCV genome.

A Representation of the HCV RNA genome[86] with the non-translated regions (NTRs) depicted as black lines, and the polyprotein coding region depicted by the blue rectangle. Individual HCV protein coding regions are delineated by their relative sizes. The structural proteins core (C) and envelope glycoproteins E1 and E2 are coded for at the 5' end of the open reading frame (ORF). The non-structural proteins are coded for at the 3' end of the ORF. The essential functions of the non-structural proteins are as follows: p7 is a viroporin, NS2 is an autoprotease, NS3 is a protease and helicase, NS4A is a cofactor for NS3, NS4B is involved in rearrangement of cellular membranes, NS5A has multiple functions interacting with cellular components, and NS5B is the polymerase. Further descriptions of the structure and function of individual regions of the HCV genome can be found in the text. **B** Predicted secondary structure of the 5' NTR[87-88]. **C** Predicted secondary structure of the 3' NTR[87,89-90].

HCV has genome of single-stranded positive sense RNA of around 9.6kb in length. The HCV genomic structure (depicted in Figure 2A) consists mostly of an open reading frame that codes for a polyprotein of approximately 3000 amino acids which is flanked by non-coding RNA at both ends of the genome.

The 5'NTR is about 341 nucleotides long and is highly conserved across HCV genotypes. It has secondary structure (Figure 2B) that plays a role both in replication of RNA and in translation of the polyprotein. The 5' NTR contains an internal ribosomal entry site (IRES), made up of domain structures II, III and IV (Figure 2B). The IRES can bind the 40S ribosomal subunit without needing the other initiation factors usually required for translation of host mRNA (including eIF3, eIF4A, eIF4B and eIF4F)[91]. An interaction has been identified between micro RNA 122 (miR122) and a short region of the 5' NTR that is required for efficient replication of HCV RNA[92].

The 3'NTR is also highly structured and made up of three regions; a variable region, a region rich in U and C residues, and a highly conserved domain called the X-tail (Figure 2C). A long poly-U/C region of 50-60 nucleotides is required for efficient replication, and the X-tail is essential for RNA replication, having very little tolerance for deletion or mutation[93-97].

The majority of the HCV genome is an open reading frame (ORF) coding for translation of a polyprotein of about 3000 amino acids in length, which, when processed, yields 10 individual proteins. Another ORF has been identified, expressing the frameshift (F) protein or alternative reading frame (ARF) protein, so called as its coding begins one nucleotide out of frame of the major ORF. The function of this protein is currently unknown, but antibodies to it have been identified in patient sera, indicating that it is naturally expressed during infection[98-100]. Translation of the ORF occurs across the endoplasmic reticulum membrane, with the different parts of the polyprotein relating to individual proteins expressed on either the ER lumen or cytoplasmic side of the membrane, depending on the function of the individual protein (Figure 3).

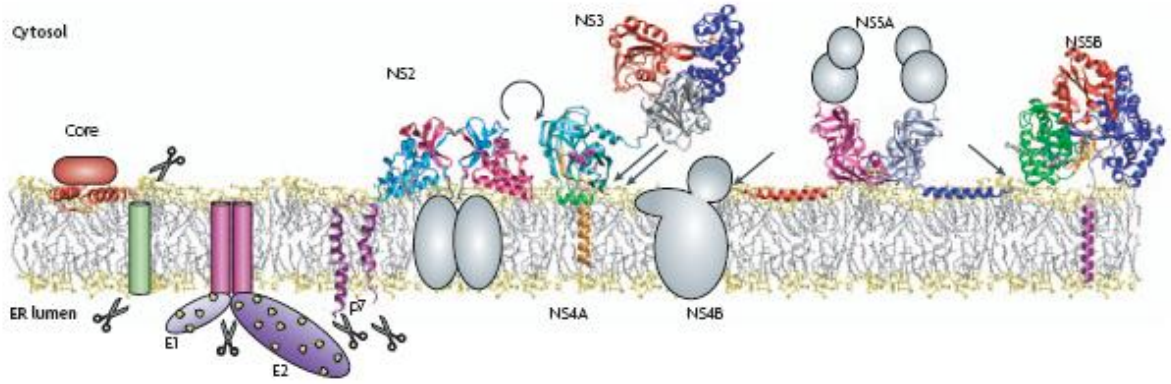


Figure 3: Structures, membrane association and processing of HCV proteins[101].
Scissors indicate cleavages by the endoplasmic reticulum (ER) signal peptidase, except on the cytosolic side where it indicates the processing of the core protein by signal peptide peptidase. The cyclic arrow denotes cleavage by the NS2–3 protease. Black arrows indicate processing by the NS3–4A protease complex. Known protein structures (as of 2007, when data were collated[101]) are shown as ribbon diagrams. The structures and the membrane bilayer are shown at the same scale. Proteins or protein segments of unresolved structures are represented as coloured spheres or cylinders.

Structural proteins are coded for at the amino terminus of the polyprotein, and non-structural proteins at the carboxy terminus of the polyprotein. There are three major structural proteins; core (C) and two envelope proteins (E1 and E2).

Core protein is about 191 amino acids in length and performs the role of capsomer for construction of the viral capsid. It is cleaved from the polyprotein by host signal peptidase[102] and further processed by host signal peptide peptidase[103]. The mature protein forms a dimer[104]. The N-terminal domain of core comprises about two-thirds of the protein and is hydrophilic[103-104]. The C-terminal domain of core is hydrophobic and is required for proper folding and localisation of the protein[103,105]. Core protein localises to endoplasmic reticulum and lipid droplets in the cell[103,106-108]. Core protein has the ability to bind RNA, which is an important feature for the packaging of genomic RNA into the capsid[109-110]. Expression of core protein in cell culture and animal models has identified a number of interactions with host cell proteins. Expression of core protein has also been shown to regulate the expression of host genes including those involved in immunity, apoptosis and proliferation, signalling and lipid metabolism[111-113] which are further described in subsequent sections.

The HCV proteins E1 and E2 are envelope glycoproteins. E1 and E2 are cleaved from the polyprotein by a host signal peptidase[106]. E1 and E2 together form a non-covalent heterodimer[114]. They localise to the ER, with the N-terminal majority of the proteins in the ER lumen (Figure 3). Both E1 and E2 are post-translationally modified by addition of N-linked glycans. E1 is glycosylated at up to 6 amino acid positions, and E2 at up to 11 positions[115-116]. These glycans play roles in envelope protein folding and viral entry[115,117-118]. E2 has been shown to bind several host cell factors, including CD81[119] and scavenger receptor class B type I (SR-BI)[120] which have been shown to be involved in HCV entry to the cell, as further described in subsequent sections. Regions of sequence heterogeneity, termed hypervariable regions (HVR), were identified in E2[121], and these have been proposed to be involved in generation of antibody escape mutants, and in modulating receptor binding and entry[122-124].

A small protein, p7, is expressed in the polyprotein after E2. This protein is likely to be a viroporin responsible for transfer of ions. Similar proteins in other viruses (e.g. influenza protein M2[125]) play a role in uncoating, but p7 has not yet been shown to be incorporated into the viral particle. It has been shown to form both hexameric and heptameric structures[126].

There are five non-structural (NS) proteins expressed by HCV. NS2 is a protein of about 216 amino acids. NS2 is a cysteine autoprotease which cleaves HCV polyprotein at the boundary between itself and NS3 (Figure 3). NS2 requires the protease domain of NS3 for autoprotease activity[127]. The active site of NS2 is formed between dimers, with histidine and glutamate residues of the catalytic triad provided by one monomer and the cysteine residue provided by the other monomer[128]. The target sequence of WRLL↓APIT is well conserved across HCV genotypes although mutations are tolerated, except to the residues at the cleavage position or those which seriously affect the structure[129]. NS2 is not essential for the formation of the RNA replication complex, as has been demonstrated in subgenomic HCV replicon cell culture models[130-131]. An HCV clone containing point mutations which inactivated NS2 protease activity was shown to infect chimpanzees but not cause a persistent infection[95]. As the non-structural proteins cannot function until NS2 has autocleaved from the polyprotein, NS2 may play a role in regulating their activity. NS2 expression has also been shown to affect expression from various host promoters including NFκB and TNFα[132]. NS2 has also been shown to inhibit apoptosis induced by CIDE-B (cell death-inducing DFF45-like effector).[133]

NS3 is around 630 amino acids in size. It is cleaved from the polyprotein at the amino terminus by the autoprotease activity of NS2-3, and at the carboxy terminus by NS3 protease activity. NS3 is a

multifunctional protein with two major domains. The amino terminal portion (180 amino acids) is a serine protease domain, and the carboxy terminal portion (450 amino acids) of NS3 is a helicase domain with NTPase activity. NS3 protease is a trypsin-like protease[134], and as such has a catalytic triad formed of the amino acids histidine (NS3 amino acid position 57), aspartate (81) and serine (139). NS3 protease is responsible for cleavage of the polyprotein at the boundaries between all the non-structural proteins from NS3 to NS5B (Figure 3)[135-140]. The protease recognises a Cys/(Ala/Ser) motif at most NS protein boundaries, but at the NS3/NS4A boundary a Thr/Ser sequence is the substrate (consensus cleavage sequence: D/EXXXXC/T↓A/SXXX). This results in slower cleavage at the NS3/4A boundary than at the other sites, possibly because the uncleaved NS3/NS4A protein is required for assembly of the replicase complex[141]. The primary function, identified so far, of the 54 amino acid long NS4A protein is to act as a cofactor for enhancing NS3 protease activity. NS3 does have protease activity alone and will cleave, for example, the NS5A/NS5B boundary. However, NS4A enhances NS3 protease activity, and is required for cleavage of the polyprotein at the remaining three boundaries between non-structural proteins[142-146]. HCV NS3 is also known to have protease activity against host proteins. This is of particular importance for the evasion of host innate immune responses to infection. NS3 is able to cleave TRIF[147], a mediator of TLR-3 signalling. TLR3 detects the presence of double stranded RNA and through the recruitment of TRIF and subsequent activation of NF-κB and IKK induces an interferon response[148]. NS3 can also cleave MAVS[149-151], a mediator of RIG-I and Mda5 signalling, both of which are involved in the initiation of innate immune systems in response to sensing of double stranded RNA. RIG-I has also been shown respond to 5' triphosphate on single stranded RNA molecules[152-153]. RIG-I, through MAVS and subsequently IRF signalling can induce an interferon response. The inactivation by cleavage of the mediator proteins TRIF and MAVS allows HCV to avoid detection through these signal pathways. The carboxy terminal domain of NS3 is a helicase with NTPase activity. The helicase domain binds RNA and has NTPase activity. NS3 is in the general class of DExD/H box helicases. The eight commonly conserved motifs of DExD/H box helicases are present in NS3, including a DECH motif at amino acid position 290[154]. NS3 helicase binds the 3' end of RNA and unwinds double stranded RNA which has a 3' overhang. Progression of the enzyme is dependent on ATP and proceeds at about 11 base pairs per step, and the helicase activity of unwinding the RNA duplex occurs at 3.6 base pairs per step, also dependent on ATP binding[155]. Recent work has indicated functions of NS3 additional to the replication of RNA. Subdomains of the helicase may also be involved in packaging of RNA and assembly of the virion[156], which is supported by evidence from research on the *Flaviviridae* members Kunjin virus[157] and Yellow Fever virus[158]. HCV NS3 has been a popular target for drug development. Protease inhibitors targeting NS3 are relatively difficult to design as the active site is a shallow groove, leaving few sites

of interaction between the protein and the drug[159]. Protease inhibitors such as Ciluprevir[64] and Telaprevir[68] have shown promise *in vitro*, but have encountered problems *in vivo*, mostly due to undesirable side effects. Helicase inhibitors have also been difficult to develop as the domains of NS3 are conserved across many cellular proteins, making specificity and toxicity the major problems.

NS4B is about 261 amino acids in length. It is hydrophobic and, once translated, is located in the ER membrane. It is involved in membrane vesicle formation and has been shown to be associated with the membranous web structures formed in HCV infected cells[160-161], implying a role in the formation of replication complexes by influencing the environment in which the HCV proteins can interact. An amphipathic helix at the amino terminal end of NS4B has been hypothesised to be responsible for association with lipid rafts[162-163]. Another amphipathic helix is present at the carboxy end of NS4B, which mediates membrane association and the formation of functional replication complexes[164]. NS4B also has GTPase activity, which is important for efficient RNA replication[165].

NS5A is a protein of about 466 amino acids which is present in either a hypophosphorylated (56kDa) or hyperphosphorylated (58kDa) state. The other non-structural proteins can influence the phosphorylation state of NS5A, and the state of NS5A influences the replication rate of HCV. In cell culture, inhibition of kinases resulting in a increase in the amount of hypophosphorylated NS5A was accompanied by an increase in replication[166]. NS5A has the ability to bind RNA, with an affinity for poly-U tracts such as the one present in the 3' NTR[167]. NS5A also interacts with a number of host cell proteins, some of which are mediated through the presence of a Src homology 3 (SH3) binding domain, including growth factor receptor bound protein 2 (Grb2)[168] and the tumour suppressor Bin1[169]. Src tyrosine kinases may contribute to phosphorylation of NS5A and NS5A may also interact with the tumour suppressor p53[170]. NS5A also interacts with host cell proteins involved in immune responses. The region of NS5A from amino acid 240 to 314, called the interferon sensitivity determining region (ISDR), was reported to contain clusters of amino acids correlating with the ability of patients to achieve SVR from interferon treatment[171]. The ISDR interacts with Protein Kinase R (PKR)[172-173], and an interaction with oligoadenylate synthase (2'-5' OAS) has also been reported[174]. NS5A interactions with host proteins also play a role in RNA replication. The membrane vesicle proteins VAP-A and VAP-B enhance HCV RNA replication and their binding to NS5A is regulated by the phosphorylation state of NS5A and may aid in positioning proteins in the replication complex[163,175]. The F box protein FBL2 also interacts with NS5A and is required for HCV replication[176].

NS5B is the RNA-dependent RNA polymerase. It has a more closed conformation than other polymerases, which is due to interactions between the hydrophobic residues in the thumb and fingers subdomains, and this may aid the initiation of RNA synthesis *de novo* as opposed to primer initiated synthesis[177-179]. NS5B also interacts with host cell factors including VAP-A and VAP-B (as NS5A also does) and cyclophilin B, which stimulates the RNA binding activity of NS5B[180]. NS5B also has a retinoblastoma protein (Rb) binding motif, which, if mutated, results in impaired replication[181]. It is also possible that binding of NS5B targets Rb for degradation and therefore promotes cell proliferation[182].

1.7 HCV Lifecycle

The HCV lifecycle is illustrated by the schematic illustration given in Figure 4[101]. The blood-borne virus binds to the hepatocyte cell using several host proteins and is internalised by endocytosis. The virus uncoats and the positive strand RNA genome is released into the cytoplasm. Protein translation and RNA replication take place in the cytoplasm, on membranous structures associated with the endoplasmic reticulum. Newly replicated RNA is then packaged in the capsid and the particles acquire a membrane and additional factors as the virus matures and is released.

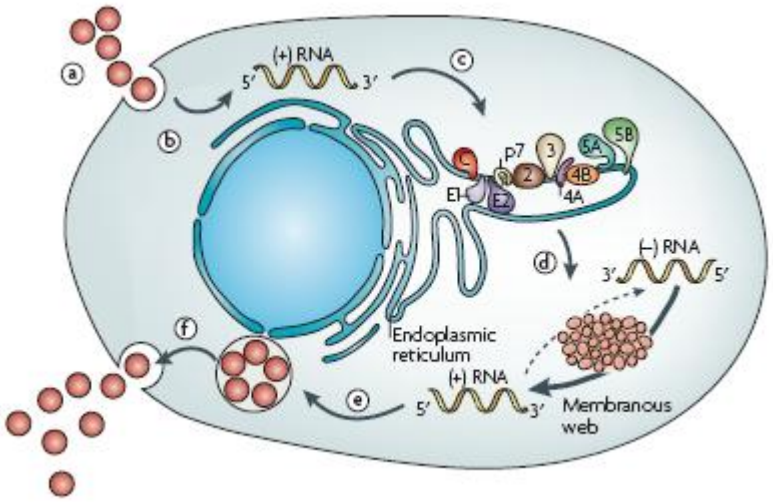


Figure 4: A schematic representation of the lifecycle of hepatitis C virus.

The lifecycle stages of HCV in its interaction with the host cell are labelled as follows: (**a**) Virus binding and internalization. (b) Cytoplasmic release and uncoating. (**c**) IRES-mediated translation and polyprotein processing. (**d**) RNA replication. (**e**) Packaging and assembly. (**f**) Virion maturation and release[101].

1.8 HCV Entry to the Cell

Entry of HCV into a host cell requires interaction between components of the viral particle and cellular factors. Current research indicates that four cell molecules are required for entry. An early host cell protein to be identified as required for HCV entry was the tetraspannin CD81[119]. Antibodies against CD81 can inhibit entry of HCV *in vitro* before or after the initial binding of the virus[183]. The scavenger receptor class B type I (SR-BI) is involved in cholesterol uptake and has affinity for LDL, which are often part of infectious virus particle in the host, and HDL which were shown to increase infectivity of virus in a dose dependent manner. SR-BI was initially identified as a candidate HCV entry receptor when it was shown to bind E2[120]. Both proteins CD81 and SR-BI bind E2 and are necessary but not sufficient for HCV entry. Claudin 1 (CLDN1) is a membrane protein involved with tight junctions that has been shown to be involved in HCV entry[184]. Occludin (OCCLN) is the most recently identified protein to be involved in HCV entry[185]. Other proteins shown to interact with HCV, but that may not be as important for entry as those already described include; the LDL receptor (LDLR), liver/lymph node-specific intercellular adhesion molecule-3-grabbing non-integrin (L-SIGN), dendritic cell-specific intercellular adhesion molecule-3-grabbing integrin (DC-SIGN) and heparan sulphate.

After binding, HCV is internalised by clathrin-mediated endocytosis[186]. This is followed by uncoating induced in a low-pH compartment[183,187].

1.9 HCV Replication Complex

As already described, the HCV proteins are translated and localise to the ER. Here, HCV rearranges internal cellular membranes into structures required for viral replication. The membranous web contains the HCV replication complex including viral proteins NS3, NS4A, NS4B, NS5A, and NS5B, as well as viral RNA and host cell factors. This membranous web forms subcellular locations which could help to optimise HCV RNA replication, as well as protect from host nucleases, proteases, dsRNA-induced immune responses and presentation of HCV antigens on MHC-I.

Membranous structures have been observed in infected chimpanzee liver cells[188], virus infected cultured cells[108], cells expressing subgenomic RNA replicons[161], as well as cells expressing only NS4A-B precursor protein[189] or mature NS4B protein[160,189]. Observations have been made using electron microscopy where NS4B was expressed alone and found only on the membranous web structure[160]. NS4B has been observed by light microscopy at the ER and at cytoplasmic foci[162,190] which seem to correspond to vesicles embedded in a membrane matrix which may be the membranous web[191]. Therefore, while all the nonstructural proteins are required for HCV RNA replication and are present in the replication complexes, expression of NS4B alone is sufficient to induce morphological changes in cellular membranes[162,190-195].

The HCV replication strategy is similar to that of other viruses with positive stranded RNA genomes[196-197]. In particular, they share the feature of using structures derived from cellular membranes as sites of RNA replication. HCV[161] and other *Flaviviridae* (including Kunjin[198-199] and Dengue[200] viruses) create vesicular structures from the ER. *Picornaviridae* (such as Polio virus[201]) create clusters of vesicles from the ER, Golgi and lysosomes. Togaviridae (such as Semliki Forest[202] and Rubella[203] viruses) create vacuoles lined with small spheres from endosomes and lysosomes.

RNA replication occurs within the replication complexes constructed inside the membranous web. Current models hypothesise a structure similar to that shown in Figure 5B. It is known that the structural proteins are not required for RNA replication, as these are not present in the subgenomic RNA replicon cell lines used for in vitro study. All non-structural proteins are required for RNA replication[131]. The 5' NTR contains the IRES required for translation[91] and is required for efficient RNA replication[204]. The 5' NTR also contains a miR122 binding site that is required for efficient RNA replication[92]. The 3' NTR contains stem loops and a U/C-rich region that are required for efficient RNA replication[93,95-97]. Cellular cofactors have also been identified which are required for, or

enhance, HCV RNA replication. These include cyclophilin B[180], which interacts with NS5B, and the combination of FKBP8 and Hsp90[205].

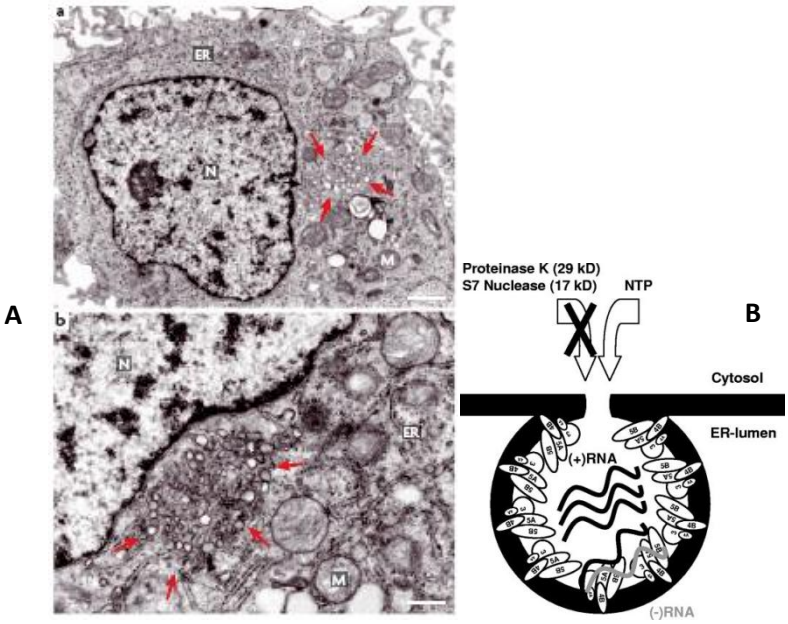


Figure 5: Membranous structures created by HCV during viral replication.

A The membranous web created in Huh7 cells harbouring a subgenomic replicon[101,161] at (**a**) low power and (**b**) higher power. The membranous web is indicated by red arrows. ER: endoplasmic reticulum, M: mitochondrion, N: nucleus. **B** A simple schematic representation of the replication complex[206].

1.10 HCV Assembly and Release

The late stages of the HCV lifecycle are less well characterised than other aspects due to the lack, until recently, of a good model for *in vitro* study. Recent research has identified roles in assembly for most of the HCV proteins, and also roles for cellular structures such as lipid droplets. Assembly and release of HCV has been linked to the VLDL synthesis and ESCRT transport pathways.

Most of the viral proteins have some role in HCV assembly. Core protein is the monomer which makes up the HCV capsid. Once core is cleaved from the polyprotein by signal peptide peptidase, it moves to the surface of lipid droplets[103], the interactions with which are mediated by the 60 amino acids in the C-terminal hydrophobic domain of core[105]. The site of capsid assembly is a point of interaction between lipid droplets, core protein and HCV RNA delivered by NS5A from the ER. The p7 protein forms α-helical hexa- or heptameric complexes[126] which have the ability to channel cations[207]. The precise function of p7 is uncertain, but it is essential for the assembly and release of infectious HCV[208-209]. It has been proposed that p7 may protect virus particles during assemble by preventing acidification of intracellular compartments[210]. NS2 is also essential for assembly, but the protease activity is not required[208,211]. NS2 may have a role in maturation after assembly of the virus[212-214]. NS3 has been implicated as having a role in the assembly process. Mutational analysis identified that domains in the NS3 helicase are required for assembly at a stage after recruitment of NS5A to the lipid droplet and before formation of dense intracellular viral particles[156]. This is supported by evidence from research on other viruses related to HCV, such as the *Flaviviridae* members Kunjin virus[157] and Yellow Fever virus[158]. NS4B may also play a role in HCV assembly. Trans-complementation studies showed that NS4B was capable of modulating infectious virus production[215]. NS5A contains three domains, of which Domain 3 has been identified to be required for HCV assembly[216-219]. Phosphorylation of a serine by casein kinase II may regulate the interaction of NS5A with core, and therefore may affect assembly[216,219]. Deletion of Domain 3 of NS5A results in NS5A and core no longer localising to the same lipid droplets[218].

Several host factors play a role in the assembly and release of HCV. Lipid droplets are an important cellular feature required for the assembly of the HCV virion. Lipid droplets are usually present in the cell and form storage organelles for neutral lipids. The association of HCV core protein with lipid droplets is essential for assembly as the inhibition of signal peptide peptidase prevents core localisation to lipid droplets and virion production[220]. Non-structural proteins, including NS5A, also interact with lipid droplets and colocalise with core. Prevention of NS5A from localising to lipid

droplets, or with core, can also block virus production[218,221]. Many of the host factors involved in the assembly and release of HCV are also involved in the VLDL pathway. VLDL assembly requires apoB and microsomal triglyceride (MTP). Briefly, apoB translocates to the ER lumen, where it forms a cavity. MTP inserts lipids (phospholipids and triglycerides) into the cavity. This process forms a spherical particle which can then be secreted[222-223]. ApoE is essential for assembly and is a component of infectious HCV particles[224-227]. ApoE has a molecular weight of 34kDa and is involved in the transport of lipids. When (the C-terminal domain of) apoE is associated with lipids, the N-terminal region of the protein is capable of binding LDL family receptors[228]. ApoB has a molecular weight of 500kDa. It is the only apolipoprotein that remains after conversion of VLDL to LDL by lipases, and there is only one molecule present per lipoprotein particle. Binding of apoB to the LDL receptor initiates endocytocis[229]. The importance of apoB to the production of infectious HCV particles is not yet clear. Some groups have found inhibition of apoB by RNA interference, or inhibition of MTP, to impair HCV production[230-231]. However, other groups have found that by RNA interference of apoE reduced virus production, but that knockdown of apoB and inhibition of MTP did not reduced virus production[224-226]. The ESCRT (endosomal sorting complex required for transport) system is involved in membrane remodelling for protein sorting, creating multivesicular bodies, cytokinesis and budding of enveloped viruses (e.g. HIV-1[232] and Ebola[233]). Briefly, ESCRT complexes I, II and III are recruited in order to the membrane of endosomes to sequester proteins for transport and encourage vesicularisation. The ESCRT system is disassembled and recycled when Vps4 (an AAA ATPase) is recruited to ESCRT III[234]. Knockdown of TSG101 (a component of ESCRT I), CHMP4b (ESCRT III), Alix (a TSG101 and CHMP4b binding protein), and Vps4b reduced extracellular infectious viral titre and the amount of core released by cells[235]. A study expressing dominant negative copies of CHMP proteins and Vps4 also showed reduced infectious virus production[236]. HCV core, but not NS5A, has been observed to colocalise with CHMP4b[235]. Heat shock cognate protein 70 (hsc70) has been seen to colocalise with HCV proteins on lipid droplets, affect the size of lipid droplets, and affect the production of infectious virus particles[237]. Annexin 2 (ANXA2) has been observed in proteomic analysis of membranous replication complexes, and knockdown of ANXA2 by RNAi resulted in impaired viral assembly [238].

There are currently two major theories as to how capsid assembly occurs. One model suggests that lipid droplets are transport vehicles which take core to the site of assembly, where it acquires RNA from the replicase or NS5A. This is supported by evidence that lipid droplets can transport along microtubules, and that use of antibodies against dyenin or nocodazole impairs HCV assembly[239]. An alternative theory is that capsids are formed on the surface of lipid droplets, and viral RNA is

delivered by NS5A which also localises to the lipid droplets. This is supported by the fact that the N-terminal domain of NS5A can target lipid droplets [240-241].

The maturation and release of the HCV particle is linked to the VLDL pathway[224,226,230-231]. Core protein has been shown to accumulate in detergent resistant lipid fractions which contain cholesterol and sphingolipids in high amounts[242], both of which are also present in HCV particles and are important factors in determining infectivity[243]. The capsid is inserted into an ER luminal lipid droplet, but it is uncertain how E1 and E2 are targeted to this site. It has been suggested that NS2 plays a role in pulling together the envelope proteins and other non-structural proteins (particularly NS3) by protein-protein interactions[212-214,244]. The precise method of incorporation of apolipoproteins into the viral particle is unclear. The ER luminal lipid droplet containing the virus and apoE may fuse with VLDL particles containing apoB, resulting in a mature lipo-viral particle. The ESCRT system has been shown to be required for the release of infectious HCV particles[235-236]. However, inhibition of ESCRT components does not prevent assembly of intracellular infectious particles, so it is likely that ESCRT is only involved in the late stages of release of the virus from the cell.

HCV particles released from cells have been profile using density gradients. There is a heterogeneous mix of HCV particle densities observed in patients, partly due to the association of HCV with VLDL/LDL and other factors[82-84,245]. These range from around 1.04g/ml to 1.25g/ml[81,83,245-246]. The lower density particles (<1.06g/ml) are more infectious than higher density particles. Around 40% of total HCV RNA in the plasma is associated with these lower density particles, although it varies between patients[84,245]. The low density particles are associated with VLDL/LDL containing apoB, apoE and apoC, as well as triglycerol, and can be complexed with antibodies[83,245,247]. Higher density particles can also be infectious, and these may include particles that contain apoE and apoC but not apoB, and therefore have less lipid volume. These are the major types of particle that have been observed by production of HCV in cell culture, with an average density of around 1.1g/ml[248]. HCV particles containing RNA, with a density between 1.06g/ml and 1.17g/ml, may be free virus particles[247,249]. HCV RNA present in particles with density above 1.18g/ml is thought to be in structures such as the capsid or capsid complexed with antibodies[249-250]. Examples of determination of HCV buoyant density in iodixanol gradients are shown in Figure 6[248,251]. These demonstrate the different densities of HCV particles produced in cell cultures and from chimpanzees, reflecting the compositional differences described above.

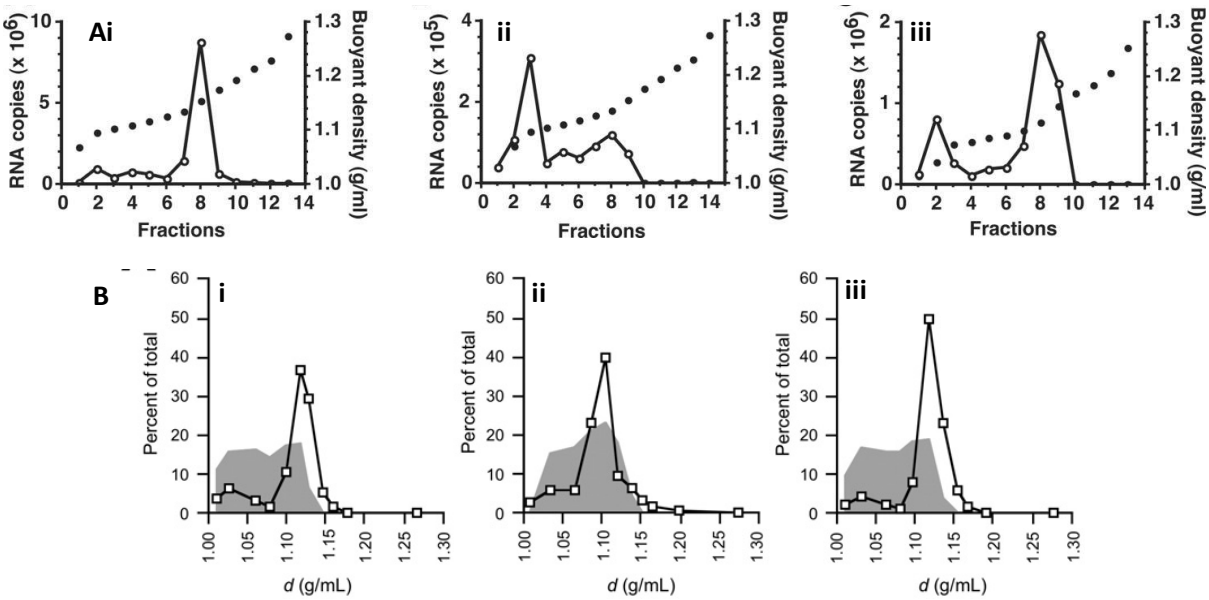


Figure 6: Density profiles of HCV particles.

These examples of density profiles show the approximate buoyant densities of HCV particles, and demonstrate the differences that can be observed in particle density. **A** Buoyant density in iodixanol gradients[248] of HCV from **i)** cell culture, **ii)** plasma from chimpanzee 4x0483 at 3 weeks postinfection, and **iii)** virus recovered from chimpanzee 4x0483 week 3, then passaged in cell culture for 9 days. **A** Buoyant density in iodixanol gradients[251] of HCV from **i)** Huh7 cell culture, **ii)** primary hepatocyte cell culture, and **iii)** virus recovered from primary hepatocyte cell culture, then re-cultured in Huh7 cells.

1.11 Immune Response to Infection and Viral Evasion

In the majority of cases, HCV is not cleared and the individual goes on to develop a chronic infection. In roughly 20% of cases, only an acute infection occurs and the virus is cleared within six months. The immune response to infection plays a role in determining the outcome of infection, and although the mechanisms are not fully understood, some of the determinants and features involved have been identified. Both the adaptive and innate aspects of the immune system have roles to play in fighting viral infection, and HCV must have means to evade these responses in order to establish a chronic infection.

The adaptive immune response to infection is made up of the humoral response (production of antibodies by B cells) and the cellular response (including $CD4^+$ helper T cells and $CD8^+$ cytotoxic T cells).

The time to seroconversion varies, but the average is around 10-12 weeks post infection with HCV[90,252]. Antibody titres are generally low and can become undetectable in some patients after resolution of acute infection. HCV has been shown to be neutralised by antibodies in chimpanzees[253-255] and cell culture[256-260]. Neutralising epitopes exist in E2[254,256,261]. However, neutralising antibodies do not always appear in acutely infected patients who resolve infection, indicating that the humoral response to HCV may not be the most important factor in clearance of the virus[262-263]. It is also possible for humans and chimpanzees who have recovered from the virus to become infected on subsequent exposure to the virus.

Adaptive cellular immunity is an important determinant of infection outcome. A T cell response is measurable in most individuals, but it is slow to develop, and it can be between 5 and 10 weeks post HCV infection before $CD8^+$ T cells are observed in blood[252,264-267]. Intrahepatic T cells have been observed in infected chimpanzees 4-8 weeks after viraemia was detected[252,264].

A strong $CD4^+$ T cell response has been associated with resolved infections[268-271], and these $CD4^+$ responses are usually aimed at non-structural proteins (including some frequently observed epitopes in NS3)[270,272]. There is a relationship between the expansion of HCV-specific $CD8^+$ T cell responses and the decline in viraemia during acute infection[252,265,269,271,273]. Strong $CD8^+$ T cell responses, targeting up to 8-12 HCV epitopes have also been reported as present in patients who resolved HCV infection[265,274]. $CD4^+$ and $CD8^+$ T cell responses can remain detectable after clearance of the

virus[265,275] even when antibodies are undetectable[276]. There have been cases of multiple acute infections of humans and chimpanzees[277-282] indicating a lack of immunity to subsequent infection. However, a study has shown that previously HCV-infected patients were about half as likely to develop new viraemia[283]. Studies in chimpanzees have also shown that second infections were cleared much more quickly that primary infections[266,284]. Chimpanzees that have been immunised with HCV proteins that are not the targets of neutralising antibodies have a reduced viraemia[90].

Animals with depleted $CD4^+$ or $CD8^+$ T cells have persistent HCV infections when re-challenged with the virus. Depletion of $CD8^+$ T cells caused prolonged viraemia[266], and depletion of $CD4^+$ T cells caused persistent infection despite the presence of memory $CD8^+$ T cells from a previous infection[284]. As clearance of the virus only occurs in about 20% of patients, the cellular immune response observed in acute resolving infections must not work in the majority of cases. This may be due to mechanisms such as primary T cell failure, T cell exhaustion, T cell dysfunction and viral escape mutations[274,285].

Patients with chronic HCV may not have strong or multispecific $CD8^+$ T cell responses. This could happen if the cells are not initially primed, and has been shown in some early acute chimpanzees and humans[252,264,286]. Impaired priming may occur where there are low numbers of antigen presenting cells[285,287-288] but this is contested[285,289-290]. Impaired T cell activation has been observed in the presence of HCV core protein, through its interaction with complement receptor gC1qR[291-292]. There have also been cases observed where a T cell response existed early in infection but then disappeared, but the mechanism for this is unknown[265,269]. $CD4^+$ help is required for a good $CD8^+$ response, so the weak $CD4^+$ response seen in chronic HCV[293] and impaired $CD4^+$ which produce low levels of IL-2[294] could contribute to a weak cellular immune response to HCV.

The programmed cell death-1 (PD-1) receptor is known to be a marker for exhaustion in $CD8^+$ T cells, and blockage of the interaction of receptor and ligand can restore cytokine secretion, cell proliferation, and cytotoxicity ability[295]. During acute HCV infection, PD-1 is upregulated on $CD8^+$ T cells. It has been observed that patients who resolved infection had an early decrease in PD-1 expression, but patients who developed a chronic infection maintained PD-1 levels[296-298].
The T cells involved in the response to infection can be influence by regulatory T cells. $CD4^+$ $CD25^+$ T cells suppress $CD8^+$ T cells and have been found in chronically infected patients at higher levels than in resolved or uninfected individuals[299-300]. There are also regulatory $CD8^+$ T cells which express IL-10, and can suppress the virus-specific $CD8^+$ T cells[301].

Viral mutation can result in alteration of epitopes recognised by T cells[302-304]. Mutation can also affect the abil[304]ity of cells to process antigens for presentation on MHC, and the ability of epitopes to bind MHC[303]. There has also been a case described where a mutation resulted in diminished T cell recognition of the presented epitope , and therefore failure to prime T cells[305].

There are therefore several potential mechanisms which could contribute to the ability of HCV to evade the cellular immune response and establish a persistent infection.

The infected individual also has innate immune responses with which it can fight infection. HCV must evade the innate response in hepatocytes in order to replicate within the cell and establish an infection. The innate response is activated when pattern associated molecular patterns (PAMPs) are detected by pattern recognition receptors (PRRs). PRRs include Toll-like receptors (TLRs), RIG-I-like receptors (RLRs), and nucleotide oligomerisation domain-like receptors (NLRs)[306]. Recognition of viral PAMPs by TLRs and RLRs leads to activation of interferon regulatory factors (IRFs), nuclear factor-κB (NF-κB) and eventually IRF3 target genes, IFN and interferon stimulated genes (ISGs), and cytokines. Recognition of PAMPs by NLRs activates caspase 1, then cytokines such as IL-1 which have an antiviral inflammatory effect. NLRs are thought to be primarily involved in sensing bacteria[307-308]. Several TLRs are involved in sensing viral PAMPs. TLR2 and 4 can detect viral proteins on the cell surface, and TLR2 has been shown to be activated by HCV core and NS3[307-308]. TLR3, TLR7/8 and TLR9 all detect nucleic acids, and are all expressed in endosomes, with TLR3 also expressed on the cell surface. TLR7/8 detects U- and G-rich ssRNA, and TLR9 detects CpG in DNA, and TLR3 detects dsRNA. Hepatocytes are deficient in TLR signalling[309], so they are unlikely to provide a primary defence against infection by HCV. However, HCV does have a method for evasion of the TLR3 mediated immune response. NS3 is able to cleave TRIF[147], a mediator of TLR-3 signalling. Without functional TRIF, TLR3 cannot signal the presence of dsRNA by subsequent activation NF-κB and IKK, and cannot induce an interferon response[148]. NS5A can prevent TLR induction of cytokines in macrophages by binding the major signalling adaptor MyD88 (which is not used by TLR3)[310].
RIG-I can detect PAMPs including dsRNA, 5’ triphosphates and U- or A-rich RNA[152-153,311-314]. When RIG-I detects a PAMP, it oligomerises and exposes its CARD domain. This CARD domain interacts with the card domain of MAVS, and signals an interferon response through IRF7[149-150,312-313,315-317].
The polyU/UC region of the 3’ end of the HCV genome, and the 5’ triphosphate end of the genome have been shown to be recognised by RIG-I[312,314,316,318]. It is possible that HCV RNAs in replication

complexes in the membranous web are protected from detection by RIG-I[160-161], however there is still likely to be RNA present at other sites in the cytoplasm. HCV can disrupt RIG-I signalling by cleavage of MAVS using the NS3/4A protease. Cleavage of MAVS releases it from the membrane and stops oligomerisation, both of which prevent signal transduction[149-151,319-320].

HCV can also evade the innate immune response by attenuation of IFN signalling through the Jak/STAT pathway. HCV core protein can bind STAT1 to prevent phosphorylation and therefore activation of ISGs[321-323]. HCV is also able to directly interfere with the action of some ISGs. E2 can inhibit PKR kinase ability by competing with eIF2 to bind PKR[324]. NS5A can also block PKR[173,325], as well as blocking 2-5' OAS by direct interaction[174].

The ability of HCV to evade innate immune responses is likely to be an important feature in the establishment of chronic infection.

1.12 HCV Animal Models of Replication

The study of HCV has been limited by the difficulty of developing and identifying suitable model systems. *In vivo* studies of HCV in animal models have been restricted to chimpanzees, which are the only animal other than humans that can truly be infected by HCV[326]. Surrogate animal models have been used with some success. The GB virus B (GBV-B) is classed as a hepacivirus (see phylogeny dendrograms Figure 1). GBV-B infects tamarins, resulting in an acute infection which lasts for 16 weeks, after which time the infection is cleared. This differs from the usual progression of HCV to chronic infection in the human host, limiting comparative studies. GBV-B also infects marmosets. There are similarities in sequence and substrate specificity of HCV and GBV-B viral proteins[327]. This has allowed the use of GBV-B animal models in the testing of some potential HCV therapeutics[328]. Chimpanzee infection with HCV is a more accurate model of human infection with HCV. The acute resolving infection lasts for 12-24 weeks, and many infections proceed to a chronic state, although with a lower rate of progression to chronicity in chimpanzees than in humans[329-330]. Fibrosis in the chimpanzee is usually milder than in humans, and occurrence of cirrhosis and HCC is less frequent. However, most countries have recently banned, or are considering banning, medical testing on chimpanzees. This means that the option to study this *in vivo* model is no longer available. The current area of development is in mouse models. There have been a number of models generated where constitutive expression of HCV proteins (individual, combinations and the full polyprotein) has been achieved. Another approach has been to introduce human liver cells into the mouse, providing a more natural habitat for the virus. SCID (severe combined immune deficient) mice have been used for this purpose to prevent immune rejection of human cells. In addition, a transgenic mouse was developed carrying the mouse urokinase type plasminogen activator (uPA) gene under the control of the mouse albumin enhancer/promoter (called SCID-Alb/uPA mice)[331]. The expression of this gene results in toxicity to the mouse hepatocytes, and therefore allows the introduced human hepatocytes a growth advantage, meaning that repopulation of the liver is performed by the human hepatocytes[332]. Another xenograft mouse model called Trimera was created by irradiating mice, then reconstituting liver with marrow from SCID mice and human liver cells[333].

1.13 HCV Replicon Cell Culture Models

An advance in the ability to study HCV *in vitro* was made when the replicon cell culture system was developed[131]. The first subgenomic replicons described were based on genotype 1b HCV (an isolate called Con1)[131]. Replicons were subsequently developed using a genotype 1a HCV consensus clone called H77[334]. Subgenomic RNA replicons typically consist of the HCV 5' NTR (containing the HCV IRES) to drive RNA replication and translation of a neomycin resistance gene (*neo*) gene for antibiotic selection of cells containing the replicon. The coding sequence for the non-structural proteins, from NS3 to NS5B, is present and under the translational control of an EMCV (encephalomyocarditis virus) IRES. The 3' NTR of the HCV genome is also present. This design may have been influenced by the existing subgenomic replicons for other viruses e.g. poliovirus[335], bovine viral diarrhoea virus (BVDV)[336], and Kunjin virus[337]. In developing the HCV replicon systems, it was found that some mutations were required for efficient replication of the replicons. Cell culture adaptive mutations were found in NS3, NS4 and NS5A, and worked individually or cooperatively[338]. Potential functions for these mutations include action by enhancing HCV polyprotein cleavage, and HCV protein interaction, by enhancing interaction with the cellular components of the replicase complex, or by more efficiently inhibiting the cellular anti-viral defences. Establishment of replicons based on genotypes other than genotype 1 did not occur until later, possibly because genotype 1 is the most common in patients from Europe and the USA and therefore the most likely to be studied. However, in 2003 a genotype 2a clone isolated from a Japanese patient with fulminant hepatitis was used to create a subgenomic replicon[339]. The consensus clone generated from this patient was designated JFH-1[340]. The JFH-1 subgenomic replicon gave a higher number of colony forming units per μg of RNA than genotype 1b replicons and, importantly, was able to replicate without the need for the cell culture adaptive mutations required by previous replicons. The major problem with the use of subgenomic replicons for the study of HCV is that they lack the coding sequence for structural proteins. This means that subgenomic replicons cannot produce infectious virus particles and the full viral life cycle cannot be studied. Therefore the description of the full-length JFH-1 HCV clone in 2005, which can replicate in Huh7 cells without adaptive mutations, was a major advance in HCV research.

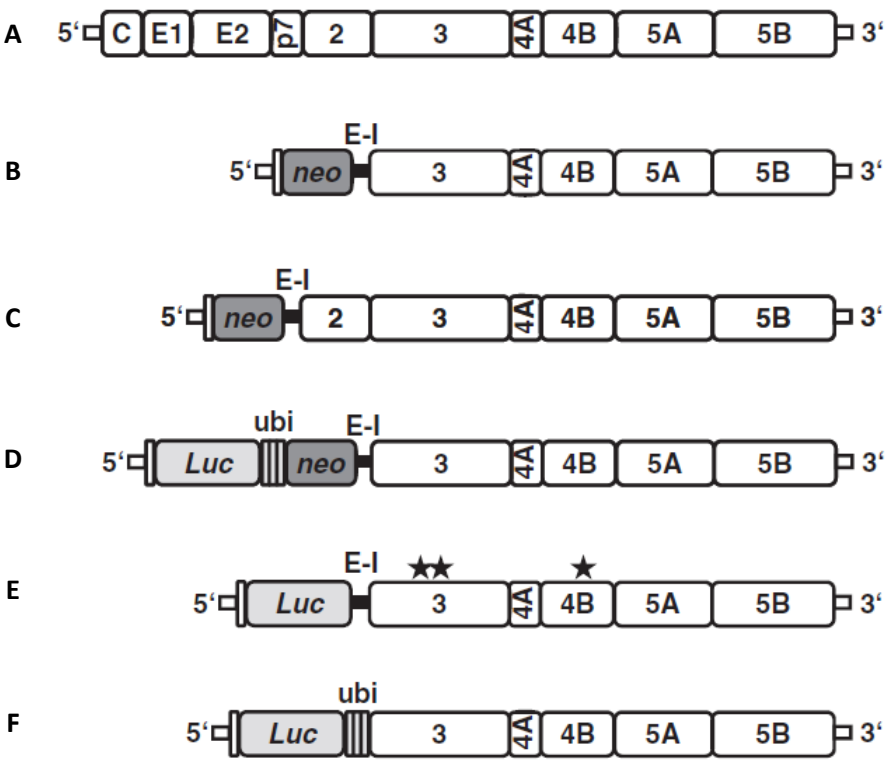


Figure 7: Structures of HCV replicons[341].

A Schematic representation of the HCV genome. The 5' and 3' NTRS are indicated by white bars. **B** and **C** The structures of bicistronic selectable subgenomic replicons. They are composed of the HCV 5'NTR directing translation of the neo gene, the IRES of the encephalomyocarditis virus (E-I), the HCV replicase genes NS3–NS5B (**A)** or NS2–NS5B (**B)** and the 3'NTR. **D** Structure of a selectable reporter replicon. This construct encodes a luciferase–ubiquitin–neomycin phosphotransferase fusion protein in the first cistron. The RNA supports stable expression of luciferase; ubiquitin (ubi) is used to trigger proteolytic removal of the neomycin phosphotransferase from the fusion protein. **E** The structure of a subgenomic Con1 luciferase (Luc) reporter replicon that is used for transient replication assays. **F** Structure of a monocistronic reporter replicon. A gene encoding luciferase is fused in frame to the viral replicase genes NS3–5B via ubiquitin. The entire polyprotein is translated by the HCV IRES.

1.14 HCV Infectious Cell Culture Models

When the full-length JFH-1 HCV clone was generated, it was found to be able to undergo complete viral replication when transfected into cultured hepatoma cells[79-80]. This was the first sequence to be identified to allow HCV replication *in vitro* and derivatives of this genome are still by far the most efficient at replication and production of HCV *in vitro*. Other HCV isolates have been tested for their ability to replicate in cell culture, with varying degrees of success. Most research has been put into genotype 1 isolates. The genotype 1a isolate H77 requires adaptive mutations for RNA replication and has shown a small amount of virus production[334,342]. Isolate H77C also showed a low level of RNA replication, and its cell culture adapted derivative H77S replicated RNA to a higher level, and produced some infectious virus [338,343-344]. The genotype 1b isolate HCV-N could replicate RNA with NS5A adaption, but did not produce virus[345-347], and isolate HCV-CG1b replicated RNA under a T7 driven system and was capable of producing some infectious virus[348]. The genotype 1b isolate Con1 wild type was capable of some RNA replication and transient virus production, but its cell culture adapted derivative, whilst capable of high levels of RNA replication, could not produce virus[130-131,349-350]. Two genotype 1b isolates with genotype 1a 3'NTRs called BK[351]and HC-J4[352] showed a small amount of RNA replication, with no reported virus production.

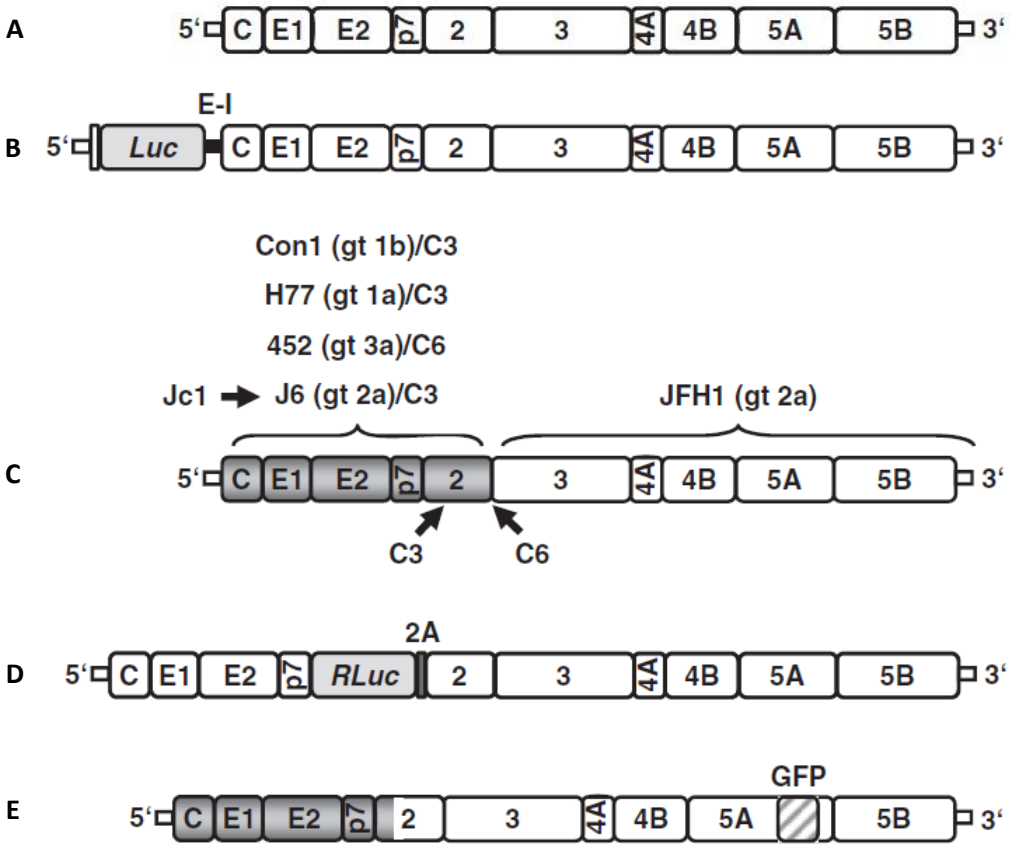


Figure 8: Structure of JFH-1 derived genomes[341].

A Schematic representation of the HCV genome. The 5' and 3' NTRS are indicated by white bars. **B** Schematic representation of a bicistronic full length JFH-1 reporter genome. The HCV 5' NTR directs translation of the firefly luciferase gene (Luc) whereas translation of the HCV polyprotein is under the control of the EMCV IRES (E-I). **C** Chimaeric genomes are composed of the region encoding core to transmembrane segment 1 of NS2 (C3 position) of HCV isolates Con1, H77 or J6 fused to the remainder of the JFH-1 isolate. In case of the 452 chimera, the region encoding core to the C-terminus of NS2 (C6 position) was fused to the JFH-1 replicase genes. Junction sites are indicated by an arrow. The highly assembly competent J6/JFH-1 chimera is also called Jc1. **D** Schematic diagram of a monocistronic Renilla luciferase (RLuc) reporter genome. **E** Structure of a monocistronic Jc1 reporter virus applicable for live cell imaging. The gene encoding the green fluorescent protein (GFP; striped box) is inserted in-frame into domain 3 of NS5A.

1.15 Chimaeric HCV Genomes

There have also been attempts to improve upon and add to the JFH-1 infectious virus system. The use of reporters in the viruses, whilst usually conferring a replicative disadvantage, is useful in that it allows for additional methods to measure the replication of the virus. Luciferase reporter viruses have been created, with several different construction morphologies. Bicistronic vectors have been created where, in a similar way to the subgenomic replicons, the reporter is under the translational control of the HCV IRES, and the HCV polyprotein is under the control of an EMCV IRES (Figure 8B). Reporter genes have been inserted into the polyprotein, for example GFP at domain 3 of NS5A[353] (Figure 8E). A common reporter virus has the reporter inserted after p7, and then has an FMDV (foot and mouth disease virus) 2A sequence between the reporter and NS2[208] (Figure 8D). The function of the FMDV 2A is to autocleave the reporter from the HCV non-structural proteins. The use of chimaeric viruses has been pursued in order to improve the replicative efficiency of viruses, and to provide models for study of genotypes other than genotype 2a. Studies have found that it is possible to exchange the structural protein coding region of JFH-1 for those of other viruses and still achieve HCV replication in cell culture. Chimaeric JFH-1 sequences were created with the junctions located at various sites in p7 and NS2, mostly at sites between the transmembrane domains. It was found that most chimaeras replicated most efficiently when the junction between sequences was located after the first transmembrane domain of NS2. Intergenotypic and intragenotypic chimeras have been made using this technique. A chimaera of the non-structural region of JFH-1 with the structural region of another genotype 2a clone, J6, created a virus that could yield infectious titres of 100 times higher than JFH-1 alone. This chimaera was designated Jc1. Replicating chimaeras were also made during the same study by fusion of the non-structural regions of JFH-1 with the structural regions from isolates of genotypes 1a (H77), 1b (Con1), and 3a (452), in the case of which, the fusion junction was at the end of NS2)[354] (Figure 8C). Chimaeric viruses incorporating the structural genes of JFH-1 and the non-structural genes of other viruses have not been able to replicate in cell culture.

Studies into the importance of non-structural regions in the replication of HCV JFH-1 have been attempted. Intergenotypic and intragenotypic chimaeras of subgenomic and full length JFH-1 have been used to identify viral determinants involved with HCV replication.
A study has been performed using intragenotypic chimaeric subgenomic replicons and full length infectious HCV as the bases for study[355]. Using the JFH-1 sequence as a backbone, J6 isolate sequences corresponding to the individual non-structural proteins were incorporated into a panel of subgenomic replicons and replication at 24 and 48 hours post electroporation was assessed by

luciferase activity. Four chimaeras were observed to have reduced replication when compared to JFH-1 wild type. These chimaeras were those containing J6 sequences in the following positions: NS5B and 3'NTR; NS3 helicase and NS5B; NS3 helicase and 3' NTR; NS3 helicase, NS5B and 3' NTR. In a complementary experiment it was shown that introduction of the JFH-1 NS3 helicase, NS5B and 3' NTR sequences could rescue the replication of a (non-JFH-1) genotype 2a replicon. These regions were also investigated in full length infectious systems. It was found that a J6 backbone (which cannot replicate alone) containing the NS3 helicase, NS5B and 3' NTR sequences from JFH-1 was able to replicate and produce infectious virus, although infectivity was about 100 times less than JFH-1 wild type. Chimaeric viruses based on a JFH-1 backbone could replicate with minimal introduction of J6 sequence, for example the chimaera with only J6 3' NTR replicated at levels approaching wild type JFH-1, but when the NS3 helicase, NS5B and 3' NTR sequences from J6 were introduced into the JFH-1 backbone, there was no replication observed.

A separate study was conducted into the importance of non-structural regions in the replication of HCV RNA using intergenotypic chimaeric subgenomic replicons[356]. This study investigated the effect of exchanging genotype 2a JFH-1 sequence for genotype 1b Con1 sequence, with emphasis on the NTRs, helicase, NS5A and NS5B. Several of the various combinations of these sequences replicated, but to levels lower than the wild type JFH-1 replicon. One chimaera which replicated almost to JFH-1 levels, although with slower kinetics, was the construct containing the NTRs, helicase, NS5A and NS5B from JFH-1 and other sequences from Con1. This study was more focused on the interactions between the NTRs and proteins, but provided evidence for genotype specific interactions between the NS3 helicase, NS5A and NS5B.

Natural chimaeras are rare but have been observed. For example a 2k/1b chimaera exists in Europe, and has the recombination site in NS2[357]. A 2b/1b chimaera has been reported in the Philippines[358], and a 2k/5a in France[359], both of which have the recombination site in NS2. A 1a/1b chimaera identified in South America has the recombination site in NS5B[360].

1.16 Mutation in the HCV Genome

The heterogeneity of the HCV genome is an important feature of its strategy for survival and has an important bearing on the scientific study of the virus.

The HCV polymerase is typical of RNA dependent RNA polymerases in that it has a relatively high error rate in replication of RNA (compared to DNA polymerases). A major contributing factor to the error rate is that the HCV polymerase lacks the ability to proofread the replicated strand by 5' to 3' exonuclease activity[361]. Estimates of the *in vivo* nucleotide mutation rate are around 1.4-1.9 x 10^{-3} substitutions per nucleotide per year, based on work performed in chimpanzees and humans[362-363]. Other estimates have suggested that there is roughly one mutation per replication of the genome. Of the mutations which occur, within the protein coding region some will be synonymous and have no effect, some will be non-synonymous but have no great effect on replication and some will have an effect on replication, although these will mostly be detrimental. The non-coding regions of the genome are much less permissive to mutation, and the mutations which occur here will largely result in defective genomes. Over the six major genotypes of HCV, nucleotide sequences can differ by 30%, and even within some genotypes there can be differences of up to 25%. The 5' NTR has 90% sequence conservation across all genotypes, and the capsid is also well conserved. The region of the HCV genome coding for the envelope proteins includes two regions of high diversity called Hyper Variable Regions (HVR) 1 and 2. HVR-1 is located at the amino terminus of the E2 protein, and can have 50% sequence diversity in different patients. This is thought to be part of a viral strategy to avoid detection by the host adaptive immune system by constantly changing the epitopes presented. Evidence for the importance of the HVR-1 in the humoral immune response is limited, and other regions may be just as important for development of immune responses[261,364]. A phylogenetic study of HCV failed to find an association between viral persistence in patients and specific mutations in E1 and E2[365]. Another key region of sequence diversity is the interferon sensitivity determining region (ISDR) located in NS5A. This region has been noted to mutate in patients as well as cell culture, and amino acid mutations have been observed to affect the ability of patients with HCV genotypes 1 and 2 to respond to interferon therapy[171,366-368]. Sequence diversity occurs more generally across the non-structural proteins and this may have an effect on the variable pathologies of different HCV genotypes, activities of their proteins, and their ability to replicate in cell culture (as discussed in section 1.15 on the study of artificial chimaeric HCV constructs). The NS3 coding region shares 70% nucleotide sequence identity and 80% amino acid identity across all genotypes (Figure 9A-C). The helicase domain has less homology between genotypes than the

protease domain (Figure 9D-E) and genotype 2a has the lowest score when compared to the other genotypes, indicating that it has more unique sequence.

A	1a	1b	2a	3	4	5	6
1a				Nucleotide Identity NS3 Full Length			
1b	79						
2a	69	69					
3	69	70	68				
4	73	74	69	70			
5	72	72	69	69	72		
6	73	70	69	69	72	71	

B	1a	1b	2a	3	4	5	6
1a				Amino Acid Identity NS3 Full Length			
1b	92						
2a	80	80					
3	81	82	80				
4	85	87	78	81			
5	84	84	79	81	82		
6	86	86	80	81	84	84	

C	1a	1b	2a	3	4	5	6
1a				Amino Acid Similarity NS3 Full Length			
1b	97						
2a	88	88					
3	89	90	89				
4	92	93	87	88			
5	92	92	88	89	90		
6	92	92	88	89	90	91	

D	1a	1b	2a	3	4	5	6
1a				Amino Acid Identity NS3 Protease			
1b	88						
2a	70	69					
3	76	77	71				
4	81	83	71	75			
5	80	79	71	76	79		
6	83	83	74	79	82	82	

E	1a	1b	2a	3	4	5	6
1a				Amino Acid Identity NS3 Helicase			
1b	94						
2a	83	84					
3	83	84	83				
4	87	88	81	83			
5	86	86	82	83	84		
6	87	87	83	82	85	85	

Figure 9: NS3 sequence similarity between different HCV genotypes.

Example sequences from each HCV genotype were selected and compared for similarity. Sequences compared were: genotype 1a HCV isolate H77 (accession number AF011753); genotype 1b Con1 (AJ238799); genotype 2a JFH-1 (AB047639); genotype 3a 452 (DQ437509); genotype 4a ED43 (NC_009825); genotype 5a SA13 (AF064490); genotype 6a EUHK2 (Y12083).

The ability to study HCV in the laboratory has been linked to specific details of the HCV sequence. The replication in cell culture of the majority of replicon models has depended on specific amino acid mutations. However the HCV isolate consensus sequences do not usually replicate efficiently in cell culture, and the ability to replicate efficiently is conferred by the presence of cell culture adaptive mutations. Sequence analysis of one of the first replicons, the genotype 1b subgenomic replicon I_{377}/NS3-3'[131], showed several mutations were selected in NS5A, each of which enhanced the transduction efficiency of the replicon when engineered into the replicon RNA[130]. A particular mutation was seen to arise on multiple occasions in separate replicon cell clones, where the serine residue at amino acid position 1179 of the subgenomic HCV polyprotein in the original replicon was mutated into an isoleucine in the adapted replicon (S1179I). It has become common practice to use replicons bearing cell culture adaptive mutations for the study of HCV. Studies of replicons in cell culture, particularly genotype 1b, have yielded a number of potential cell culture adaptive mutations, some of which are described in Figure 10[86,350]. Most mutations found prove not to

endow a replicative advantage when deliberately recloned[349]. Some mutations, such as S1179I (described as S2204I in Figure 10), have been shown to give a strong replicative advantage, and some mutations have been shown to confer weak replicative advantages. A few mutations have been shown to work together in producing additive effects (such as E1202G, T1280I and S2197P increasing the number of colony forming units per microgram of replicon RNA used to transfect Huh7 cells[349]).

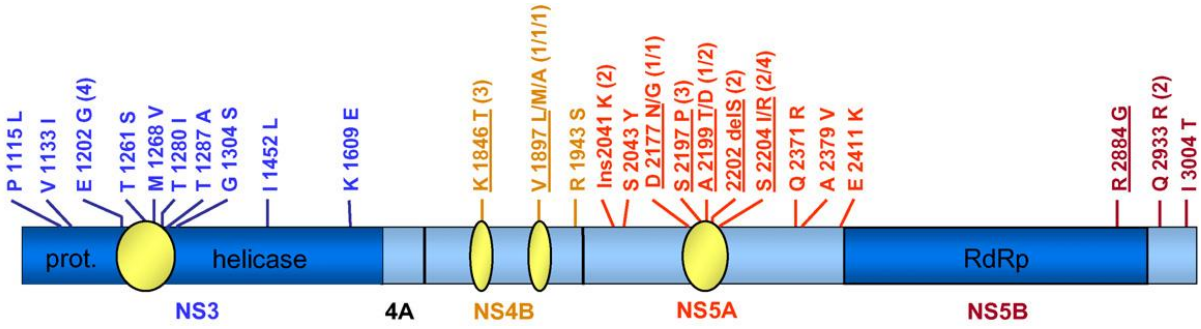


Figure 10: Mutations observed in replicon cell clones[86].

The conserved mutations in Con1 replicons isolated from 26 independently selected cell clones[350] are shown on a schematic representation of the HCV non-structural proteins from NS3 to NS5B. Amino acid positions given refer to the Con1 polyprotein (AJ238799). Numbers in parenthesis indicate the frequency with which a given mutation was found in independent replicon cell clones. Mutations identified as the only conserved alteration in at least one cell clone are underlined. The circles illustrate clusters of adaptive mutations.

It has been shown that some mutations that are beneficial to the replicative ability of the virus in cell culture can be detrimental *in vivo*. Intra-hepatic transfections of chimpanzees with a cell culture adapted Con1 genome carrying the mutations E1202G, T1280I and S2197P[349] did not result in the production of infectious virus, whereas the wild-type Con1 did produce infectious virus[369].

1.17 Cell Lines Capable of Supporting Replication of Infectious HCV

The viral sequence is not the only determinant involved in achieving *in vitro* HCV RNA replication or virus production. The search for appropriate host cells has been as difficult as that of finding replicative HCV isolates. The cell line shown to achieve the highest levels of HCV replication is the hepatocellular carcinoma line Huh7 and its derivatives. This cell line has supported all isolates so far

found to replicate *in vitro*. A few other cell lines have also been shown to support replication of some HCV isolates, such as the hepatoma lines HuH6 (supporting Con1 and JFH-1[370]), HepG2 (JFH-1[371]) and IMY-N9 (JFH-1[371]). The cervical carcinoma line HeLa (Con1, JFH-1[372-373]) and the embryonic kidney line 293 (Con1, JFH-1[372]), as well as the mouse lines MEF[374] and Hepa1-6[373], have shown some ability to support HCV RNA replication. Huh7 cells were isolated from a 57 year old Japanese male patient with liver cancer in 1982. These cells support HCV replication, and there has also been the development of cell lines, derived from Huh7, with enhanced capacity for HCV replication. Many of these have been achieved by selecting for cells which host efficiently replicating HCV replicons. It was found that Huh7 cells which had hosted HCV replicons, and were cured of their replicons, subsequently often became more permissive to HCV replication. These cells include the lines Huh7.5 and Huh7.5.1. To generate Huh7.5 cells[375], interferon cured replicon cells were separated by limiting dilution in order to obtain clonal lines, before their ability to support HCV RNA replicon replication was assessed. This study discovered a line, Huh7.5, which supported higher levels of RNA replication than the parental Huh7 cell line. Other cured cell lines have been generated, from Huh7 cell lines hosting different replicons, and by using interferon or other anti-virals. It has not always been possible to identify the properties of the cured cells that make them more permissive to HCV replication. In the case of Huh7.5 cells, a mutation was identified in a gene called RIG-I (retinoic acid inducible gene I)[318]. This gene was known to be involved in immune regulation, and was later found to be a sensor for double-stranded RNA and 5' triphosphates on RNA[152-153]. The detection of these patterns by RIG-I initiates an interferon response, signalled through a protein called MAVS (mitochondrial antiviral signalling protein, also known as IPS-1, VISA and Cardif). MAVS is associated with membranes near the mitochondria and, in response to signals from the RIG-I and Mda5 proteins, will induce an interferon response via IRF7[149-150,315].

There may be additional determinants which contribute to the ability of Huh7 cells to support HCV replication. For example, Huh7 cells do not express toll-like receptor 3 (TLR3)[376] that initiates an immune response upon sensing double-stranded RNA. The Huh7 cell line is a hepatocellular carcinoma line, and certain properties of these differentiated cells may contribute to their ability to support HCV replication. This is not simply a product of the fact that Huh7 is a cancer line, as most of the cell lines so far tested for the ability to support HCV replication were cancer lines. It may be properties specific to the Huh7 cancer. Studies involving HCV have tended to be performed in Huh7.5 cells since their discovery, rather than Huh7 cells. This is because of the higher levels of RNA replication that can be attained in Huh7.5 cells. A study has compared several clonal lines of Huh7 cells from different sources, and Huh7.5 cells[377]. Similar HCV replication kinetics were demonstrated

in Huh7 and Huh7.5 cell lines. Both cell types could therefore be viable options for performing gene expression analyses, and results from different studies may be compared.

Cell culture is a very useful model for studying human disease but there are limitations to this model. The cells used here are cultured cancer cells in culture not primary hepatocytes. This means that the cells have already undergone changes in order to make them immortal. In addition, these cells have been cultured since isolation from the donor (in the cases of Huh7, since 1982) during which time other phenotypic alterations may have occurred to alter them from the normal state of primary hepatocytes. In the JFH-1 culture model of HCV, all cells can be infected whereas only a proportion (maybe 10%) of hepatocytes in a liver will be infected, and hepatocytes themselves are only part of the cell population of the liver. A higher intracellular titre of HCV RNA can be achieved in cell culture than in the liver. There will be fewer quasispecies in culture, where there is less time for them to develop (days rather than years). If mutations do arise in HCV during cell culture this may be advantageous to the study of the virus. Any cell culture adaptive mutations which allow for a higher titre virus will aid the study of HCV. This situation is already apparent from the work on subgenomic replicons, where all replicons used in cell culture now have adaptive mutations to allow more efficient replication. This has become a standard model. There is also less of a selection pressure on HCV in culture as there are no antibodies, and Huh7 cells have impairments to their innate immune responses. There is also a more homogenous cell population (i.e. all hepatocytes, no other cells such as white blood cells). This will lead to different intercellular signalling so some gene inductions may be different.

There are clear advantages to using a cell culture model however. It is possible to perform destructive tests where samples cannot be recovered, and which are not harmful to a patient. It is possible to perform larger numbers of multiple tests, with more samples, and these can be controlled much more easily than is possible in tests using clinical samples.

1.18 HCV and Host Cell Gene Expression

The investigation of host cell gene expression changes due to the presence of HCV has so far been performed in models using replicons, and by expression of individual HCV proteins. These studies have identified gene expression changes in the host cell in both cases; during HCV RNA replication, and due to the presence of HCV proteins. Gene expression has also been investigated in chimpanzees infected with HCV.

Microarray analyses of gene expression in acutely and chronically infected chimpanzees have been performed. HCV infection of chimpanzees is more likely to be an acute infection than in humans, as greater than 60% of inoculated animals will clear the virus[330,378]. The first microarray studies performed on chimpanzees were therefore performed on animals with acute infections. Bigger *et al*[379] infected an individual chimpanzee with genotype 1a HCV, which experienced loss of viraemia at 8 weeks and clearance of viral RNA from the liver at 14 weeks post infection. Microarray analyses were performed on RNA from liver biopsies taken at 2 and 7 days post infection and 2, 4, 6, 8, and 12 weeks post infection. Changes in gene expression were made in comparison to day 0, before HCV infection. 327 genes were observed to change by a fold change of ≥3.5, with 162 of these at more than one timepoint. Expression levels of interferon response genes were observed to have changed, as well as cytokines and growth factors, genes involved in cell regulation and replication, and immune cell markers. Genes involved in other aspects of HCV infection were also onserved to change in expression levels. These genes included adipophilin (involved in steatosis), IFI44 (also known as HCV-associated microtubule aggregate protein), and Mac-2BP (a possible marker for IFN-α unresponsiveness). Su *et al*[380] performed a study using three chimpanzees, all infected genotype 1a HCV, but from different sources. One animal achieved sustained clearance, one was persistently infected but initially transiently cleared, and one was persistently infected. Gene expression changes were measured from liver biopsy RNA. All chimpanzees showed expression changes in IFN-α response genes, but only the animals which cleared the virus showed an induction of IFN-γ induced genes. Genes involved in lipid metabolism were also observed to be regulated in the animals which cleared the virus. These included PPARα, hepatic lipase C, UDP-glucose ceramide glucosyltransferase, and SREBP pathways related genes. A study looking at gene expression 10 persistently infected chimpanzees was performed by Bigger *et al*[329]. One animal was infected with HCV genotype 3a, three with genotype 1b and six with genotype 1a. The animals had been infected for between 7 and 20 years, and had varying levels of viraemia. Gene expression was compared to six controls, from four uninfected animals and two pools of uninfected material. Up to 971 genes were observed to be altered in expression level in infected chimpanzees compared to uninfected

animals. As in the previous studies of acutely infected animals, these chronically infected chimpanzees were shown to have many interferon stimulated genes transcriptionally elevated. Expression changes of several ISGs were confirmed by quantitative PCR. Other genes observed to change in expression included those involved in modulation of immune cell activity, cytokines and chemokines, MHC-related components, and lipid metabolism.

Studies performed using replicon models have shown expression changes in genes involved in biological processes including lipid metabolism, immunity, cell proliferation and apoptosis, and intracellular transport. Several studies have utilised subgenomic replicon models to identify gene expression changes that occur during HCV RNA replication. Abe *et al* compared gene expression in Huh7 cells harbouring genotype 1b subgenomic replicons with expression in their interferon-cured counterparts[381]. This study used microarrays containing probes to around 10,000 genes to identify 8 genes commonly regulated in the replicon cell lines. In total, 101 and175 genes were regulated in the two different replicon lines tested, with 12 and 24 genes being regulated by more than three fold. Commonly regulated genes included the upregulated genes phosphatidylserine-specific phospholipase A1α and oncostatin M receptor, and the downregulated genes large multifunctional protease 2, large multifunctional protease 7, and serine proteinase inhibitor clade C. Nishimura-Sakuri *et al* compared gene expression in genotype 1b and genotype 2a subgenomic replicons with their interferon cured counterparts, and with their parental line of naive Huh7 cells[382]. This study used whole genome microarrays to identify 372 probe sets which were regulated by more than 1.2 fold in replicon cells compared to cured cells, of which 15 changed by more than two fold. This study also showed altered gene expression in cured cells compared to parental naive Huh7 cells. Steroid biosynthesis, MAPK signalling and TGF-β signalling processes were identified as altered in replicon cells compared to cured cells. Steroid biosynthesis, sphingolipid biosynthesis and TGF-β signalling processes were identified as altered in cured cells compared to naive cells. This study emphasised the role that alterations in lipid metabolism including cholesterol and sphingolipid biosynthesis may be important for HCV replication. Agonists of peroxisome proliferator activated receptor alpha (PPARα) were shown to suppress HCV replication and agonists of PPARγ augmented HCV replication, suggesting HCV replication was affected by the production of fatty acids. Expression studies have also been undertaken which focused on specific groups of genes. Fillebeen *et al* used a microarray targeted to iron metabolism genes[383]. This study identified expression changes which resulted in reduced iron uptake and increased iron release capacity. Several genes were observed to be altered in expression in replicon cells compared to Huh7 cells, including upregulation of ceruloplasmin and ferroportin and downregulation of transferrin. As NS5B has

previously been shown to be inactivated by iron[384], these gene expression changes were hypothesised as possibly providing a mechanism to avoid NS5B inactivation by iron. Curing replicon cells with interferon partially reversed the iron-deficient phenotype and restored the ability of cells to retain iron. Itsui *et al* performed a study focused on interferon stimulated genes (ISGs)[385]. 17 ISGs were identified as being downregulated in replicon cells compared to naive Huh7 cells, and when overexpressed in replicon cells, eight of these ISGs had inhibitory effects on HCV replication.

As well as using subgenomic replicons, some groups have made use of full length replicons to perform expression studies. This allows for gene expression changes induced by the complete range of HCV proteins, however, there is still no entry or exit of infectious virus, and there are the additional genetic elements of the replicon present in these systems. Ciccaglione *et al* compared gene expression in two cell lines harbouring a full length genotype 1b replicon with naive parental Huh7 cells and cured replicon cells[386]. This study used whole genome microarrays to identify 38 genes commonly regulated in all comparisons of replicon clones versus naive or cured cells. In each individual comparison, between 534 and 654 genes were seen to be regulated by presence of the replicon. Genes involved in biological processes including lipid metabolism, the extracellular matrix, cytoskeleton, histones, ribosomal proteins, and intracellular transport were observed to be regulated by presence of the HCV replicon. Scholle *et al* used whole genome microarrays to identify changes in gene expression between cells harbouring a full length genotype 1b replicon with cured cells[387]. This study identified 57 genes regulated by more than two fold by one replicon clone. This study showed HCV genome replication to be dependent on cellular proliferation, and that replication was enhanced in the S phase of the cell cycle. However, this study did not identify a significant alteration of the cell cycle by presence of the replicon at times up to 24 hours after release from the cell cycle block. Cao *et al* used microarray analysis to identify arginase 1 as being elevated in HepG2 cells harbouring a full length replicon[388]. A three fold increase in expression was observed in cell culture. The expression of arginase 1 was observed to be elevated in 75% of HCV patients (compared to patients with hepatocellular carcinoma). This study observed that the presence of the replicon induced growth of HepG2 cells (but not Huh7 cells). Inhibition of arginase 1 by siRNA inhibited the ability of the replicon to induce growth, and also increased nitric oxide synthase, nitric oxide and cell death. It was hypothesised that HCV regulation of cell growth and survival could occur through altering arginine metabolism.

The influence of individual HCV proteins on host gene expression has also been investigated by some groups. Whilst these studies do not involve any HCV RNA replication, the proteins are effectors of

changes in the host cell. These studies have used a variety of protein delivery methods and cell lines. Vandermeeren *et al* expressed the full polyprotein from a vaccinia virus vector in HeLa cells[389]. After 6 hours morphological changes were observed in the ER, Golgi and mitochondria, and gene expression changes were observed. Microarray analysis of around 20,000 genes identified 231 genes regulated at 6 hours and 81 genes regulated at 16 hours after induction of polyprotein expression. This study identified genes involved in apoptosis, oxidative stress, mitochondrial functions, lipid metabolism, cell cycle, signalling and immune responses to be regulated during polyprotein expression. Budhu *et al* used adenoviral vectors to express core, NS3 and NS5A, separately and in combination, in primary human hepatocytes[390]. Using microarray profiling of around 22,000 genes, these HCV proteins were found to induce expression changes in genes involved in cell regulation, transcription, immune response transport and metabolism. This study also compared expression levels in HCV infected patients liver with samples from chronic liver disease patients, and highlighted the upregulation of interferon inducible gene 27 in HCV liver and in cells expressing HCV core protein. Dou *et al* used plasmid expression vectors to deliver core protein of genotypes 1b, 2a and 4d into HepG2 cells[391]. This study identified 264 genes associated with expression of the genotype 1b core, 172 with 2a, and 285 with 4d. There was some overlap in the genes observed to be expressed in the presence of the different genotypes, but most genes were unique to each genotype. However, the biological processes these genes were involved in were common to all genotypes. This study identified that expression of HCV core protein regulated expression of genes involved in transport, signal transduction, transcription regulation, protease activity and both pro- and anti-apoptotic functions. Another study performed by Dou *et al* used whole genome microarrays to compare the expression profiles induced by genotype 1b core protein and core shadow protein (the core protein equivalent translated from the alternative reading frame) in Huh7 cells[392]. This study identified that the core shadow protein could also influence the expression of genes involved in both pro- and anti-apoptotic mechanisms. Aizaki *et al* used cDNA expression vectors to express full and partial HCV polyproteins in HepG2 cells[393]. Microarray analysis of the cell line expressing full length polyprotein identified 16 genes to be regulated compared with control. These included genes involved in cell growth regulation and major histocompatibility complex (MHC) regulation. Basu *et al* used a plasmid expression vector to introduce genotype 1a core protein into primary hepatocytes[394]. Using whole genome microarrays, 1918 transcripts were identified as being differentially expressed by more than two fold in cells with core. This study focused on the increase in genes involved in Stat3 signalling (IL-6, gp130, leptin receptor, stat3). Presence of core was also found to regulate genes involved in biological processes including cellular growth, immune regulation, oxidative stress and apoptosis.

Some gene expression studies have been performed using liver material from HCV infected patients. Hagist *et al* focused on the role of iron and oxidative stress in liver disease[395]. This study used a combination of microarray data from HepG2 cells challenged with iron and oxidative stress, and microarray data from HCV patient liver. One gene (natriuretic peptide precursor B) was observed to be regulated in HepG2 challenged with iron, in HCV patient liver but not in patients with severe iron deposition. A small number of genes involved in oxidative stress, iron metabolism, RNA processing and cell proliferation were also observed to be regulated in HCV patients. Smith *et al* used microarrays to compare expression levels of around 13,600 genes between HCV infected cirrhotic liver material and control normal liver material[396]. This study excluded cancer related genes and identified 132 annotated genes to be regulated in at least 5 of their 7 experiments. These genes were categorised into functions including genes expressed in activated lymphocytes and macrophages, extracellular matrix and cell-cell interactions, cytoskeleton, Bcl-2 anti-apoptotic pathway, oxidative stress, and anti-viral immune response. Other studies using HCV infected liver have focused on specific functions. A study performed by Walters *et al* in HCV infected patients observed a subset of patients where there was a decrease in genes involved in the FAS-apoptotic pathway, and impaired interferon responses, which was similar to gene expression patterns in patients who develop fibrosis soon after liver transplant[397]. Helbig *et al* used whole genome microarray analysis to compare gene expression HCV infected liver with normal liver[398]. This was performed using both human and chimpanzee liver samples. This study found that CXCR3 family cytokines were elevated in expression, including CXCL10 and CCXCL11. CXCL10 was also observed to be elevated in serum. CXCL11 was observed to increase in response to IFNγ and TNFα in cell culture using JFH-1, but this feature was also observed using dsRNA, indicating that this is a general response, and not specific to HCV.

The fact that these observations have been made in previous studies is a good indication that it is worth pursuing the investigation of host cell gene expression changes during HCV infection. These studies have provided important information on host gene expression during HCV RNA replication, and the interaction between HCV and the cell. However, the use of infectious virus in a gene expression study would induce a more biologically relevant change in the host cells. Areas of potential significance include genes involved in RNA replication, immune responses, lipid metabolism, oxidative stress, apoptosis and cellular proliferation. The use of infectious virus would mean that the processes of entry, assembly and exit were affecting the cell. The proper interactions of all HCV proteins with each other, and with host cell proteins, will also be allowed to take place. Thus, the use of the infectious JFH-1 HCV in a whole genome expression study could yield useful and novel information about the state of HCV infected cells.

1.19 Aims and Hypotheses

The genotype 2a HCV isolate JFH-1is the only isolate discovered to replicate efficiently in cell culture. It is predicted that this quality is due to specific sequence determinants unique to JFH-1. It has been shown that the structural regions of JFH-1 can be exchanged for those of other genotypes, and still replicate in cell culture. This implies that the viral determinants for the ability of JFH-1 to replicate in cell culture lie in the non-structural region of the genome. This work will focus on the NS3 region, as this is a multifunctional protein with vital roles in RNA replication as a helicase, in polyprotein processing as a protease and in interactions with cellular proteins as a protease. The hypothesis that genotype specific NS3 sequence determinants are required for efficient HCV replication in cell culture will be tested by creating chimaeric JFH-1 genomes containing genetic sequence from other HCV genotypes, and assessing the replication capacity of these chimaeras in cell culture.
Hypothesis: The NS3 coding regions contain genotype specific sequence determinants that allow JFH-1 to replicate efficiently in cell culture.

The host cell has been found to be crucial in the efficient replication of HCV in cell culture. It is predicted that HCV infection will induce expression changes in the host genes involved in processes related to HCV replication. These are predicted to include genes involved in the regulation of the biological processes required for the HCV lifecycle. Genes involved in lipid metabolism are predicted to change in expression as the virus alters cell membranes and lipid droplets. Genes involved in cell cycle including proliferation and death are predicted to change as the virus replicates and the cell responds to its presence. Genes related to oxidative and ER stresses are predicted to change as the virus replicates. It is also predicted that innate immune genes involved in the host's response to infection with HCV will be altered in expression levels. These predictions will be tested by application of whole genome expression analysis of HCV JFH-1 infected cells using microarray technology.
Hypothesis: HCV infection will alter the host gene expression patterns, including those of processes directly related to the replication of HCV and the host response to infection.

It is predicted that, of the host genes identified to be regulated in expression level during HCV infection, some host genes will be required for the replication of HCV. Selected genes, identified as being upregulated during HCV infection, will be inhibited prior to infection of cells with HCV to determine whether these genes are required for HCV replication.
Hypothesis: Genes upregulated in expression levels during HCV infection are required for efficient HCV replication.

Methods

2.1 Cell Culture

Huh7 and Huh7.5 cells were grown in Dulbecco's modified Eagles Medium (DMEM) supplemented with 10% foetal bovine serum (FBS), 100U/ml penicillin and 100µg/ml streptomycin at 37°C with a 5% CO_2 atmosphere. All cell culture reagents were purchased from Invitrogen. Cell lines containing selectable sub-genomic HCV replicons (Rep4 and Rep4.5) were grown as for Huh7 cells, but in medium supplemented with 500µg/ml geneticin. Cells were passaged by trypsinisation. Huh7.5 cells were obtained from Charles Rice.

2.2 HCV Constructs

The infectious clone JFH-1, replication deficient mutant JFH-1 GND, and envelope protein deletion mutant JFH-1 deE1E2 were obtained in their plasmid vectors from Takaji Wakita. Jc1p7FLuc2A was created by Shihyun You using Jc1p7GLuc2A from Charles Rice. Genotype 1b subgenomic replicon S1179I, also known as BB7, was obtained from Charles Rice. Replicon cell line 15.53 contains a genotype 2a subgenomic replicon created by Cindy Richards at GlaxoSmithKline (GSK).

2.3 JFH-1 Infectious Virus Cell Culture System

2.3.1 Plasmid Preparation

Plasmid pJFH-1 was produced by transformation of Library Efficiency *E. coli* DH5α (Invitrogen) according to manufacturer's instructions. 10ng of JFH-1 plasmid DNA was mixed with 50µl of *E. coli* and incubated on ice for 30 minutes. Bacteria were heat shocked at 42°C for 40 seconds and incubated on ice for two minutes. 450µl SOC medium was added and the bacteria were shaken at 200rpm for one hour at 37°C. 200µl of the transformation mix was plated onto Luria Bertani (LB) agar containing 100µg/ml ampicillin and incubated overnight at 37°C. The following day, transformed bacterial colonies were picked and grown overnight at 37°C in 5ml LB medium containing 100µg/ml ampicillin. pJFH-1 DNA was prepared from the transformed DH5α cultures using the Plasmid Mini Kit (Qiagen) according to the manufacturer's instructions.

For larger scale plasmid preparations, 5µl of pJFH-1 DH5α glycerol stock was used to seed 5ml of LB medium containing 100µg/ml ampicillin and grown for 8 hours at 37°C with shaking at 200rpm. 50µl of the 5ml culture was used to seed 50ml of LB medium containing 100µg/ml ampicillin and grown overnight at 37°C with shaking at 200rpm. pJFH-1 DNA was prepared from the 50ml cultures using the HiSpeed Plasmid Midi Kit (Qiagen) according to the manufacturer's instructions.

2.3.2 *In Vitro* RNA Transcription

20µg of pJFH-1 was linearised with 150 units of 100U/µl restriction enzyme XbaI (NEB) and 5µl 10x NEBuffer 2 (NEB) in a final volume of 50µl, which was incubated at 37°C for 2 hours. The linearised DNA was purified by phenol-chloroform extraction and ethanol precipitation. The 50µl restriction digestion was made upto 200µl with tris-EDTA (1mM Tris-Cl, 1mM EDTA, pH8.0). An equal volume of phenol-chloroform (25:24:1 phenol:chloroform:isoamyl alcohol, Sigma) was added, the mixture shaken vigorously, and then centrifuged at 16,000g for 15 minutes. The upper, aqueous phase was transferred to a new 1.5ml eppendorf tube, and an equal volume of chloroform was added. Samples were shaken, and then centrifuged at 14,000g for 5 minutes. The upper, aqueous phase was transferred to a new 1.5ml eppendorf tube, where 0.1 volume 3M sodium acetate and 2.5 volumes of ethanol were added, and incubated overnight at -20°C. DNA was pelleted by centrifugation at 14,000g for 20 minutes at 4°C, and the supernatant removed. The pellet was washed by adding 0.5ml 75% ethanol and centrifuging at 14,000g. After air-drying, the pellet was resuspended in 45µl nuclease-free water. 3' overhanging DNA was removed by digestion with 30 units Mung Bean Nuclease (NEB) for 30 minutes at 30°C. The digestion mix was treated with 0.5% SDS and 40µg Proteinase K (Invitrogen) in a final volume of 200µl for 1 hour at 50°C. The DNA was purified by phenol-chloroform extraction and ethanol precipitation as before, and the DNA pellet resuspended in 20µl nuclease-free water. JFH-1 RNA transcripts were generated from pJFH-1 using the T7 MEGAscript *In Vitro* RNA Transcription kit (Ambion). RNA transcription was performed using 1µg of linearised plasmid DNA and T7 MEGAscript *In Vitro* RNA Transcription reactions were incubated at 37°C for 6 hours. 1µl DNase was added and incubated at 37°C for 15 minutes. 15µl stop solution was added, and water was added to a final volume of 250µl. 750µl Trizol LS (Invitrogen) was added, and JFH-1 RNA transcripts were purified according to the Trizol LS manufacturer's instructions. RNA was finally resuspended in 20µl nuclease-free water.

2.3.3 RNA Transfection of Huh7.5 Cells

The JFH-1 RNA transcript was transfected into Huh7.5 cells using Lipofectamine 2000 (Invitrogen). Huh7.5 cells were seeded at a density of $6x10^5$ in a 6-well plate. The following day, with cells at 80% confluency, growth medium was replaced with OptiMEM medium (Invitrogen) and the cells were incubated for four hours. 5µg JFH-1 RNA and 10µl Lipofectamine 2000 were each diluted in 500µl of OptiMEM and incubated at room temperature for 20 minutes. The dilutions were then mixed, and incubated at room temperature for 20 minutes. The growth medium was removed from the cells and they were washed with 1ml OptiMEM. The 1ml RNA/Lipofectamine 2000 transfection mixture

was then added to the cells. After an eight hour incubation period, the transfection medium was replaced with 2ml normal growth medium and the cells were incubated overnight. The following day, transfected cells were passaged into a 25cm^2 flask. Transfected cells were then expanded into 75cm^2 flasks for large scale production of JFH-1 infectious virus. 1.5ml of growth medium containing infectious virus was used to infect naive Huh7.5 cells at 50% confluency in 75cm^2 flasks.

2.3.4 Harvest of Infectious JFH-1 Virus

Growth media were collected from 75cm^2 flasks of Huh7.5 cells infected with JFH-1 virus. Pooled media were clarified by centrifugation in a Mistral 3000 Benchtop Centrifuge (MSE) at 1500rpm for 10 minutes, after which the supernatant was filtered through 0.45µm sterile filter units. JFH-1 virus in the filtered medium was concentrated using Amicon Ultra-15 filtration units (Millipore) by centrifugation at 3600 rpm at 4°C for 20 minutes. Retentate containing concentrated JFH-1 virus was collected and stored at -20°C.

2.3.5 Titration of JFH-1 Virus Stocks

Huh7.5 cells were seeded into 8-well chamber slides at a density of 0.8x10^5 to be at 100% confluency for infection. Three 10-fold serial dilutions of the concentrated JFH-1 virus stocks (corresponding to 1µl, 0.1µl and 0.01µl per well) were used to infect the Huh7.5 cells in duplicate. After 36 hours, the chamber slides were stained for HCV core protein and foci were counted using immunofluorescence microscopy. Total numbers of HCV Core-positive foci were counted per well at the appropriate dilution and averaged. Titres of infectious JFH-1 virus in the concentrated stock were calculated as focus forming units per ml (ffu/ml).

2.3.6 Staining for HCV Core Protein

Chamber slides were fixed in 4% paraformaldehyde for 30 minutes. Cells were washed in PBS for 10 minutes and permeabilised in 0.1% Triton X-100 for 20 minutes. The anti-core antibody, mouse monoclonal C7-50 (Abcam), was diluted 1 in 400 in 1% BSA in PBS. 20µl of diluted C7-50 was applied to each well and incubated for one hour in a humidity chamber. Chamber slides were washed in PBS times in PBS for five minutes each wash. Fluorescent secondary antibody, AlexaFluor 594 conjugated donkey anti-mouse polyclonal (Invitrogen), was diluted 1 in 1000 in 1% BSA in PBS. 20µl of the diluted secondary antibody was applied to each well and incubated for one hour in a humidity chamber. Chamber slides were again washed three times with PBS, and briefly rinsed once with water to remove salts. The slides were mounted using 10µl per chamber of Mowiol mounting medium, containing the nuclear stain DAPI. Fluorescent staining was observed using the Zeiss Axiovert 200M fluorescent microscope, and Axiovision 4.6 software for image acquisition.

2.3.7 JFH-1 Virus Production by Media Passage

Huh7.5 cells were seeded to be 25% confluent in 75cm^2 cell culture flasks. The cells were infected with JFH-1 virus at a multiplicity of infection (MOI) of 0.1. Infected Huh7.5 cells were incubated for four days and the growth medium was collected and clarified. Huh7.5 cells were also seeded in 75cm^2 flasks, were each infected with 1.5ml of clarified medium containing JFH-1 virus. The remaining clarified medium was concentrated, as described, and stored at -20°C. Infectious clarified medium was serially passaged onto naive Huh7.5 cells every four days to provide a supply of high titre JFH-1 stocks.

The growth media from flasks of uninfected Huh7.5 cells were also collected and treated by the same method to generate mock medium for mock infected controls in infection experiments.

2.4 Jc1 Infectious Virus Production

2.4.1 Plasmid Preparation

Plasmid pJc1p7FLuc2A was produced as pJFH-1. All work using Jc1p7FLuc2A was performed at the GSK laboratories, NC, USA.

2.4.2 *In Vitro* RNA Transcription

10µg of pJc1p7FLuc2A was linearised with 100 units of restriction enzyme XbaI (NEB) and purified using the PCR MinElute Clean-Up kit (Qiagen). Jc1 RNA transcripts were generated from pJc1p7FLuc2A using the T7 RiboMax Express kit (Promega). RNA transcription was performed using 2µg of linearised plasmid DNA and reactions were incubated at 37°C for one hour. The transcription reaction was treated with DNA-free Turbo DNAse (Ambion) to remove the remaining linearised pJc1p7FLuc2A DNA. Jc1 RNA transcripts were purified using the RNeasy kit (Qiagen), and eluted in 80µl nuclease-free water.

2.4.3 RNA Electroporation of Huh7.5 Cells

10µg Jc1 RNA transcript was mixed with 1 x 10^7 Huh7.5 cells suspended in 0.8ml PBS, in a 4mm gap electroporation cuvette. Gene Pulser Xcell (Bio-Rad) electroporation equipment was set to deliver a pulse with voltage of 270V and capacitance at 975µF. The electroporated cells were left to stand for 5 minutes and then transferred into a 225cm^2 flask containing growth medium. The following day, growth medium was replaced. On the second day post-electroporation the Huh7.5 cells were split into two 225cm^2 flasks.

2.4.4 Harvest of Infectious Jc1 Virus

Growth media containing infectious Jc1 virus from 225cm^2 flasks of Jc1 RNA electroporated Huh7.5 cells were collected every day for five days after electroporation and pooled.

2.4.5 Titration of JFH-1 Virus Stocks (TCID50)

Huh7.5 cells were seeded in a 96-well plate at a density of 8 x 10^3. Two separate 10-fold serial dilutions (from 10^{-1} to 10^{-5}) of the Jc1 virus stock were prepared and added to the wells, with eight replicates per dilution. Infected cells were incubated for 72 hours, at which time the cell culture medium was removed and replaced with 25µl of SteadyGlo Luciferase reagent (Promega). After 10 minutes incubation shaking at room temperature in the dark, luciferase activity was measured. Wells were scored as positive or negative for luciferase activity and TCID50 was calculated.

2.5 Microarray Studies

2.5.1 Titration Assay

Cells were seeded at a density of 0.5 x 10^5 in 24-well plates, and infected with JFH-1 virus at MOIs from 0.01 to 3. After 48 hours incubation, total intracellular RNA was extracted and JFH-1 RNA levels were quantified using quantitative real-time PCR. Cells were also seeded at a density of 0.5x10^5 on glass coverslips placed into 24-well plates. These cells were infected with JFH-1 virus at MOIs ranging from 0.01 to 3, incubated for forty-eight hours and then stained for HCV core protein. The percentage of cells infected with JFH-1 was estimated by counting the numbers of cells which stained positively for HCV core protein within a field of view.

2.5.2 Infection of Huh7.5 Cells (Initial Method)

Huh7.5 cells were seeded at a density of 5 x 10^5 cells in 4ml of growth medium in 25cm^2 flasks. The next day, either concentrated JFH-1 stock or mock medium was added to the flasks. Cells were infected at an MOI of 3, and the volume added to each flask was 1ml. Conditions were performed in triplicate. Four hours post-infection, the media were removed from all flasks and cells were washed with PBS at 37°C. 5ml of normal growth medium at 37°C was added to each flask. At the indicated timepoints, media were removed from the flasks of infected and mock infected cells. The cells were washed with PBS at 37°C. 3ml of Trizol (Invitrogen) was added to each flask and incubated for five minutes at room temperature. Trizol-cell lysates were then homogenised by pipetting up and down, and transferred into cryovials for storage at -80°C.

2.5.3 Infection of Huh7.5 (Revised Method)

Huh7.5 cells were seeded at a density of 5 x 10^5 cells in 4ml of growth medium in 25cm^2 flasks. The next day, either concentrated JFH-1 stock or mock medium was added to the flasks. Cells were infected at an MOI of 3, and the volume added to each flask was 1ml. Conditions were performed in triplicate. At the indicated timepoints, media were removed from the flasks of infected and mock infected cells. 3ml of Trizol was added to each flask and incubated for five minutes at room temperature. Trizol-cell lysates were then homogenised by pipetting up and down, and transferred into cryovials for storage at -80°C.

2.5.4 Infection of Huh7 Cells and Addition of Protease or Polymerase Inhibitors

Huh7 cells were seeded at a density of 5 x 10^5 cells in 3.5ml of growth medium in 25cm^2 flasks. The next day, either concentrated JFH-1 stock or mock medium was added to the flasks. Cells were infected at an MOI of 3, and the volume added to each flask was 1ml. At 12 hours post-infection,

NM107 (final concentration of 50µM), BILN2061 (final concentration of 10µM), or DMSO control was added to the flasks in a volume of 0.5ml normal growth medium. Conditions were performed in triplicate. At the indicated timepoints, media were removed from the flasks of infected and mock infected cells. 3ml of Trizol was added to each flask and incubated for five minutes at room temperature. Trizol-cell lysates were then homogenised by pipetting up and down, and transferred into cryovials for storage at -80°C.

2.5.5 RNA Extraction

Extraction of total cell RNA from Trizol-cell lysates, was performed by Expression Analysis (North Carolina, USA). RNA quality was assured to be suitable for microarray analysis by assessment with Agilent Bioanalyzer equipment.

2.5.6 Microarray Data Aquisition

Hybridisation to microarrays and fluorescent data acquisition was performed by Expression Analysis. The GeneChip Human Genome U133 Plus 2.0 array (Affymetrix) was used to obtain expression profiles of all genes in the human genome. One array was used per RNA sample extract.

2.5.7 Microarray Data Processing

Fluorescence data were analysed at GSK (North Carolina, USA) using Array Studio software (OmicSoft). Affymetrix CEL data files were imported into Array Studio using RMA signal extraction. A $\log_2$ transformation was performed on the data prior to analysis. Quality control of the data obtained from the arrays was performed by the principal components analysis and correlation based quality control methods available in Array Studio. For correlation based quality control, arrays with a MADScore of less than -5 were considered outliers. For the Huh7.5 JFH-1 infection study, one array was identified as an outlier and excluded from the study before data analysis. This was a 6 hour timepoint, JFH-1 infected sample. Therefore the 6 hour JFH-1 infected data analysis and comparison with mock infected samples were performed with duplicate infected sample data. For the Huh7 study, two outliers were identified and excluded before further analysis. These were a 0 hour sample, and a 6 hour JFH-1 infected sample. Again, this meant that the data analysis of the 6 hour infected timepoint, and its comparison with mock infected samples were performed with duplicate infected sample data. Data were analysed by two-way analysis of variance (ANOVA) in Array Studio to compare the differences in gene expression between JFH-1 infected and mock infected samples at each timepoint. The cut off criteria applied for identification of genes differentially expressed between infected and mock infected samples were a modulus fold change of

greater than 2 and a p-value of less than 0.05. Fold changes were not considered significant if the average fluorescence levels of compared conditions were both within background fluorescence levels. In the Array Studio analysis this meant that the maximum LSMean (least squares mean – the statistically adjusted average data for a condition group) for probe sets in comparisons had to be greater than 5 on the $\log_2$ scale.

Analysis of biological pathways was performed using Panther and Ingenuity software programs. Panther (http://www.pantherdb.org/)[399-400] was used to identify the biological pathways containing genes regulated during HCV infection. Using the gene expression data analysis tool, the list of genes observed to change by at least 2-fold with JFH-1 infection, were input into the online program. Separate lists were used for each timepoint, and a list compiled of these genes from all timepoints was also used. Panther statistically compared uploaded lists of genes to a reference list (all *H.sapiens* genes in the NCBI reference) to look for under- and over-represented biological processes. The Bonferroni correction for multiple testing was applied.
Ingenuity Pathway Analysis (http://www.ingenuity.com/) was used to analyse the fold change data for all probe sets. This program was used as a reference tool to obtain further information on the functions of genes of interest, and the associated pathways.

Heatmaps for representation of gene expression were created using MeV (MultiExperiment Viewer), part of the TM4 Microarray Software Suite[401]. Data were imported into MeV using tab delimited text files containing gene descriptors and fold change data expressed on a $\log_2$ scale. Hierarchical clustering was performed in MeV using Pearson correlation.

2.6 Validation of Microarray Data by Quantitative PCR

2.6.1 Infection and RNA Extraction

Huh7 and Huh7.5 cells were seeded at a density of 5 x 10^5 cells in 4ml of growth medium in 25cm^2 flasks. The next day, either concentrated JFH-1 stock or mock medium was added to the flasks. Cells were infected at an MOI of 3, and the volume added to each flask was 1ml. Conditions were performed in triplicate. At the indicated timepoints, media were removed from the flasks of infected and mock infected cells. 3ml of Trizol was added to each flask and incubated for five minutes at room temperature. Trizol-cell lysates were then homogenised by pipetting up and down, and transferred into 15ml tubes. 600µl chloroform was added, samples shaken for 20 seconds and incubated at room temperature for 2 minutes. Each 3.6ml sample was divided between four 1.5ml eppendorf tubes, and centrifuged at 12,000g for 10 minutes at 4°C. The upper, aqueous phase was transferred to a new 1.5ml eppendorf tube, an equal volume of isopropanol added, and incubated at -20°C for 1 hour. RNA was pelleted by centrifugation at 12,000g for 20 minutes at 4°C, and the supernatant removed. The pellets were washed twice by adding 1ml 75% ethanol and centrifuging at 10,000g. Pellets were resuspended in nuclease-free water and the four pellets from each sample recombined. RNA was rigorously treated with 2 units DNA-free Turbo DNAse (Ambion) per 5µg RNA to remove any genomic DNA.

2.6.2 Synthesis of cDNA

Reverse transcription was performed on total cell RNA samples to generate cDNA. 2µg of total RNA and 1µg of oligo dT primer (Invitrogen) were heated to 70°C for 5 minutes to melt secondary structure, after which the sample was placed immediately on ice. 200 units Moloney Murine Leukaemia virus reverse transcriptase (M-MLV RT, Promega), 5µl 5x M-MLV buffer, 1µl 40mM dNTP mix, 25 units RNasin ribonuclease inhibitor (Promega) and nuclease-free water were added to a final reaction volume of 25µl. The reaction was incubated at 42°C for 1 hour and then reverse transcriptase activity was inactivated by heat treatment at 70°C for 10 minutes.

2.6.3 Quantitative PCR

Validation of host gene expression seen in microarray data was performed by real-time quantitative PCR (qPCR) on cDNA samples generated from separate infection experiments from those used in the microarray studies. qPCR was performed using QuantiTect SYBR Green PCR kit (Qiagen) and Lightcycler equipment (Roche). 10µl reactions were performed using 125ng cDNA as template, and 0.5µM final concentration of each primer. Primers were designed using Primer 3 software to amplify a 100 -150bp product. The annealing temperature used for all primer pairs was 57°C. Data

acquisition was performed at a temperature 3°C below the melting temperature of the PCR product. Please see Appendix (A1) for sequences of primers. For each run, a reaction was performed with water as template to control for contamination of reagents with RNA or DNA. The threshold cycle (CT) was determined by the LightCycler software using the second derivative maximum method. Relative gene expression was calculated using the comparative CT method, with GAPDH as the normalising control gene.

Validation of host gene expression seen in microarray data was also performed by real-time quantitative reverse transcription PCR (qRT-PCR) on RNA samples generated from separate infection experiments from those used in the microarray studies, as well as the remaining material from original samples used in microarray studies. JFH-1 intracellular RNA titres were also measured by qRT-PCR. qRT-PCR was performed using QuantiTect SYBR Green RT-PCR kit (Qiagen) and Lightcycler equipment (Roche). 10µl reactions were performed using 125ng RNA as template, and 0.5µM final concentration of each primer. Primers were designed using Primer 3 software to amplify a 100 - 150bp product. The annealing temperature used for all primer pairs was 57°C. Data acquisition was performed at a temperature 3°C below the melting temperature of the PCR product. Please see Appendix (A1) for sequences of primers. For each run, a reaction with no reverse transcriptase and a reaction with water as template were included to control for genomic DNA contamination of the samples and contamination of other reagents respectively. The threshold cycle (CT) was determined by the LightCycler software using the second derivative maximum method. Relative gene expression was calculated using the comparative CT method, with GAPDH as the normalising control gene.

Absolute expression of RNA was calculated by including a series of six standards of known amount in 10-fold dilutions from 4ng to 40fg. The standards were generated by *in vitro* transcription. The qPCR amplicon was amplified from pJFH-1 and introduced by the TA cloning method into plasmid pCR2.1 (Invitrogen), generating plasmid pCR2.1HCV2aRTqPCR. To prepare for transcription this plasmid was linearised with restriction enzyme HindIII (NEB). RNA was transcribed from linearised pCR2.1HCV2aRTqPCR using the T7 MEGAscript *In Vitro* RNA Transcription kit (Ambion). RNA transcription was performed using 1µg of linearised plasmid DNA and reactions were incubated at 37°C for 6 hours. RNA transcripts were purified using phenol-chloroform extraction and isopropanol precipitation. RNA was rigorously treated with 2 units DNA-free Turbo DNAse (Ambion) per 5µg RNA to remove the remaining linearised plasmid DNA.

2.7 The Effect of Host Gene Knockdown by RNA Interference on HCV Replication

2.7.1 Jc1 Infectious Virus Model System

0.2µl Lipofectamine 2000 and 0.1µl 20µM siRNA were separately diluted into 17.5µl OptiMEM each and left to incubate at room temperature for 5 minutes. Both solutions were then added into a 96-well plate and left to incubate at room temperature for 20 minutes. 5×10^3 Huh7.5 cells in 50µl normal growth medium were added to the well giving a final siRNA concentration of 25nM. After 48 hours incubation at 37°C, the transfection medium was replaced with 100µl of normal growth medium containing Jc1 virus at an MOI of 0.1. Infection was allowed to proceed for 48 hours before measuring Jc1 replication by luciferase assay. The media were removed from the wells and replaced with 25µl SteadyGlo luciferase assay reagent (Promega). 96-well plates were incubated on an orbital shaker, at room temperature, in the dark for 10 minutes. Luciferase activity was read on an EnVision Luminometer (Perkin-Elmer). For each experiment, four replicates were performed per siRNA. Viability of cells after transfection with siRNA was tested by Cell Titer-Glo assay (Promega). Cells were transfected with siRNA as described and at 48 hours post-transfection medium was replaced with 25µl Cell Titer-Glo reagent. 96-well plates were incubated on an orbital shaker, at room temperature, in the dark for 10 minutes. Luciferase activity was read on an EnVision Luminometer (Perkin-Elmer). For each experiment, four replicates were performed per siRNA. Please see Appendix (A2) for siRNA sequences. All siRNAs were transfected as individual duplexes, except for DDX3X, used as a positive control known to knockdown HCV replication, which was a pool of four siRNA duplexes. Luciferase activities for all four replicates of the negative control siRNA were averaged. The luciferase activity of each replicate was then expressed as a ratio of the negative control. These ratios were used to calculate averages and standard deviations for each siRNA.

2.7.2 JFH-1 Infectious Virus Model System

1×10^5 cells were seeded in 0.5ml normal growth medium in 24-well plates. The next day, growth medium was removed, cells were washed with OptiMEM, and then incubated in 0.5ml OptiMEM for 2 hours, during which time transfection mixtures were prepared. 1µl Lipofectamine 2000 and 1.5µl 20µM siRNA (consisting of two duplexes targeted against the same gene) were separately diluted into 50µl OptiMEM each and incubated at room temperature for 5 minutes. The two solutions were mixed together and incubated at room temperature for 20 minutes. The 100µl mixture was then added to the 0.5ml OptiMEM already in the well, giving a final siRNA concentration of 50nM for the combination of the two duplexes. After 8 hours incubation, transfection medium was replaced with 0.5ml normal growth medium. 48 hours post-transfection, cells were infected with JFH-1 virus at an MOI of 3. After 48 hours, the cell culture medium was removed and cells washed with PBS. 150µl

Trizol was added, and left to incubate for 5 minutes. The Trizol-cell lysate was then homogenised by pipetting up and down, and then transferred into a 1.5ml eppendorf tube. 30µl chloroform was added, shaken for 20 seconds and incubated at room temperature for 2 minutes, before centrifugation at 12,000g for 10 minutes at 4°C. The upper, aqueous phase was transferred to a new 1.5ml eppendorf tube, an equal volume of isopropanol added, and incubated at -20°C for 1 hour. RNA was pelleted by centrifugation at 12,000g for 20 minutes at 4°C, and the supernatant removed. The pellet was washed twice by adding 0.5ml 75% ethanol and centrifuging at 10,000g. After air-drying, the pellet was resuspended in nuclease-free water. RNA was rigorously treated with 2 units DNA-free Turbo DNAse (Ambion) per 5µg RNA to remove any genomic DNA. RNA levels of target host gene and JFH-1 were measured by qRT-PCR as described.

2.8 Protein Level Analysis of Genes of Interest

2.8.1 Protein Preparation

Cells were harvested from 25cm^2 flasks after treatment (timecourse infection, or 48 hour siRNA transfection followed by 48 hour infection). 0.5ml Lysis buffer (please see Appendix A3 for recipe) was added to the flask and incubated at room temperature for 2 minutes. Any remaining adherent cells were scraped from the flask, the lysate was transferred to a 1.5ml eppendorf tube, and incubated on ice on a rocker for 30 minutes. The lysate was homogenised by passing through a narrow bore blunt needle, and stored at -80°C. Protein was quantified by Bradford Assay or absorbance at 280nm. For Bradford assay a series of bovine serum albumin (BSA) standards of known concentration were prepared. Dilutions of protein lysate or BSA standard were mixed with Bradford Assay Reagent, and absorbance at 495nm was measured. Protein concentrations of cell lysates were calculated by comparison with a curve generated from the BSA standards.

2.8.2 SDS-PAGE and Western Blotting

SDS-PAGE gels were made with 10% acrylamide resolving and 4% acrylamide stacking phases please see Appendix A3 for recipes). 100µg protein lysate was mixed with denaturing loading buffer and heated to 90°C for 10 minutes to denature the protein and then placed on ice. Samples were loaded on the gel, and BenchMark protein ladder (Invitrogen) was included in one well. Gels were run at 200V for one hour in Mini-Protean Tetra (Bio-Rad) apparatus. For western blotting in Mini Trans-Blot (Bio-Rad) apparatus, pre-soaked nitrocellulose membrane was used, and the blot was performed at 100V for one hour at 4°C. The membrane was washed in 5ml PBS-T (PBS with 0.1% Tween 20), and blocked with 5ml 4% milk in PBS for 1 hour at room temperature. Primary antibodies were diluted 1:1000 in blocking buffer, and membranes were incubated in 4ml dilute primary antibody overnight at 4°C. HCV Core was detected with mouse monoclonal C7-50 (Abcam), TXNIP with mouse monoclonal anti-VDUP (MBL), metallothioneins by anti-MT (MBL) and β-actin with mouse monoclonal anti- β-actin (Abcam). The membrane was washed in 5ml PBS-T three times for five minutes each, and then incubated with 4ml 1:1000 HRP-conjugated anti-mouse secondary in blocking buffer, for 1 hour at room temperature. The membrane was washed in PBS-T three times for five minutes each to remove excess unbound antibody. 1ml of SuperSignal West Pico detection reagent (Thermo Scientific) was added to the membrane for 5 minutes, then the excess shaken from then blot. Western blots were visualised using the ChemiDoc-It system (UVP), with dynamic integration of images taken every minute for 40 minutes (alternatively, blots were visualised by exposure of photographic film to the blot for five minutes).

2.9 Sequencing of JFH-1

2.9.1 RNA Transfection of Huh7.5 Cells

JFH-1 RNA transcript was transfected into Huh7.5 cells using Lipofectamine 2000 (Invitrogen). Huh7.5 cells were seeded at a density of $6x10^5$ in a 6-well plate. The following day, with cells at 80% confluency, growth medium was replaced with OptiMEM medium and the cells were incubated for four hours. 5µg JFH-1 RNA and 10µl Lipofectamine 2000 were each diluted in 500µl of OptiMEM and incubated at room temperature for 20 minutes. The dilutions were then mixed, and incubated at room temperature for 20 minutes. The growth medium was removed from the cells and they were washed with OptiMEM. The 1ml RNA/Lipofectamine 2000 transfection mixture was then added to the cells. After an eight hour incubation period, the transfection medium was replaced with normal growth medium and the cells were incubated overnight.

2.9.2 Passage of Transfected Huh7.5 Cells

The following day, 50% of the transfected cells were passaged into a $25cm^2$ flask. The remaining 50% of cells were prepared for RNA extraction by Trizol. Every three days, 25% of the transfected cells were passaged into a new $25cm^2$ flask, and 50% of the transfected cells were prepared for RNA extraction by Trizol.

2.9.3 Reverse Transcription

Reverse transcription was performed on total cell RNA samples to generate cDNA of JFH-1 RNA. 2µg of total RNA and 1µg of primer HVC2aRT9482 were heated to 70°C for 5 minutes to melt secondary structure, after which the sample was placed immediately on ice. 200 units Moloney Murine Leukaemia virus reverse transcriptase (M-MLV RT, Promega), 5µl 5x M-MLV buffer, 1µl 40mM dNTP mix, 25 units RNasin ribonuclease inhibitor (Promega) and nuclease-free water were added to a final reaction volume of 25µl. The reaction was incubated at 42°C for 1 hour and then reverse transcriptase activity was inactivated by heat treatment at 70°C for 10 minutes.

2.9.4 PCR and Sequence Analysis

To amplify cDNA in preparation for sequencing, PCR was performed to generate fragments of JFH-1 cDNA. PCR was performed using Accuzyme polymerase (Bioline) and 1µl cDNA reaction as template. Annealing temperature for all primer sets was 57°C, and extension time was one minute per kb amplicon size. PCR products were then purified using PCR Purification Kit (Qiagen) and eluted in 30µl water. PCR products were sequenced using the same forward and reverse primers as for amplification. Sequencing reactions were performed by the Imperial Genomics Core Facility at Hammersmith Hospital Campus. Sequences were compared and analysed using BioEdit software[402].

2.10 Chimaeric JFH-1 Construction and Replication

2.10.1 Cloning of Chimaeric JFH-1 Constructs

The large size of pJFH-1 means that there are few unique restriction sites to facilitate cloning. In order to create chimaeric JFH-1 constructs containing NS3 regions from other genotypes, a cloning strategy was devised, using an NS3 shuttle plasmid in which cloning could be more easily performed. Briefly, the AflII- NsiI region of JFH-1 was introduced into pCR2.1 (Invitrogen) at the corresponding restriction sites by ligation with T4 DNA ligase (Invitrogen). This vector had a BlpI restriction site introduced by site directed mutagenesis using the QuikChange kit (Stratagene) and primers QCNS32aBlpIF and QCNS32aBlpIR. NS3 sequence from other HCV genotypes was then introduced into the shuttle plasmid using the appropriate restriction enzymes. Finally the AflII-NsiI region from the shuttle vectors were introduced back into pJFH-1, creating a panel of chimaeric JFH-1 constructs.

20µg pJFH-1 and 10µg pCR2.1 were double digested with 50 units of both restriction enzymes AflII and NsiI (NEB) in NEBuffer 2 at 37°C for 2 hours. Restriction digests were run on a 1% agarose TBE gel and the required DNA fragments excised and purified by Qiaquick Gel Extraction kit (Qiagen). 100ng vector fragment and 300ng insert fragment were ligated overnight at 4°C using 2 units T4 DNA ligase in a 10µl reaction.

5µl ligation reaction was mixed with 50µl of Library Efficiency *E. coli* DH5α (Invitrogen) and incubated on ice for 30 minutes. Bacteria were heat shocked at 42°C for 40 seconds and incubated on ice for two minutes. 450µl SOC medium was added and the bacteria were shaken at 200rpm for one hour at 37°C. 200µl of the transformation mix was plated onto Luria Bertani (LB) agar containing 100µg/ml ampicillin and incubated overnight at 37°C. The following day, transformed bacterial colonies were picked and grown overnight at 37°C in 5ml LB medium containing 100µg/ml ampicillin. Plasmid DNA was prepared from the transformed DH5α cultures using the Plasmid Mini Kit (Qiagen) according to the manufacturer's instructions.

A BlpI restriction site was introduced into the shuttle plasmid by site directed mutagenesis using the QuikChange kit (Stratagene). PCR was performed using primers QCNS32aBlpIF and QCNS32aBlpIR for 15 cycles, with an extension time of 6m30s. DpnI was incubated with the PCR reaction for 1 hour at 37°C to remove the parent plasmid. *E. coli* XL-1 Blue were transformed with 5µl PCR reaction according to manufacturer's protocol, and plasmid prepared as described above.

NS3 sequence fragments were generated by PCR from plasmids pS1179I (genotype 1b) and pHCV1a. The primers used are given in the Appendix (A1.1). PCR was performed using Accuzyme polymerase (Bioline) in 50µl reactions. PCR reactions were purified by Qiaquick PCR Purification kit (Qiagen). Purified PCR reactions were digested with the appropriate restriction enzymes. Digestions were then treated with 0.5% SDS and 200µg/ml Proteinase K (Invitrogen) for 1 hour at 50°C. Samples were made up to 200µl with water, and 200µl phenol-chloroform was added. Samples were shaken, and then centrifuged at 16,000g for 20 minutes at 4°C. The upper, aqueous phase was transferred to a new 1.5ml eppendorf tube, an equal volume of chloroform was added. Samples were shaken, and then centrifuged at 14,000g for 20 minutes at 4°C. The upper, aqueous phase was transferred to a new 1.5ml eppendorf tube, where 0.1 volume 3M sodium acetate and 2.5 volumes of ethanol with were added, and incubated overnight at -20°C. DNA was pelleted by centrifugation at 14,000g for 20 minutes at 4°C, and the supernatant removed. The pellet was washed by adding 0.5ml 75% ethanol and centrifuging at 14,000g. After air-drying, the pellet was resuspended in nuclease-free water.

Digested PCR products and complementary vector fragments of shuttle vector were ligated with T4 DNA ligase as described above. Transformation into *E. coli* DH5α, and plasmid production were also performed as described above.

In vitro transcription of chimaeric constructs was performed as for pJFH-1. 20µg of plasmid was linearised with 150 units of restriction enzyme XbaI (NEB) and purified using phenol-chloroform extraction and ethanol precipitation. 3' overhanging DNA was removed by digestion with 30 units Mung Bean Nuclease (NEB) for 30 minutes at 30°C, and DNA purified by phenol-chloroform extraction and ethanol precipitation. RNA transcripts were generated from plasmid using the T7 MEGAscript *In Vitro* RNA Transcription kit (Ambion). RNA transcription was performed using 1µg of linearised plasmid DNA and reactions were incubated at 37°C for 6 hours. RNA transcripts were purified using phenol-chloroform extraction and isopropanol precipitation. RNA was treated with DNA-free Turbo DNAse (Ambion) to remove the remaining linearised plasmid DNA.

2.10.2 RNA Transfection of Huh7.5 Cells

The RNA transcripts were transfected into Huh7.5 cells using Lipofectamine 2000. Huh7.5 cells were seeded at a density of $6x10^5$ in a 6-well plate with 2ml DMEM. The following day, with cells at 80% confluency, growth medium was replaced with 1ml OptiMEM medium and the cells were incubated

for four hours. 5µg RNA and 10µl Lipofectamine 2000 were each diluted in 500µl of OptiMEM and incubated at room temperature for 20 minutes. The dilutions were then mixed, and incubated at room temperature for 20 minutes. The growth medium was removed from the cells and they were washed with 2ml OptiMEM. The 1ml RNA/Lipofectamine 2000 transfection mixture was then added to the cells. After an eight hour incubation period, the transfection medium was replaced with 2ml normal growth medium (DMEM) and the cells were incubated overnight. For each experiment, transfections were performed in triplicate.

2.10.3 Passage of Transfected Huh7.5 Cells

The following day, 50% of the transfected cells were passaged into a 25cm^2 flask. The remaining 50% of cells were prepared for RNA extraction by Trizol. Every three days, 25% of the transfected cells were passaged into a new 25cm^2 flask, and 50% of the transfected cells were prepared for RNA extraction by Trizol.

2.10.4 Quantification of Intracellular JFH-1

Levels of intracellular JFH-1 and its derivatives were measured by real-time qRT-PCR using QuantiTect SYBR Green RT-PCR kit (Qiagen) and Lightcycler equipment (Roche). 10µl reactions were performed using 125ng RNA as template, and 0.5µM final concentration of each primer. Primers (described in the Appendix A1.4) amplify a 150bp product. The annealing temperature used was 57°C. Data acquisition was performed at 80°C. For each run, a reaction with no reverse transcriptase and a reaction with water as template were included to control for non-specific amplification and contamination of other reagents respectively. The threshold cycle (CT) was determined by the LightCycler software using the second derivative maximum method. Absolute expression of RNA was calculated by including a series of six standards of known concentration in 10-fold dilutions from 4ng to 40fg. The standards were generated by *in vitro* transcription. The qPCR amplicon was amplified from pJFH-1 and introduced by the TA cloning method into plasmid pCR2.1 (Invitrogen), generating plasmid pCR2.1HCV2aRTqPCR. To prepare for transcription this plasmid was linearised with restriction enzyme HindIII (NEB). RNA was transcribed from linearised pCR2.1HCV2aRTqPCR using the T7 MEGAscript *In Vitro* RNA Transcription kit (Ambion). RNA transcription was performed using 1µg of linearised plasmid DNA and reactions were incubated at 37°C for 6 hours. RNA transcripts were purified using phenol-chloroform extraction and isopropanol precipitation. RNA was rigorously treated with 2 units DNA-free Turbo DNAse (Ambion) per 5µg RNA to remove the remaining linearised plasmid DNA.

2.11 Magnetic Resonance Spectroscopy

$5x10^5$ Huh7.5 cells were seeded per $25cm^2$ flask in 4ml normal growth medium. The next day JFH-1 virus at an MOI of 3, or mock medium was added to the cells in a volume of 1ml. At 48 hours post-infection, media were removed from the flasks, the cells were washed with 5ml warm PBS and trypsinised with 0.5ml of 1x trypsin-EDTA (Invitrogen). Trypsinisation was stopped with 4.5ml normal growth medium (containing FBS), and cells were counted so that each sample had the same number of cells. The cell suspensions were centrifuged for 5 minutes at 1500rpm in a Mistral 3000 Benchtop Centrifuge (MSE). The supernatant was discarded and the cell pellets resuspended in PBS to wash away any medium. Cells were centrifuged for 5 minutes at 1500rpm and the supernatants discarded. The cell pellets were resuspended in PBS to a final volume of 20µl and loaded into MRS sealing cells (XC4 Kel-F, Doty Scientific). Samples were transported on ice to the 500MHz MRS facility at Hammersmith Hospital where ^1H MAS MRS was performed. Further details on the MRS machine, its operational procedures and procedures for obtaining data can be found in the cited references[403-404]. Briefly, the sealing cell was inserted into the ceramic rotor (XC4 Kel-F, Doty Scientific) and placed in the MAS probe (Doty Scientific). The probe was interfaced with a JEOL Eclipse 500+ spectrometer and an 11.75T superconducting magnet (Oxford Instruments). Samples were spun at 4000Hz, and maintained at 4°C to minimise sample degradation. Suppression of the water signal was performed to allow better resolution of metabolite signals.

Results and Discussion

3.1 Viral Determinants for JFH-1 Replication

3.1.1 Role of NS3 Sequence Determinants in JFH-1 Replication

It has been shown by other groups that replication levels of JFH-1 can be maintained and even enhanced by the substitution of the structural protein coding region for that from other genotypes. However, the same is not true for the non-structural coding region. This implies that the non-structural protein coding region contains determinants essential for the efficient replication of JFH-1. To investigate whether the NS3 region contains essential determinants for JFH-1 replication, chimaeric viruses were constructed. These viruses contained the coding region either for full length NS3, the helicase or protease domain, or subdomain regions. Inserted coding regions were from HCV genotypes 1a and 1b. Chimaeric RNA was transfected into Huh7.5 cells by either electroporation or lipofection. In each experiment, wild type JFH-1 RNA was included as a positive control and GND and delE1E2 mutants were included as negative controls. Intracellular HCV RNA was measured at multiple time points. The method for construction of chimaeric JFH-1 genomes is outlined in Figure 11, and images from gel electrophoresis of restriction digestions performed as confirmation of cloning steps are shown in Figure 12-Figure 16.

3.1.2 Construction of Chimaeric JFH-1

In order to study the effects of NS3 components from different genotypes in the JFH-1 infectious culture system, a strategy was designed to create chimaeric viruses. pJFH-1 is a large plasmid of 12kb and therefore has few unique restriction sites to facilitate cloning. Therefore, it was decided to move the region of interest, NS3, into another vector where it could be more easily manipulated. Unique restriction sites AflII and NsiI were the closest to the NS3 boundaries. The AflII site is 129 amino acids upstream of NS3 in NS2, and the NsiI site is 4 amino acids into the C-terminal end of NS3.

Figure 11 shows the cloning strategy represented by plasmid maps with the relevant restriction sites indicated. Some examples of the confirmatory agarose gels generated at each step of the process are shown in Figure 12-Figure 16.

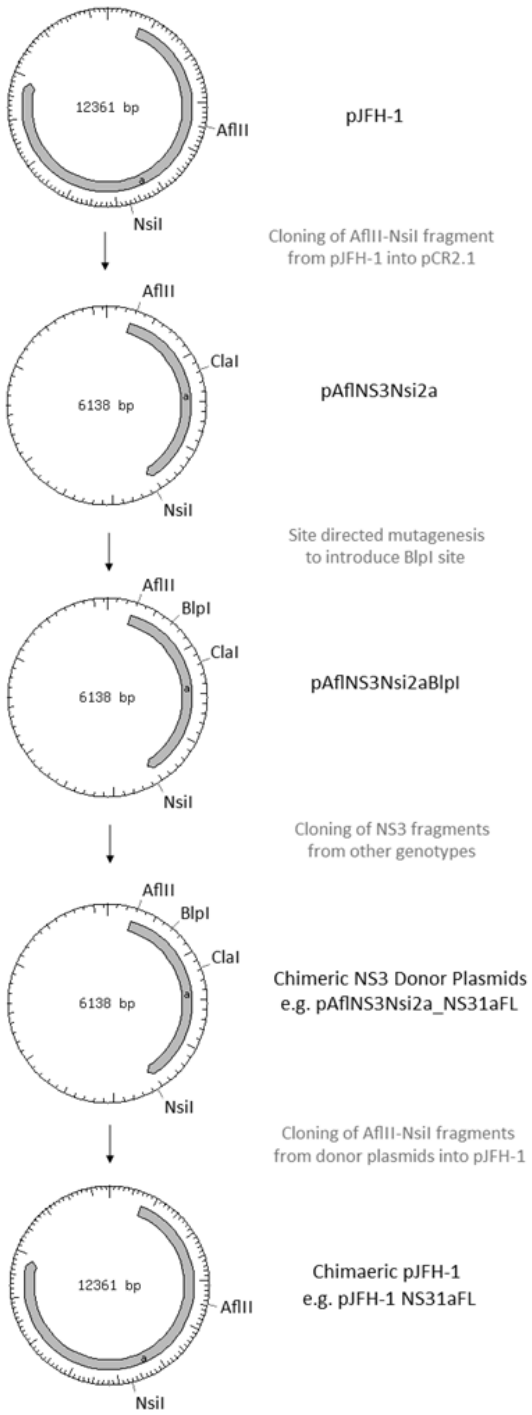


Figure 11: Major steps in the cloning of chimaeric JFH-1 viruses.

Plasmid diagrams include the restriction sites of importance. Protein coding regions are shown by the grey arrows, corresponding to the polyprotein in plasmids containing the complete genome, and NS3 in the intermediate vectors. Construction of chimaeric plasmids was performed as follows. The AflII-NsiI fragment of pJFH-1 was amplified by PCR and TA cloned into the vector pCR2.1. A second NsiI site in this plasmid was removed by digestion with NsiI and re-ligation of the plasmid. The resulting plasmid was designated pAflNS3Nsi2a. This plasmid has a unique ClaI restriction site at the protease/helicase boundary of NS3, but no unique site at the N terminal end of NS3. A BlpI site was introduced by site directed mutagenesis to a position six amino acids into NS3, creating plasmid pAflNS3Nsi2aBlpI. This plasmid was now ready to receive NS3 sequences from other genotypes. Sequences corresponding to the full length NS3 and protease and helicase domains were amplified by PCR from plasmid pHCV1aFull Length (genotype 1a) and plasmid S1179I (genotype 1b), incorporating the appropriate restriction site into the primers. These fragments were TA cloned into pCR2.1, creating vectors pNS31aFL, pNS31aPro, pNS31aHel, pNS31bFL, pNS31bPro and pNS31bHel. These plasmids were then digested with the relevant pair of enzymes to release the desired NS3 fragment. pAflNS3Nsi2aBlpI was digested with the same enzymes, and the vector portion was ligated with the desired NS3 fragments. This resulted in the donor plasmids pAflNS3Nsi2a_NS31aFL, pAflNS3Nsi2a_NS31aPro, pAflNS3Nsi2a_NS31aHel, pAflNS3Nsi2a_NS31bFL, pAflNS3Nsi2a_NS31bPro and pAflNS3Nsi2a_NS31bHel. The final stage in the construction of the chimaeric plasmids was to digest pJFH-1 and the donor plasmids with AflII and NsiI, and perform a sticky-end ligation.

The AflII-NsiI fragment of pJFH-1 was cloned into pCR2.1 to create plasmid pTANS32a. This plasmid was then altered by site directed mutagenesis to create plasmid pTANS32aBlpI, which contains a BlpI restriction site at the start of the NS3 coding region. Figure 12A shows pTANS32a digested using AflII, NsiI and BlpI and demonstrating the electrophoresis pattern consistent with pCR2.1 containing the AflII-NsiI fragment of pJFH-1, and that the fragment contains only AflII and NsiI sites (not BlpI). Figure 12B shows pTANS32aBlp (the product of site directed mutagenesis of pTANS32a) also digested with AflII, NsiI and BlpI and demonstrating the electrophoresis pattern consistent with the introduction of a BlpI site to the plasmid.

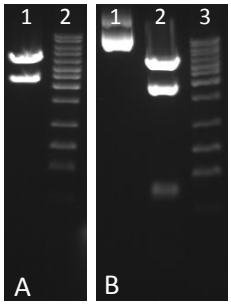


Figure 12: Agarose gel electrophoreses as confirmation of site directed mutagenesis insertion of BlpI restriction site in pTANS32a.

A Lane 1: TANS32a digested with AflII, NsiI and BlpI, Lane 2: 1kb DNA ladder. **B** Lane 1: Undigested TANS32aBlp, Lane 2: TANS32aBlp digested with AflII, NsiI and BlpI, Lane 3: 1kb DNA ladder.

The regions of HCV genotype 1a and 1b sequence corresponding to the full length NS3, protease and helicase domains were amplified by PCR using primers incorporating the required restriction sites. The AflII-NsiI region of JFH-1 was also amplified for TA cloning. Example agarose gels of PCRs are given in Figure 13A-C.

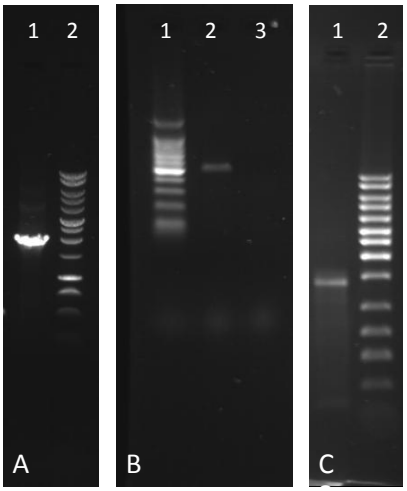


Figure 13: Agarose gel electrophoreses as confirmations of successful PCR of NS3 coding sequences.

A Lane 1: Full length NS3 PCR product, Lane 2: 1kb DNA ladder. **B** Lane 1: 100bp DNA ladder, Lane 2: NS3 protease domain PCR product, Lane 3: No template negative control PCR. **C** Lane 1: NS3 helicase domain PCR product, Lane 2: 1kb DNA ladder.

After cloning the PCR products (Figure 13) into pTANS32aBlp, the resulting plasmids and pJFH-1 were digested with AflII and NsiI for cloning of the chimaeric NS3 regions into pJFH-1. The digested plasmids are shown in Figure 14, in agarose gels prior to gel extraction and cloning.

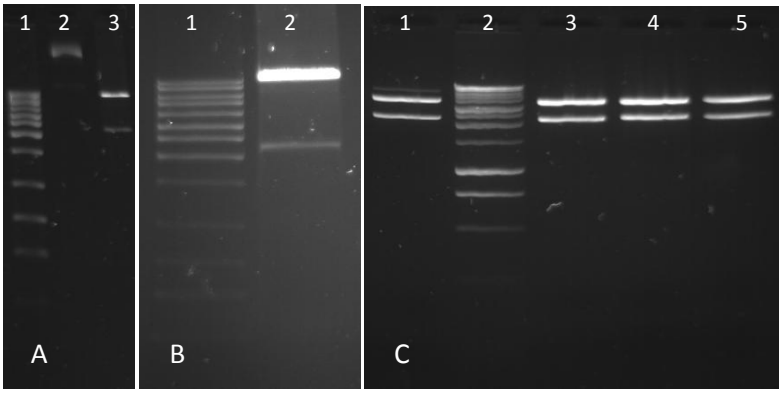


Figure 14: Agarose gel electrophoresis of AflII/NsiI digests of constructs prior to final cloning step.

A Lane 1: 1kb DNA ladder, Lane 2: Undigested pJFH-1, Lane 3: pJFH-1 digested with AflII and NsiI. This analytical gel shows the expected pattern of bands after complete digestion of pJFH-1. **B** Lane 1: 1kb DNA ladder, Lane 2: pJFH-1 digested with AflII and NsiI. This gel was used for gel extraction of the large band, which contains the majority of pJFH-1. **C** Lane 1: Incomplete digestion of pTANS32a_NS31aFL with AflII and NsiI, Lane 2: 1kb DNA ladder, Lane 3: pTANS32a_NS31aFL digested with AflII and NsiI, Lane 4: pTANS32a_NS31aPro digested with AflII and NsiI, Lane 5: pTANS32a_NS31aHel digested with AflII and NsiI. The largest band in Lane 1 shows the linearised form of pTANS32a_NS31aFL, a result of incomplete digestion. This band is absent from Lanes 3-5, indicating complete digestion of these plasmids.

After cloning the chimaeric AflII-NsiI sequences into the JFH-1 backbone, the final constructs were analysed by gel electrophoresis to confirm the cloning was successful (Figure 15). Example restriction digests are shown in Figure 16, with comparison to the original JFH-1 constructs.

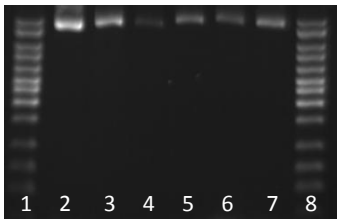


Figure 15: Agarose gel electrophoresis of final chimaeric constructs.
Lane 1: 1kb DNA ladder, Lane 2: pJFH_NS31aFL, Lane 3: pJFH_NS31aPro, Lane 4: pJFH_NS31aHel, Lane 5: pJFH_NS31bFL, Lane 6: pJFH_NS31bPro, Lane 7: pJFH_NS31bHel, Lane 8: 1kb DNA ladder. This gel shows all the final constructs to be of the same size, and therefore incorporating the chimaeric AflII-NsiI fragments (all plasmids are in their supercoiled form, as derived from DNA miniprep).

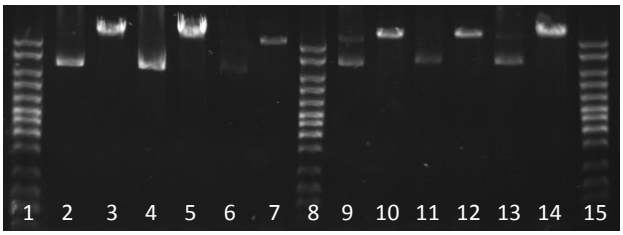


Figure 16: Agarose gel electrophoresis of JFH-1 constructs digested with AflII and NsiI.
Lane 1: 1kb DNA ladder, Lane 2: Undigested pJFH-1, Lane 3: Digested pJFH-1, Lane 4: Undigested pJFH-1 GND, Lane 5: Digested pJFH-1 GND, Lane 6: Undigested pJFH-1 delE1E2, Lane 7: Digested pJFH-1 delE1E2, Lane 8: 1kb DNA ladder, Lane 9: Undigested pJFH_NS31aFL, Lane 10: Digested pJFH_NS31aFL, Lane 11: Undigested pJFH_NS31aPro, Lane 12: Digested pJFH_NS31aPro, Lane 13: Undigested pJFH_NS31aHel, Lane 14: Digested pJFH_NS31aPro, Lane 15: 1kb DNA ladder.

3.1.3 Replicative Ability of Chimaeric JFH-1

Chimaeric RNA was transfected into Huh7.5 cells by lipofection. In each experiment, wild type JFH-1 RNA was included as a positive control and GND and delE1E2 mutants were included as negative controls. Intracellular HCV RNA was quantified as a measure of the ability of the chimaeric genomes to replicate in cell culture.

As can be seen in Figure 17, the replacement of JFH-1 full length NS3 with that from genotypes 1a or 1b resulted in a replication deficient virus. The RNA observed in the initial measurements is input RNA, and follows a similar pattern of decline in titre to the replication deficient GND mutant.

Having established that substitution of full length NS3 resulted in replication deficient RNA, domain level chimaeras were constructed in an attempt to identify which region of the NS3 coding sequence conferred replicative deficiency. The protease and helicase domains of JFH-1 were substituted for those of genotypes 1a and 1b. Figure 17 shows that these chimaeric RNAs also failed to replicate when transfected into Huh7.5 cells.

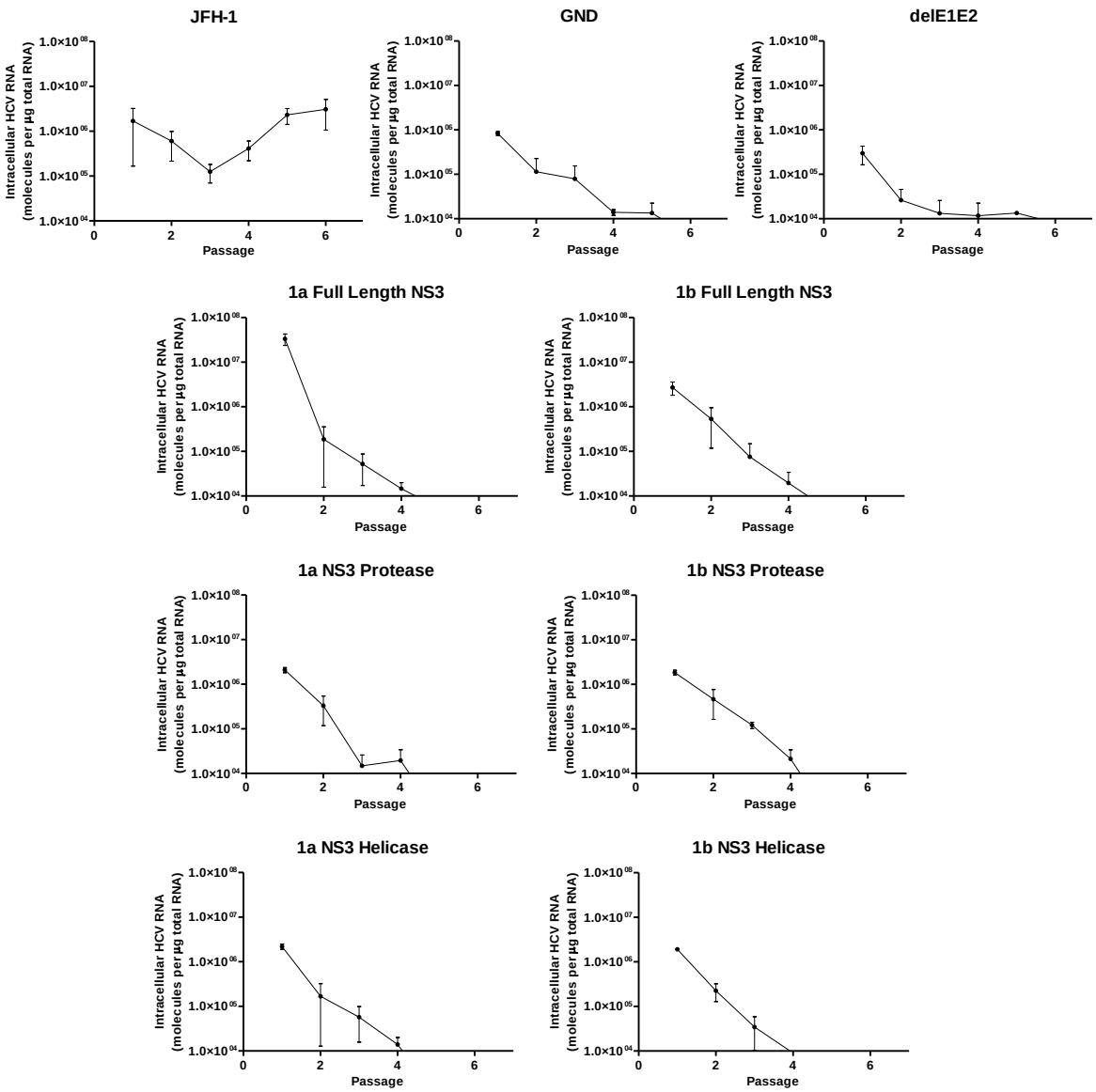


Figure 17: Replication of chimaeric JFH-1.

Huh7.5 cells were transfected by lipofection with viral RNA and intracellular RNA titres were measured every passage by qRT-PCR. JFH-1 RNA. Data presented are the means and standard errors from two separate experiments performed with duplicate transfections. JFH-1, the wild type virus, shows an initial decrease in RNA levels followed by an increase as replication occurs. GND, the non-replicative mutant, shows a decrease in RNA levels which does not recover. The delE1E2 mutant shows a more gradual decline in RNA levels. Quantitation of RNA levels of transfected the JFH-1 chimaeric RNAs containing sequence elements from the NS3 region of genotype 1a and genotype 1b HCV all showed a pattern of decline in RNA over time. The decline in levels of chimaeric RNAs were similar to that of the non-replicating GND construct, and as there were also no increases in RNA levels as achieved by wild type JFH-1, it can be concluded that the chimaeric viruses were unable to replicate and establish a persistent infection.

3.1.4 NS3 Sequence Determinants for JFH-1 Replication

JFH-1 is the only natural isolate of HCV capable of highly efficient replication in cell culture. Some other isolates have achieved lower levels of replication[344], and some isolates have been adapted to confer replicative ability[338], but these do not match JFH-1. This implies that JFH-1 possesses some specific genetic features which enable its ability to replicate in cell culture. It has been shown that the structural region of the JFH-1 genome can be exchanged for those of other genotypes (Figure 8C), and a relatively high replication rate be maintained[354]. However, it is not possible to exchange the non-structural regions of the virus for those of other genotypes and maintain efficient replication. This implies that the major sequence determinants for the ability of JFH-1 to replicate in cell culture may be in the non-structural protein coding region of the genome.

The NS3 protein plays a number of roles in HCV replication including a role as a protease with viral and cellular targets, a role as a helicase involved in RNA replication, and a role in viral assembly. Across HCV genotypes, shared nucleotide identity of NS3 sequence is around 70%, and amino acid identity around 80%, with amino acid similarity approaching 90% (see Figure 9). There is therefore potential for unique sequence determinants to exist in JFH-1 NS3 that allow replication in cell culture.

Chimaeric JFH-1 genomes incorporating genetic elements from genotype 1 HCV NS3 were created to test this hypothesis. Genotypes 1a and 1b are the most common in Europe and the USA, and most research is focused on these genotypes when possible. Chimaeric JFH-1 genomes were tested for their replication ability by transfection of *in vitro* transcribed RNA (corresponding to the viral genome) into Huh7.5 cells. The control constructs used were wild type JFH-1, JFH-1 GND and JFH-1 delE1E2. JFH-1 GND is a replication deficient virus with a mutation in the viral polymerase, NS5B. JFH-1 delE1E2 is RNA replication competent, but cannot produce infectious virus as it lacks the envelope proteins E1 and E2. The first constructs to be tested were JFH-1 genomes containing full length NS3 from genotypes 1a and 1b. It can be seen in Figure 17 that neither full length NS3 chimaera replicated in cell culture. This implies that NS3 contains genotype specific sequence elements which determine replication capacity of the virus. In this case, it was demonstrated that genotype 1 NS3 genes were not compatible with genotype 2a JFH-1 for replication. It was then attempted to elucidate which specific regions of the NS3 sequence were responsible for this observation. Chimaeric JFH-1 genomes were constructed containing only the protease or helicase

domains from genotype 1 sequences. Figure 17 shows that none of these chimaeras were capable of establishing a persistent infection of cultured cells.

The data obtained from the experiments performed here imply that both the protease and helicase sequences are essential for the ability of JFH-1 to replicate in cell culture. The method used measured RNA levels, and therefore only the replication capacity of the virus. It is hard to distinguish, using this method, between viruses which are RNA replication incompetent (such as the JFH-1 GND) and those which cannot produce infectious viral particles (such as JFH-1 delE1E2). As both domain level chimaeras failed to replicate in cell culture, it may be that both the protease and helicase functions of JFH-1 NS3 are determinants in allowing JFH-1to replicate in cell culture. However, it is also possible that the sequence of each domain is capable of influencing the function of the other. Possible ways to test this would be to knock out the specific functionality of each domain. Helicase activity can be eliminated by mutating the aspartate of the essential DECH motif to an alanine (resulting in a non-functional AECH motif)[405]. Protease activity can be eliminated by mutating any of the amino acids which make up the catalytic triad His-Asp-Ser[140]. The functionality of NS3 in the chimaeric viruses should be tested to determine whether the loss of ability to replicate in cell culture is due to an inability to replicate RNA or a loss of protease function. The protease function could be assessed by performing *in vitro* translation of the polyprotein from the chimaeric genomes and observing the level of polyprotein cleavage. This observation could be made either by radiolabelling protein with ^{35}S-methionine and photographing a protein blot of SDS-PAGE, or by SDS-PAGE and western blotting for the cleaved forms of viral proteins. Alternatively, purified bacterially-expressed chimaeric NS3 proteins could be assessed *in vitro* for protease function by measuring their ability to cleave polypeptides labelled with a fluorescent marker and quencher. Confirmation of the ability of chimaeric genomes to proteolytically cleave the polyprotein would imply that any inability to replicate in cell culture is not caused by protease deficiency, but by RNA replication deficiency. It is possible to test helicase functionality *in vitro* by purifying bacterially expressed chimaeric NS3 protein and performing a dsDNA or dsRNA unwinding assay, using oligonucleotide duplexes containing one strand labelled with a fluorophore and the other strand labelled with a quencher[406]. Since the functional elements of all chimaeras created were still in place, it is unlikely that the protease and helicase activities of NS3 were completely lost. It is more probable that there was a reduction of activities due to genotype specificities. The proposed experiments would be able to quantify the reduction in protease and helicase activities of the chimaeras. The reduction in activities was sufficient that HCV replication was reduced to a level where it could not combat the host cell defences and achieve a persistent infection of the cultured cells. Further assessments could

then be performed on sub-domain level chimaeras, where sequence exchange focused on smaller regions where there is genetic divergence between genotypes. This focusing down on particular amino acids would identify the precise sequence determinants which allow JFH-1 to replicate in cell culture.

Whilst performing this work, a similar study was published by Imhof and Simmonds in which protease elements from different genotypes were inserted into a genotype 2a backbone[407]. In common with the work presented in this thesis, it was found that insertion of the NS3 protease domain alone resulted in replication deficient viral genomes. The one exception was where a genotype 5a sequence was inserted, where replication was achieved after acquiring adaptive mutations. In an attempt to rescue the replication deficient chimaeras, NS4A sequences from the same genotype as the introduced NS3 protease sequences were inserted into the viral genomes. As NS4A is a cofactor that can greatly enhance NS3 protease activity and this would also have been the next logical step to rescue replication deficient chimaeras created during the work presented in this thesis. Replication competent chimaeras were created by Imhof using sequence from genotypes 1b, 2a, 3a, 5a and 6a, with varying degrees of success. The chimaera containing genotype 1b sequence was detected in 50% of cells four days post transfection, but subsequently cleared. Genotype 2a and 5a chimaeras were detected in almost all cells at two days post transfection. Genotype 3a and 6a chimaeras were detected in 80% of cells after eclipse periods of 6 and 33 days respectively. This study indicates that incorporating NS4A sequences, of the same genotype as the NS3 protease sequences, into the chimaeras created for the work presented in this thesis may be a method for acquiring replicative ability.

3.2 Mutation in the JFH-1 Genome during Cell Culture

Replication of the JFH-1 in cell culture is possible by the isolate consensus sequence[79]. This differs from replicon models based on genotypes 1a[334] and 1b[131], which require adaptive mutations to replicate in cell culture. However, it has been previously observed[79] that the titre of infectious JFH-1 virus produced in cell culture, and the titre of intracellular JFH-1 RNA, will increase over time. This indicates that the virus may be adapting to the cell culture environment. It is possible that these adaptations could be at the genetic level. In order to monitor the mutations that could arise in JFH-1, a strategy for sequencing was devised involving reverse transcription of intracellular JFH-1 RNA and PCR amplification of multiple regions of the genome in order to acquire material for sequencing.

3.2.1 Testing of Primers for PCR of Regions of JFH-1 to be Sequenced

In order to establish the efficacy of the primers chosen for sequencing, test PCRs were performed using plasmid DNA (Figure 18A) and cDNA (Figure 18B) templates. All reactions were observed to produce amplified target sequence. The cDNA template resulted in some non-specific products, but in all reactions the desired product was the most highly amplified.

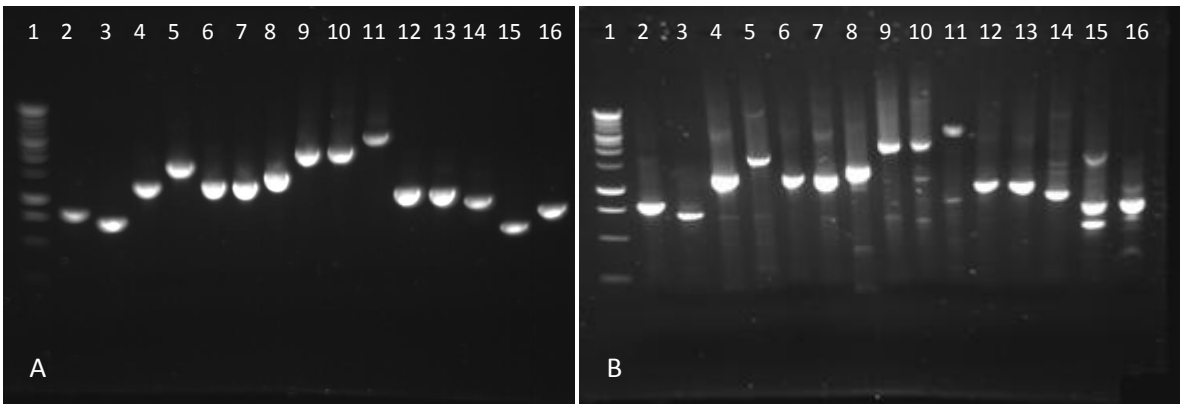


Figure 18: Amplification of targets for sequencing of JFH-1 genome.

PCRs of JFH-1 plasmid DNA (**A**) and cDNA (**B**) were performed as described in the Methods section (2.9) and 10µl of the reactions were run on 1% agarose gels. The reactions in both images are in the same order. Lane 1: 1kb ladder, Lane 2: Product of reaction using primer JFH 64F + primer JFH 829R, Lane 3: 637F + 1303R, Lane 4: 1158F + 2348R, Lane 5: 637F + 2348R, Lane 6: 2305F + 3491R, Lane 7: 3484F + 4648R, Lane 8: 4566F + 5951R, Lane 9: 2305F + 4648R, Lane 10: 3489F + 5951R, Lane 11: 2305F + 5951R, Lane 12: 5902F + 6983R, Lane 13: 6967F + 8015R, Lane 14: 7472F + 8872R, Lane 15: 8700F + 9262R, Lane 16: 8700F + 9482R.

3.2.2 Identification of Mutations in Cell Cultured JFH-1

Mutations accumulated by the virus over time in cell culture were identified by sequencing JFH-1 RNA isolated after 23 passages of JFH-1 transfected cells. The six mutations identified are shown in Table 1. Two occurred in the NS5A coding region, and one each in NS4b, NS3, E2 and the IRES. All the mutations in the protein coding region were nucleotide point mutations that resulted in a change of amino acid at their codon.

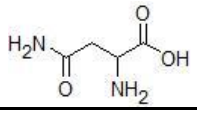
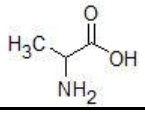
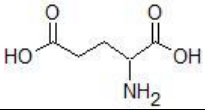
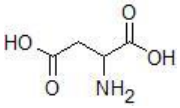
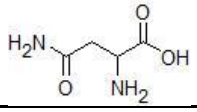
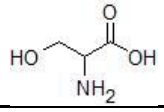
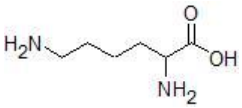
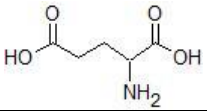
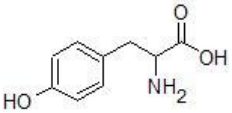
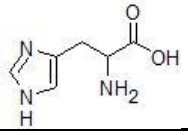
	Nucleotide Mutation			Amino Acid Mutation		
Region	From	Position	To	From	Position	To
IRES	G	179	A	-	-	-
E2	A	1590	G	Asparagine 	416	Alanine 
NS3	G	3715	T	Glutamate 	1171	Aspartate 
NS4B	A	6132	G	Asparagine 	1930	Serine 
NS5A	A	6587	G	Lysine 	2350	Glutamate 
NS5A	T	7217	C	Tyrosine 	2292	Histidine 

Table 1: Mutations identified in cell cultured JFH-1.

Huh7.5 cells were transfected with JFH-1 RNA and continuously passaged. After 23 passages of transfected JFH-1 cells, intracellular JFH-1 RNA was extracted, the positive strand converted to cDNA, amplified by PCR and sequenced. Six point mutations were identified and the corresponding amino acid change is given where relevant. Nucleotide positions refer to the JFH-1 genome, and amino acid positions refer to the JFH-1 polyprotein.

3.2.3 Mutation in the JFH-1 Genome during Cell Culture

The ability of full length JFH-1 to replicate in cell culture made it unique amongst HCV isolates when first identified. Since then, other HCV isolates, even of other genotypes, have been identified that can replicate in cell culture, but none as efficiently as JFH-1. The exception is the artificial chimaera J6/JFH-1. Many of the genomes so far described to replicate in cell culture require the presence of cell culture adaptive mutations. Cell culture adaptive mutations were identified in the replicon models developed since the late 1990s, originally by observation of spontaneous mutation in the subgenomic replicons.

In this study, after continuous passage of Huh7.5 cells harbouring JFH-1 for 3 months, the intracellular JFH-1 RNA was sequenced, revealing six mutations from the consensus sequence.
A mutation was observed to occur in the IRES region of the genome. The nucleotides of the IRES do not contribute to protein coding, but are still vital to the lifecycle of HCV. The IRES is strongly conserved both intra- and inter-genotypically (as observed when comparing the sequences stored on www.HCVdb.org). The IRES is known to be of importance in interactions with other molecules, such as miR122, for which mutations have been shown to disrupt the base pairing and therefore impair replication efficiency. The secondary structure of the IRES is also known to be of importance in controlling HCV RNA replication and translation. The IRES stem-loop structures are predicted to be important in interaction with proteins and other regions of the HCV genome. The nucleotide mutation observed, G179A, is located in the stem-loop III. This base is predicted to be paired with a cytosine. However, there was no complementary mutation to this nucleotide observed. G179A would therefore result in a bulge in the stem, possibly an enlargement of the loop. This could further be investigated by a bioinformatic prediction of the structure of the IRES including the observed mutation, as well as studies into crystal structures or protein binding affinity assays. There was one observed mutation in the E2 coding region, A1590G which results in amino acid substitution N416A. E2 contains two hypervariable regions (HVRs) which, in vivo, are observed to be regions of sequence diversity. E2, as an envelope glycoprotein, is visible to antibodies and its sequence variability helps the virus to evade detection. As the model system used in this study is a cell culture system, there is no antibody pressure on the virus to select mutations at this region, so there is unlikely to be a mutation rate higher than for other parts of the genome. The mutation observed lies between the two HVRs. The mutation from asparagines to alanine is one from a polar uncharged residue to a small hydrophobic residue. One amino acid change, E1171D, was observed in the NS3 coding region, located in the protease domain. This change was between two amino

acids of very similar properties. Glutamate was converted to aspartate, both of which have a –COOH group, but with inverted =O, and is therefore unlikely to have a significant effect on interactions or conformation, but may subtly enhance some positioning. The point mutation observed in the NS4B coding region converts an asparagine into a serine (N1930S). Both residues are polar and uncharged, but the serine contains an –OH group, which is often reactive in proteins and could, for example, be phosphorylated. Two mutations resulting in amino acid changes were observed in NS5A. This protein coding region is also known to be a region for the occurrence of mutations. In particular, the region known as the interferon sensitivity determining region (ISDR) has been documented as a region for accumulation of adaptive mutations in replicon cell models and *in vivo*. The mutation of lysine to glutamate (K2350E) converted a long positive amino acid into a long negatively charged amino acid. In the second mutation, Y2292H, both tyrosine and histidine contain rings, but tyrosine is a hydrophobic six carbon ring with an –OH group, and histidine is a positively charged residue with a five membered ring containing two nitrogen atoms. Of the mutations observed by this study, only one has been reported before. The mutation K2350E in NS5A was seen in another study based on replicon cells[349], but showed no significant enhancement of replication when deliberately introduced as a mutation in the parental replicon. It is unlikely that any consistently recurring mutations will be found in JFH-1 during cell culture to explain the increase in titre over time. A number of different mutations have been seen by groups at many positions, and very few of these have been shown to have a large effect on HCV replication. A larger scale investigation would need to be performed to identify any mutations that may induce a replicative advantage. The observed mutations would need to be artificially engineered into the JFH-1 genome both individually and in combination, to identify any replicative advantage conferred.

A similar recent study[408] identified only one mutation out of many observed that had a significant effect on replication when deliberately engineered into JFH-1 (and other intergenotypic chimaeras). Since starting this work, other groups have attempted to identify cell culture adaptive mutations in JFH-1. As with the studies performed in replicon models, only a few of the mutations identified confer a replicative advantage to the virus. A study focusing on the structural region of the genome was performed using JFH-1 in Huh7 cells[409]. JFH-1 was sequenced after six serial infections with virus harvested from cell culture (with two cell passages between each infection). Three mutations were identified in the E2 gene, comprising two silent nucleotide mutations (G1843A and U1912C) and one mutation (U1942A) which lead to a change in amino acid from asparagine to lysine (N534K). This N534K mutation occurred at a site of *N*-glycosylation. Introduction of this mutation into the JFH-1 genome created a virus which gained a slight replicative advantage over the wild type JFH-1 ($10^{3.9}$

f.f.u./ml, compared to $10^{3.3}$ f.f.u./ml for wild type). This same study observed that a chimaera of JFH-1 containing the core gene from a genotype 1a isolate had a replicative advantage over JFH-1. Incorporation of two amino acids from the genotype 1a sequence into JFH-1 (cysteine and serine at positions 172 and 173), plus the N534K resulted in a virus which produced higher infectious virus titres in cell culture much more quickly than wild type JFH-1 ($10^{5.7}$ f.f.u./ml, compared to $10^{2.9}$ f.f.u./ml for wild type after one infection).

Another study continuously passaged infected Huh7.5 cells in order to identify possible cell culture adaptive mutations[408]. Two cultures were performed. In the culture passaged 11 times, 7 mutations were identified, and in the culture passaged 6 times, 3 mutations were identified. Of these mutations, two conferred an increase in released infectious virus when deliberately introduced into the genome. One of these mutations was amino acid substitution N765D in the p7 protein. In addition, when this mutation was incorporated along with two others (I1316V in NS3 and Y2103H in NS5A), an increase in released infectious virus was observed compared to wild type JFH-1. The other mutation observed to enhance viral titres was amino acid substitution V2440L in NS5A. This mutation was also capable of enhancing viral titres in intergenotypic chimaeras (including those in Figure 8C), but not in the intragenotypic chimaera Jc1. Again, most of the mutations observed in cultured JFH-1 did not confer a replicative advantage upon the virus when deliberately introduced.

The protocol for sequencing described, involved taking total intracellular RNA samples and synthesising cDNA from the positive strand of the HCV genome, and generating PCR products from this cDNA for sequencing. Multiple rounds were performed on the same sample of RNA. Similar methods have also been used in other published work[409]. This method has certain advantages and disadvantages in sequencing analysis, e.g. it will generate a consensus sequence from the culture. The advantage of a consensus is that it identifies the mutations which occur in the majority of genomes in the cell. It is possible that there are time-dependent mutations which may occur at a certain passage and disappear over time so that if the same culture were sequenced at a later timepoint the same mutations may not appear. However this method will not identify mutations in individual genomes in the population. In the human host HCV is a heterogeneic virus with a population made up of genetic quasispecies. In order to identify mutations in each genome present, the original RNA isolate would have to be diluted out so that samples containing (less than) one genome could be synthesised for cDNA synthesis. PCR products of cDNA would have to be cloned into bacterial vectors and multiple clones sequenced for each region of interest and for each genome. Given the high number of genomes (10^8 per μg total cellular RNA), this would be a massive

task, but would provide excellent data on quasispecies genetic makeup. This was not required here, however as the goal was to find potential cell culture adaptive mutations responsible for the overall higher levels of replication.

Alternative explanations, not part of this study, for the apparent increasing fitness of JFH-1 in cell culture over time include selection of cells for those which can support higher viral and cellular replication. It is known that cultured cells mutate over time. The Huh7 line is a hepatocellular carcinoma line, and as a cancer line it may inherently have some deficiencies in the proofreading element of their replication machinery. Huh7 cultures are known to be heterogeneous both within individual cultures and between different laboratory sources. The line was first isolated in 1982, and nearly 30 years is a long time when considering cell doubling times of around 24 hours, giving lines plenty of time to diverge genetically and phenotypically, even with good laboratory practice of making stocks of low passage cells. As already described, the clearest evidence for a case of the host cell being responsible for an observed high level of HCV replication is that of Huh7.5 cells[375], which contain a defect in the RIG-I gene, thus impairing the cell's ability to detect HCV RNA.

3.3 Identification of Host Genes Regulated During HCV Infection

The ability of JFH-1 to replicate in cell culture allows for the investigation of events occurring in the cell during HCV infection. The goal of these experiments was to identify host genes and biological processes regulated during HCV infection. To this end, the described infection experiments were performed and the RNA extracted from samples for microarray analysis. The use of Affymetrix GeneChip Human Genome U133 Plus 2.0 arrays allowed relative expression levels of all genes in the human genome to be quantified. These arrays contain around 55,000 probe sets corresponding to the roughly 30,000 genes in the human genome, with some genes represented by more than one probeset. An initial timecourse experiment was performed which yielded information on the most appropriate protocols to use in these experiments. This information was used to perform the experiments from which the data on the effect of HCV infection on host gene expression is drawn. An experiment was performed comparing the gene expression between JFH-1 infected and mock infected Huh7.5 cells. A second experiment was performed to compare the gene expression between JFH-1 infected and mock infected Huh7 cells. This experiment using Huh7 cells also incorporated an experiment investigating the effect of anti-viral inhibitors on the expression of host genes in JFH-1 infected Huh7 cells.

3.3.1 Initial Timecourse

An initial timecourse experiment was designed to establish the correct protocol for infection of samples for microarray analysis, and to determine the effect of HCV infection on gene expression in Huh7.5 cells. The MOI used in experiments was essentially determined by the amount and titre of virus it was possible to produce. The highest MOI possible would give the most cells infected for the course of the experiment. The highest MOI it was possible to consistently obtain, given the target experimental setup of $25cm^2$ flasks and a 1 ml volume of virus to be added, was an MOI of 3. Figure 53 (Appendix A6) shows that any MOI of above 1 would have given maximal infection levels at 48 hours post-infection, as represented by intracellular RNA levels. In addition to the experimental evidence, it can be calculated theoretically using a Poisson distribution, that there is a 95% chance that any given cell will be infected by at least one focus forming unit when infecting with an MOI of 3 focus forming units.

The infection protocol for the microarray experiment was performed (as described in the Methods 2.5.2). Briefly, Huh7.5 cells were seeded in $25cm^2$ cell culture flask. The next day, cells were washed with PBS and then were either infected at an MOI of 3 or mock infected. At 4 hours post-infection, the infection and mock media were removed, cells were washed with PBS, and normal growth medium was added. At 0, 6, 12, 18, 24, and 48 hours post-infection, growth medium was removed and cells were washed with PBS before total cell RNA was extracted by the Trizol method. Microarray hybridisation and data analyses were performed as described using Affymetrix GeneChip Human Genome U133 Plus 2.0 arrays and Array Studio software.

		Fold Change in Expression				
Gene Symbol	**Probe Set**	**6 hours**	**12 hours**	**18 hours**	**24 hours**	**48 hours**
RPS6	211690_at	580.04	592.22	942.27	744.43	1552.09
SAA1	214456_x_at	1.00	1.28	1.19	1.07	2.28
---	232504_at	1.26	1.12	1.12	1.23	2.13
ATF3	202672_s_at	1.04	1.29	0.73	0.96	2.04
MLCK	238834_at	1.93	0.63	1.04	0.86	0.49
OLFML2A	213075_at	0.39	0.51	0.60	0.81	0.44
GPC4	204984_at	0.67	0.65	0.82	0.84	0.44
TCF7L1	221016_s_at	1.03	1.00	0.93	1.17	0.41
FAT3	236029_at	0.48	0.70	0.69	0.78	0.34

Table 2: Host genes most highly regulated during JFH-1 infection of Huh7.5 cells identified by the initial microarray experiment.

Huh7.5 cells were infected with JFH-1 at an MOI of 3 or mock infected, and RNA was extracted at 0, 6, 12, 18, 24, and 48 hours post-infection. All conditions were performed in triplicate. Affymetrix GeneChip Human Genome U133 Plus 2.0 arrays were used for hybridisation and Array Studio software was used for analysis. One array was used per RNA sample. Genes listed are those that were observed to change in expression by more than 2 fold at 48 hours post-infection in JFH-1 infected cells compared to mock infected cells.

To determine the consistency of the assay over time, gene expression at each designated time point was compared with gene expression at the 0 hour time point. Changes in gene expression were observed over time in both the mock infected and the infected cells. When compared against the time 0 hours mock infected Huh7.5 cells, 3414 genes were seen to change in expression levels in the mock infected Huh7.5 cells over all timepoints. These genes were discounted from the analysis, generating a list of the genes which changed in expression level only between infected cells and mock infected cells. 284 genes are listed in this analysis. Genes exhibiting expression changes of 4 fold or more were chosen as significant for further investigation. As can be seen in Table 2, very few genes were observed to change in expression by a modulus fold change of greater than 2 during infection at 48 hours post infection. Only one gene changed by more than 4 times: RPS6 (ribosomal protein S6). RPS6 had a greater than 512 fold increase in transcript levels across all time points. More genes were observed to be down-regulated by a significant amount, especially at early timepoints, although most had highly variable expression levels across time points. This variability across timepoints is demonstrated in Figure 19, where the number of genes overlapping between different timepoints is very small.

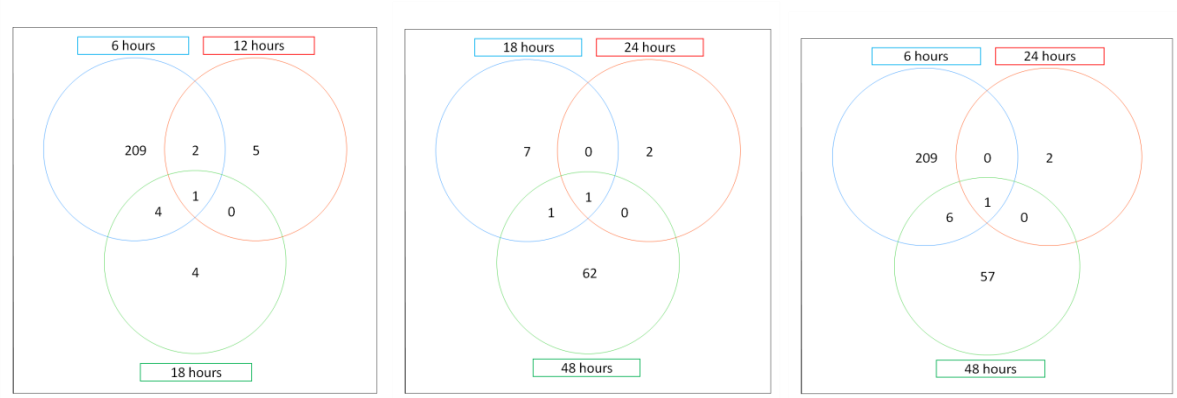


Figure 19: Number of genes changing in expression level at multiple time points in the initial microarray analysis of JFH-1 infected Huh7.5 cells.

The number in each circle represents the number of genes that changed in expression level, to any degree, in infected Huh7.5 cells compared to mock infected Huh7.5 cells. **A** Comparison infected versus mock at 6 (blue), 12 (red) and 18 (green) hour timepoints. **B** Comparison infected versus mock at 18 (blue), 24 (red) and 48 (green) hour timepoints. **C** Comparison infected versus mock at 6 (blue), 24 (red) and 48 (green) hour timepoints. These diagrams show that genes seen to change in expression level changed at only one time point. Only one gene, ribosomal protein S6, was seen to change in expression level over all time points

It was therefore determined that analysis of this data would not yield useful information. A new experiment with a modified protocol for infection was designed. The primary function of the revised protocol, used in all further infection experiments, was to limit the number of manipulations of the cells, and therefore limit as far as possible the physical and environmental stresses put on the cells.

3.3.2 Identification of Host Genes Regulated During HCV Infection of Huh7.5 Cells

A timecourse experiment with a revised infection protocol was designed to determine the effect of HCV infection on gene expression in Huh7.5 cells by microarray analysis. The infection protocol was performed, as described in Methods (2.5.3), with the aim of reducing the number of manipulations of the cells to an absolute minimum. Briefly, Huh7.5 cells were seeded in 25cm^2 cell culture flask. The next day, cells were infected at an MOI of 3, mock infected or not infected. At 0, 6, 12, 18, 24, and 48 hours post-infection, growth medium was removed and total cell RNA was extracted by the Trizol method. Microarray hybridisation and data analyses were performed as described. Raw microarray data were analysed using Array Studio software. After consultation with statisticians and researchers with experience of microarray analysis, specific parameters were decided upon for the analyses. Fold changes identified were not considered significant if the mean fluorescence signal of the maximally fluorescent condition was below the background level. A cut-off of 2-fold change in expression and a p-value of 0.05 were used to determine whether a gene was significantly regulated during infection.

After analysis, 2851 probe sets (comprising of 1477 named genes and 996 poorly characterised loci or transcripts) were found to be altered in expression by at least 2-fold for at least one timepoint in JFH-1 infected cells compared to mock infected cells. Table 3 describes the number of probe sets found to be significantly differentially expressed between JFH-1 infected and mock infected Huh7.5 cells. The genes observed to be most highly regulated during JFH-1 infection are described in Table 4, and the genes observed to be significantly regulated across all timepoints are described in Table 5.

	6 hours	12 hours	18 hours	24 hours	48 hours
Fold change > 2	527	203	226	179	180
Fold change < -2	891	433	719	525	413
|Fold Change| > 2	1418	636	945	704	593

Table 3: Number of probe sets significantly regulated between JHF-1 infected and mock infected Huh7.5 cells.

Huh7.5 cells were infected with JFH-1 at an MOI of 3 or mock infected, and RNA was extracted at 0, 6, 12, 18, 24, and 48 hours post-infection. All conditions were performed in triplicate. Affymetrix GeneChip Human Genome U133 Plus 2.0 arrays were used for hybridisation and Array Studio software was used for analysis. One array was used per RNA sample. Microarray data were analysed by Array Studio software, and cut-offs for significant changes in expression were set selected as a fold change in expression of greater than two, with a significance of $p<0.05$. The number of probe sets identified as meeting these conditions at each timepoint is given.

To aid interpretation of the data comprising the large number of genes identified as changing during infection, further bioinformatic analysis was performed. Use of Panther software allowed identification of the biological pathways represented in the genes identified as changing during infection. Table 6 describes the major biological processes identified to be affected during infection. Several processes of particular interest to the study of HCV, based on current knowledge, were identified. These included immunity, apoptosis, cellular proliferation, signalling, and lipid metabolism.

The results obtained by microarray analysis were validated by a second method, in this case, quantitative PCR. A separate infection experiment was performed, using the same infection protocols, and RNA was extracted by the Trizol method. However, in this case, the relative expression levels of specific genes were quantified by quantitative PCR instead of microarray analysis. This process allows the confirmation of expression changes for specific genes of interest, and, if most gene expression levels assessed by quantitative PCR a shown to be in agreement with microarray data, it validates the use of microarray analysis for studying gene expression in this model system. Figure 22 and Figure 23 show that most expression levels determined by quantitative PCR were in agreement with the data generated by microarray analysis.

Genes were identified that exhibited increased expression during HCV infection. Some of these genes were selected for investigation of their requirement for HCV replication. Genes were chosen for further study based primarily on two criteria; the levels of fold change observed, and the potential for roles in HCV replication based on current knowledge or predictions of their function.

			Fold Change in Expression				
Gene	**Gene Title**	**Probe Set Id**	**6 hr**	**12 hr**	**18 hr**	**24 hr**	**48 hr**
MGAM	maltase-glucoamylase (alpha-glucosidase)	206522_at	1.01	1.31	1.06	1.43	5.62
CD300LF	CD300 molecule-like family member f	1553043_a_at	2.22	3.05	3.94	2.75	4.56
RIN2	Ras and Rab interactor 2	233811_at	1.34	1.04	-1.25	1.12	3.89
LGALS3	lectin, galactoside-binding, soluble, 3	1557197_a_at	1.21	1.36	-1.16	1.44	3.53
CCL3	chemokine (C-C motif) ligand 3	205114_s_at	1.13	1.85	1.46	1.39	3.36
LBP	lipopolysaccharide binding protein	214461_at	1.09	1.45	2.19	2.51	3.34
ANKRD60	Ankyrin repeat domain 60	230683_at	1.09	1.64	1.16	-1.72	3.34
SLC10A7	solute carrier family 10, member 7	1555108_at	-1.25	1.80	1.62	-1.03	3.23
SOD2	superoxide dismutase 2, mitochondrial	215078_at	1.06	1.88	2.14	2.50	3.20
TXNIP	thioredoxin interacting protein	201008_s_at	1.24	1.92	1.66	1.21	3.18
ANXA13	annexin A13	208323_s_at	1.92	-1.16	1.28	-1.61	3.18
RECQL5	RecQ protein-like 5	1561720_at	-2.27	-1.47	-1.35	1.15	3.16
TXNIP	thioredoxin interacting protein	201010_s_at	2.04	1.52	2.60	1.40	3.03
LBP	lipopolysaccharide binding protein	211652_s_at	1.26	1.27	1.79	2.03	2.99
SAA1/2	serum amyloid A1 / A2	208607_s_at	1.22	1.97	2.33	3.07	2.97
BATF2	basic leucine zip tcriptn factor, ATF-like 2	228439_at	3.05	-1.25	1.01	1.13	2.95
SLC6A4	solute carrier family 6, member 4	242009_at	2.33	1.12	1.31	1.37	2.91
VNN3	vanin 3	220528_at	1.04	2.28	2.53	1.78	2.89
ZNF24	zinc finger protein 24	1554045_at	-1.20	-1.14	1.27	1.39	2.89
MBD2	methyl-CpG binding domain protein 2	214397_at	-1.45	-1.61	-1.02	1.75	2.87
ABLIM3	actin binding LIM protein family, 3	205730_s_at	-1.64	-1.32	1.14	1.68	2.85
FXYD3	FXYD dom. cont. ion transport regulator 3	202489_s_at	1.31	1.04	1.06	-1.10	2.85
STAT4	signal tducer and activator of tcriptn 4	206118_at	-1.16	-1.49	-1.41	-2.78	-4.17
COL1A1	collagen, type I, alpha 1	202310_s_at	-1.67	-3.85	-2.33	-6.67	-4.17
MT1M	metallothionein 1M	217546_at	-1.64	-2.78	-5.00	-7.69	-4.17
SUSD4	sushi domain containing 4	219389_at	-4.35	-5.00	-3.57	-8.33	-4.35
SDPR	serum deprivation response	222717_at	-1.67	1.01	-2.13	-2.50	-4.35
MAB21L2	mab-21-like 2 (C. elegans)	210302_s_at	-1.75	-2.33	-1.56	-5.00	-4.35
NOX4	NADPH oxidase 4	219773_at	-1.04	1.05	-1.49	1.13	-4.55
ERBB4	v-erb-a erythroblastic leukemia viral oncogene homolog 4 (avian)	214053_at	-3.23	-2.00	-2.50	-3.70	-4.55
MT1G	metallothionein 1G	204745_x_at	-1.33	-2.13	-2.86	-3.57	-4.55
FBN1	fibrillin 1	235318_at	-2.44	-3.03	-3.85	-4.17	-5.00
NPPB	natriuretic peptide precursor B	206801_at	-2.04	-2.50	-5.88	-7.69	-5.00
MT1F	metallothionein 1F	217165_x_at	-1.59	-2.56	-3.23	-4.17	-5.26
LOXL4	lysyl oxidase-like 4	227145_at	-3.45	-3.57	-4.17	-4.55	-5.26
MT1F	metallothionein 1F	213629_x_at	-1.43	-2.50	-3.03	-4.00	-5.26
ADH1A	alcohol dehydrogenase 1A,α polypeptide	207820_at	-1.45	-1.32	2.33	-1.75	-5.56
TAGLN	transgelin	1555724_s_at	-2.00	-2.27	-3.85	-6.25	-5.56
MT1E	metallothionein 1E	212859_x_at	-1.79	-2.94	-3.23	-3.57	-5.56
FAT3	FAT tumor suppressor homolog 3	236029_at	-3.23	-2.78	-1.43	-7.69	-6.25
FLRT2	Fibronectin Leu rich transmembrane 2	240259_at	-2.17	-2.22	-3.45	-4.76	-6.25
NPNT	nephronectin	225911_at	-2.86	-3.03	-3.03	-4.17	-7.14
NCF2	neutrophil cytosolic factor 2	209949_at	-6.25	-8.33	-14.29	-25.00	-7.69
TAGLN	transgelin	205547_s_at	-1.96	-2.27	-4.55	-7.14	-8.33
LEFTY2	left-right determination factor 2	206012_at	-14.29	-8.33	-12.50	-16.67	-12.50
COL1A1	collagen, type I, alpha 1	1556499_s_at	-5.26	-8.33	-4.35	-16.67	-14.29

Table 4: Host genes most highly regulated at 48 hours post-infection of Huh7.5 cells.

Huh7.5 cells were infected with JFH-1 at an MOI of 3 or mock infected, and RNA was extracted at 0, 6, 12, 18, 24, and 48 hours post-infection. All conditions were performed in triplicate. Affymetrix GeneChip Human Genome U133 Plus 2.0 arrays were used for hybridisation and Array Studio software was used for analysis. One array was used per RNA sample. Probe sets which were not ascribed to a specific named gene have not been included in this table.

Gene Symbol	Gene Title	probe set id	6	12	18	24	48
CD300LF	CD300 molecule-like family member f	1553043_a_at	2.22	3.05	3.94	2.75	4.56
HLF	hepatic leukemia factor	204754_at	2.19	2.75	2.14	2.00	2.03
ACADL	acyl-Coenzyme A dehydrogenase, long chain	206069_s_at	-4.59	-3.78	-2.50	-3.84	-2.06
UACA	uveal autoantigen with coiled-coil domains and ankyrin repeats	238868_at	-4.69	-4.00	-3.71	-3.76	-2.23
SEMA3C	sema domain, immunoglobulin domain (Ig), short basic domain, secreted, (semaphorin) 3C	203789_s_at	-2.04	-2.50	-2.79	-4.29	-2.28
LMCD1	LIM and cysteine-rich domains 1	242767_at	-4.72	-3.12	-3.03	-7.57	-2.39
SERPINE2	serpin peptidase inhibitor, clade E (nexin, plasminogen activator inhibitor type 1), member 2	212190_at	-2.11	-2.20	-2.79	-3.01	-2.41
NRP2	Neuropilin 2	228699_at	-3.97	-4.14	-4.59	-3.27	-2.41
DPYSL3	dihydropyrimidinase-like 3	201431_s_at	-2.03	-3.34	-2.83	-6.15	-2.43
TIMP4	TIMP metallopeptidase inhibitor 4	206243_at	-3.32	-2.50	-2.60	-5.03	-2.48
CUX2	cut-like homeobox 2	213920_at	-3.46	-2.14	-2.39	-2.31	-2.50
MICAL2	microtubule associated monoxygenase, calponin and LIM domain containing 2	212472_at	-2.58	-3.05	-2.60	-3.68	-2.55
JAK1	Janus kinase 1 (a protein tyrosine kinase)	239695_at	-4.66	-2.36	-3.18	-2.23	-2.58
KLRC1 /// KLRC2	killer cell lectin-like receptor subfamily C, member 1 /// killer cell lectin-like receptor subfamily C, member 2	206785_s_at	-3.46	-2.75	-3.51	-2.85	-2.60
NODAL	nodal homolog (mouse)	230916_at	-13.00	-7.01	-4.35	-6.68	-2.60
PRSS23	protease, serine, 23	202458_at	-2.19	-2.33	-3.18	-3.68	-2.66
MICAL2	microtubule associated monoxygenase, calponin and LIM domain containing 2	212473_s_at	-2.71	-2.77	-2.83	-3.43	-2.69
ANGPTL2	angiopoietin-like 2	213004_at	-5.10	-5.66	-2.45	-7.89	-2.79
HAO2	hydroxyacid oxidase 2 (long chain)	220801_s_at	-4.41	-6.06	-4.44	-4.56	-2.83
LOC728449	hypothetical protein LOC728449	1557094_at	-2.22	-2.20	-2.45	-2.69	-2.85
DPYSL3	dihydropyrimidinase-like 3	201430_s_at	-3.16	-3.81	-4.86	-8.17	-2.99
ENTPD4 /// LOXL2	ectonucleoside triphosphate diphosphohydrolase 4 /// lysyl oxidase-like 2	202998_s_at	-2.07	-2.99	-2.81	-6.82	-3.27
TNFRSF19	tumor necrosis factor receptor superfamily, member 19	227812_at	-4.29	-2.77	-3.46	-4.29	-3.27
PRSS23	protease, serine, 23	226279_at	-2.39	-2.20	-3.76	-10.06	-3.56
NRP2	Neuropilin 2	228103_s_at	-4.11	-3.43	-4.29	-5.35	-3.56
PALMD	palmdelphin	218736_s_at	-2.62	-2.31	-2.30	-3.34	-3.86
ANGPTL2	angiopoietin-like 2	213001_at	-5.39	-7.01	-5.21	-4.32	-3.89
LEFTY1	left-right determination factor 1	206268_at	-3.10	-8.63	-5.78	-9.45	-3.97
DACT1	dapper, antagonist of beta-catenin, homolog 1 (Xenopus laevis)	219179_at	-14.03	-8.51	-3.68	-11.24	-3.97
SUSD4	sushi domain containing 4	219389_at	-4.26	-4.99	-3.63	-8.06	-4.32
FBN1	fibrillin 1	235318_at	-2.43	-2.99	-3.86	-4.08	-4.92
NPPB	natriuretic peptide precursor B	206801_at	-2.06	-2.51	-5.82	-7.94	-4.96
LOXL4	lysyl oxidase-like 4	227145_at	-3.51	-3.53	-4.17	-4.53	-5.28
TAGLN	transgelin	1555724_s_at	-2.00	-2.27	-3.92	-6.15	-5.54
FLRT2	Fibronectin leucine rich transmembrane protein 2	240259_at	-2.16	-2.23	-3.41	-4.82	-6.23
NPNT	nephronectin	225911_at	-2.83	-2.99	-3.05	-4.20	-7.26
NCF2	neutrophil cytosolic factor 2	209949_at	-6.28	-8.63	-13.64	-23.10	-7.73
LEFTY2	left-right determination factor 2	206012_at	-13.93	-8.46	-12.38	-16.68	-12.04
COL1A1	collagen, type I, alpha 1	1556499_s_at	-5.39	-8.17	-4.44	-18.00	-15.35

Table 5: Probe Sets regulated during infection of Huh7.5 cells by a greater than 2-fold change at all timepoints.

46 probe sets were observed to be regulated by greater than 2-fold across all timepoints during infection of Huh7.5 cells with JFH-1. These probe sets are sorted by fold change at 48 hours post-infection. Probe sets without an assigned named gene are not shown.

	6 hours			12 hours			18 hours			24 hours			48 hours		
Biological Process	Observed	Expected	P-Value	Observed	Expected	P-Value	Observed	Expected	P-Value	Observed	Expected	P-Value	Observed	Expected	P-Value
Biological process unclassified	31	95.27	1.64E-19	17	49.41	1.71E-09	143	201.21	4.55E-07	99	146.01	2.25E-06	93	122.87	5.00E-03
Signal transduction	75	28.66	2.67E-14	36	14.87	6.56E-06	113	60.54	8.85E-10	96	43.93	1.52E-12	63	36.96	4.30E-04
Cell surface receptor mediated signal transduction	37	13.78	6.18E-06	22	7.15	3.12E-04	50	29.11	2.32E-02	39	21.13	2.69E-02	34	17.78	3.46E-02
Developmental processes	41	18.11	2.09E-05	24	9.39	5.06E-04	86	38.25	4.10E-11	62	27.76	6.34E-08	55	23.36	7.07E-08
Immunity and defence	28	11.09	2.23E-04	15	5.75	1.95E-02	41	23.43	1.36E-02	36	17	6.92E-04	27	14.3	4.01E-02
Angiogenesis	4	0.45	2.40E-01	4	0.24	2.01E-02	6	0.96	9.29E-02	6	0.7	1.67E-02	6	0.59	6.47E-03
Inhibition of apoptosis	6	1.08	1.20E-01	5	0.56	3.86E-02	6	2.28	1.00E+00	9	1.65	7.74E-03	3	1.39	1.00E+00
Lipid, fatty acid and steroid metabolism	14	6.48	1.88E-01	10	3.36	6.42E-02	29	13.69	4.94E-03	17	9.93	7.34E-01	17	8.36	1.53E-01
Receptor protein tyrosine kinase signalling pathway	7	1.78	4.47E-01	6	0.92	6.96E-02	14	3.75	6.90E-03	10	2.72	9.79E-02	8	2.29	4.74E-01
Apoptosis	16	4.47	4.27E-04	8	2.32	7.37E-02	22	9.44	8.61E-03	22	6.85	7.06E-05	17	5.76	2.72E-03
Cell communication	28	10.21	2.19E-04	14	5.29	1.22E-01	50	21.56	6.60E-06	41	15.64	3.63E-06	31	13.16	1.56E-03
Proteolysis	15	8.08	1.00E+00	12	4.19	1.49E-01	19	17.06	1.00E+00	26	12.38	5.26E-02	25	10.42	8.62E-03
Cell adhesion	9	5.23	1.00E+00	8	2.71	1.89E-01	22	11.06	6.48E-02	23	8.02	2.62E-04	18	6.75	5.86E-03
Intracellular signalling cascade	25	7.33	1.70E-05	11	3.8	2.24E-01	34	15.48	3.15E-03	31	11.23	7.11E-05	15	9.45	1.00E+00
Granulocyte-mediated immunity	6	0.54	2.93E-03	3	0.28	4.19E-01	6	1.14	1.63E-01	6	0.83	3.05E-02	6	0.69	1.20E-02
Mesoderm development	12	4.64	3.92E-01	8	2.4	4.31E-01	36	9.79	6.43E-09	26	7.11	3.21E-06	19	5.98	1.80E-03
Cell proliferation and differentiation	22	8.65	2.05E-03	10	4.49	4.57E-01	34	18.27	1.48E-02	28	13.26	6.12E-03	21	11.16	1.41E-01
Neurogenesis	11	4.94	1.00E+00	8	2.56	8.60E-01	23	10.43	8.70E-02	16	7.57	8.94E-01	19	6.37	5.79E-03
Cell structure and motility	22	9.66	9.63E-03	10	5.01	8.96E-01	47	20.4	4.48E-06	33	14.81	5.75E-04	28	12.46	2.03E-03
Protein biosynthesis	1	4.97	1.00E+00	0	2.58	1.00E+00	1	10.5	4.13E-02	3	7.62	1.00E+00	1	6.41	1.00E+00
Ectoderm development	13	5.82	9.04E-01	8	3.02	1.00E+00	25	12.3	1.16E-01	17	8.93	1.00E+00	21	7.51	4.11E-03
Cell motility	13	2.96	1.64E-03	5	1.54	1.00E+00	20	6.26	1.11E-03	23	4.54	5.71E-08	15	3.82	1.38E-03
Ligand-mediated signalling	18	3.54	5.25E-06	6	1.84	1.00E+00	21	7.48	6.07E-03	14	5.43	2.67E-01	13	4.57	1.62E-01
Cell adhesion-mediated signalling	5	3.19	1.00E+00	5	1.65	1.00E+00	12	6.74	1.00E+00	16	4.89	8.80E-03	9	4.11	1.00E+00
Oncogenesis	14	3.97	1.75E-03	6	2.06	5.51E-01	17	8.39	1.67E-01	14	6.09	1.16E-01	8	5.12	1.00E+00
NF-kappaB cascade	6	0.6	7.10E-03	2	0.31	1.00E+00	3	1.26	1.00E+00	3	0.92	1.00E+00	4	0.77	1.00E+00
Cytokine and chemokine mediated signalling pathway	10	2.12	1.30E-02	4	1.1	1.00E+00	11	4.48	1.00E+00	6	3.25	1.00E+00	7	2.73	1.00E+00
Steroid metabolism	8	1.54	2.69E-02	4	0.8	1.00E+00	5	3.25	1.00E+00	6	2.36	1.00E+00	5	1.99	1.00E+00
Sulphur metabolism	5	0.78	3.85E-02	3	0.41	2.51E-01	3	1.65	1.00E+00	4	1.2	1.00E+00	2	1.01	1.00E+00

Table 6: Host cellular biological processes identified to be affected by transcriptional regulation during JFH-1 infection of Huh7.5 cells.

Panther analysis was performed using all genes which met the cut-off of a 2-fold change. Processes identified as having an enriched number of genes (with a p-value cut-off of 0.05, stringently calculated using the Bonferroni correction option), represented in the microarray data compared with the expected random number of genes based on the whole human genome, for at least one timepoint, are shown. Given for each timepoint and biological process are the observed number of genes regulated during infection, the expected number of genes based on the proportion of genes involved in that process in the entire human genome, and finally a p-value representing the probability that the difference between observed and expected numbers is not significant.

A striking pattern observed in the microarray data was the downregulation of metallothionein genes. Figure 20 shows that expression of all forms of MT1, and MT2A, were down during JFH-1 infection of Huh7.5 cells. Expression levels of MTs in infected cells were also observed to decrease over time.

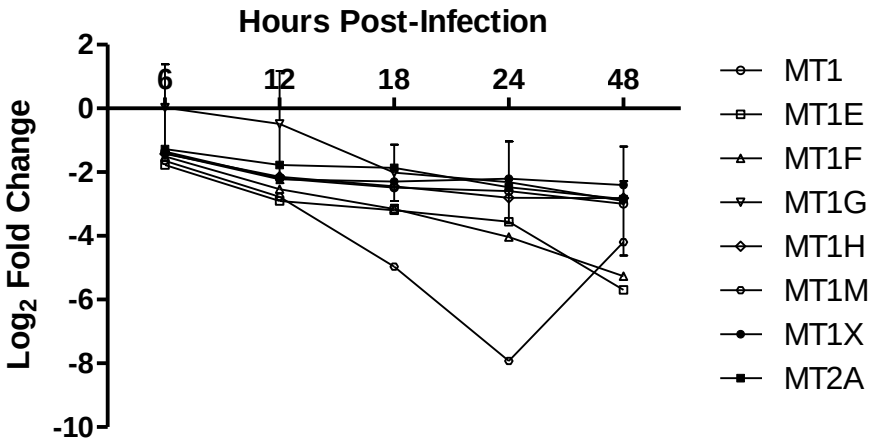


Figure 20: Fold change in expression of Metallothioneins during JFH-1 infection of Huh7.5 cells. Metallothioneins were clearly seen to be down regulated in infected Huh7.5 cells, with expression levels in infected cells decreasing over time. Where a gene is represented on the microarray by more than one probe set, data were averaged and displayed with error bars. The data set MT1 corresponds to a probe set which recognises all MT1 isoforms

Genes observed to be regulated by more than two fold at 48 hours post-infection have been presented in heatmap form. Figure 21 presents these genes grouped by biological processes identified in the Panther analysis of microarray data (Table 6, Figure 21). As a visual aid, heatmap data is presented on a $\log_2$ scale. Upregulated genes are shown in red and downregulated genes are shown in green. Maximal colour intensity is assigned to genes with a relative expression change of 3 fold or higher (1.5 fold on the $\log_2$ scale).

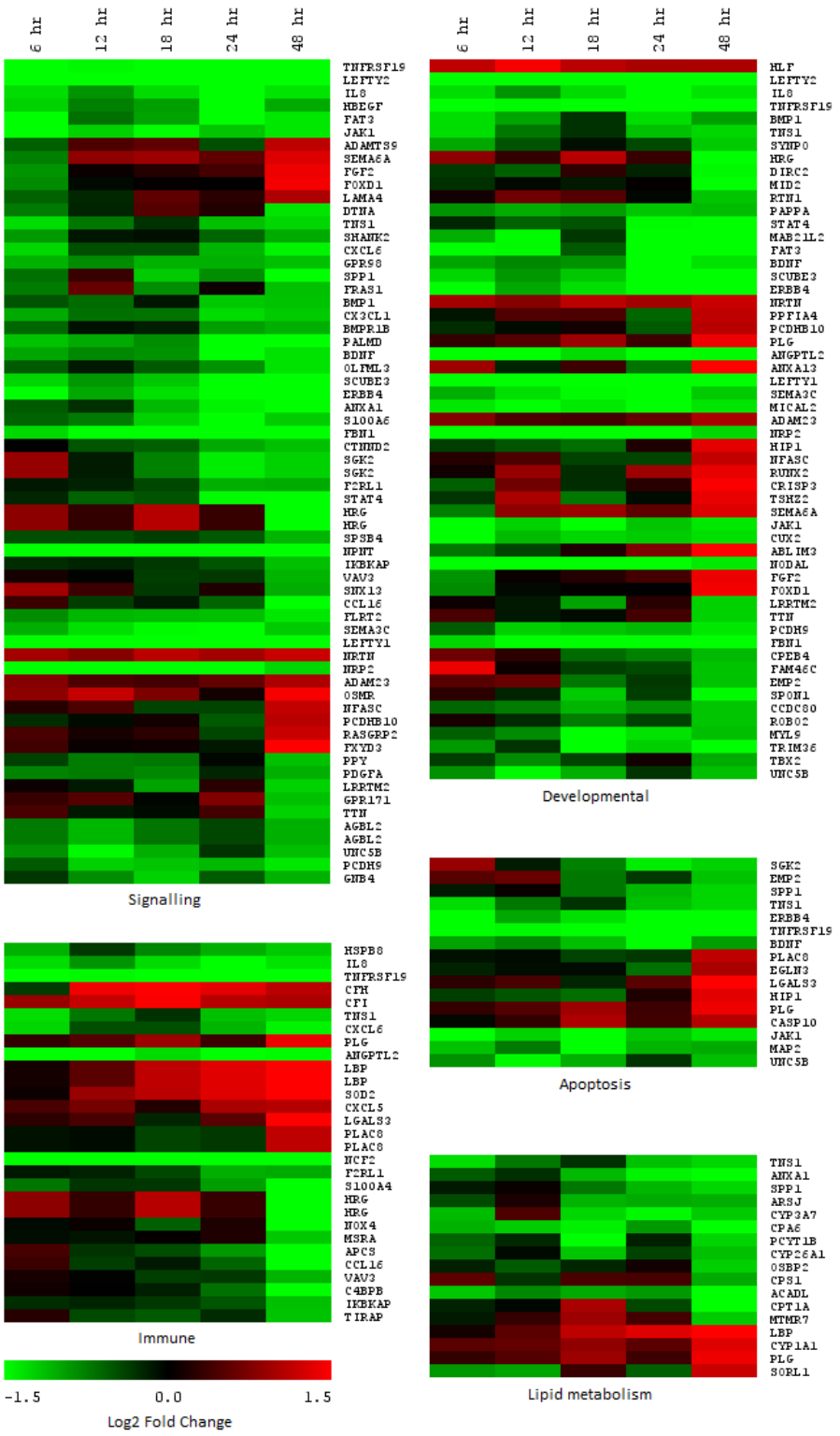


Figure 21: Host biological processes regulated during JFH-1 infection of Huh7.5 cells.

Genes identified to be regulated during JFH-1 infection of Huh7.5 cells are presented in heatmap form with each heatmap corresponding to biological processes identified using Panther analysis. Heatmaps were generated using MeV software and genes are clustered within heatmaps by Pearson correlation. Genes shown in red were upregulated and genes shown in green were downregulated, displayed on a $\log_2$ fold change scale. Data presented is an average calculated from the three replicates each performed for JFHF-1 infected and mock infected Huh7.5 cells.

To confirm the validity of the data obtained from the microarray study, gene expression level changes were measured by qPCR. A new set of replicate infections was performed in Huh7.5 cells, and the expression levels of a number of genes were measured by qPCR. A small number of genes only were chosen, as the purpose of the experiment was just to validate the principal that the microarray data were true representations of the expression changes occurring during infection. Validation was performed on the genes presented in Figure 22 and Figure 23. Figure 22A shows the correlation between PCR and microarray data for genes upregulated at 6 hours post-infection, and Figure 22B for genes upregulated at 48 hours post-infection. Figure 23 shows the correlation between PCR and microarray data for genes in the metallothionein family at 48 hours post-infection, all of which were observed to be downregulated during infection.

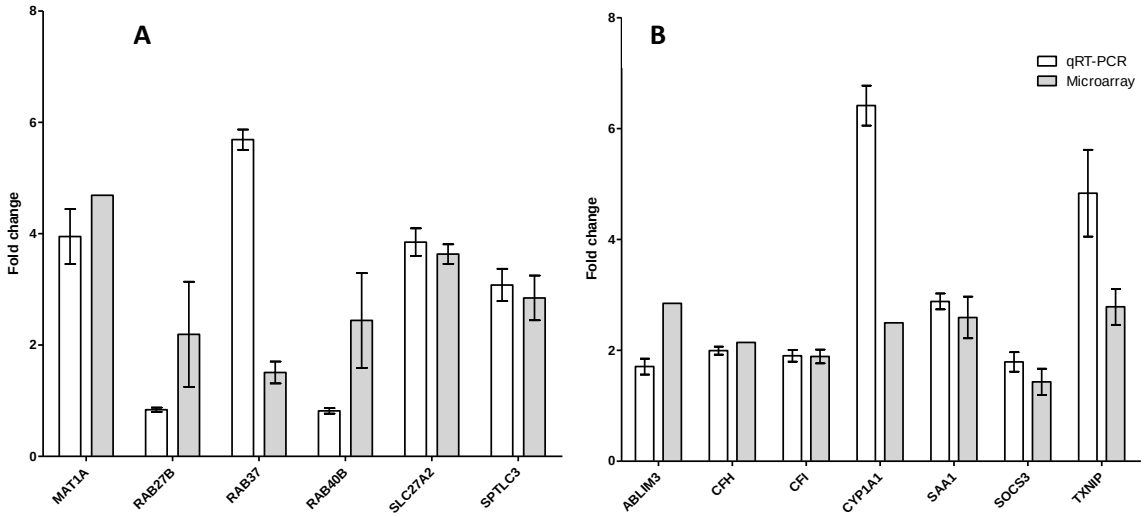


Figure 22: Validation by PCR of gene expression levels in Huh7.5 cells infected with JFH-1.
Huh7.5 cells were infected with JFH-1 at an MOI of 3 or mock infected for 6 hours (**A**) or 48 hours (**B**). PCR quantification of relative expression levels for a selection of genes was performed (as described in methods 2.6). Mean and SEM are presented for quantitative PCR results which were obtained from triplicate infections in two separate experiments. For microarray data, where more than one probeset corresponding to a single gene was present in the array, the data presented is the mean and standard error of the mean. The majority of gene expression levels determined by PCR and microarray were observed to be in agreement.

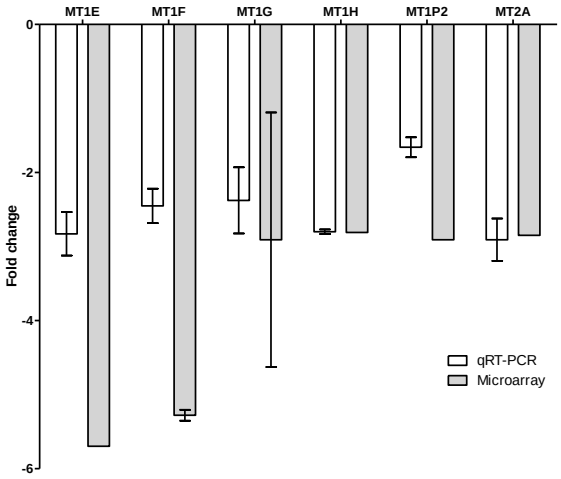


Figure 23: Validation by PCR of metallothionein gene expression levels in Huh7.5 cells infected with JFH-1.

Huh7.5 cells were infected with JFH-1 at an MOI of 3 or mock infected for 48 hours. PCR quantification of relative expression levels for a selection of metallothionein genes was performed as described in methods. Mean and SEM are presented for quantitative PCR results which were obtained from triplicate infections in two separate experiments. For microarray data, where more than one probeset corresponding to a single gene was present in the array, the data presented is the mean and standard error of the mean. All metallothioneins identified by microarray analysis to be downregulated were also identified by PCR to be downregulated.

3.3.3 Identification of Host Genes Regulated During HCV Infection of Huh7 Cells

Huh7.5 cells are a useful model for the study of HCV infection. However, they are a cell line that has been created by selection for their ability to support HCV replication. In particular, they are known to lack functional RIG-I, and hence do not have that mechanism for the detection of HCV RNA. This is not the case in human liver, where RIG-I is functional. Alteration of gene expression due to infection in the absence of RIG-I may not reflect the situation found in infected liver cells. Huh7 cells have functional RIG-I. In order to more closely replicate the situation that may exist in liver cells, Huh7 cells were used in a microarray experiment to determine the effect of HCV infection on host cell gene expression.

A timecourse experiment was designed to determine the effect of HCV infection on gene expression in Huh7 cells by microarray analysis. The infection protocol was performed as described, with the aim of reducing the number of manipulations of the cells to an absolute minimum. Briefly, Huh7 cells were seeded in 25cm^2 cell culture flasks. The next day, cells were infected at an MOI of 3 or mock infected. At 0, 6, 12, 18, 24, and 48 hours post-infection, growth medium was removed and total cell RNA was extracted by the Trizol method. Microarray hybridisation and data analyses were performed as described.

After analysis 2885 probe sets (comprising of 1726 named genes and 461 poorly characterised loci or transcripts) were found to be altered in expression by at least 2-fold for at least one timepoint in JFH-1 infected cells compared to mock infected cells.

	6 hours	12 hours	18 hours	24 hours	48 hours
Fold change > 2	74	270	146	617	1275
Fold change < -2	165	117	232	383	870
|Fold Change| > 2	239	387	378	1000	2145

Table 7: Number of probe sets significantly regulated between JHF-1 infected and mock infected Huh7 cells.

Huh7.5 cells were infected with JFH-1 at an MOI of 3 or mock infected, and RNA was extracted at 0, 6, 12, 18, 24, and 48 hours post-infection. All conditions were performed in triplicate. Affymetrix GeneChip Human Genome U133 Plus 2.0 arrays were used for hybridisation and Array Studio software was used for analysis. One array was used per RNA sample. Microarray data were analysed by Array Studio software, and cut-offs for significant changes in expression were set selected as a fold change in expression of greater than two, with a significance of $p<0.05$. The number of probe sets identified as meeting these conditions at each timepoint is given.

To aid interpretation of the data comprising the large number of genes identified as changing during infection, further bioinformatic analysis was performed. Use of Panther software allowed identification of the biological pathways containing genes observed to be changing during infection. Table 10 describes the major biological processes identified to be affected during infection. Several processes of particular interest to the study of HCV, based on current knowledge, were identified. These included immunity, apoptosis, proliferation, and lipid metabolism.

			Fold Change in Expression				
Gene	**Gene Title**	**Probe Set Id**	**6 hr**	**12 hr**	**18 hr**	**24 hr**	**48 hr**
TXNIP	thioredoxin interacting protein	201010_s_at	1.38	9.3	6.03	20.51	21.96
STC2	stanniocalcin 2	203438_at	1.55	8.65	4.68	18.35	20.5
INHBE	inhibin, beta E	210587_at	-1.77	7.16	2.44	22.93	18.01
TXNIP	thioredoxin interacting protein	201008_s_at	1.3	8.39	5.26	20.15	15.32
STC2	stanniocalcin 2	203439_s_at	1.32	9.49	5.52	21.94	14.32
TXNIP	thioredoxin interacting protein	201009_s_at	1.15	6.56	4.99	13.55	14.3
ALDH1L2	Aldehyde dehydrogenase 1 family, member L2	231202_at	1.05	2.05	2.47	8.6	11.78
SLC16A14	solute carrier family 16, member 14	238029_s_at	1.52	1.3	1.04	3.08	11.23
ASNS	asparagine synthetase	205047_s_at	1.08	5.82	6.76	15.53	11.22
ARRDC4	arrestin domain containing 4	225283_at	-1.14	4.1	3.22	11.77	10.77
SAMD5	sterile alpha motif domain containing 5	228653_at	1.4	1.56	2.25	3.71	9.06
ATF3	activating transcription factor 3	202672_s_at	-1.99	5.28	1.54	6.97	8.57
PRNP	prion protein	201300_s_at	1.09	1.07	1.49	2.21	8
SOCS2	suppressor of cytokine signaling 2	203372_s_at	-1.69	1.6	-1.86	4.56	7.91
BEX1	brain expressed, X-linked 1	218332_at	1.18	1.08	2.32	2.28	7.56
LYPD1	LY6/PLAUR domain containing 1	212909_at	-1.72	-1.43	-1.47	2.16	7.33
PPARGC1A	peroxisome proliferator-activated receptor gamma, coactivator 1 alpha	219195_at	1.23	1.12	1.02	2.17	6.94
SLC1A4	solute carrier family 1 (glutamate/neutral amino acid transporter), member 4	212810_s_at	-1.28	2.51	2.12	5.45	6.84
C10orf10	chromosome 10 open reading frame 10	209183_s_at	1.28	2.08	2.11	3.42	6.63
FABP3	fatty acid binding protein 3, muscle and heart	214285_at	1.13	-1.06	1.43	1.12	6.58
KLF10	Kruppel-like factor 10	202393_s_at	-1.83	1.93	1.44	4.25	6.36
RORA	RAR-related orphan receptor A	210426_x_at	1.25	-1.04	1.38	1.68	6.28
RBM14	RNA binding motif protein 14	204178_s_at	-1.04	-1.01	-1.46	-1.26	-4.6
FDFT1	farnesyl-diphosphate farnesyltransferase 1	210950_s_at	-1.23	-1.63	-1.74	-4.16	-4.6
ID4	Inhibitor of DNA binding 4, dominant negative helix-loop-helix protein	226933_s_at	1.16	-1.66	-1.3	-2.54	-4.61
TESC	tescalcin	218872_at	-1.19	-1.39	-1.55	-2.47	-4.62
SMAD9	SMAD family member 9	227719_at	-1.05	-1.44	-1.48	-3.09	-4.77
ID4	inhibitor of DNA binding 4, dominant negative helix-loop-helix protein	209293_x_at	-1.2	-1.65	-1.28	-2.21	-4.82
BTD	biotinidase	214117_s_at	1.19	-1.11	-1.19	-1.64	-4.83
TPCN2	two pore segment channel 2	229250_at	-1.16	1.01	-1.42	-1.5	-4.87
FSCN1	fascin homolog 1, actin-bundling protein	210933_s_at	-1.43	-1.66	-1.99	-4.18	-4.88
CDKN3	cyclin-dependent kinase inhibitor 3	209714_s_at	1.01	-1.49	-1.29	-2.26	-5.09
ID4	inhibitor of DNA binding 4, dominant negative helix-loop-helix protein	209291_at	-1.2	-1.51	-1.44	-3.11	-5.14
CCNB1	cyclin B1	214710_s_at	1.06	-1.51	-1.23	-2.38	-5.23
SMAD6	SMAD family member 6	209886_s_at	-1.39	-1.67	-1.49	-2.17	-5.24
CDKN3	cyclin-dependent kinase inhibitor 3	1555758_a_at	1.04	-1.46	-1.34	-2.21	-5.34
SMAD6	SMAD family member 6	207069_s_at	-1.22	-1.74	-1.45	-5.19	-5.61
HIST1H2BC	histone cluster 1, H2bc	214455_at	1.05	1.05	-1.57	-2.36	-5.62
FAM83D	family with sequence similarity 83, member D	225687_at	1.14	-2.34	-1.32	-2.6	-5.64
GATM	glycine amidinotransferase	216733_s_at	-1.01	-1.33	-1.55	-3.08	-5.71
MYCBP	c-myc binding protein	203360_s_at	-1.2	-1.19	-1.42	-1.62	-5.78
GATM	glycine amidinotransferase	203178_at	1.05	-1.03	-1.64	-3	-5.9
RBM14	RNA binding motif protein 14	1555639_a_at	1.02	1.05	-1.68	1.04	-6.04
CDKN2C	cyclin-dependent kinase inhibitor 2C (p18, inhibits CDK4)	204159_at	1.39	-1.53	-1.2	-4.12	-6.87
B3GNT1	UDP-GlcNAc:betaGal beta-1,3-N-acetylglucosaminyltransferase 1	203188_at	1.79	1.11	-1.03	-2.63	-6.95

Table 8: Host genes most highly regulated at 48 hours post-infection of Huh7 cells.

Huh7.5 cells were infected with JFH-1 at an MOI of 3 or mock infected, and RNA was extracted at 0, 6, 12, 18, 24, and 48 hours post-infection. All conditions were performed in triplicate. Affymetrix GeneChip Human Genome U133 Plus 2.0 arrays were used for hybridisation and Array Studio software was used for analysis. One array was used per RNA sample. Probe sets which were not ascribed to a specific named gene have not been included in this table.

Gene Symbol	Gene Title	probe set id	6	12	18	24	48
TGFB1I1	transforming growth factor beta 1 induced transcript 1	209651_at	-2.92	-3.13	-5.5	-2.63	5.73
RAB27B	RAB27B, member RAS oncogene family	228708_at	2.56	2.5	3.43	2.43	5.19
RASSF9	Ras association (RalGDS/AF-6) domain family (N-terminal) member 9	210335_at	3.28	4.28	2.53	3.62	4.45
GPR109B	G protein-coupled receptor 109B	205220_at	2.03	6.06	2.77	3.41	3.18
CYP1A1	cytochrome P450, family 1, subfamily A, polypeptide 1	205749_at	2.17	4.18	2.28	5.19	2.58
SLC7A2	solute carrier family 7 (cationic amino acid transporter, y+ system), member 2	225516_at	2.3	2.75	2.62	2.88	2.52
---	---	1570561_at	29.92	12.44	17.39	2.65	2.28
SLC26A3	solute carrier family 26, member 3	206143_at	2.64	2.35	4.49	3.34	2.06
DPYSL3	dihydropyrimidinase-like 3	201431_s_at	-2.46	-3.63	-5.97	-3.12	-2
---	---	222281_s_at	-2.32	-2.7	-3.07	-2.49	-2.89

Table 9: Probe Sets regulated during infection of Huh7 cells by a greater than 2-fold change at all timepoints.

10 probe sets were observed to be regulated by greater than 2-fold across all timepoints during infection of Huh7.5 cells with JFH-1. These probe sets are sorted by fold change at 48 hours post-infection. The two probe sets without an assigned named gene are shown.

.

	6 Hours			12 Hours			18 Hours			24 Hours			48 Hours			All Hours Combined		
Biological Process	Observed	Expected	P-Value	Observed	Expected	P-Value	Observed	Expected	P-Value	Observed	Expected	P-Value	Observed	Expected	P-Value	Observed	Expected	P-Value
Nucleoside, nucleotide and nucleic acid metabolism	20	19.32	1.00E+00	46	32.86	3.54E-01	22	30.76	1.00E+00	115	80.71	1.86E-03	267	167.08	2.00E-13	336	222.42	2.83E-13
Cell proliferation and differentiation	15	5.94	2.99E-02	20	10.11	9.81E-02	20	9.46	4.55E-02	44	24.82	7.20E-03	99	51.38	2.98E-08	134	68.4	1.27E-11
mRNA transcription	17	11.06	1.00E+00	27	18.82	1.00E+00	13	17.61	1.00E+00	70	46.21	5.77E-02	166	95.66	7.81E-10	211	127.34	1.15E-10
Developmental processes	33	12.44	5.92E-06	37	21.16	2.00E-02	48	19.8	2.69E-07	76	51.96	1.89E-02	161	107.55	8.09E-06	225	143.18	5.64E-10
mRNA transcription regulation	14	8.43	1.00E+00	24	14.34	1.00E+00	9	13.42	1.00E+00	54	35.23	2.84E-01	132	72.92	1.48E-08	168	97.07	1.73E-09
Amino acid metabolism	5	1.33	3.48E-01	13	2.26	2.00E-05	17	2.12	2.57E-09	21	5.55	1.12E-05	38	11.5	1.29E-08	46	15.3	4.49E-09
Lipid, fatty acid and steroid met.	10	4.45	4.49E-01	11	7.57	1.00E+00	16	7.09	7.08E-02	40	18.59	2.33E-04	77	38.48	5.12E-07	94	51.23	9.72E-07
Transport	10	7.55	1.00E+00	23	12.84	1.65E-01	21	12.02	3.04E-01	60	31.53	6.37E-05	103	65.27	1.66E-04	138	86.89	3.56E-06
Oncogenesis	8	2.73	2.00E-01	17	4.64	1.79E-04	11	4.34	1.47E-01	23	11.4	4.52E-02	40	23.59	3.57E-02	64	31.4	4.99E-06
Steroid metabolism	4	1.06	1.00E+00	5	1.8	1.00E+00	6	1.68	1.00E+00	18	4.42	1.26E-04	31	9.15	1.37E-06	35	12.18	9.16E-06
Cell structure and motility	20	6.64	3.55E-04	20	11.29	3.16E-01	29	10.56	3.18E-05	43	27.72	1.07E-01	75	57.38	3.94E-01	120	76.38	4.12E-05
Cell cycle	13	5.83	1.85E-01	12	9.92	1.00E+00	10	9.28	1.00E+00	26	24.36	1.00E+00	79	50.43	2.63E-03	107	67.13	8.41E-05
Cell cycle control	11	2.42	5.23E-03	7	4.11	1.00E+00	5	3.85	1.00E+00	16	10.09	1.00E+00	38	20.89	6.29E-02	57	27.81	9.17E-05
Other metabolism	4	3.23	1.00E+00	8	5.5	1.00E+00	6	5.14	1.00E+00	23	13.5	3.29E-01	50	27.94	2.71E-03	67	37.19	1.64E-04
Intracellular signalling cascade	14	5.03	8.25E-02	18	8.56	3.92E-01	17	8.01	4.61E-01	38	21.03	6.24E-02	60	43.53	1.00E+00	96	57.95	2.76E-04
Signal transduction	43	19.69	1.23E-05	56	33.48	2.14E-03	57	31.34	1.39E-04	111	82.23	1.98E-02	184	170.23	1.00E+00	284	226.61	1.27E-03
Immunity and defence	18	7.62	2.00E-02	32	12.96	8.36E-05	28	12.13	1.17E-03	51	31.82	2.36E-02	73	65.87	1.00E+00	125	87.69	2.04E-03
Sulphur metabolism	3	0.54	5.32E-01	3	0.91	1.00E+00	7	0.86	9.16E-04	5	2.25	1.00E+00	15	4.65	3.11E-03	18	6.19	2.48E-03
Apoptosis	10	3.07	3.47E-02	10	5.22	1.00E+00	11	4.89	3.38E-01	16	12.82	1.00E+00	40	26.54	2.53E-01	59	35.33	4.41E-03
Cell structure	9	3.97	1.00E+00	9	6.75	1.00E+00	15	6.32	2.83E-01	22	16.59	1.00E+00	49	34.34	1.00E+00	75	45.71	4.88E-03
Olfaction	1	1.14	1.00E+00	0	1.95	1.00E+00	0	1.82	1.00E+00	0	4.78	1.00E+00	0	9.9	9.60E-03	1	13.17	5.10E-03
Cell communication	14	7.01	1.00E+00	22	11.92	6.64E-01	23	11.16	1.33E-01	46	29.29	2.92E-01	77	60.62	1.00E+00	118	80.7	5.50E-03
Mesoderm development	12	3.18	1.39E-02	13	5.42	5.10E-01	18	5.07	6.64E-04	25	13.3	3.47E-01	37	27.54	1.00E+00	63	36.66	5.67E-03
Homeostasis	3	1.13	1.00E+00	8	1.93	2.52E-02	7	1.8	7.66E-02	15	4.73	3.62E-03	18	9.8	3.58E-01	28	13.04	6.23E-03
Chemosensory perception	1	1.2	1.00E+00	0	2.03	1.00E+00	0	1.9	1.00E+00	0	5	9.59E-01	1	10.35	5.11E-02	2	13.77	1.59E-02
Stress response	3	1.16	1.00E+00	7	1.97	5.75E-01	5	1.84	1.00E+00	11	4.83	1.00E+00	20	10	4.80E-01	29	13.31	1.78E-02
Cell motility	8	2.03	1.59E-01	15	3.46	4.18E-04	15	3.24	1.85E-04	17	8.5	9.04E-01	23	17.59	1.00E+00	43	23.42	2.35E-02
Cholesterol metabolism	1	0.39	1.00E+00	2	0.67	1.00E+00	0	0.63	1.00E+00	12	1.64	3.24E-05	14	3.4	2.57E-03	14	4.52	5.12E-02
Ligand-mediated signalling	6	2.43	1.00E+00	14	4.14	1.78E-02	8	3.87	1.00E+00	20	10.16	7.53E-01	28	21.04	1.00E+00	47	28.01	1.15E-01
Amino acid activation	0	0.22	1.00E+00	3	0.37	9.46E-01	1	0.35	1.00E+00	7	0.92	6.91E-03	5	1.9	1.00E+00	9	2.53	1.77E-01
MAPKKK cascade	9	1.05	2.64E-04	7	1.78	4.56E-01	5	1.67	1.00E+00	8	4.37	1.00E+00	11	9.05	1.00E+00	24	12.04	2.93E-01
Ion transport	5	3.56	1.00E+00	13	6.06	1.00E+00	15	5.67	9.75E-02	32	14.87	8.82E-03	38	30.79	1.00E+00	60	40.98	4.08E-01
Blood clotting	5	0.53	3.13E-02	4	0.9	1.00E+00	6	0.85	3.44E-02	7	2.22	1.00E+00	6	4.6	1.00E+00	14	6.12	6.13E-01
Amino acid biosynthesis	1	0.27	1.00E+00	3	0.45	1.00E+00	5	0.42	1.12E-02	6	1.11	1.45E-01	6	2.3	1.00E+00	9	3.06	6.20E-01
Amino acid transport	2	0.27	1.00E+00	4	0.46	1.87E-01	4	0.43	1.47E-01	7	1.13	2.54E-02	8	2.35	4.21E-01	9	3.13	7.11E-01
Cell adhesion	9	3.6	3.28E-01	8	6.11	1.00E+00	15	5.72	2.30E-02	21	15.02	1.00E+00	36	31.09	1.00E+00	53	41.38	1.00E+00
Muscle contraction	2	1.14	1.00E+00	5	1.95	1.00E+00	8	1.82	1.75E-02	7	4.78	1.00E+00	9	9.9	1.00E+00	18	13.17	1.00E+00
Other homeostasis activities	1	0.4	1.00E+00	1	0.68	1.00E+00	2	0.63	1.00E+00	8	1.67	4.79E-02	4	3.45	1.00E+00	10	4.59	1.00E+00

Table 10: Host cellular biological processes affected during JFH-1 infection of Huh7 cells.

Panther analysis was performed as described (2.5.7) using all genes which met the cut-off of a 2-fold change, and the Bonferroni correction was employed for stringent calculation of p-values. Processes identified as having an enriched number of genes (with a p-value cut-off of 0.05), represented in the microarray data compared with the expected random number of genes based on the whole human genome, for at least one timepoint, are given. Given for each

timepoint and biological process are the observed number of genes regulated during infection, the expected number of genes based on the proportion of genes involved in that process in the entire human genome, and finally a p-value representing the probability that the difference between observed and expected numbers is not significant.

The downregulation of metallothionein genes observed in infected Huh7.5 cells was also observed in Huh7 cells (Figure 24). In Huh7 cells there was more fluctuation in the regulation, including a lesser fold change at 48 hours post infection.

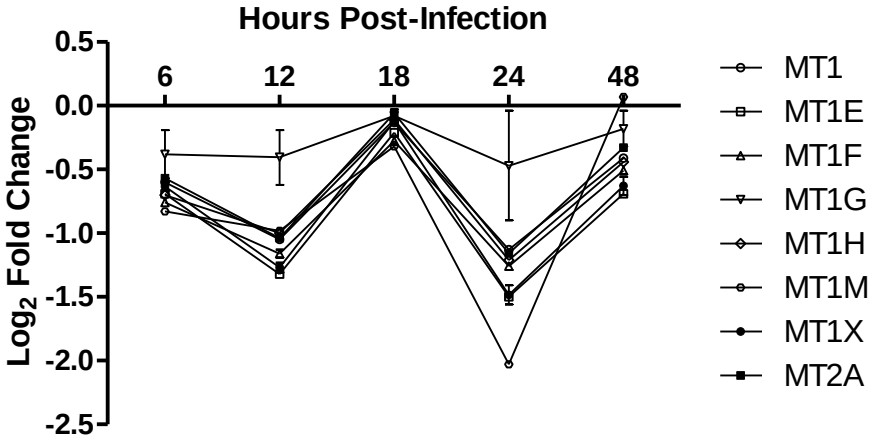


Figure 24: Fold change in expression of Metallothioneins during JFH-1 infection of Huh7 cells. Metallothioneins were seen to be down regulated in infected Huh7.5 cells, and can also be seen to be downregulated here in infected Huh7 cells. In Huh7 cells a trend of downregulation of metallothioneins is seen across all timepoints, but with a rebound towards normal levels at 48 hours. Where a gene is represented on the microarray by more than one probe set, data were averaged and displayed with error bars. The data set MT1 corresponds to a probe set which recognises all MT1 isoforms

Genes observed to be regulated by more than two fold at 48 hours post-infection have been presented in heatmap form. Figure 25, Figure 26, Figure 27, Figure 28, Figure 29 and Figure 30 present these genes grouped by biological processes identified in the Panther analysis of microarray data (Table 10, Figure 21). As a visual aid, heatmap data is presented on a $\log_2$ scale. Upregulated genes are shown in red and downregulated genes are shown in green. Maximal colour intensity is assigned to genes with a relative expression change of 3 fold or higher (1.5 fold on the $\log_2$ scale). The biological processes displayed fall into the general categories of apoptosis, cell cycle regulation, protein synthesis, cytoskeleton, intracellular transport, immunity, oxidative stress, and lipid metabolism.

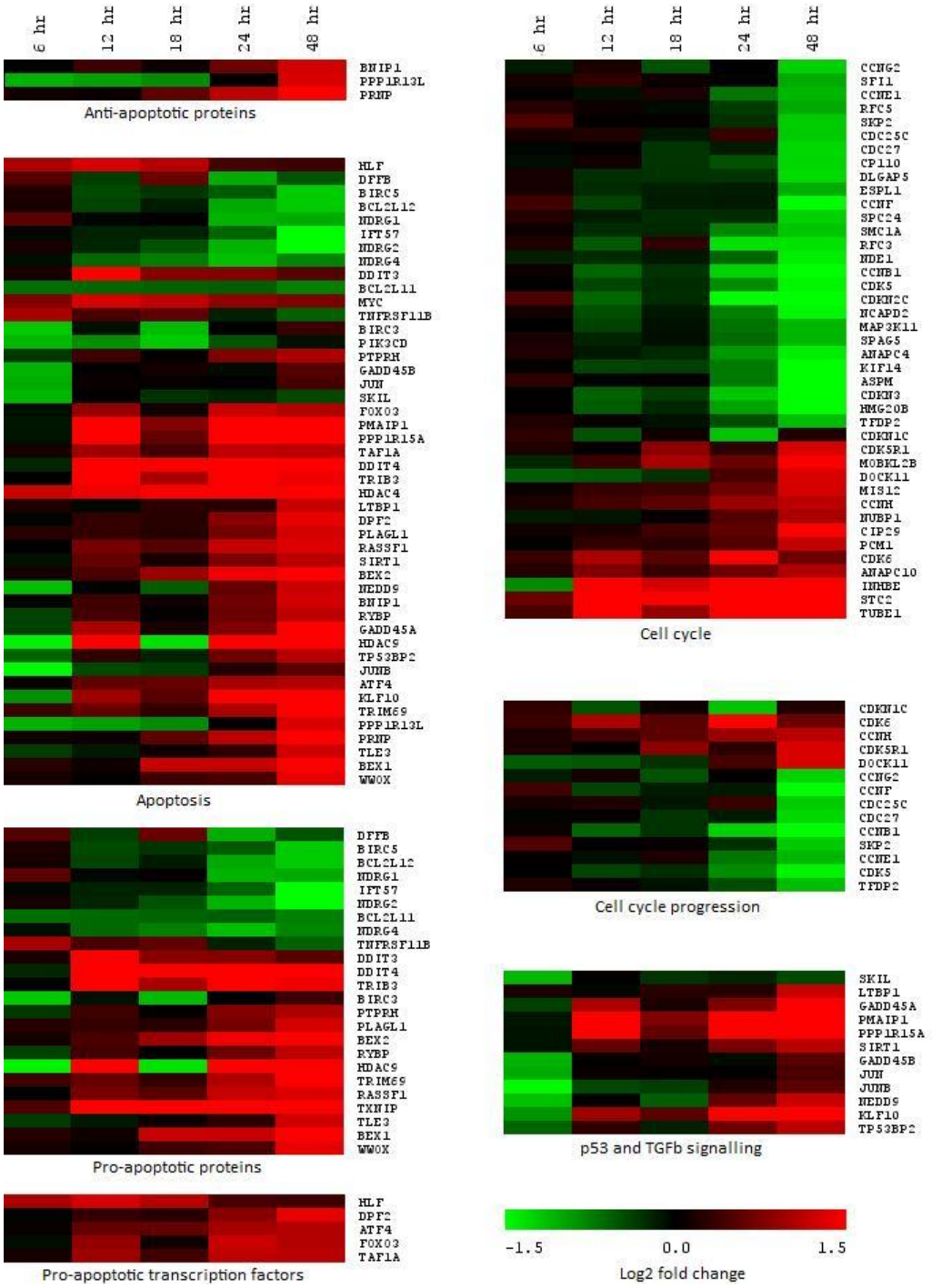


Figure 25: Host biological processes regulated during JFH-1 infection of Huh7 cells (apoptosis and cell cycle).

Genes identified to be regulated during JFH-1 infection of Huh7 cells compared to mock infected Huh7 cells are presented in heatmap form with each heatmap corresponding to biological processes identified using Panther analysis. Heatmaps were generated using MeV software and genes are clustered within heatmaps by Pearson correlation. Genes shown in red were upregulated and genes shown in green were downregulated, displayed on a $\log_2$ fold change scale. Genes are identified by their gene symbol, and relative expression levels are presented for 6, 12, 18, 24 and 48 hours post-infection.

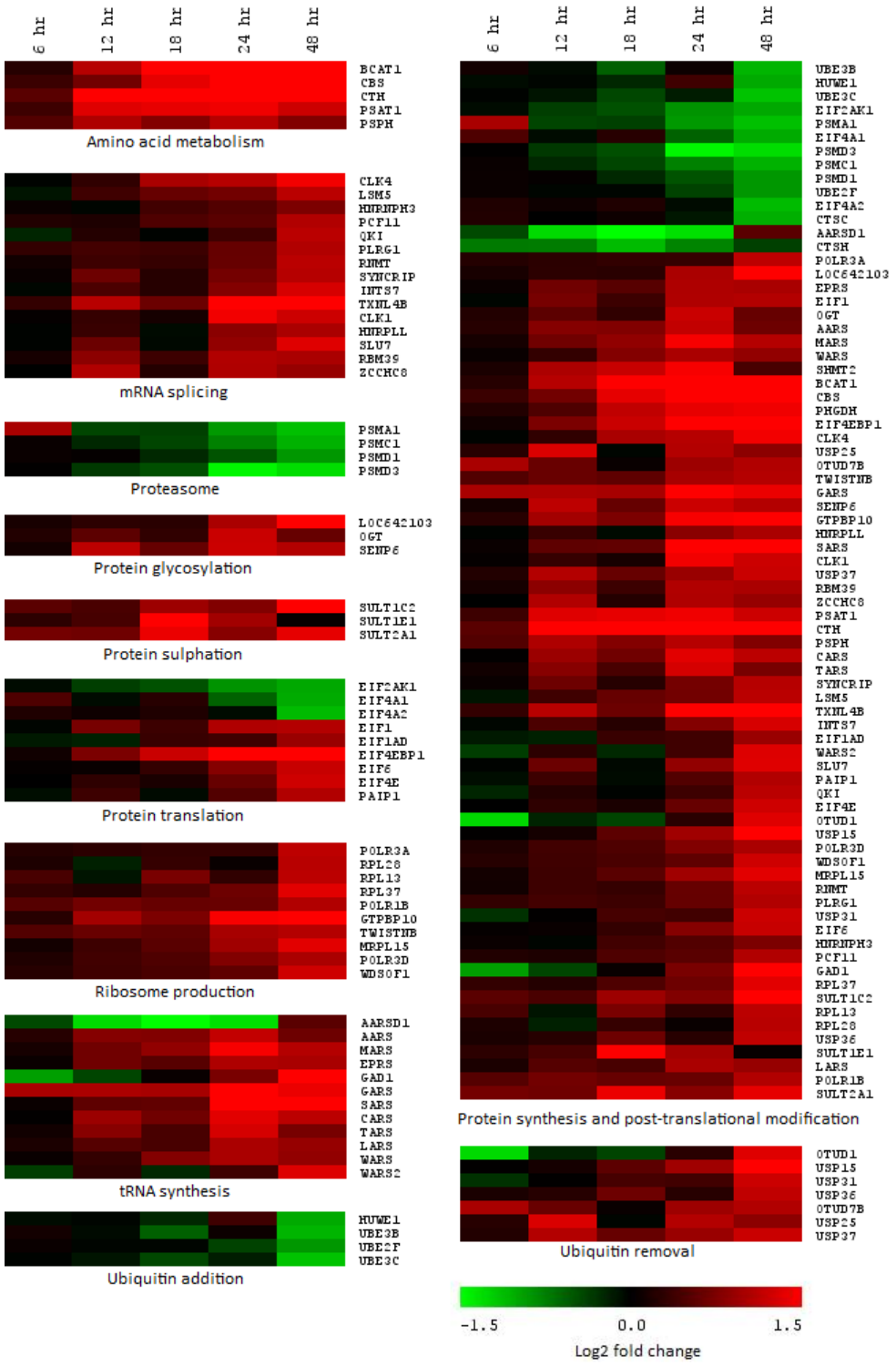


Figure 26: Host biological processes regulated during JFH-1 infection of Huh7 cells (protein synthesis).

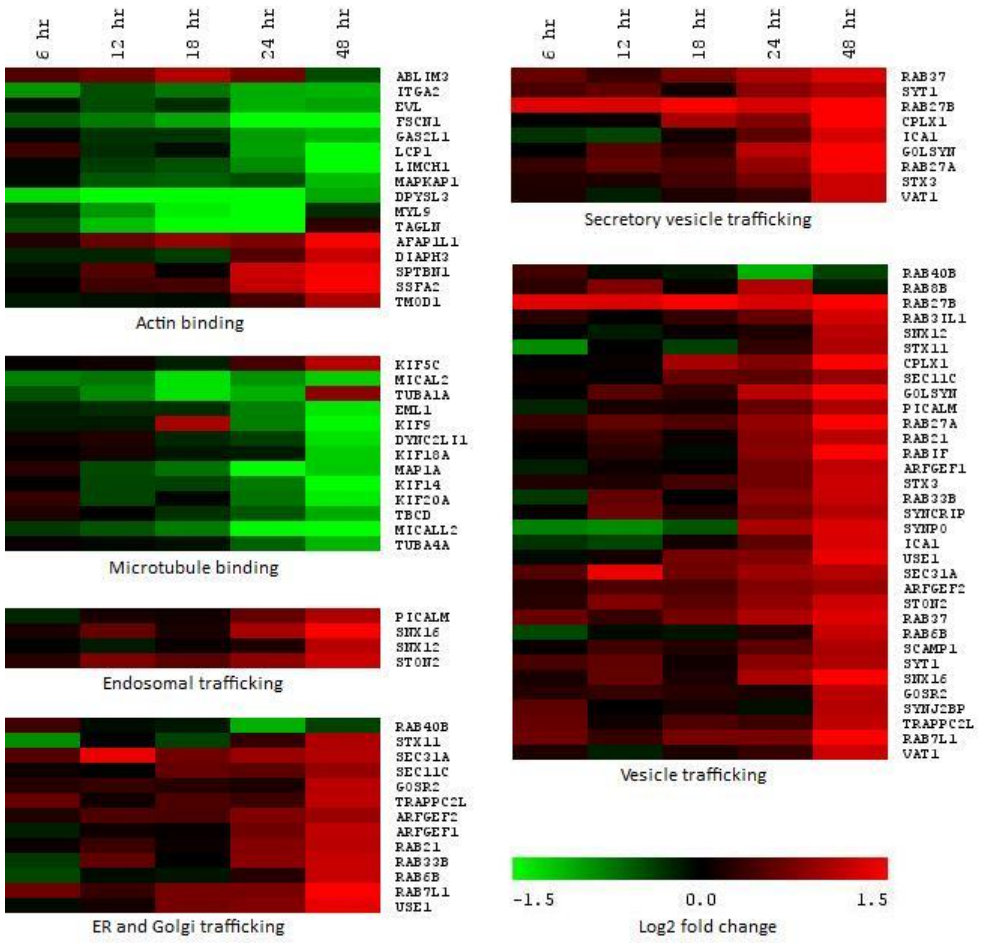


Figure 27: Host biological processes regulated during JFH-1 infection of Huh7 cells (cytoskeleton and transport).

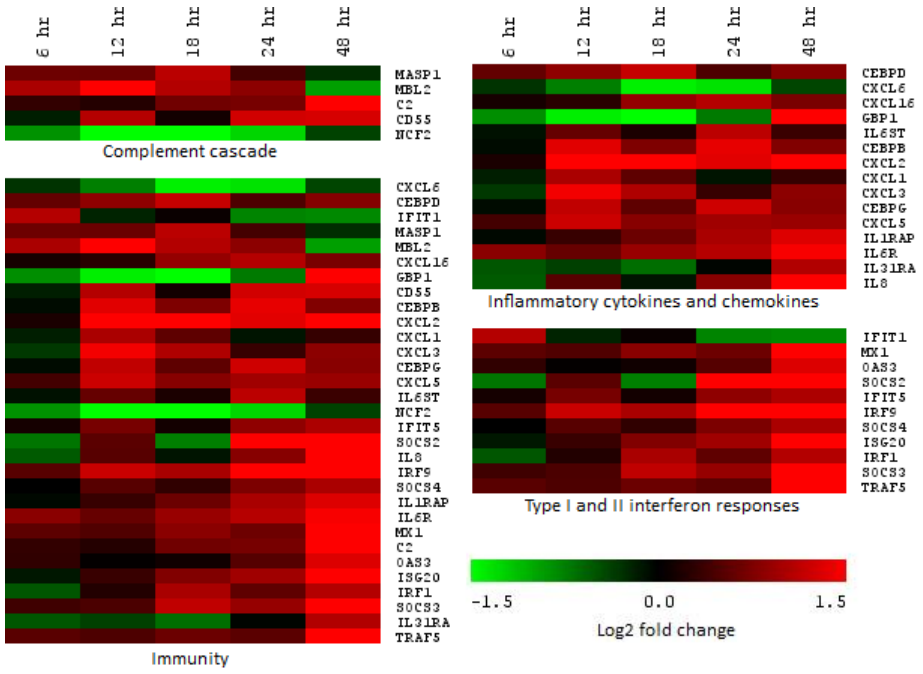


Figure 28: Host biological processes regulated during JFH-1 infection of Huh7 cells (immunity).

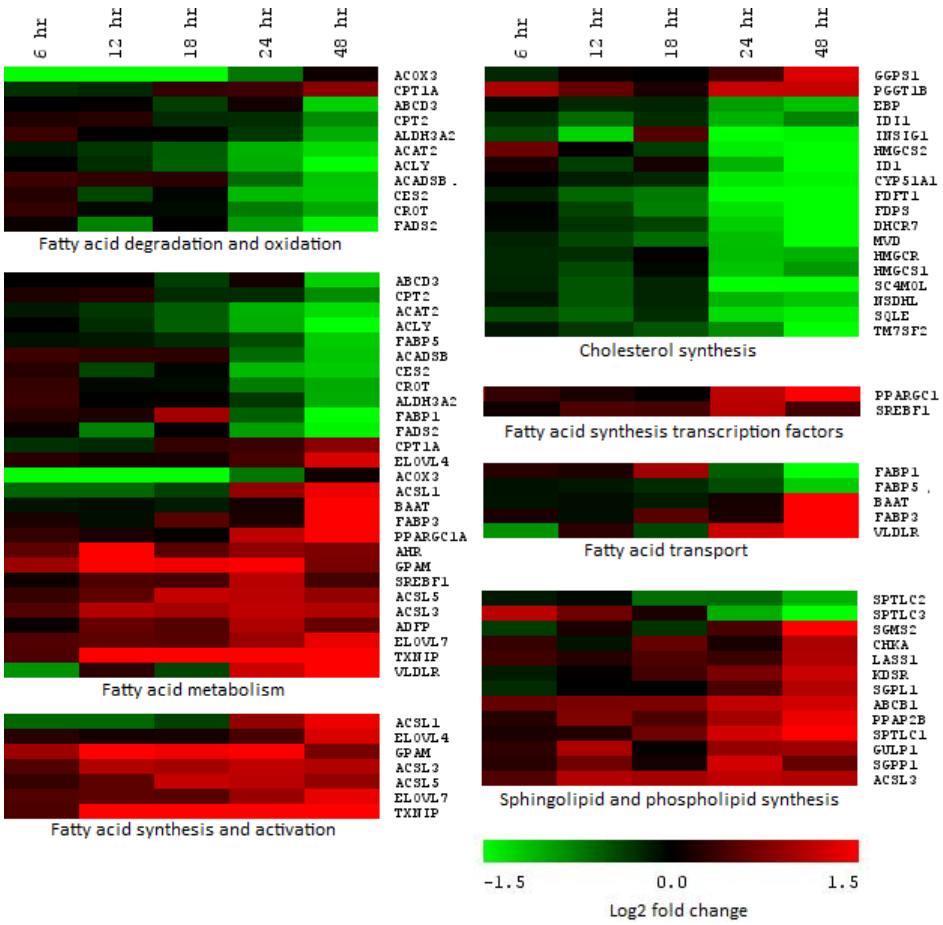


Figure 29: Host biological processes regulated during JFH-1 infection of Huh7 cells (lipid metabolism).

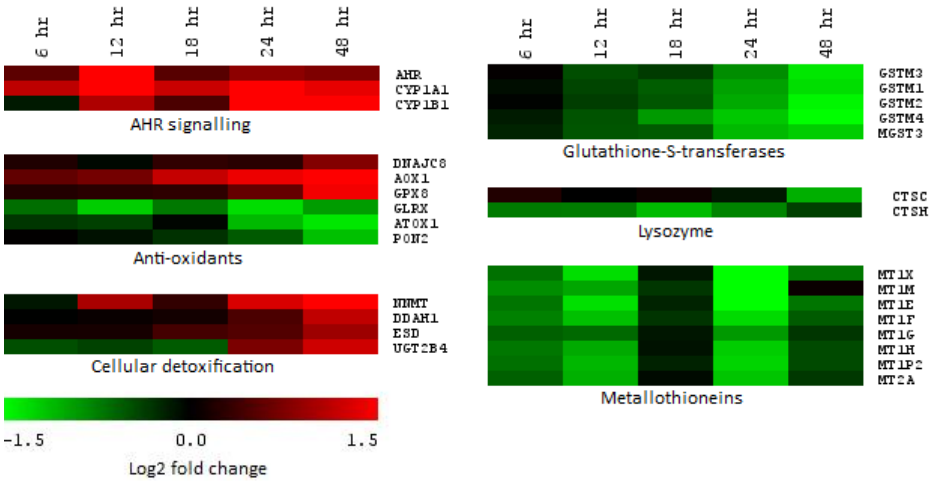


Figure 30: Host biological processes regulated during JFH-1 infection of Huh7 cells (oxidative stress and detoxification).

An extensive validation of the microarray expression findings was performed. Using infection experiments separate from the microarray experiment, a wide range of genes were tested for expression changes by qPCR. The genes chosen were observed to have significant expression changes with infection at the 48 hour post-infection timepoint. Genes chosen were those involved in the biological processes identified to be affected during infection. Gene expression changes are presented in Figure 31. Figure 31A shows the expression levels of genes involved in oxidative stress and it includes detoxification genes CYP1A1 and CYP1B1. Figure 31B shows genes involved in lipid metabolism functions including cholesterol synthesis (EBP, FDFT1, HMGCR, MVD, SQLE), sphingolipid synthesis (SGMS2, SGPL1, SGPP1, SPTLC1) and fatty acid metabolism (ACLY, ACSL3, FABP3, SREBF1). Figure 31C also shows genes involved in fatty acid metabolism (PPARC1A, ELOVL4, ELOVL7) including TXNIP. Figure 31D shows genes involved in immunity including cytokines (CXCL2, CXCL16, CXCR4) and genes involved in interferon signalling (IRF9. MX1, SOCS2, SOCS3). Figure 31E shows genes involved in the cytoskeleton (ABLIM3) and vesicle trafficking (RAB27B, RAB37, RAB40B). Figure 31F shows expression levels of metallothioneins. It can be seen that the vast majority of qPCR data agreed with the microarray data. The correlation between data obtained from the two techniques confirms the validity of using microarray to study expression level changes, the fact that gene expression level changes do occur during HCV infection, and that these changes are reproducible between infections.

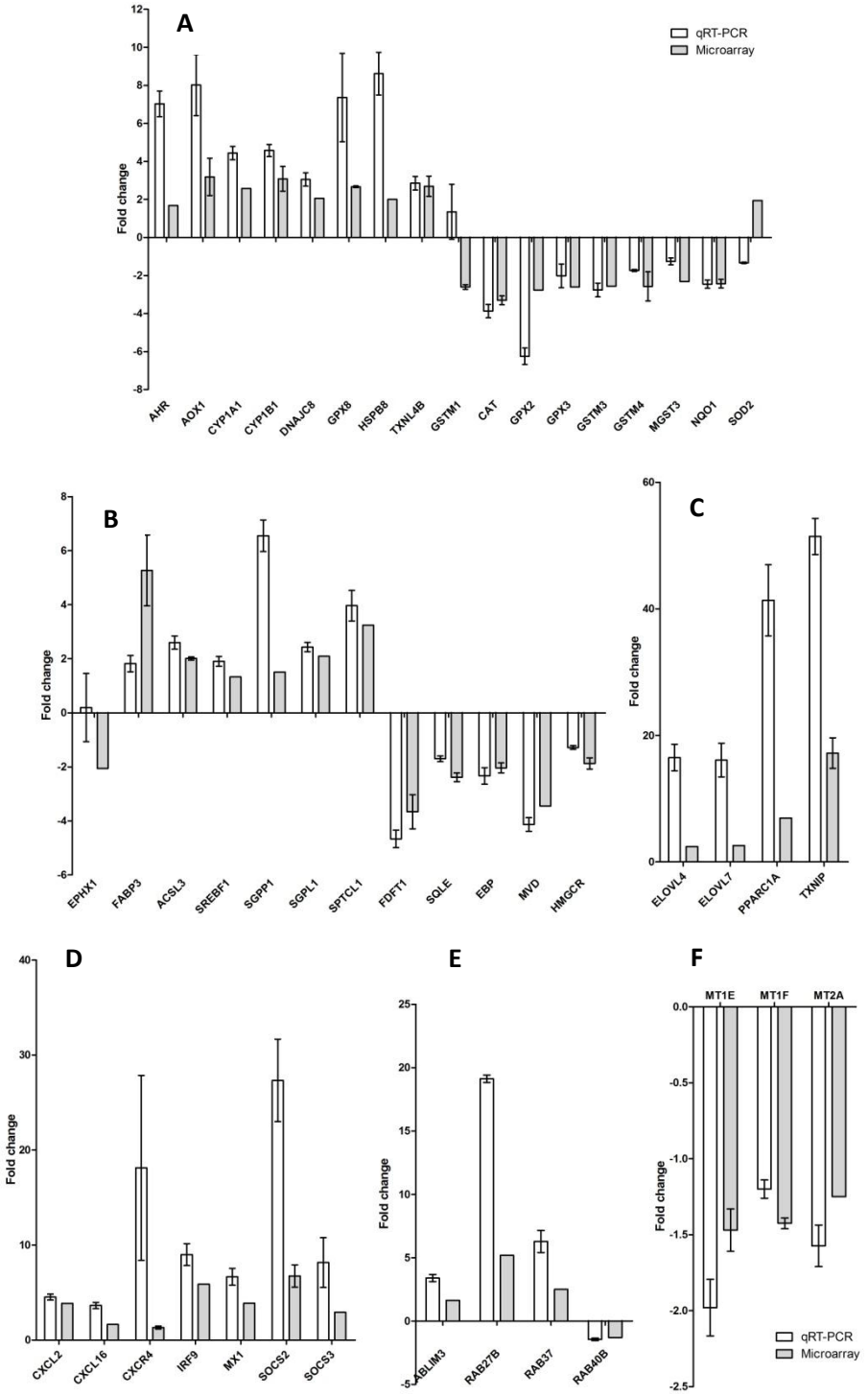


Figure 31: Validation by PCR of gene expression levels in Huh7 cells infected with JFH-1.

Huh7 cells were infected with JFH-1 at an MOI of 3 or mock infected for 48 hours. Data are presented as in previous figures. PCR quantification results were obtained from duplicate infections in three separate experiments or triplicate infections in two separate experiments. The majority of gene expression levels determined by PCR and microarray were observed to be in agreement. Genes are grouped by biological processes: oxidative stress (**A**), lipid metabolism (**B** and **C**), immunity (**D**), cytoskeleton and intracellular transport (**E**), metallothioneins (**F**).

3.3.4 Host Cell Biological Processes Altered during HCV Infection

The analysis of gene expression in HCV infected cells has identified several biological processes of relevance to the HCV lifecycle to have a significant number of genes regulated during infection. These include lipid metabolism, immune responses, intracellular transport, oxidative stress and apoptosis. These processes and specific genes involved are discussed in the following sections with reference to their potential impact on the HCV lifecycle and the pathology of disease in humans.

The use of microarray technology to perform large scale expression studies has become increasingly common, and is usually observed to return reliable data. In order to validate the data obtained from the microarray studies described in the work presented here, quantitative PCR was performed. Selected genes were quantified by qRT-PCR using cellular RNA material from separate infection experiments. Most quantitative PCR data agreed with microarray data in the direction of regulation of genes during infection. It was observed in many cases that the fold changes in gene expression seen by qPCR were not exactly the same as the microarray results. A general pattern was observed between qPCR and microarray data. In the case of genes that increased in expression with infection, qPCR generally indicated a higher expression level with infection. For genes that decreased in expression with infection, qPCR generally indicated a lower expression level with infection. The pattern observed, of larger expression level changes when measured by qPCR, may indicate that this technique is more sensitive than microarray technology in identifying gene expression changes. This phenomenon has been observed in previous work by other groups[410-411].

A recently performed study investigated gene expression changes in Huh7.5 cells infected with a J6/JFH-1 chimaera[411], providing a useful comparison study for the data described here. Whole genome microarrays were used to identify gene expression changes at 24, 48, 72, 96 and 120 hours post-infection. This study used a MOI of 1 to infect cells, lower than was used in the work presented here. This study also demonstrated that the expression of a large number of host genes was altered during infection, with 860 genes differentially regulated at 72 hours post infection. This study also differed from the work presented here by using cells treated with UV-inactivated virus as a control to remove any gene expression changes induced in cells by the binding of virus during the initial infection event. However, few genes were observed to be regulated by treatment of Huh7.5 cells with the UV-inactivated HCV. This may either be due to the amount of virus not being sufficient to induce anti-viral responses, or that the viral detection mechanisms (including RIG-I and TLR3) are impaired in Huh7.5 cells. This study highlights the observations of gene expression changes in

apoptotic, cell cycle and oxidative stress processes. There is good correlation between these observations and the work presented here. Three areas of interacting components involved in oxidative stress responses were described, p53 signalling, NRF2-mediated oxidative stress response, and TGFβ signalling. There is correlation in gene expression between their study and the work presented here for the following, upregulated, genes involved in p53 signalling: TP53BP, GADD45A, GADD45B, MYC, PMAIP, JMY, JUN and SIRT1. For TGFβ signalling correlation is also generally upregulated and seen in genes LTBP1, NEDD9, SKIL, NHBA, BMP2, KLF10, JUN and JUNB. For NRF2 signalling correlation is seen in genes MAFF, JUN, JUNB, MAFK (all upregulated), MAP2K6, EPHX1 and CAT (all downregulated). The gene expression data from both this study and the work presented here support each other in the indication that there are changes in both cell cycle and oxidative stress factors occurring in HCV infected cells, potentially leading to apoptosis and providing a possible cause for liver damage observed in HCV infected patients.

3.3.4.1 Immune Modulation

The work presented here has shown genes involved in immunity and defence to be regulated during HCV infection.

There was an observed increase in expression of cytokines and chemokines during infection. HCV infected patients can develop inflammation in the liver. The observed increase in expression of cytokines and chemokines in the work presented here correlates with previous studies indicating a role for infected hepatocytes as sources of inflammation in the liver[411]. The CXCL chemokines were generally observed to be upregulated, in particular CXCL 1, 2, 3, 5, 6 and 8. These chemokines bind CXCR1 and CXCR2 receptors which have been shown to induce hepatocyte proliferation and liver regeneration[412], as well as being able to stimulate infiltration and respiration of neutrophils and monocytes[413]. The chemokines were similarly upregulated in Huh7 and Huh7.5 cells (including in the study performed using J6/JFH-1 in Huh7 cells[411]), which implies that the regulation of this response is probably not initiated through RIG-I signalling. Chemokines and receptors (including CXCL11 and CXCR3) have previously been observed to be upregulated in HCV infected humans and chimpanzees[398]. In expression studies performed in chimpanzees[329,379-380], a variety of interferon stimulated genes were observed to be upregulated. This was not observed to such an extent in this work. This may reflect the more complicated immune situation *in vivo*, compared to cell culture, which includes other cell types and aspects of the adaptive immune response.

There was an observed increase in the expression of SOCS genes during HCV infection. SOCS genes are negative regulators of cytokine responses[414]. Upregulation of SOCS genes has been reported in previous studies[411,415], and has been implicated as a possible reason for interferon resistance in some HCV patients[416].

Acute phase response genes were upregulated during infection, particularly in Huh7.5 cells. These included SAA1, PLG and complement factors. Acute phase genes such as these are produced by the liver in response to infection and cytokine stimulation. Complement factors were also observed to be regulated during HCV infection. Factors MASP1 and MBL2 were observed to be increased in expression during infection. These genes can induce fibrosis, and may provide a mechanism that contributes to the fibrosis observed in the liver of HCV infected patients[417-418]. Complement factors CFH and CFI were observed to be upregulated during HCV infection (more highly in Huh7.5 than Huh7). These are negative regulators of the complement system[419], and as such may be in part

responsible for a mechanism to allow virus to escape host defences. Flaviviruses including West Nile virus and Dengue virus have been observed to target complement factors with the effect of inhibiting complement activation and therefore evading complement control of infection[420-421]. However, siRNA silencing of CFH and CFI did not inhibit HCV replication in cell culture, implying that complement is not a major mechanism for the host to defend against HCV infection in cell culture.

3.3.4.2 Lipid Metabolism

Lipids have been shown to play an important role in the HCV lifecycle. As described in the introduction, HCV requires an envelope made of lipid membrane, endocytotic pathways reliant on lipids are used for entry into the cell, replication occurs on membranous structure in the cell, assembly of the virus requires the presence of lipid droplets, and lipid secretion pathways are required for exit from infected cells.

The work presented here has identified that genes involved in lipid metabolism are regulated during HCV infection. Analysis of microarray data showed lipid, fatty acid and steroid metabolism genes to be regulated during HCV infection (Figure 21, Table 6, Figure 29, and Table 10). The regulation of several of these genes was confirmed by qRT-PCR (Figure 22, Figure 31B and C). Genes involved in the synthesis of sphingolipids, phospholipids and fatty acids were generally observed to be upregulated during HCV infection. This is consistent with the requirement of these molecules for the efficient replication of HCV. Previous studies have also shown the upregulation of expression of genes involved in sphingolipid and fatty acid metabolism. This has been demonstrated in a variety of systems including in replicon models[382], *in vivo*[380], and by expression of core protein[422]. This implies that transcriptional regulation of lipid metabolism is induced by HCV infection, and may be a result of action of the HCV proteins. A key gene in the production of sphingolipids, SPTLC3, was observed to be upregulated during infection, and siRNA silencing of the gene was found to impair efficient HCV replication (Figure 40E). This gene is discussed in more detail in a subsequent section (3.5.2.3).

A common factor in the regulation of several of the lipid metabolism genes observed to be upregulated during HCV infection is the transcription factor PPARα. Previous studies have identified hepatic lipid metabolism target genes of PPARα, including CPT1A, ACSL1, ADFP, MBL2 and CYP1A1[423]. The siRNA silencing of two genes involved in PPARα signalling, TXNIP and CYP1A1, was shown, in the work presented here, to inhibit efficient HCV replication (Figure 40B and F). TXNIP has

been shown to be a negative regulator of PPARα (and SREBP)[424]. A study has shown that agonists of PPARα can suppress HCV replication[382], suggesting that TXNIP suppression of PPARα could be important in ensuring efficient HCV replication. The silencing of a glucose responsive transcription factor capable of inducing TXNIP, MXLIPL, was recently identified as reducing HCV replication[425], further indicating the possible importance of TXNIP to efficient HCV replication. CYP1A1 is involved in both PPARα and AHR pathways, and activation of CYP1A1 through either pathway can control lipid metabolism events[423,426-427]. These two genes, TXNIP and CYP1A1, are discussed in more detail in following sections (3.5.2.4 and 3.5.2.2).

Genes involved in the synthesis of cholesterol were also observed to be regulated during HCV infection (Figure 29). There was a general trend for these genes to be down regulated. Reduced cholesterol levels have been observed in patient serum[428]. It is also possible for other RNA viruses to reduce the levels of cholesterol synthesis, such as the Measles virus[429]. A study performed using an HCV replicon system found that cholesterol synthesis genes were increased in expression levels[382]. This may be a feature of the reduced interferon response in the Huh7.5 cells used in this replicon study, as interferon can downregulate expression of miR122, which in turn would prevent miR122 from upregulating cholesterol synthesis genes. Further discussion of the involvement of miR122 in gene expression regulation and the HCV lifecycle is given in a following section (3.3.4.2.1).

Since performing these experiments it has been shown that expression of genes involved in cholesterol synthesis are upregulated in JFH-1 infected cells at 72 hours post-infection (personal communication from M. J. McGarvey). Genes have been observed to be expressed at levels between 1.5- and 5-fold higher in JFH-1 infected cells than in mock infected cells. This indicates a biphasic mechanism of control of gene expression during HCV infection. It appears that HCV may play a role in upregulation of the lipid metabolism genes essential for the efficient replication of HCV. However before this can happen, the expression of these genes is downregulated possibly due to immune responses and competition from miR122 as discussed in the following section on miR122.

3.3.4.2.1 Micro RNA 122 (miR122)

As has already been established, miR122 is known to be required for efficient replication of HCV[92]. There are a number of cellular genes already known to be regulated by miR122. Of particular interest to the study of HCV, miR122 has been shown to regulate cholesterol production. Inhibition of miR122 by use of antisense oligonucleotide has been shown to reduce plasma cholesterol levels[430-431]. This study demonstrated by microarray analysis that a number of genes involved in the production of cholesterol were down regulated during infection of Huh7 cells with JFH-1 up to 48 hours post-infection. This may represent competition for miR122 by the abundant HCV genomes, resulting in less miR122 available for genes involved in cholesterol synthesis. This state is unlikely to continue as cholesterol is required for the HCV lifecycle, in particular for composition of the lipoprotein particles that HCV forms as it is released from the cell, which form the most infectious particles. It is known that expression of miR122 itself is downregulated by an interferon-β response[431-432], so an anti-viral response by the host cell may also lead to conditions where there is less miR122 available.

The micro RNA miR122 is also known to regulate other cellular genes, and the microarray data was analysed for transcriptional changes in these genes. The cationic amino acid transporter SLC7A1 is known to be regulated by miR122[433-434], with SLC7A1 levels decreasing as miR122 increases. In Huh7 cells, SLC7A1 was upregulated 2-fold at 12 hours and over 4-fold at 24 and 48 hours, Implying that, if miR122 was responsible for the expression changes, miR122 levels were dropping. This could potentially be due to sequestration of miR122 by HCV. N-myc downstream regulated 3 (NDRG3) was not observed to be regulated by at least 2-fold during JFH-1 infection, but NDRG1, NDRG2, and NDRG4 were observed to be downregulated by an average of 2-fold by 24 hours post-infection. These genes are involved in cell cycle control, but there is debate as to their precise functions. It is interesting to note that the N-myc gene is often rearranged in tumours occurring in woodchucks with woodchuck hepatitis virus. Aldolase A (ALDOA) was previously shown to be downregulated in mouse AML12 cells on treatment with a miR122 antagomir[431]. ALDOA is involved in glycolysis, but is usually suppressed in human adult liver. In Huh7 cells it was found to be downregulated by 2-fold at 48 hours post-infection. Downregulation of ALDOA in the Huh7 microarray indicated that miR122 was being sequestered, possibly by HCV. Cyclin G1 (CCNG1) is known to have its 3'UTR targeted by miR122 and they have been shown to have an inverse relationship in some HCC, where CCNG1 is upregulated and miR122 is downregulated[435], although miR122 is expressed in Huh7 cells. CCNG1 was not observed to change in the microarray study during infection of Huh7 with JFH-1, but the related gene CCNG2 was observed to be downregulated by 2-fold at 48 hours post-infection,

although as CCNG2 is more tightly regulated during the cell cycle and has an additional C-terminal PEST protein destabilisation motif, so the downregulation may not be related to miR122. Overall, given the direction of changes in expression of several genes known to be regulated by miR122, which are not known to be regulated by other means in common, it is tempting to propose that HCV is sequestering the available miR122 for its own replication, leaving little for the cellular genes which require miR122 for their own regulation. This demonstrates a method for HCV to affect the expression of host cellular genes, and therefore potentially to induce pathologies in the host. However, it is possible that if longer timeframes were studied, it may be found that miR122 levels increase to compensate, or that the genes identified use regulation by another method to compensate.

The apparent reduction in miR122, as determined by the direction of expression changes of genes it regulates, may be explained by another hypothesis. It is known that miR122 is downregulated by an interferon-β response[431-432]. It is possible that the immune response induced by the infection of Huh7 cells by JFH-1 is causing a decrease in miR122 expression and therefore the expression changes observed in the microarray study. This possibility is tentatively supported by the fact that the expression changes seen during infection of Huh7 cells were not seen to the same extent in Huh7.5 cells.

3.3.4.3 Oxidative Stress

Infection with HCV has been shown to induce production of reactive oxygen species (ROS) in patients, which leads to oxidative damage of the liver[418]. ROS are particularly destructive and can attack most molecules, and when ROS inflict damage on host DNA, errors may occur leading to cancer. It has also been suggested that oxidative stress damage can contribute to steatosis in HCV patients[436]. Analysis of the gene expression data presented here has shown an overall downregulation in the expression of genes involved in the oxidative stress response. This implies that any production of ROS due to HCV infection will not be dealt with as efficiently as usual by the cell, indicating a further mechanism for oxidative stress damage. A decrease in expression of antioxidant genes such as catalase (CAT) have previously been shown to occur following stimulation by cytokines[437]. As an increase in cytokine expression was observed in the work presented here, this may provide a mechanism for the observed expression pattern. The metallothionein family of genes are involved in antioxidant responses and were strongly downregulated in expression during HCV infection. This gene family is discussed in further detail below. Other oxidative stress genes were observed to be upregulated (Figure 30). This indicates that there are still some mechanisms in place for detection and combat of ROS.

3.3.4.3.1 Metallothionein (MT)

In both the microarray studies on Huh7.5 and Huh7 cells there was a decrease in metallothionein expression during JFH-1 infection compared to mock infected cells. All isoforms of the MT1 family and also isoform MT2A were downregulated at all timepoints. MTs were some of the most strongly downregulated of all genes, with expression of MT1E, F and G in JFH-1 infected Huh7.5 cells at only 20% of the levels in mock infected Huh7.5 cells 48 hours post-infection.

Metallothioneins are low molecular weight proteins, usually of less than 10kDa. MTs are cysteine rich proteins with 20 – 30% cysteine content. For example, the isoform MT1E has 20 cysteine amino acids out of a total 61 amino acids. MTs have metal-binding capacity. MTs typically bind 4 Zn^{2+} ions, and can also bind Cu and Cd. This ability seems to be important to its identified functions of zinc regulation and protection against oxidative stress. MTs can scavenge free radicals in the cell preventing damage, especially protecting DNA. This anti-oxidant function of MT may be particularly important in the reduction of damage induced during viral infection. If this function is removed, as

seems to be the case with the downregulation of MT expression observed in this study, it may contribute to the damage of cells and initiation of cancer that occurs in HCV infected liver.

MT1 and MT2 are the forms of MT found in the liver, as well as in the kidneys and other peripheral epithelial tissues. Two other forms of MT exist; MT3 which is expressed in the brain, and MT4 which is expressed in squamous epithelial cells. Heavy metals, particularly zinc, copper and cadmium can regulate the expression of MTs, with an increased presence of metals inducing MT expression. PPARγ agonists have been shown to downregulate the expression of MTs[438]. Infection with other viruses, including the measles virus[439], can affect the expression of MTs.

There is evidence from other studies that MT may be important in HCV infection. Other studies have shown a decrease in MT expression, followed by an increase at later timepoints post-infection than were measured in this study[411]. This could indicate a disregulation of MT expression during HCV infection. MT1E has been shown to be associated with regulation of cancer cell migration[440], but most studies indicate tumour suppressor roles for MTs. MTs have been shown to be down regulated in some cancers. This could be a contributory factor to the emergence of cancer, as the MT provides a protective function for DNA against stress damage. Expression of MT1F by exogenous induction in the liver cell line HepG2 has been shown to slow cell growth[441]. MT1G deletion has been shown to be associated with hepatocellular carcinoma[442], and the MT1G gene has been shown to be hypermethylated (which usually results in transcriptional silencing) in renal cell carcinoma[443]. MT2A has been implicated as being able to regulate p53 by Zn exchange, and that increased Zn, and therefore MT, can help restore wild type p53 function in tumours[444]. MT protein expression has also been shown to be three times lower in the liver of patients infected with HCV, compared to uninfected controls[445].

Metallothioneins have been identified to play a role in protection of cells from oxidative stress and seem to be tumour suppressive. These features may be important in the context of HCV infection. If MT levels are indeed reduced in HCV infected liver, then this may partially account for oxidative stress damage and eventual progression to cancer. As MT expression has been shown to be regulated by Zn, it may be advantageous to have HCV patients take Zn supplements to their diet. It has been previously shown that Zn can increase the therapeutic response to IFN in HCV patients[446-447]. In these studies, Zn was given as 300mg/day of zinc sulphate, corresponding to 68mg of Zn. MT can be induced by IFN, but if Zn levels are depleted MT will not be induced[448], indicating another reason to maintain Zn in HCV patients.

3.3.4.4 Protein Synthesis

During infection of Huh7 cells with HCV JFH-1, genes involved in protein synthesis were observed to be upregulated. These genes included those involved in protein synthesis, turnover, post-translational modification, and tRNA synthesis. This effect of HCV on gene expression has not been shown before. However, other viruses have been shown to induce similar changes in the host. HIV has been show to induce protein synthesis and use host protein sulphation processes for modification of viral proteins[449-450].

The host gene MGAM was observed to be upregulated during infection with HCV. This gene is a glucosidase known to be required for maturation of HCV structural proteins. It is involved in the processing of *N*-linked oligosaccharides on envelope proteins[451]. The potential importance of MGAM for HCV replication is illustrated by the clinical trials which are underway to test the efficacy and safety of a MGAM inhibitor in combination therapy for treatment of HCV[452].

3.3.4.5 Intracellular Transport

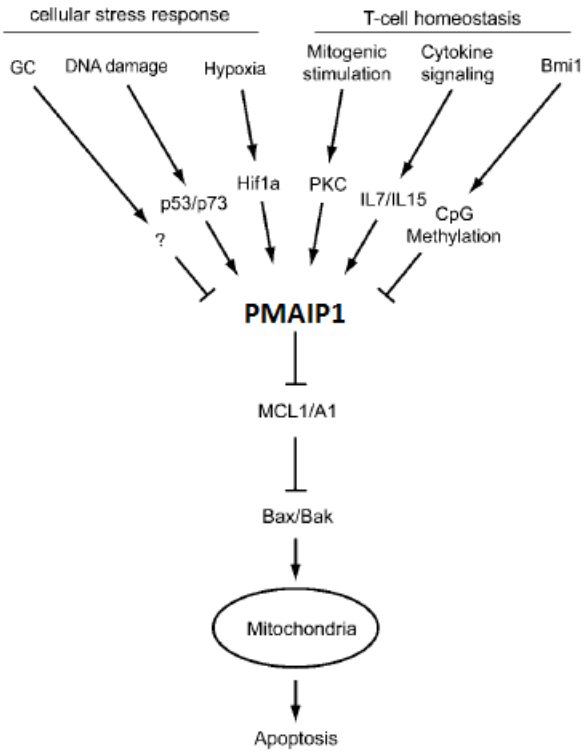
The work presented here has shown that genes involved in the regulation of vesicle trafficking between ER, Golgi and plasma membranes were regulated during HCV infection. This indicates a potential role for these genes in viral processes including entry, exit and construction of replication complexes. Host proteins which regulate intracellular transport have been shown to be important in the HCV lifecycle[175,453-454].

Genes coding for proteins involved in endocytosis (e.g. SNX12, SNX16) were observed to be upregulated during infection. HCV is known to enter the cell through clathrin-mediated endocytosis, and regulation of expression of these genes may aid HCV entry of cells. Genes RAN6B and RAB33B, involved in retrograde transport from the Golgi to the ER, were observed to be increased in expression levels during HCV infection. These genes may aid in the accumulation of viral proteins required for formation of the replication complex[455-456]. RAB33B is also involved in autophagy, and has been shown to be important for HCV replication and assembly[457-458]. Increased expression of RAB27A, RAB27B and RAB37 was observed during HCV infection. These genes are expressed in cells which require high levels of secretion[459-460], indicating that these genes may facilitate viral exit.

3.3.4.6 Apoptosis and Cell Proliferation

Genes involved in the control of apoptosis and cellular proliferation were observed to be regulated during HCV infection. Other studies have found increases in pro-apoptotic gene expression, and regulation of cell cycle[411,461]. It has been shown that HCV replication is dependent on the cell cycle, and that most efficient replication occurs in S phase[411]. An increase in the proportion of cultured cells in S phase has been observed after infection with HCV by others[411] (and in data not shown). The combination of data presented here and data from recent studies indicates that the liver damage seen in patients due to hepatocyte death may be due not only to the action of cytotoxic immune cells, but also due to apoptosis of cells induced by viral infection.

Phorbol-12-myristate-13-acetate-induced protein 1 (PMAIP1), also known as Noxa, is a protein of 103 amino acids. It is a member of the Bcl-2 protein family, and contains a BH3 domain. PMAIP1 can be induced by a number of signals. These include cellular stress responses such as hypoxia (mediated through Hif1a) and DNA damage (mediated through p53). PMAIP1 can then induce apoptosis by targeting the pro-survival proteins MCL1/A1 for degradation, thus facilitating the activation of Bax/Bak proteins, which induce apoptosis associated with mitochondrial disfunction[462]. PMAIP1 was upregulated in JFH-1 infected Huh7 cells, but not Huh7.5 cells, at the 48 hour post infection timepoint. This could indicate that PMAIP1 is part of a cellular response to HCV infection in Huh7 cells of which Huh7.5 cells are not capable.



PMAIP1 transcription and expression can be activated by diverse apoptotic or mitogenic signals in a p53-dependent and p53-independent manner (Figure 32). PMAIP1 exerts its pro-apoptotic function mainly by neutralizing the pro-survival Bcl2 proteins Mcl1/A1, facilitating activation of Bax and/or Bak proteins

Figure 32: Induction and action of PMAIP1[462].

3.4 Inhibition of JFH-1 Replication by Anti-Viral Inhibitors

The microarray analysis comparing gene expression in RNA isolated from infected and mock infected cells identified the genes altered in expression during JFH-1 infection. By inhibiting the replication of JFH-1, the differentiation can be made between genes which are altered in expression due to a stimulus during the initial stages of infection, and those which either require the presence of actively replicating HCV or are a response to a later stage of infection.

A number of anti-HCV molecules have been developed with the intention of use in patients, but have ultimately failed clinical trials. BILN2061 (Figure 33A) is an HCV protease inhibitor which has shown good anti-viral activity but had to be withdrawn from clinical trials after inducing side-effects. BILN2061 is very effective at inhibiting HCV in cell culture models. BILN2061 has an EC50 of 4nM in genotype 1 based replicon cells models, and 250nM in JFH-1 cell culture. NM107 (Figure 33B) is a 2'-C-methyl cytidine analogue HCV polymerase inhibitor which showed strong inhibition of HCV and other flaviviruses. In clinical trials NM107 is the active constituent of the pro-drug NM283. NM107 also has EC50 of around 4µM in genotype 1 replicon cells models, and 12µM in JFH-1 cell culture.

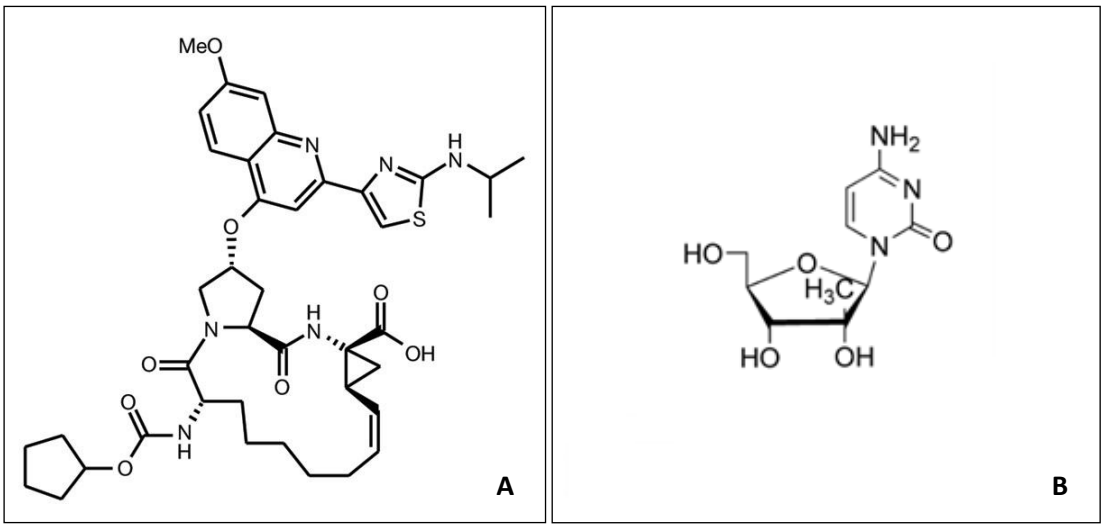


Figure 33: Structures of anti-viral molecules.

A BILN2061, an HCV protease inhibitor[64] (molecular weight 776.919) **B** NM107, an HCV polymerase inhibitor[74] (molecular weight 257.24)

Literature suggested EC50 values of around 4nM for BILN2061 and 4µM for NM107 in genotype 1 replicon cell culture, and EC50 values between 4 and 10 times higher in JFH-1 cell culture. To

establish the EC50s in the JFH-1 infected Huh7 cells and obtain a working concentration for each inhibitor, dose responses were generated (Figure 34).

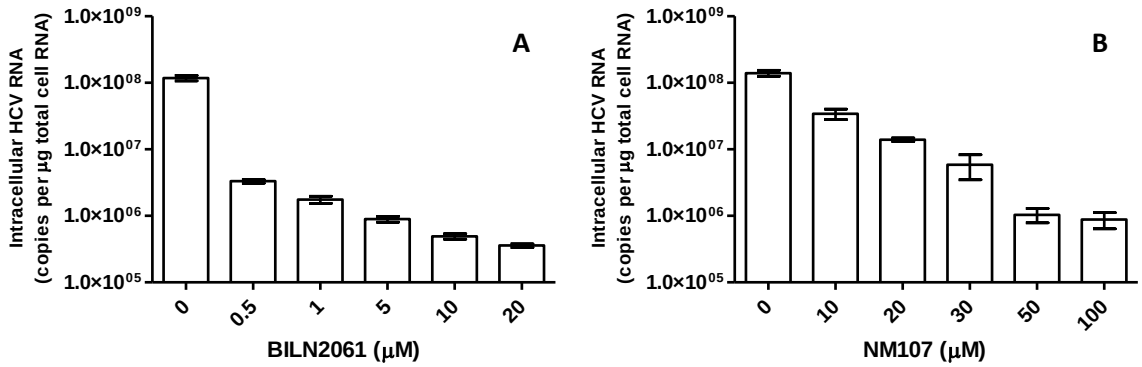


Figure 34: JFH-1 dose responses to anti-viral treatment.

Huh7 cells were infected with JFH-1 at an MOI of 3. At 12 hours post infection, cells were treated with anti-HCV inhibitors. At 48 hours post-infection, intracellular RNA was isolated and JFH-1 RNA levels quantified by qRT-PCR. Conditions were performed in triplicate, and two experiments were performed. **A** Dose response to BILN2061 **B** Dose response to NM107

BILN2061 was found to have anti-JFH-1 activity at low µM concentrations, and activity increased at concentrations tested, up to 20µM. NM107 was not as potent as BILN2061, especially at low µM concentrations, but a dose of 50µM could induce a 2-log drop in intracellular JFH-1 RNA titre. Cell culture studies employing a compound typically use working concentrations of 10-50x EC50, depending on efficacy and toxicity.

Before performing the microarray analysis of Huh7 cells infected with JFH-1 and treated with anti-viral compounds, the effect of anti-viral treatment on cell viability was assessed. Treatment of cells with a cytotoxic compound could affect the expression of host cell genes in a non-HCV dependent manner.

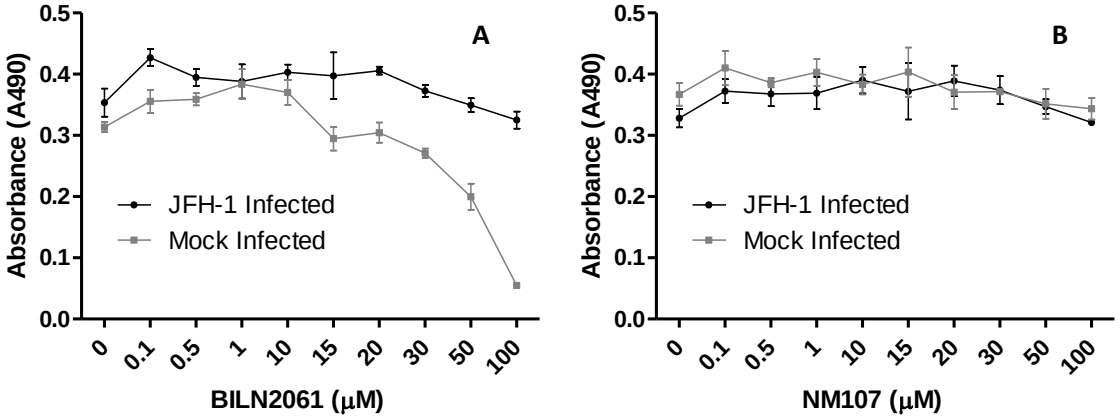


Figure 35: Cellular toxicity of anti-viral compounds.

Huh7 cells were infected with JFH-1 at an MOI of 3, or mock infected. At 12 hours post infection, cells were treated with anti-HCV inhibitors. At 48 hours post-infection, methyl violet staining of cells was performed and absorbance at 490nm was read to give an assessment of the survival of cells exposed to the anti-viral compounds. Four replicates were performed per condition.

The toxicity of anti-viral compounds on Huh7 cells was tested by methyl violet assay. The polymerase inhibitor NM107 was shown not to have a significant effect on the viability of Huh7 cells at any concentration tested, up to 100μM as seen in Figure 35B. The protease inhibitor BILN2061 was shown to be decrease cell viability in mock infected cells at concentrations of 15μM and greater (Figure 35A). Mock infected cells were nearly all killed by treatment with 100μM BILN2061. Cells infected with JFH-1 were to a large extent protected from the cytotoxic effect seen in the mock infected cells. This indicated that BILN2061 probably has some anti-protease activity on essential host cell proteases. A small effect on cell viability was seen at BILN2061 concentrations of 20μM and greater in cells infected with JFH-1.

The dose response data described in Figure 34 indicated that treatment with NM107 at a concentration of 50μM gave the greatest knockdown of intracellular JFH-1 RNA achievable. The mean intracellular JFH-1 RNA concentration in cells treated with 100μM NM107 was slightly lower than that in cells treated with 50μM, but this difference was not significant (determined by t-test in GraphPad Prism). An NM107 dose of 50μM was found not to be cytotoxic (Figure 35B), so this was selected as the dose at which to perform microarray analysis.

The dose response data described in Figure 34A indicated that treatment with BILN2061 at a concentration of 20μM gave the greatest knockdown of intracellular JFH-1 RNA achievable. A BILN2061 dose of 20μM was found to be slightly cytotoxic (Figure 35A) in mock infected cells. A

dose of 10μM was seen not to be toxic, and gave a strong knockdown of intracellular JFH-1 RNA, so this was selected as the dose at which to perform microarray analysis.

Gene expression changes between anti-viral treated samples and infected samples were calculated using Array Studio as before. No genes were observed to change in expression significantly ($|FC| \geq 2$, $p \leq 0.05$) on analysis of the comparison of NM107-treated infected samples with mock-treated infected samples. Eight probe sets were observed to change in expression significantly ($|FC| \geq 2$, $p \leq 0.05$) on analysis of the comparison of BILN2061-treated infected samples with mock-treated infected samples, as can be seen in Table 11.

Gene Symbol	Probe Set ID	Fold Change Infected, BILN2061-treated vs Infected, mock-treated
CYP1B1	202435_s_at	2.68
	202436_s_at	2.62
	202437_s_at	3.16
MT1E	212859_x_at	2.07
MT1F	213629_x_at	2.04
MT1M	217546_at	2.5

Table 11: Effect of BILN2061 treatment on gene expression in JFH-1 infected Huh7 cells.
Host cell gene expression changes between JFH-1 infected Huh7 cells treated with BILN2061, and JFH-1 infected Huh7 cells. Expression changes were observed in CYP1B1 and three metallothionein family members

Three probe sets observed to indicate a change in expression levels corresponded to one gene, CYP1B1 (cytochrome P450 1B1). In the analysis of infected Huh7 cells compared to mock infected Huh7 cells, CYP1B1 was one of the most highly up-regulated genes during infection. Three probe sets identified belonged to members of the metallothionein gene family. Metallothioneins were identified in both Huh7 cells and Huh7.5 cells as a gene family highly down-regulated during JFH-1 infection. The inhibition of HCV replication by BILN2061 may have also removed the stimulus that was inhibiting expression of metallothionein genes. Comparison of infected and mock infected Huh7 cells indicated that metallothioneins were expressed at lower levels in infected cells (Figure 24, Figure 30). The BILN2061-treated infected Huh7 cells expressed metallothioneins at double the level seen in mock treated infected Huh7 cells. This may indicate a return to normal expression levels for the metallothioneins.

3.5 Host Genes with a Role in HCV Replication

The microarray analysis of Huh7 and Huh7.5 cells infected with JFH-1 identified host genes that were regulated during HCV infection. It was hypothesised that some of the genes seen to be regulated during HCV infection may be changing in expression level because it confers an advantage on HCV replication efficiency.

3.5.1 Identification of Host Genes with a Role in HCV Replication

In order to identify genes which have an effect on HCV replication, a selection of genes were targeted for knockdown by RNA interference. Genes were selected based on the magnitude of fold change seen in their expression during HCV infection, and genes were selected based on the existence of evidence pointing to potential functional roles in the cell which may enhance efficient HCV replication.

In this part of the study a modified chimaeric HCV was used in addition to the wild type JFH-1. Jc1p7FLuc2A (hereon referred to as Jc1) is based on the chimaera of genotype 2a isolates J6 and JFH-1. As shown in the introduction (Figure 8) and here in Figure 36, the chimaeric genome Jc1 is formed from the structural region of J6 and the non-structural regions of JFH-1. This construct also incorporates a luciferase reporter gene, and a Foot and Mouth Disease virus (FMDV) 2A gene for autocleavage of the luciferase from the polyprotein. The advantage of using this reporter virus is that a large number of experiments can be performed using a simple luciferase reporter assay, rather than performing the multiple steps required for measurement of viral RNA by quantitative PCR.

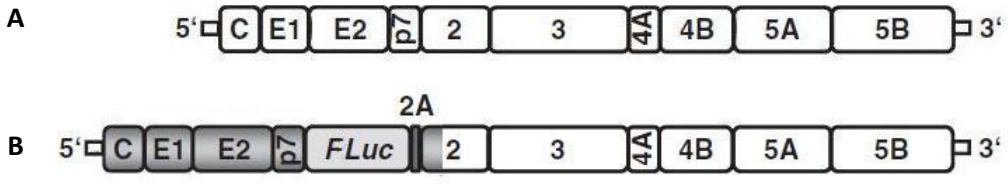


Figure 36: HCV constructs used to identify host genes with a role in HCV replication.

A Representation of the JFH-1 genome. **B** Representation of the Jc1 genome. The genetic elements C, E1, E2, p7 and NS2 (up to C3 position as shown in Figure 8) are from the J6 isolate. A firefly luciferase gene (FLuc) is positioned after p7, and an FMDV 2A gene immediately after FLuc to allow for autocleavage of FLuc from the expressed polyprotein. All other genetic elements are from isolate JFH-1.

Gene	Probe Set	Huh7 JFH-1 vs Mock Fold Change in Expression					Huh7.5 JFH-1 vs Mock Fold Change in Expression					Functions
		6 hr	12 hr	18 hr	24 hr	48 hr	6 hr	12 hr	18 hr	24 hr	48 hr	
ABLIM3	205730_s_at	1.43	1.58	2.1	1.63	-1.37	-1.64	-1.32	1.14	1.68	2.84	cytoskeleton organisation
CFH	213800_at	1.48	1.47	1.65	1.46	1.51	-1.28	2.68	5.02	2.55	2.14	complement
	215388_s_at	1.44	1.37	1.19	1.17	1.03	1.62	2.36	2.49	1.2	1.33	
CFI	203854_at	1.27	1.19	1.49	1.16	1.53	1.86	2.24	2.79	2.11	2.02	complement
	1555564_a_at	1.28	1.21	1.49	1.33	1.34	1.98	2.51	2.25	2.01	1.77	
CYP1A1	205749_at	2.17	4.18	2.28	5.19	2.58	1.44	1.5	1.82	1.45	2.5	cytochrome p450
MAT1A	205813_s_at	1.26	1.05	1.12	1.05	-1.03	4.69	1.96	4.35	1.71	1.57	makes methyl donor (SAMe)
MT1F	213629_x_at	-1.7	-2.19	-1.24	-2.45	-1.46	-1.43	-2.53	-3.03	-3.93	-5.35	oxidative stress, metal regulation
	217165_x_at	-1.69	-2.28	-1.18	-2.34	-1.39	-1.58	-2.54	-3.28	-4.14	-5.19	
MT1G	204745_x_at	-1.49	-1.54	-1.09	-1.87	-1.25	-1.34	-2.15	-2.9	-3.6	-4.62	oxidative stress, metal regulation
	210472_at	-1.14	-1.14	-1.02	-1.03	-1.03	1.38	1.17	-1.14	-1.04	-1.19	
MT2A	212185_x_at	-1.49	-2.06	-1.04	-2.24	-1.25	-1.28	-1.77	-1.87	-2.47	-2.85	oxidative stress, metal regulation
RAB40B	204547_at	1.31	-1.05	-1.1	-2.07	-1.31	3.3	1.78	1.13	1.07	1.81	vesicle transport
	217597_x_at	-1.13	-1.02	1.22	-1.11	-1.2	1.59	1.1	1.28	-1.32	1.28	
RAB27B	207017_at	1.47	1.22	1.32	1.25	1.25	1.24	1.2	1.07	-1.11	1.21	vesicle transport
	207018_s_at	1.45	-1.01	1.48	1.43	1.46	-1.06	1.34	1.27	-1.02	-1.33	
	228708_at	2.56	2.5	3.43	2.43	5.19	3.13	3.62	2.52	2.08	1.59	
RAB37	228113_at	1.53	1.26	1.63	2.07	2.5	1.71	1.04	1.35	1.24	1.74	vesicle transport
	244124_at	1.06	-1.32	1.02	-1.08	-1.14	1.31	-1.05	1.55	1.23	1.08	
SLC27A2	205768_s_at	1.21	-1.02	1.35	-1.09	-1.41	3.47	2.53	2.84	1.59	1.29	lipid metabolism
	205769_at	1.17	1.29	1.18	1.04	-1.29	3.8	2.33	2.74	1.67	1.39	
SOCS3	206359_at	-1.05	-1.07	1.41	1.11	1.41	1.09	1.19	1.09	1.04	1.2	cytokine signalling
	206360_s_at	1.07	-1.1	-1.04	1.08	-1.04	1.3	-1.11	1.32	1.06	-1.26	
	214105_at	1.07	-1.07	1.18	-1.07	-1.11	1.18	-1.06	1.12	1.11	1.19	
	227697_at	1.3	1.36	2.2	1.86	2.92	1.03	1.4	1.33	1.15	1.9	
SPTLC3	220456_at	1.28	1.01	-1.17	1.04	-1.3	2.44	1.51	1.29	1.2	-1.17	sphingolipid synthesis
	227752_at	2.14	1.57	1.12	-2.04	-3.05	3.26	1.79	1.96	1.42	-1.04	
TXNIP	201008_s_at	1.3	8.39	5.26	20.15	15.32	1.24	1.92	1.66	1.22	3.18	oxidative stress, apoptosis, cell proliferation, sugar metabolism
	201009_s_at	1.15	6.56	4.99	13.55	14.3	1.2	1.39	1.38	1.55	2.14	
	201010_s_at	1.38	9.3	6.03	20.51	21.96	2.05	1.52	2.6	1.41	3.03	

Table 12: Expression level changes, during JFH-1 infection of Huh7 and Huh7.5 cells, of genes selected for RNA interference studies.

This table presents fold change data from both Huh7 and Huh7.5 microarray studies for every probe set of the genes selected. Also presented are biological functions and potential biological functions of selected genes as identified from literature and databases

Optimal concentration of siRNA for transfection was previously determined. In order to show that siRNAs were being efficiently delivered to the majority of cells, a control was performed using a fluorescently labelled oligonucleotide designed for this purpose. Figure 37 shows the efficient delivery of fluorescent oligonucleotide to Huh7.5 cells. Red staining indicates the presence of fluorescent oligonucleotide, and this can be seen in the majority of cells. The diffuse red staining seen throughout the cytoplasm and also localised to the nucleus indicates that siRNA has been delivered to the cells. The reason for the presence of discrete points of bright staining is unknown, but may correspond to endosomes or p-bodies (or some other nucleic acid degradation structure). This result indicates that transfection by the described protocol is efficient and suitable for further studies.

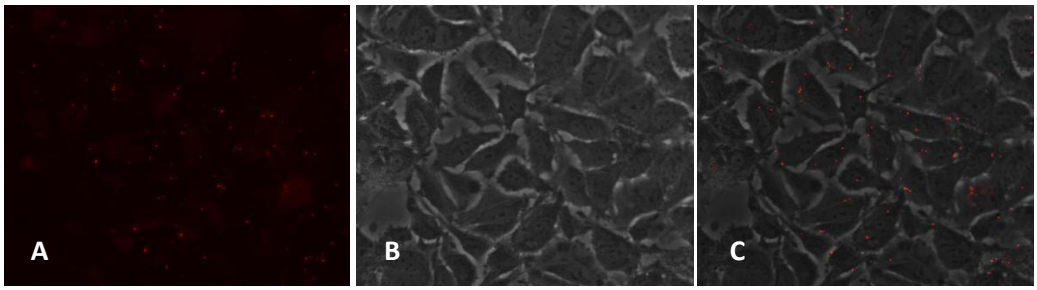


Figure 37: Efficiency of siRNA delivery.

Huh7.5 cells were transfected with 25nM Block-iT AlexaFluor Red oligo. Cells were photographed at 40x magnification. Images were obtained in the red (**A**) and phase (**B**) channels, and a merged image was created (**C**). It can be seen that Block-iT AlexaFluor Red oligo is present in the greater than of 90% of cells.

Having established the efficient delivery of siRNA, the potency of the siRNAs was tested. For each of the 15 cellular targets, two siRNAs were synthesised. For the initial testing, the two siRNAs were pooled. A control pool of siRNAs directed against DDX3X, known to knockdown both the target host gene and HCV, was used as a positive control in these experiments. The efficiency of the pooled siRNAs to knockdown their host gene targets was measured by qRT-PCR. As can be seen in Figure 38 the efficiency of knockdown varied for each target. Knockdowns achieved ranged from 85% for CYP1A1 to 60% for CFH. The siRNA pool directed against DDX3X had already been determined to give target knockdown of greater than 80%.

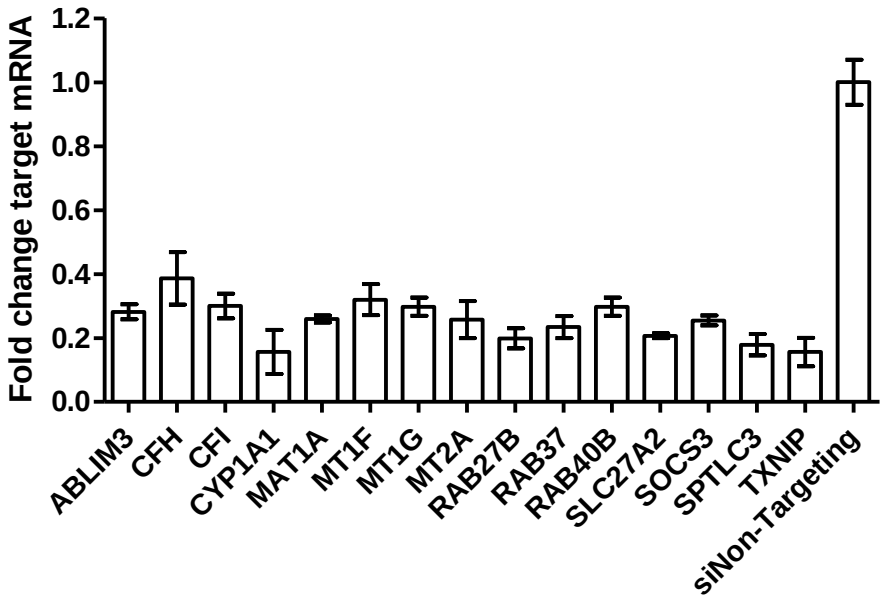


Figure 38: Knockdown efficiency of siRNAs targeted to the 15 host genes selected for study by RNA interference.

Huh7.5 cells were transfected with 25nM of two pooled siRNAs per target for 48 hours, and target transcript levels were measured by RT-qPCR. Data were normalised to average host gene levels in cells separately transfected with two different non-targeting siRNAs.

The pooled siRNAs for each host gene target were then tested for any anti-HCV effect. The HCV Jc1 virus carrying a firefly luciferase reporter gene was used for this purpose. The target cells were transfected with siRNA to knockdown the host gene transcript levels, before being infected with virus. Luciferase activity was measured as a determination of HCV replication efficiency.

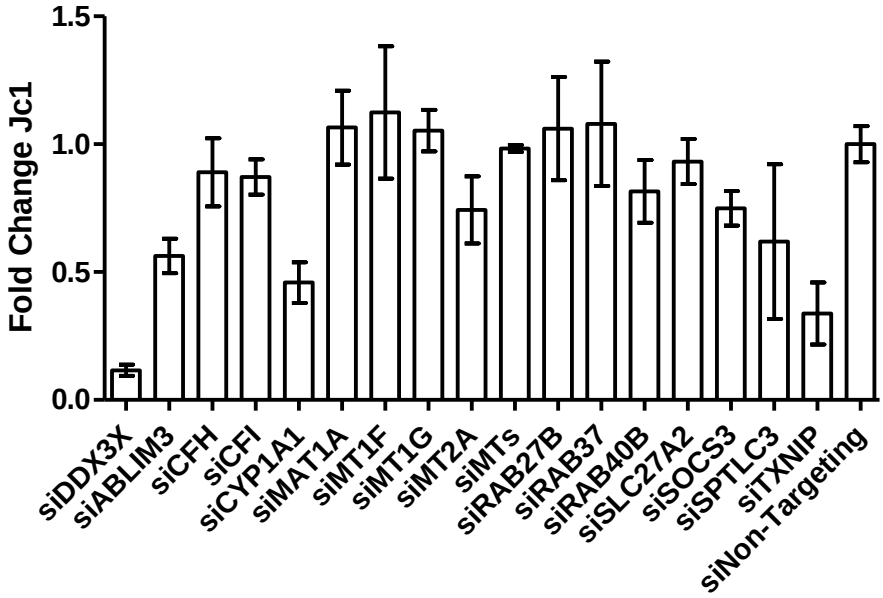


Figure 39: Effect of host gene knockdown on HCV replication using pooled siRNAs.
Huh7.5 cells were transfected with 25nM of two pooled siRNAs per target 48 hours before infection with Jc1. 48 hours post infection, luciferase activity was measured. Data were normalised to average host gene levels in cells separately transfected with two different non-targeting siRNAs. The pool siDDX3X was used as a positive control, as knockdown of this host cell gene was known to inhibit HCV replication. An additional pool of all the metallothionein siRNAs combined was also tested (column labelled siMTs).

A range of responses was seen to the use of these siRNAs. Knockdown of some host targets had an effect on HCV replication, and knockdown of other host targets having no effect on HCV replication. The siRNAs seen to have the most inhibitory effects on HCV replication were selected for further testing. These were the siRNAs against the genes ABLIM3, CYP1A1, SPTLC3, and TXNIP.

To obtain more precise data on the effect on HCV replication of the individual siRNAs, the pools were no longer used. Instead, the individual siRNAs were used in transfections. This meant that there were two separate siRNAs for each host gene which could be tested for their inhibition of HCV replication.

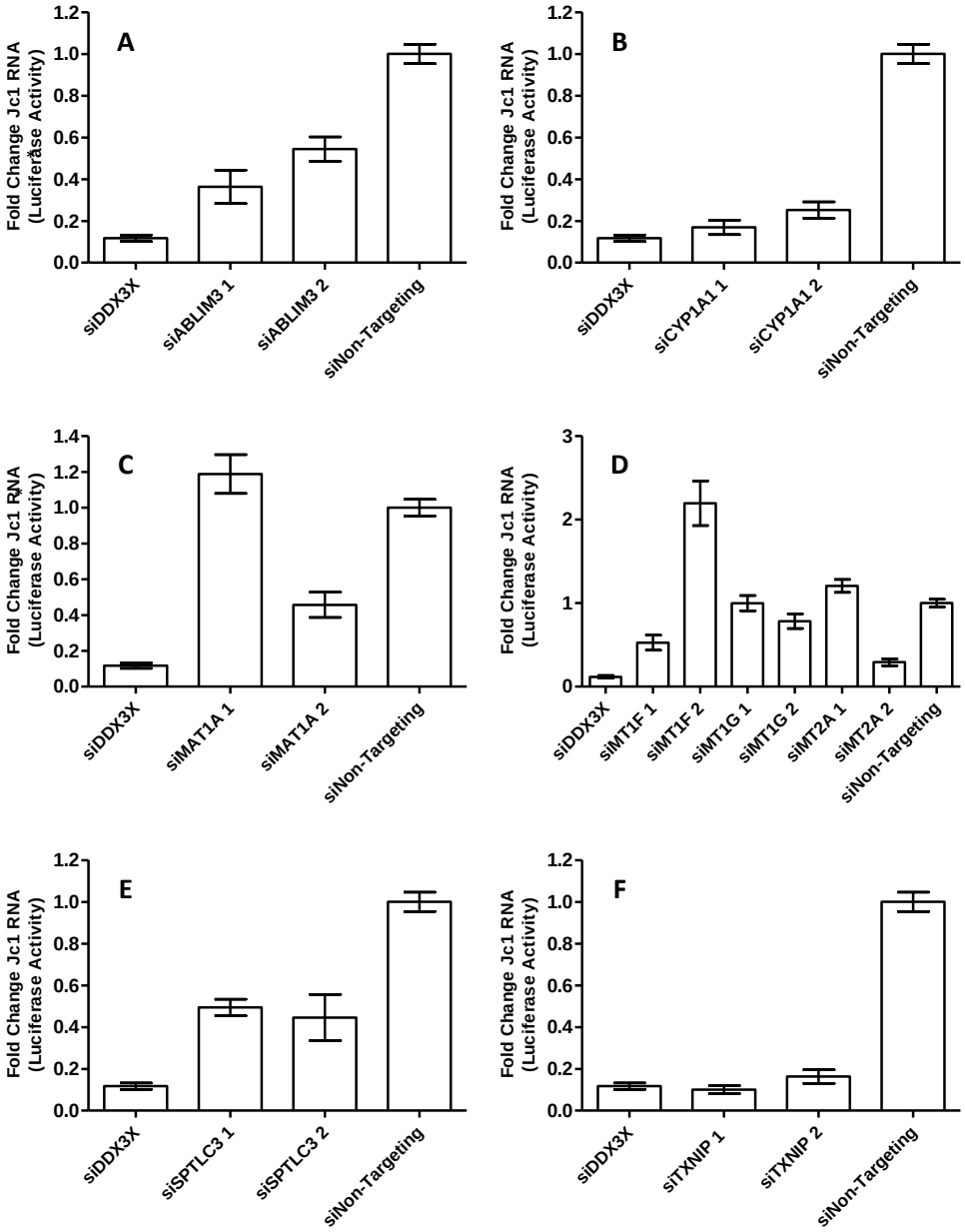


Figure 40: Effect of host gene knockdown on HCV replication using deconvoluted siRNAs.

Huh7.5 cells were transfected with 25nM siRNA 48 hours before infection with Jc1. 48 hours post infection, luciferase activity was measured. Four replicates were performed in each experiment, and three experiments performed. Data were normalised to the average luciferase level in cells separately transfected with two different non-targeting siRNAs. The pool siDDX3X was used as a positive control, as knockdown of this host cell gene was known to inhibit HCV replication. T-tests were performed to calculate whether there was a statistically significant difference in luciferase levels between cells treated with siRNAs targeting host genes and the non-targeting siRNAs. F-testing indicated a difference in variance when comparing siDDX3X, siTXNIP 1, siMAT1A 1 and siMT1F 2 with siNon-Targeting data so a Welch's correction was applied to these t-tests. A significant difference ($p \leq 0.05$) in Jc1 levels was found for all siRNAs except siMAT1A 1 and siMT1G 1.

The effect of knockdown of host cell genes by individual siRNAs on Jc1 replication can be seen in Figure 40. The positive control siDDX3X inhibits HCV replication (as measured by luciferase activity) by 90%. The most effective inhibition of HCV on knockdown of a host gene was seen when targeting TXNIP. Both siTXNIP 1 and 2 inhibited HCV replication by greater than 80% (Figure 40F). Knockdown of CYP1A1 inhibited HCV replication by 75% (Figure 40B). Knockdown of genes ABLIM3 and SPTLC3 (Figure 40A and E) also inhibited HCV replication, but to a lesser extent, by around 50% each.

The effect of knockdown of metallothionein genes on HCV replication was also tested. The microarray analysis indicated that metallothionein expression is decreased during HCV infection. Knockdown of MT genes prior to infection was therefore predicted not to inhibit HCV replication. As can be seen in Figure 40D, a range of changes in HCV replication was seen in response to inhibition of MT genes. Knockdown of MT1G did not affect HCV replication. Use of siMT1F 1 inhibited HCV replication, but siMT1F2 increased HCV replication. MT2A is the most abundant form of metallothionein in the liver, use of siMT2A 1 did not inhibit HCV replication, but siMT2A 2 did inhibit HCV replication by 70%.

In order to show that the inhibitory effects observed on HCV replication were not due to stress effects on the cells induced by knockdown of the host genes, cell viability assays were performed. A standard technique for assessing the viability of cells by measuring their ATP content was performed. Figure 41 shows that the act of transfection with siRNA results in a very small increase in the viability of cells, as indicated by comparison of cells transfected by non-targeting siRNAs with untransfected cells. The siRNA siTXNIP 2 had a small effect on the viability of cells, decreasing the observed light levels by about 10%. Overall, the transfections of siRNAs targeting host cell genes were shown not to have a major effect on cell viability. This supports the hypothesis that the effects on HCV replication observed were due to knockdown of the host cell genes targeted by RNA interference.

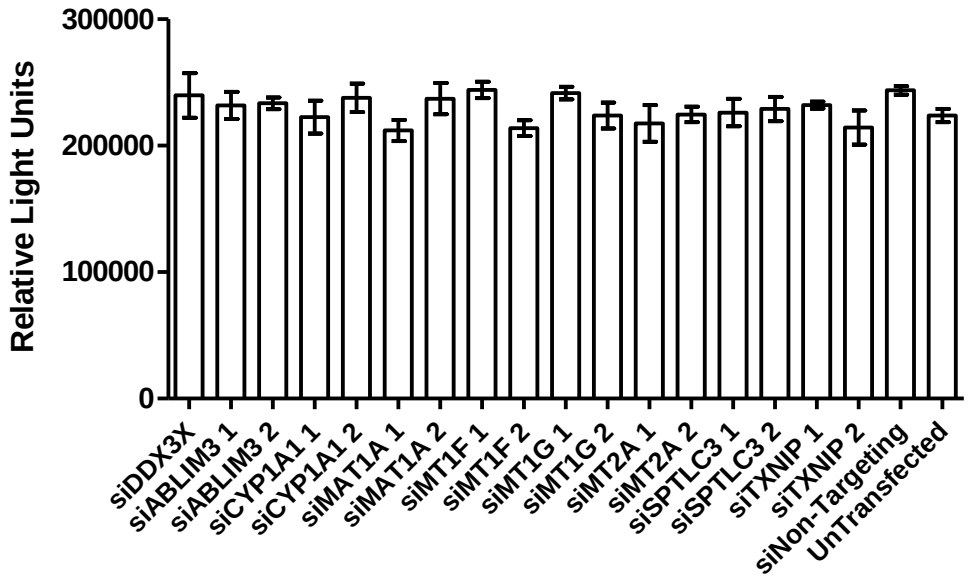


Figure 41: Cellular toxicity of siRNAs.

Huh7.5 cells in a 96-well plate were transfected with 25nM siRNA for 48 hours, and the viability of transfected cells was measured by Cell Titer-Glo assay. Each transfection was performed as four replicates, with the mean data and standard error plotted. Wells containing no cells gave an average fluorescence of 40 relative light units. As a positive control for cytotoxicity, cells were treated with 100μM H_2O_2, giving an average fluorescence of 2000 relative light units.

To establish whether the gene expression changes observed in the microarray studies were limited to the infectious HCV model, the transcript levels of genes of interest were quantified in replicon cells relative to the parental line. All experiments were performed in Huh7.5 cells. Two replicon cell lines were used, both based on Huh7.5 cells, one line harbouring a genotype 1b replicon (cell line Rep4.5) and one line harbouring a genotype 2 replicon (cell line 15.53). The expression levels of genes of interest in replicon lines compared to Huh7.5 cells are reported in Figure 42. The most striking differences in expression were seen for genes MAT1A and TXNIP. Both of these genes were observed to be expressed at significantly lower levels in replicon cells compared to Huh7.5 cells. It was also observed that expression in 2a replicon cells was lower than that in 1b replicon cells. This may indicate a relationship between gene expression genotype, or it may be a function of the level of HCV replication. HCV replicon RNA titres are higher in genotype 2a replicon cells than in genotype 1b replicon cells. The low levels of TXNIP in replicon cells are the opposite of the highly induced levels seen in JFH-1 infected cells.

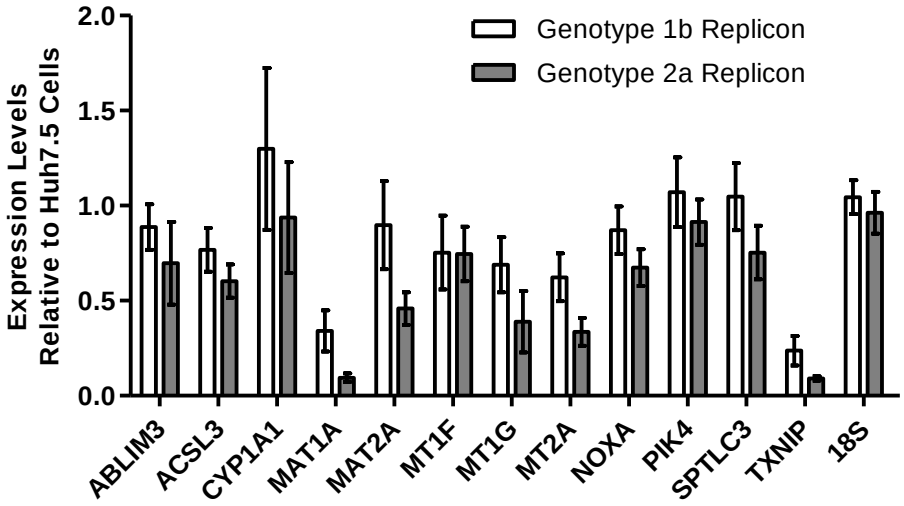


Figure 42: Relative expression of genes observed to change in microarray studies in Huh7.5 cells harbouring subgenomic replicons compared to Huh7.5 cells.

Cells harbouring a genotype 1b replicon (Rep4.5), a genotype 2a replicon (15.53) and Huh7.5 cells were seeded in duplicate. 48 hours later, total cell RNA was extracted and qRT-PCR performed. Gene expression was normalised using GAPDH. Mean expression levels with standard error are shown for each gene, with genotype 1b replicon data in white and genotype 2a replicon data in grey bars. Another housekeeping gene, 18S, is displayed as a control to demonstrate a gene known not to be affected by the presence of replicon. Three separate experiments were performed.

3.5.2 Genes Identified as Required for HCV Replication

The microarray analysis of Huh7 and Huh7.5 cells infected with JFH-1 identified host genes that were regulated during HCV infection. This information may be of importance for the understanding of the influence that HCV has on patient physiology. However, it does not tell us why the genes are regulated and, importantly, whether these genes are regulated because they have an effect on HCV replication (or whether they are, for example, a secondary effect or part of the host's reaction to infection).

Several genes were identified as being upregulated during JFH-1 infection, and having potential functional roles in the HCV lifecycle (Table 12). These genes were silenced by siRNA to investigate whether they were required for HCV replication (Figure 39). Four genes were identified as being required for efficient HCV replication, based on an inhibition of HCV replication when these genes were silenced (Figure 40). These genes were ABLIM3, CYP1A1, SPTLC3 and TXNIP.

3.5.2.1 Actin binding LIM protein family, member 3 (ABLIM3)

The levels of ABLIM3 were observed to be deregulated during infection with HCV. At most timepoints ABLIM3 was slightly upregulated, however at 48 hours post-infection in Huh7 cells and at 6 hours post infection in Huh7.5 cells, expression was downregulated in infected cells. Knockdown of ABLIM3 by RNA interference inhibited HCV replication by up to 60%.

Actin binding LIM protein family, member 3 (ABLIM3) is not yet well studied. It is the third member in a family of three ABLIM proteins, each of which contain four LIM domains and a villin head piece domain[463]. LIM domains are double zinc fingers, and have been found in proteins involved in cell development and cancer determination. Proteins containing LIM domains can interact with each other. The villin head piece domain enables the protein to bind actin[464-465]. ABLIM and its drosophila homologue UNC-115 have been shown to be involved in axon guidance [466-467].

A recent study identified ABLIM3 as a component of the adherens junction in several epithelial cell types, including hepatocytes[468]. This study revealed colocalisation of ABLIM3 with the adherens junction marker protein β–catenin, but not with the tight junction marker ZO-1 (zona occludens 1). Tight junctions have been shown to be involved in cell to cell transmission of HCV[469], and certain tight junction proteins (including occludin and claudin-1) are important molecules for entry of HCV to the cell. Adherens junctions are the first junctions to form between cells, including before tight junctions. The reduction in levels of ABLIM3 due to knockdown by siRNA may disrupt or impair adherens junction formation and therefore subsequent tight junction formation. This could inhibit the ability of HCV to be transmitted from cell to cell within culture. Clathrin-coated pits are found in close proximity to adherens junctions, and adherens junctions are known to be associated with microtubules[470]. Both of these structures are involved in the entry and internalisation of HCV, so their disruption could impede HCV replication. The recent evidence that ABLIM3 is a component of the adherens junction, its ability to interact with actin, its ability to interact with other proteins through its LIM domains, and the siRNA data indicating that its reduction impairs the efficient replication of HCV all suggest that ABLIM3 may be worth further investigation.

3.5.2.2 Cytochrome P450, family 1, subfamily A, polypeptide 1 (CYP1A1)

In this study, CYP1A1 and CYP1B1 were observed to be upregulated during HCV infection. CYP1A1 was upregulated in both Huh7 and Huh7.5 cells with slight initial upregulations increasing to 2.5-fold (Huh7.5) and 5-fold (Huh7) changes in expression compared to mock infected cells at 48 hours post infection. A small increase in expression of CYP1B1 was observed in Huh7 cells, but not in Huh7.5 cells. As CYP1A1 was amongst the more highly regulated genes and given its potential involvement in lipid metabolism, CYP1A1 was chosen as a target for RNA interference to determine whether knockdown would impair HCV replication. Knockdown of CYP1A1 prior to infection was found to inhibit HCV replication by up to 80%.

Cytochrome P450 (CYP) proteins are haeme-containing monoxygenase enzymes which play a role in the metabolism of xenobiotic environmental chemicals including drugs, as well as endogenous molecules such as lipids, steroids, cholesterol and bile acids. Lipophilic xenobiotics are oxygenated by CYP enzymes as a first step in transforming the xenobiotics into hydrophilic, and therefore excretable, molecules. CYP1A1 localises to the ER in the cell, and CYP proteins are most common in the liver. CYP1 can metabolise molecules including polycyclic aromatic hydrocarbons (PAH)[471], aflatoxin B1[472-474] and arylamines[475-476]. CYP1A1 expression can also be induced by polycyclic aromatic hydrocarbons, which it can then convert into carcinogenic intermediates[477-478]. CYP1A1 has been associated with risk of lung cancer. CYP1A1 and CYP1B1 can also metabolise endogenous estradiol into 2-hydroxyestradiol and 4-hydroxyestradiol (which is mutagenic) respectively[475]. CYP1A1 is also known to be able to convert ethylene into ethylene oxide[479-480].

The biological action of CYP on xenobiotics means that the efficacy of many drugs can be affected by its action. It is now common for drugs to be tested for metabolism by CYP during development. Tamoxifen, a treatment for breast cancer is catalysed into its active form tamoxifen to 4-hydroxytamoxifen by CYP[481]. CYP have been shown to be decreased in expression in hepatoma cells[482]. Treatment of hepatoma cell lines with the anti-cancer drug emodin rapidly induced expression of CYP1A1 and CYP1B1, and cell cycle arrest[483].

CYP1A1 induction is mediated through the aryl hydrocarbon receptor (AhR). AhR-mediated induction of CYP1A1 expression has been shown to be impaired in cells harbouring a subgenomic HCV replicon. Constitutive expression of CYP1A1 was shown to be higher in these replicon cells than their parental cells[484]. It has been reported that CYP1A1 activity can lead to oxidative stress[485-486],

and it is possible that increased expression of CYP1A1 during HCV infection could be contributing to the oxidative stress that has been previously observed in HCV infected cells. It has also been shown that there is a link between smoking and development of liver lesions in HCV patients[487-488], and this could be linked to the ability of CYP1A1 to convert PAH into carcinogenic compounds, or oxidative stress effects.

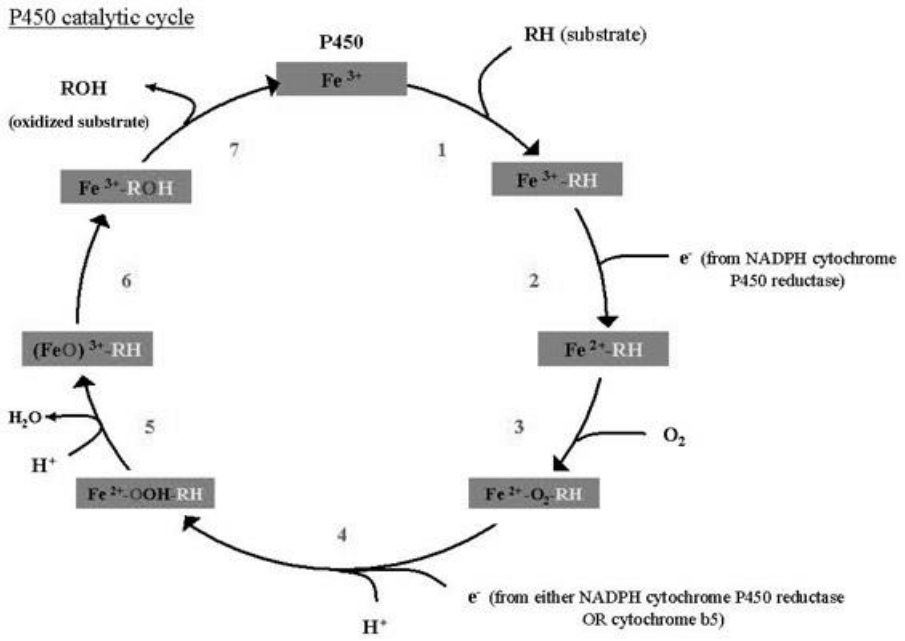


Figure 43: The cytochrome P450 catalytic cycle.

This diagram shows the steps involved when a substrate binds to the cytochrome P450 enzyme. (1) The normal state of a P450 with the iron in its ferric [Fe^{3+}] state. (2) The substrate binds to the enzyme. (3) The enzyme is reduced to the ferrous [Fe^{2+}] state by the addition of an electron from NADPH cytochrome P450 reductase. The bound substrate facilitates this process. (4,5) Molecular oxygen binds and forms an $Fe^{2+}OOH$ complex with the addition of a proton and a second donation of an electron from either NADPH cytochrome P450 reductase or cytochrome b5. A second proton cleaves the $Fe^{2+}OOH$ complex to form water. (6) An unstable $[FeO]^{3+}$ complex donates its oxygen to the substrate (7). The oxidised substrate is released and the enzyme returns to its initial state (1).

3.5.2.3 Serine palmitoyltransferase long chain base subunit 3 (SPTLC3)

The levels of SPTLC3 were observed to be deregulated during infection with HCV. At early timepoints SPTLC3 was upregulated by 2-fold in infected Huh7 and 3-fold in infected Huh7.5, but levels reduced over time and were downregulated in infected cells at 48 hours post infection. Knockdown of SPTLC3 by RNA interference inhibited HCV replication by around 50%.

SPT catalyses the condensation of serine and palmitoyl coA to produce 3-ketodihydrosphingosine. This is the first, and rate limiting, step in the production of sphingolipids. Sphingolipids are important constituents of cellular membranes, and are important in the formation of lipid rafts[489-492]. SPT is upregulated in response to some stresses, and sphingolipids have also been shown to be involved in apoptosis, indicating that SPT could be upregulated in order to induce apoptosis[493-495].

It has been proposed that the stoichiometry of the SPTLC1/2/3 complex, and therefore its activity, depends on the SPTLC2 and 3 expression levels[496]. It has also been shown that SPTLC3 forms C(16)-sphingoid bases and that a significant proportion of sphingolipids (about 15%, found in HDL and LDL) have C(16) backbones[497]. This may explain why only SPTLC3 levels were observed to change during HCV infection, and would indicate that a change in only SPTLC3 levels will still be important in determining the activity of the final enzyme complex.

In agreement with the finding here, that RNA interference of SPTLC3 inhibits HCV replication, other studies have shown the ability of a chemical SPT inhibitor to suppress HCV[498-499]. These studies indicate that NS5B binds sphingomyelin and that the inhibitor disrupts this binding, resulting in the movement of NS5B to from detergent resistant membranes to detergent soluble fractions. Combination therapy of humanised chimaeric mice infected with HCV with the SPT inhibitor and PEG-IFN resulted in a 3-log drop in serum HCV RNA.

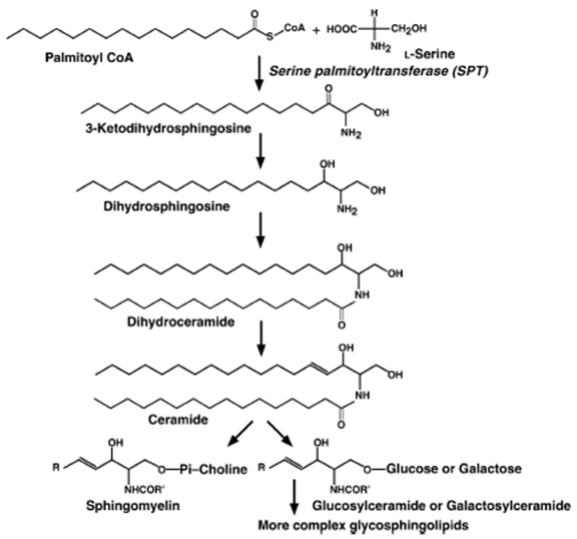


Figure 44: Biosynthetic pathway of sphingolipids in mammalian cells[500].

3.5.2.4 Thioredoxin-interacting protein (TXNIP)

The most significant finding of these studies has been the importance of TXNIP to HCV replication. TXNIP was identified, through microarray analyses validated by qRT-PCR, to be highly upregulated during HCV infection. In both Huh7 and Huh7.5 cell lines, TXNIP was found to be one of the most highly upregulated host genes (Table 4 and Table 8). The three probe sets identifying TXNIP expression present in the microarrays showed similar expression levels at all timepoints. Validation performed by qRT-PCR of RNA from Huh7 cells at 48 hours post-infection also showed very strong upregulation of TXNIP expression (Figure 31C). Expression of TXNIP was seen to have increased significantly by 12 hours post-infection, and transcript levels increased at each timepoint. Knockdown of TXNIP by RNA interference inhibited HCV replication by up to 90%

There is evidence to suggest that TXNIP, also known as VDUP1 and TBP-2, has roles in multiple cellular processes. As its name suggests, TXNIP binds and inhibits the activity of thioredoxin thus providing a regulatory role for cellular redox state and oxidative stress[501-504]. TXNIP can affect cell proliferation and cell cycle by acting as a tumour suppressor[505-511], and can promote apoptosis[503,512]. Natural killer cell development is affected in mice lacking TXNIP[513]. Most research so far on TXNIP has focused on its role in glucose and lipid metabolism. Many of the functions of TXNIP are a result of its interaction with thioredoxin (TRX). TRX is a 12kDa thiol reductase which is conserved across kingdoms and has several functions in the cell. The two cysteine residues in the WCGPC active site provide sulphydryl groups for the reducing activity of TRX. Once oxidised, TRX can be reduced to a dithiol again by NADPH and TRX reductase[514-515]. TRX exists in several locations. In the cytoplasm it protects against oxidative stress[516-517] and regulates signal transduction[518-519]. It has been shown to exist in the mitochondrial intermembrane space[507]. In the nucleus it regulates transcription factors including NF-κB and AP-1[520-521]. It can also be secreted to act like a cytokine[522-524].

TXNIP transcriptional expression is not fully understood, but it is known that the promoter region contains two ChoREs (carbohydrate response elements), two CCAATs and one FOXO (forkhead box O)[525]. There are also a vitamin D response element and a glucocorticoid response element present in the promoter. TXNIP is known to be stimulated by vitamin D[526], glucocorticoid[527-528], PPAR agonist[423-424,529], TGF-β[509], an inhibitor of histone deacetylase (HDAC) called suberoylanilide hydroxamic acid[511,530], molecules containing adenosine[531] and heat shock factors[532]. TXNIP is known to be inhibited by insulin[533], and stimulated by glucose[531,534-536].

There is increasing evidence that TXNIP regulates glucose uptake in humans. It has been shown that glucose can induce the expression of TXNIP in several cell types. It has also been found that forced expression of TXNIP will reduce glucose uptake and inhibition of TXNIP will increase glucose uptake, and that the presence of insulin will reduce TXNIP expression[533]. The same study found levels of TXNIP to be elevated in diabetics and pre-diabetics. Patients with HCV can develop insulin resistance[537-539] and therefore type 2 diabetes. The observed increase in TXNIP expression during HCV infection described in this thesis may indicate a mechanism for this pathology. Insulin resistance can be a predictor for non-response to anti-viral therapy[540-544]. It has been proposed that glucose and glutamine can affect the state of the transcription factor ModoA, for which there is a binding site (ChoRE) in the TXNIP promoter. Glutamine has been shown to repress TXNIP through this mechanism[545]. Elevated levels of TXNIP would result in reduced glucose in the cell. As glucose is essential for cell growth this may also have the effect of inhibiting proliferation. TXNIP has been shown to be a regulator of hepatic glucose production, and study of $TXNIP^{-/-}$ mice found them to be hypoglycaemic and hypoinsulinemic[546]. Regulation of glucose metabolism by TXNIP has been shown to be possible independently of TRX, and the TXNIP-related protein ARRDC4 can also inhibit glucose uptake, indicating that the arrestin domain is important for this function[547].

TXNIP plays a role in regulation of oxidative stress through its ability to bind and inhibit TRX[501-504]. TRX can reduce reactive oxygen species (ROS) and protects against damage by H_2O_2. It follows that increases in TXNIP will inhibit TRX and therefore inhibit the cellular response to ROS. Conditions promoting TXNIP expression such as hyperglycaemia have been shown to promote oxidative stress through this mechanism[535]. It has been shown that in response to ROS, TXNIP dissociates from TRX. As well as freeing TRX to perform anti-oxidant functions, this makes TXNIP available. TXNIP can associate with NLRP3 leading to activation of the inflammasome[548-549]. The inflammasome activates caspase 1, which in turn generates mature IL-1β. This may be a mechanism for the inflammation observed in diabetics (who have raised levels of TXNIP). The drug glibenclamide, which is used in the treatment of diabetes, can inhibit the induction of TXNIP by glucose and also NLRP3 inflammasome activation[548,550].

Oxidative stress is observed in cells infected with HCV. Upregulation of TXNIP in infected cells would inhibit the ability of the cell to respond to oxidative stress, and could increase the damage suffered by infected cells.

Several lines of investigation point to the role of TXNIP as a tumour suppressor, and there is some evidence for a role in apoptosis. An important target for TRX reduction is ribonucleoside reductase, which is required for DNA synthesis[551], and inhibition of TRX by TXNIP could slow DNA synthesis. $TXNIP^{-/-}$ mice have been shown to develop HCC in 40% of cases with slightly increased prevalence in males[505]. Fibroblasts deficient in TXNIP had reduced levels of $p27^{kip1}$, a cyclin dependent kinase inhibitor, seemingly due to the interaction of TXNIP and JAB1 promoting the destabilisation of $p27^{kip1}$ and blocking $p27^{kip1}$ translocation to the nucleus. As a result, these cells were observed to proliferate more rapidly, supporting the evidence for the role of TXNIP as a tumour suppressor[506]. Overexpression of TXNIP has been shown to induce apoptosis (in pancreatic β cells) by measurement of expression of Bax, Bcl-2 and caspases 3 and 9[534], and TXNIP upregulation was shown in neuronal apoptosis[552]. TRX has been shown to have anti-apoptotic effects through ASK1 binding, and TXNIP, as an inhibitor of TRX, can induce apoptosis through this mechanism. The haematopoietic stem cell (HSC) population is quickly lost in $TXNIP^{-/-}$ mice, and expression of TXNIP is decreased in HSC activation, indicating that TXNIP can maintain HSC quiescence[553]. TXNIP expression is lost in adult T-cell leukaemias that are induced by human T-cell leukaemia virus type 1, indicating the role of TXNIP in tumour suppression[508]. Ceramide, which is generated as part of sphingolipid metabolism in response to apoptotic stimuli, is a promoter of TXNIP expression. Knockdown of TXNIP by siRNA has been shown to inhibit ceramide induced ASK1, p38 and JNK phosphorylation, and cell apoptosis[512]. Degradation of TXNIP can occur in an ubiquitin-dependent manner, regulated by the E3 ubiquitin ligase Itch, leading to an anti-apoptotic effect[554]. TXNIP expression is upregulated by TGF-β1 and 1,25-dihydroxyvitamin D_3, and can arrest the cell cycle at G_0/G_1 phase[509].
The tumour suppressive role of TXNIP would aid the response to liver damage by HCV infection. Apoptosis induced by increased levels of TXNIP could help to account for the damage suffered to the liver during HCV infection.

TXNIP has been shown to play a role in cell differentiation. In the $TXNIP^{-/-}$ mice, a deficiency of NK cells was observed and it was suggested that TXNIP is required for CD121 expression and NK cell maturation[513].

TXNIP plays a role in lipid metabolism. Both $TXNIP^{-/-}$ and HcB-19 mice (which have a nonsense mutation in TXNIP) have hyperlipidaemia, with elevated levels of triglyceride and cholesterol in plasma[555-557]. TXNIP expression is also downregulated in PPARα-null mice, and it is possible that the lipid and glucose metabolism changes seen in these mice are in some part to do with the altered TXNIP expression[423]. The lack of TXNIP in $TXNIP^{-/-}$ mice was shown to inhibit the development of

steatohepatitis (during a methionine and choline deficient diet) by lowering oxidative stress, inhibiting release of cytokines and inhibiting cellular infiltration and fibrosis[558]. As TXNIP levels were greatly increased during HCV infection in the work presented here, this could contribute to HCV related steatosis.

TXNIP has been reported to be stimulated by glucocorticoid, and this stimulation resulted in apoptosis[527]. A case in which an HCV patient was treated with a glucocorticoid (prednisolone, for polymyositis), resulted in a large increase in serum HCV RNA titre[559]. It would be interesting to determine whether a similar reaction occurs *in vitro*, and whether glucocorticoid stimulation of TXNIP occurred, and was responsible for the increase in HCV.

All of these points make an attractive proposition for further research into TXNIP inhibition as a therapeutic for HCV patients.

3.6 Cellular Metabolites in JFH-1 Infected Cells

The microarray analyses have identified gene expression changes in JFH-1 infected cells. The genes identified may have functions resulting in changes in levels of metabolites in the host cells. In particular, as many of the genes identified are involved in lipid and carbohydrate metabolism, a study was undertaken to investigate any corresponding changes in metabolites during JFH-1 infection.

3.6.1 Spectroscopic Profiling of Cellular Metabolites

Protocols have been developed to quantify the levels of metabolites in cells by proton magic-angle spinning (MAS) magnetic resonance spectroscopy (MRS)[403]. The technique employed primarily identifies lipid molecules, as well as some amino acids, and sugar molecules such as glucose and glycogen. The MRS technique used has been performed on liver biopsy material. The experiment described here was the first time that live, infected cultured cells had been used in MRS. Figure 45 shows an example MRS profile with the major metabolite peaks identified.

Figure 46 shows the four profiles obtained for mock infected (Figure 46A-D) and JFH-1 infected (Figure 46E-H) Huh7.5 cells. The average area of each metabolite peak was then calculated for mock infected and infected cells (Figure 47). The most distinct change in a metabolite level observed is the decrease in height of the phosphocholine (PC) and glycerophosphocholine (GPC) peak with infection. The phosphatidylcholine (PtdC) peak was seen to increase in height with infection. The height of each peak of interest was measured to give a quantitative estimate of the amount of each metabolite in each sample.

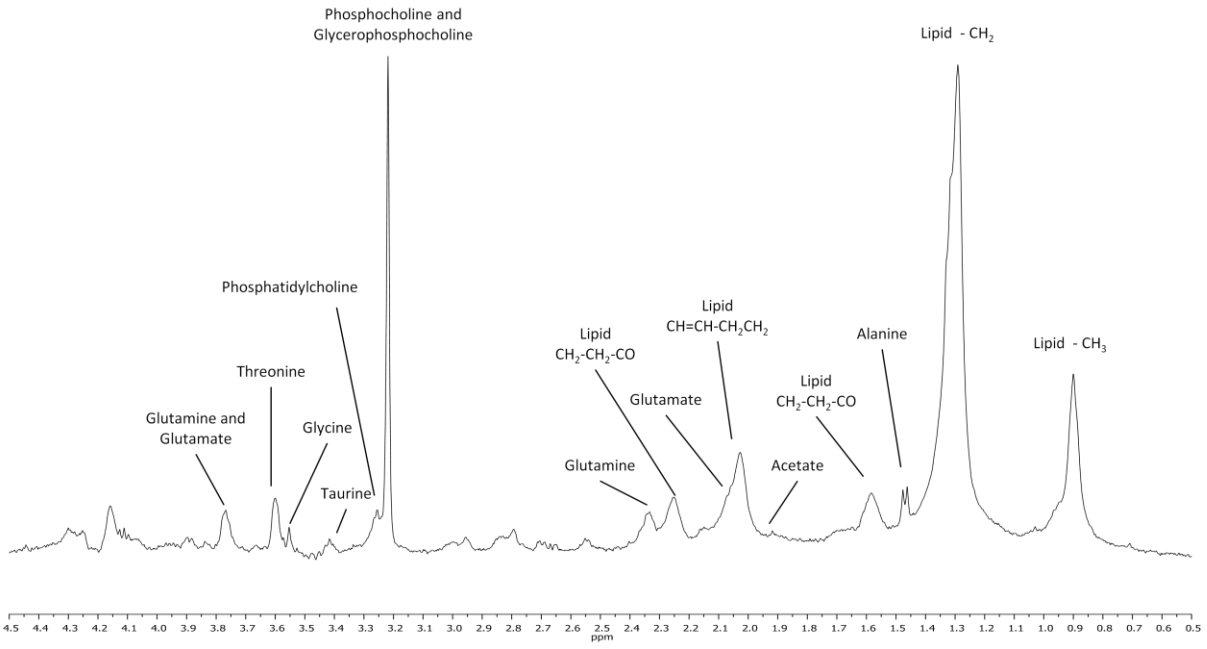


Figure 45: An example proton MAS MRS profile with the major metabolite peaks identified.

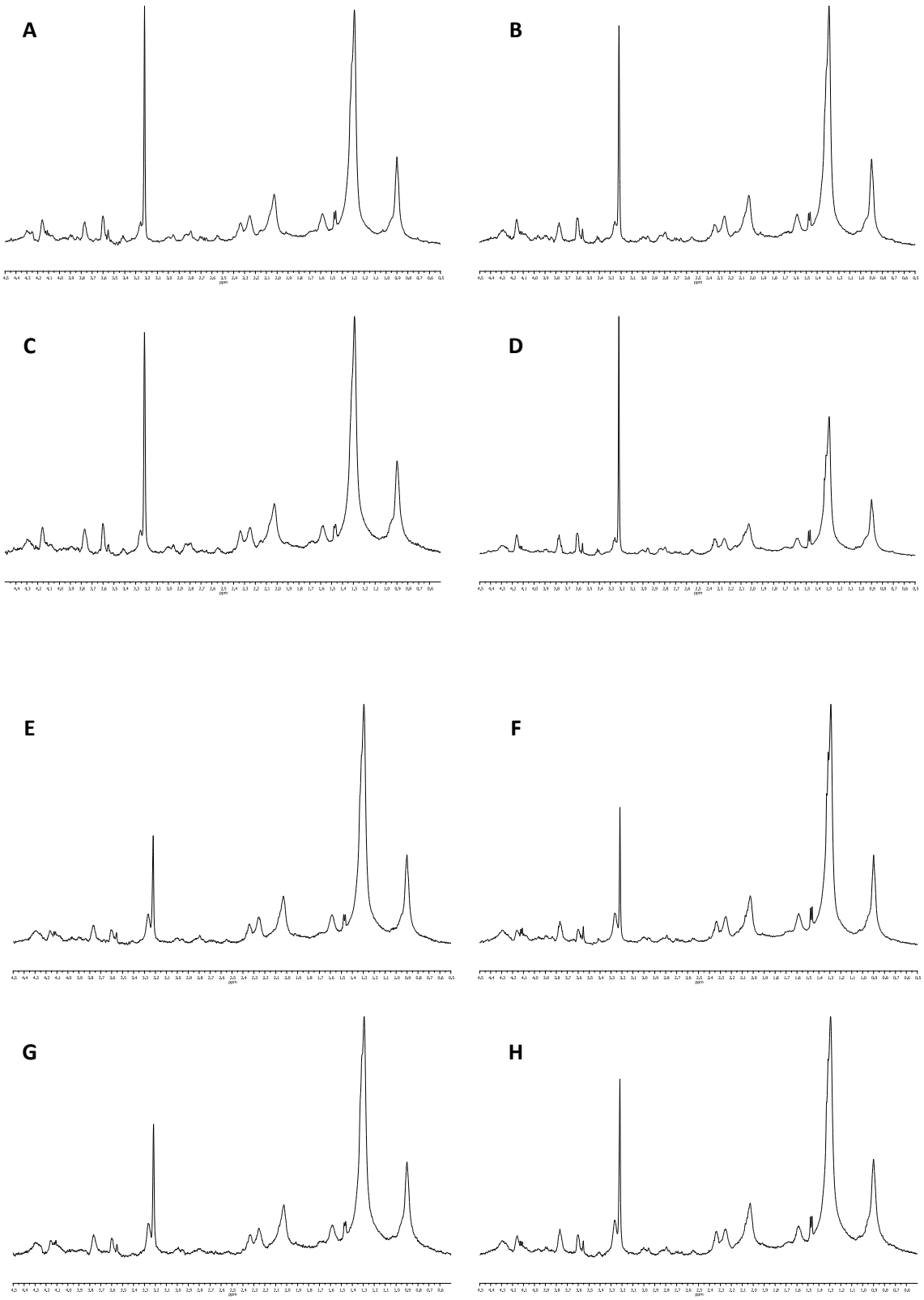


Figure 46: Magnetic resonance spectra of mock infected and JFH-1 infected Huh7.5 cells.
Huh7.5 cells were mock infected (**A**-**D**) or infected with JFH-1 virus at an MOI of 3 (**E**-**F**). 48 hours post-infection MAS MRS was performed. Spectra were obtained for four replicates each of infected and mock infected cells, performed in two experiments

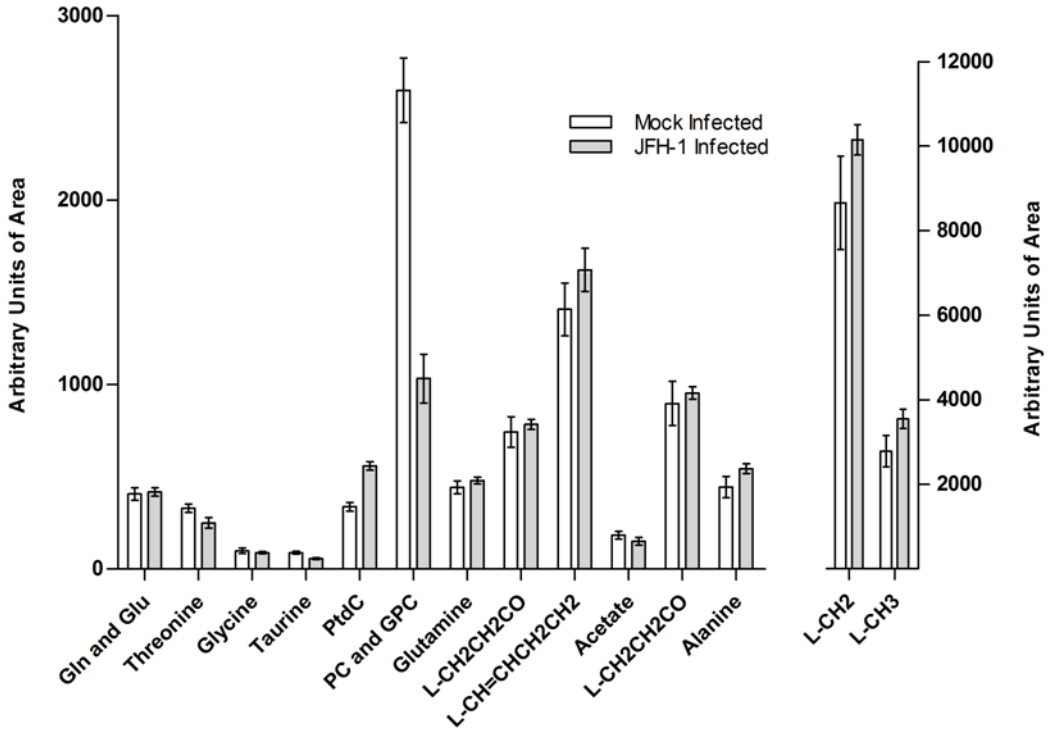


Figure 47: Relative areas of magnetic resonance spectra peaks for mock infected and JFH-1 infected Huh7.5 cells.

The areas under each peak were calculated using ImageJ (NIH) and GraphPad Prism. Average data and standard error are presented for the four replicates of each condition. T-tests were performed in GraphPad Prism to identify significant differences in metabolite levels between Mock Infected (white bars) and JFH-1 Infected (grey bars) samples (differences where $p \leq 0.05$). Statistically significant differences were identified in the phosphocholine and glycerophosphocholine (PC and GPC) levels and in the phosphatidylcholine (PtdC) levels between infected and mock infected Huh7.5 cells.

3.6.2 Choline Metabolites

The analysis by MAS MRS of metabolite levels in Huh7.5 cells infected with JFH-1 indicated that there were significant changes in choline compound levels during infection. During infection with JFH-1, glycerophosphocholine (GPC) and phosphocholine (PC) levels decreased, and phosphatidylcholine (PtdC) levels increased compared to mock infected cells (Figure 46 and Figure 47).

This change may have significance in the context of HCV replication. PtdC is a major component of cell membranes, and is required for normal secretion of VLDL and HDL. The HCV lifecycle requires cell membranes at several stages (as described in the introduction). During replication of RNA, replication complexes are formed in a membranous web made from the ER. Lipid droplets are required for construction of viral particles, and the mature virion requires its own lipid envelope. It is therefore advantageous to the virus to induce conditions where there is increased production of the required lipids.

The change in choline metabolite levels also has significance for HCV patients, as whether this helps the virus or not, a change does happen during infection, and therefore alters the pathology of the liver. Another group has performed MRS on liver biopsy material from HCV infected patients and correlated lipid quantities and fibrosis severity[560]. In their study, total choline levels were observed to decrease with increasing fibrosis, and total choline levels decreased with increasing hepatic lipid levels. It has previously been observed that there is decreased PC in non-alcoholic fatty liver disease[561]. Decreased PtdC can lead to accumulation of intracellular triglycerides[562], and as this would inhibit normal secretion of VLDL[563], it would not benefit the virus, but could explain fatty liver. The observations presented here, of increased PtdC, would seem to benefit the viral lifecycle. However, it does not quite match up with observations by others, performed on liver biopsy, that show decreased total choline (including PtdC). It may be that the situation inside the cell changes over time. The acute model of infection presented here may represent the situation where the virus is inducing optimal conditions for replication. The conditions seen in cirrhotic liver biopsy of chronic HCV may indicate the later stages, when HCV does not need to spread, and liver pathology has altered many normal metabolic processes over the long period of time infection has occurred. It is also known that mice fed on a diet deficient in choline and methionine develop steatosis[564], so if there is a reduction in choline in the liver of HCV patients due to biochemical abnormalities, a similar process could be at work.

Summary

4. Summary

JFH-1[79] was the first HCV isolate to be identified to replicate *in vitro*, and derivatives of this genome are still by far the most efficient at replication and production of HCV. Chimaeric JFH-1 genomes including the structural (but not the non-structural) coding regions of other HCV isolates and genotypes have been shown to replicate[354], suggesting that viral determinants for the ability of JFH-1 to replicate in cell culture are in the non-structural coding region. The NS3 protein is essential to the HCV lifecycle, providing multiple functions including helicase and protease activities, and as such was chosen as the target for study. Chimaeric JFH-1 genomes were created, containing full length NS3, NS3 protease or NS3 helicase coding regions from genotype 1a and 1b isolates (section 3.1.2). The replicative ability of these chimaeras was assessed by transfection into Huh7.5 cells and measurement of intracellular HCV RNA over time. None of the genomes created were observed to have the ability to persist by replicating in cell culture (section 3.1.3). The chimaeric JFH-1 genomes created have shown that NS3 and both its individual protease and helicase domains are essential genotype specific determinants for replication. The method employed has not specified, to further than domain level, the sequence determinants within NS3 that enable JFH-1 to replicate. This could be pursued by creating sub-domain level chimaeras to pinpoint the specific regions and amino acids involved. This would provide more information to identify the interactions involved, such as those between NS3 and other HCV proteins, substrates, or cellular proteins. The interaction between NS3 and NS4A enhances protease activity, and inclusion of genotype matched NS4A sequence into the existing chimaeras may restore replicative ability in some or all of the chimaeras. This has recently been demonstrated by creating chimaeras using a J6/JFH-1 backbone and inserting NS3 and NS4A sequence from several genotypes[407]. Acquisition of replicative ability for chimaeric JFH-1 would provide a useful tool for the study of the effects of NS3 from different genotypes on the host cell, including on host gene expression. It could also provide a tool for the study of the effect, on different genotypes, of potential NS3 inhibitors to be used as antiviral drugs.

The host cell environment is of great importance in determining the ability of HCV to replicate. HCV naturally replicates in hepatocytes, and *in vitro* work has found that the most efficient cell line for hosting HCV replication is Huh7, and its HCV replicon-cured derivatives[79,318,375]. HCV can induce changes in host gene expression during infection, as indicated by studies in human[395-398] and chimpanzee liver[329,379-380], replicon cell lines[381-388], and protein expression systems[389-394] . Use of the JFH-1 culture system for investigation of changes in host gene expression has several advantages

over other models including the presence of all HCV proteins, the occurrence of entry, assembly, release, and RNA replication, and the ease of material acquisition and experimental control compared to *in vivo* models.

Whole genome microarray analyses were performed to identify gene expression changes in Huh7.5 cells (section 3.2.2) and Huh7 cells (section 3.3.3) that had been infected with JFH-1. Gene expression changes were observed in cells infected with JFH-1 at an MOI of 3 for 6, 12, 18, 24, and 48 hours compared to mock infected cells. For Huh7.5 cells, between 593 and 1418 probe sets were observed to change by more than two-fold at each timepoint, with a total of 2473 genes and transcripts observed to change during at least one timepoint. For Huh7 cells, between 239 and 2145 probe sets were observed to change by more than two-fold at each timepoint, with a total of 2187 genes and transcripts observed to change during at least one timepoint. In addition, the gene expression was measured in Huh7 cells infected with HCV and treated with polymerase or protease inhibitors (section 3.4), but very few genes were observed to change compared to infected cells (further validation of this microarray data by quantitative PCR analysis of separate infection experiments is required to determine if this is a replicable result). The expression changes of selections of genes were also assessed by quantitative PCR (of infection experiments separate from those used in microarray analysis) for both Huh7.5 (section 3.2.2) and Huh7 cells (section 3.3.3). The quantitative PCR data was in general agreement with the microarray data, providing validation for the microarray data both through use of another technique and by repeat infection experiments. Analysis of the microarray data found that many host genes regulated during JFH-1 infection are involved in biological processes of importance to HCV replication and disease.

These processes included lipid metabolism, immune modulation, oxidative stress, apoptosis and intracellular transport. Genes involved in lipid metabolism, including cholesterol and sphingolipid synthesis, were observed to be regulated during infection. This is of importance as lipid structures including membranes and lipid droplets are vital to the HCV replication. Profiling of cellular metabolites 48 hours post HCV infection by magnetic resonance spectroscopy identified changes in the level of choline metabolites (section 3.6.1). The observed increase in phosphatidylcholine was of particular interest as this is an important component of the cellular membranes and lipid structures required by HCV. The pathological changes to the livers of infected patients usually take long periods of time to manifest, so observations of large scale changes in lipid metabolites may not necessarily be made in this model. Measurement of lipid metabolites at timepoints longer than 48 hours (days or weeks) after infection may yield more discernable differences, as transcriptional

changes have their effect. Changes in expression of genes involved in immune modulation were observed, including in cytokines, SOCS and acute phase response proteins, but the same large range of interferon stimulated genes observed to be regulated *in vivo*[329,379-380] was not observed. This may be an indication of the lack of complexity in the cell culture model, where interactions and signalling between other cell types (such as immune cells) are not present, and cannot have the effect that they would *in vivo*. Genes involved in the cellular response to oxidative stress were observed to be regulated during infection. These included the metallothionein family of genes, which were observed to be downregulated during infection. Regulation of genes involved in apoptosis and cell proliferation was observed, indicating that both cell cycle regulation and apoptotic cell death may be induced by viral infection. A similar study looking at gene expression has since been performed in Huh7.5 cells infected with a J6/JFH-1 chimaera[411]. This study focused on p53 signalling, NRF2-mediated oxidative stress response, and TGFβ signalling, and the correlations between this study and the work presented here support each other in indicating that there are changes in cell cycle and oxidative stress factors, potentially leading to apoptosis and providing a possible cause for liver damage. Genes involved in vesicle trafficking between ER, Golgi and plasma membranes regulated during HCV infection, indicates potential roles for these genes in viral processes such as entry, exit and construction of replication complexes. It has been demonstrated that HCV infection does induce gene expression changes in the host cell, and that many of these are involved in processes of importance to the HCV lifecycle.

It was hypothesised that genes regulated during HCV infection may be required for efficient HCV replication. To test this, a selection of genes observed to be highly regulated in microarray studies (with potential roles in the HCV lifecycle suggested by their known functions) were inhibited by RNA interference prior to infection. Other groups have since identified host genes important for HCV replication by RNA interference methods, including PI4K and Rab7[565-566], indicating the value of this approach. Of 15 genes tested, knockdown of 4 genes resulted in impaired HCV replication, as measured by quantitative PCR 48 hours post infection (section 3.5.1). This indicates that although not all genes regulated during HCV infection may be required for HCV replication, nevertheless the observation of the regulation of gene expression can serve as a guide to identify genes of importance to HCV replication. The knockdown by siRNA of genes ABLIM3, CYP1A1, SPTLC3 and TXNIP resulted in significant impairment of HCV replication (section 3.5.1). These are novel findings, and only SPTLC3 had previously been shown to reduce HCV replication when chemically inhibited[498]. The knockdown by siRNA of gene TXNIP (thioredoxin interacting protein) resulted in the greatest

reduction in HCV replication. This may be of importance to the study of HCV as TXNIP plays roles in oxidative stress, lipid metabolism and glucose metabolism, all of which have potential roles in HCV replication and disease. Genes required for the efficient replication of HCV have therefore been identified through RNA interference of genes observed by microarray and quantitative PCR analyses to be highly regulated during HCV infection.

Further Work

5.1 Viral Determinants of HCV Replication

HCV JFH-1 chimaeric genomes containing the NS3 coding regions from genotypes 1a and 1b were constructed and shown to be replication deficient in Huh7.5 cells. This indicates the presence of genotype specific viral determinants in efficient HCV replication. As the NS3 proteins generated retained all the functional elements required for activity, it is likely that the chimaeras have reduced activity rather than no activity. This activity was not enough to establish a persistent infection of cultured cells. The reduced activity of chimaeric NS3 may still be quantifiable by other methods. These include measurement of protease activity by processing of *in vitro* translated polyprotein, and measurement of helicase activity by nucleotide duplex unwinding assays. In order to identify the specific regions of the NS3 gene which are responsible for the efficiency of genotype specific activity, subdomain level HCV JFH-1 chimaeric genomes should be constructed, and tested for their replication ability. Regions identified as starting points for this study are those which show significant diversity in amino acid sequence across the different HCV genotypes. Any chimaeric viruses with the ability to replicate could be passaged in cell culture multiple times in an attempt to identify any compensatory mutations which occur in other regions of the HCV genome, indicating interactions between either HCV proteins or the RNA itself. In order to aid NS3 protease function, genotype matched NS4a sequence could be introduced into the chimaeras already made. The cofactor activity of NS4A may rescue the replication incompetent NS3 protease chimaeras, and possibly the full length NS3 chimaeras. Any non-replicative chimaeric viruses, including those already created, should have their translation efficiency and their subsequent polyprotein processing investigated by *in vitro* translation.

5.2 Metabolic Changes during HCV Replication

The analysis of Huh7.5 host cell metabolites at 48 hours post-infection, using magnetic resonance spectroscopy (MRS), showed a change in choline metabolite levels compared to mock infected cells. Additional MRS experiments should be performed on cells hosting a sub-genomic replicon to determine whether HCV non-structural proteins alone can induce this change in the host cell metabolite profile. It is also possible to gain further details of the relative amounts of metabolites in infected cells compared to mock infected cells by performing methanol/chloroform extraction of the cells. This allows analysis of the lipid soluble metabolites (e.g. choline) and water soluble metabolites (e.g. phosphatidylcholine) separately. Microarray analysis of host gene expression also identified genes involved in lipid metabolism to be regulated during HCV infection, including genes

involved in cholesterol and sphingolipid metabolism. These metabolites should be investigated by MRS, and this work could be supported by HPLC (high pressure liquid chromatography) analysis. It would also be beneficial to analyse the metabolite levels in cells infected with HCV for time periods greater than 48 hours. MRS analysis of cells infected for several days may allow for the time required for the changes in gene expression to have an effect on the metabolite levels in cells. As pathologies such as steatosis in patients take years to develop, longer infection periods may help to identify slowly progressing changes in metabolite levels.

5.3 Host Gene Expression Changes during HCV Replication

The work presented here has identified several areas of interaction between HCV and the host cell which would benefit from further investigation.

Whole genome microarray analysis of gene expression has identified many genes to be regulated during HCV infection. There is further analysis to be performed on genes which were observed to be highly regulated during HCV infection. These genes may not have fit easily into the previously described categories of biological process, or there may be little currently known about their function. However, the magnitude of regulation of some of these genes indicates further investigation may be of interest to the study of the interaction between HCV and the host cell. For example inhibin beta E and stanniocalcin C were observed to be upregulated by around 20 times in Huh7 cells infected with JFH-1 at 24 and 48 hours post-infection. The microarray results will initially need to be validated by quantitative PCR as before. Any potential relationships with HCV can then be explored such as protein interaction, roles in cellular processes required for HCV replication, or roles in cellular anti-viral mechanisms.

Analysis of the genes regulated during HCV infection identified groups of genes involved in cellular processes of importance to HCV replication. Further analysis of the genes involved in pathways highlighted by these analyses could determine the mechanisms of regulation. For example in the cholesterol synthesis pathway genes were observed to be downregulated upto 48 hours post-infection, and have recently been shown to be upregulated at 72 hours post-infection. The investigation of the mechanisms of this regulation would be of interest, including the investigation of the involvement of miR122 sequestration by HCV or downregulation by interferon response, and the subsequent upregulation of gene expression by HCV. Further exploration of the pathways involved

could include siRNA knockdown of genes that were not necessarily regulated by HCV but are involved in the processes identified as generally regulated during HCV infection.

Four host genes (TXNIP, ABLIM3, CYP1A1 and SPTLC3) have been identified through these studies which are required to varying extents for HCV replication. So far, the absence of these genes has been determined to be detrimental to the ability of HCV to replicate. Overexpression studies should be performed in order to establish whether there is also an advantage to HCV replication conferred by the presence of additional quantities of these proteins. These overexpression studies could be performed by transfection of Huh7.5 cells with mammalian expression vectors (e.g. plasmid pCR3.1, Invitrogen). As stable transfection will require antibiotic selection for cells containing the vector, controls should include cells containing empty vector, and cells containing vector with a control protein (e.g. lacZ). Cells overexpressing proteins of interest can then be infected with HCV and replication efficiencies measured as before.

Follow up studies should be performed in order to identify how these host genes are relevant to the HCV lifecycle. The role of CYP1A1 in the metabolism of cellular molecules such as lipids, steroids and cholesterol could be investigated in the context of the requirement of lipids for HCV replication. SPTLC3 is already a target of research for the development of inhibitory drugs for combination therapy of HCV.

Knockdown of ABLIM3 by siRNA showed a moderate impairment of HCV replication. ABLIM3 has the capacity to bind actin, which implies a role for it in transport of HCV or HCV elements around the cell. The likely interaction between ABLIM3 and other proteins is through the LIM domains. The recent study showing ABLIM3 to be a component of the adherens junction suggests that it may be important for cell-cell interaction. Investigation of the capacity for cell-cell transmission of HCV in the cells with knocked down ABLIM3 would be of interest. The role of ABLIM3 in regulation of intracellular transport through its interaction with actin could also be of interest to the study of HCV.

TXNIP is of interest as it was very highly upregulated during infection, its knockdown strongly inhibited HCV replication, and it has multiple functions in the cell. TXNIP has functions in lipid metabolism, glucose metabolism and oxidative stress responses, all of which can be linked to HCV replication. These biological functions should be separated to determine which plays the major role in allowing the replication of HCV. It is known that glucose induces expression of TXNIP. Huh7.5 cells could therefore be induced to express TXNIP through addition of glucose to the culture

medium, before infection with HCV. It is known that different cell lines respond in different ways to stimuli, so in the event that glucose does not stimulate TXNIP in Huh7.5 cells, another sugar could be used, such as *D*-allose, which has been shown to induce TXNIP in Huh7 cells[567]. TXNIP is involved in lipid metabolism and the HCV lifecycle is dependent on cellular lipids for functions such as formation of replication complexes and formation of the viral envelope. The effect of TXNIP inhibition by RNA interference and TXNIP overexpression on cellular lipid content should be investigated. Total lipid content analyses can be performed by staining cells with lipid dyes such as Oil Red O and microscopic observation, and direct biochemical assays. Quantification of specific lipid metabolites could also be performed by MRS as before. TXNIP plays a role in determining the redox state of the cell and regulating oxidative stress by inhibition of TRX. It would be interesting to investigate whether the role of TXNIP in HCV replication is a function of its interaction with TRX. This could be performed by treating cells with both TXNIP siRNA and a chemical TRX inhibitor to determine whether HCV replication is rescued by the chemical TRX inhibitor. Alternatively, inhibition of the enzyme thioredoxin reductase would also ultimately have the effect of inhibiting TRX, by disabling its ability to return to its active state (methylarsenicals and arsinothiols have been shown to inhibit thioredoxin reductase[568]). It is also possible that TXNIP is assisting HCV by inhibiting the ability of TRX to reduce essential disulphide bonds present in HCV proteins. For example, the envelope proteins of HCV contain nine conserved disulphide bonds which are required for correct folding of the proteins[569].

References

1 Organisation, W. H. Hepatitis C - global prevalence (update). *Weekly Epidemiological Record* **74**, 421-428 (1999).

2 Hepatitis C Strategy for England. (Department of Health Publications, London, 2002).

3 Armstrong, G. L. *et al.* The prevalence of hepatitis C virus infection in the United States, 1999 through 2002. *Ann Intern Med* **144**, 705-714, doi:144/10/705 [pii] (2006).

4 El-Zanaty, F. & Way, A. Egypt Demographic and Health Survey 2008. 241-251 (2009).

5 Kenny-Walsh, E. Clinical outcomes after hepatitis C infection from contaminated anti-D immune globulin. Irish Hepatology Research Group. *N Engl J Med* **340**, 1228-1233 (1999).

6 Frank, C. *et al.* The role of parenteral antischistosomal therapy in the spread of hepatitis C virus in Egypt. *Lancet* **355**, 887-891, doi:S0140673699065277 [pii] (2000).

7 Kamel, M. A. *et al.* High HCV prevalence in Egyptian blood donors. *Lancet* **340**, 427 (1992).

8 Ferron, F., Bussetta, C., Dutartre, H. & Canard, B. The modeled structure of the RNA dependent RNA polymerase of GBV-C virus suggests a role for motif E in Flaviviridae RNA polymerases. *BMC Bioinformatics* **6**, 255, doi:1471-2105-6-255 [pii]
10.1186/1471-2105-6-255 (2005).

9 Simmonds, P. Variability of hepatitis C virus. *Hepatology (Baltimore, Md* **21**, 570-583 (1995).

10 Simmonds, P. *et al.* Consensus proposals for a unified system of nomenclature of hepatitis C virus genotypes. *Hepatology (Baltimore, Md* **42**, 962-973, doi:10.1002/hep.20819 (2005).

11 Ina, Y., Mizokami, M., Ohba, K. & Gojobori, T. Reduction of synonymous substitutions in the core protein gene of hepatitis C virus. *J Mol Evol* **38**, 50-56 (1994).

12 Friedman, S. L. Stellate cells: a moving target in hepatic fibrogenesis. *Hepatology (Baltimore, Md* **40**, 1041-1043, doi:10.1002/hep.20476 (2004).

13 de Lalla, C. *et al.* Production of profibrotic cytokines by invariant NKT cells characterizes cirrhosis progression in chronic viral hepatitis. *J Immunol* **173**, 1417-1425 (2004).

14 Schulze-Krebs, A. *et al.* Hepatitis C virus-replicating hepatocytes induce fibrogenic activation of hepatic stellate cells. *Gastroenterology* **129**, 246-258, doi:S0016508505008942 [pii] (2005).

15 Mazzocca, A. *et al.* Binding of hepatitis C virus envelope protein E2 to CD81 up-regulates matrix metalloproteinase-2 in human hepatic stellate cells. *The Journal of biological chemistry* **280**, 11329-11339, doi:M410161200 [pii]
10.1074/jbc.M410161200 (2005).

16 Okuda, M. *et al.* Mitochondrial injury, oxidative stress, and antioxidant gene expression are induced by hepatitis C virus core protein. *Gastroenterology* **122**, 366-375, doi:S0016508502212214 [pii] (2002).

17 Moriya, K. *et al.* Hepatitis C virus core protein induces hepatic steatosis in transgenic mice. *The Journal of general virology* **78 (Pt 7)**, 1527-1531 (1997).

18 Moriya, K. *et al.* Oxidative stress in the absence of inflammation in a mouse model for hepatitis C virus-associated hepatocarcinogenesis. *Cancer Res* **61**, 4365-4370 (2001).

19 Czaja, A. J., Carpenter, H. A., Santrach, P. J. & Moore, S. B. Host- and disease-specific factors affecting steatosis in chronic hepatitis C. *J Hepatol* **29**, 198-206 (1998).

20 Asselah, T., Rubbia-Brandt, L., Marcellin, P. & Negro, F. Steatosis in chronic hepatitis C: why does it really matter? *Gut* **55**, 123-130, doi:55/1/123 [pii]

10.1136/gut.2005.069757 (2006).

21 Adinolfi, L. E. *et al.* Steatosis accelerates the progression of liver damage of chronic hepatitis C patients and correlates with specific HCV genotype and visceral obesity. *Hepatology (Baltimore, Md* **33**, 1358-1364, doi:S0270913901658336 [pii]

10.1053/jhep.2001.24432 (2001).

22 Rubbia-Brandt, L. *et al.* Hepatocyte steatosis is a cytopathic effect of hepatitis C virus genotype 3. *J Hepatol* **33**, 106-115, doi:S0168-8278(00)80166-X [pii] (2000).

23 Hezode, C., Roudot-Thoraval, F., Zafrani, E. S., Dhumeaux, D. & Pawlotsky, J. M. Different mechanisms of steatosis in hepatitis C virus genotypes 1 and 3 infections. *J Viral Hepat* **11**, 455-458, doi:10.1111/j.1365-2893.2004.00528.x

JVH528 [pii] (2004).

24 Moradpour, D., Englert, C., Wakita, T. & Wands, J. R. Characterization of cell lines allowing tightly regulated expression of hepatitis C virus core protein. *Virology* **222**, 51-63, doi:S0042-6822(96)90397-9 [pii]

10.1006/viro.1996.0397 (1996).

25 Patton, H. M. *et al.* The impact of steatosis on disease progression and early and sustained treatment response in chronic hepatitis C patients. *J Hepatol* **40**, 484-490, doi:10.1016/j.jhep.2003.11.004

S0168827803005828 [pii] (2004).

26 Bach, N., Thung, S. N. & Schaffner, F. The histological features of chronic hepatitis C and autoimmune chronic hepatitis: a comparative analysis. *Hepatology (Baltimore, Md* **15**, 572-577, doi:S0270913992000843 [pii] (1992).

27 Lefkowitch, J. H. *et al.* Pathological diagnosis of chronic hepatitis C: a multicenter comparative study with chronic hepatitis B. The Hepatitis Interventional Therapy Group. *Gastroenterology* **104**, 595-603, doi:S0016508593000678 [pii] (1993).

28 Burt, A. D., Mutton, A. & Day, C. P. Diagnosis and interpretation of steatosis and steatohepatitis. *Semin Diagn Pathol* **15**, 246-258 (1998).

29 Marchesini, G. *et al.* Nonalcoholic fatty liver, steatohepatitis, and the metabolic syndrome. *Hepatology (Baltimore, Md* **37**, 917-923, doi:10.1053/jhep.2003.50161 S0270913903001216 [pii] (2003).

30 Marchesini, G. *et al.* Association of nonalcoholic fatty liver disease with insulin resistance. *Am J Med* **107**, 450-455, doi:S0002-9343(99)00271-5 [pii] (1999).

31 Pagano, G. *et al.* Nonalcoholic steatohepatitis, insulin resistance, and metabolic syndrome: further evidence for an etiologic association. *Hepatology (Baltimore, Md* **35**, 367-372, doi:S0270913902660720 [pii] 10.1053/jhep.2002.30690 (2002).

32 Neuschwander-Tetri, B. A., Brunt, E. M., Wehmeier, K. R., Oliver, D. & Bacon, B. R. Improved nonalcoholic steatohepatitis after 48 weeks of treatment with the PPAR-gamma ligand rosiglitazone. *Hepatology (Baltimore, Md* **38**, 1008-1017, doi:10.1053/jhep.2003.50420 S027091390300778X [pii] (2003).

33 Douglas, M. W. & George, J. Molecular mechanisms of insulin resistance in chronic hepatitis C. *World J Gastroenterol* **15**, 4356-4364 (2009).

34 Shintani, Y. *et al.* Hepatitis C virus infection and diabetes: direct involvement of the virus in the development of insulin resistance. *Gastroenterology* **126**, 840-848, doi:S0016508503019978 [pii] (2004).

35 Kawaguchi, T. *et al.* Hepatitis C virus down-regulates insulin receptor substrates 1 and 2 through up-regulation of suppressor of cytokine signaling 3. *Am J Pathol* **165**, 1499-1508, doi:165/5/1499 [pii] (2004).

36 Aytug, S., Reich, D., Sapiro, L. E., Bernstein, D. & Begum, N. Impaired IRS-1/PI3-kinase signaling in patients with HCV: a mechanism for increased prevalence of type 2 diabetes. *Hepatology (Baltimore, Md* **38**, 1384-1392, doi:10.1016/j.hep.2003.09.012 S0270913903009522 [pii] (2003).

37 Pazienza, V. *et al.* The hepatitis C virus core protein of genotypes 3a and 1b downregulates insulin receptor substrate 1 through genotype-specific mechanisms. *Hepatology (Baltimore, Md* **45**, 1164-1171 (2007).

38 Miyamoto, H. *et al.* Involvement of the PA28gamma-dependent pathway in insulin resistance induced by hepatitis C virus core protein. *Journal of virology* **81**, 1727-1735, doi:JVI.01683-06 [pii]
10.1128/JVI.01683-06 (2007).

39 Georgopoulou, U., Tsitoura, P., Kalamvoki, M. & Mavromara, P. The protein phosphatase 2A represents a novel cellular target for hepatitis C virus NS5A protein. *Biochimie* **88**, 651-662, doi:S0300-9084(05)00277-4 [pii]
10.1016/j.biochi.2005.12.003 (2006).

40 Bernsmeier, C. *et al.* Virus-induced over-expression of protein phosphatase 2A inhibits insulin signalling in chronic hepatitis C. *J Hepatol* **49**, 429-440, doi:S0168-8278(08)00283-3 [pii]
10.1016/j.jhep.2008.04.007 (2008).

41 Bensinger, S. J. & Tontonoz, P. Integration of metabolism and inflammation by lipid-activated nuclear receptors. *Nature* **454**, 470-477, doi:nature07202 [pii]
10.1038/nature07202 (2008).

42 Tanaka, N. *et al.* PPARalpha activation is essential for HCV core protein-induced hepatic steatosis and hepatocellular carcinoma in mice. *J Clin Invest* **118**, 683-694, doi:10.1172/JCI33594 (2008).

43 Korenaga, M. *et al.* Hepatitis C virus core protein inhibits mitochondrial electron transport and increases reactive oxygen species (ROS) production. *The Journal of biological chemistry* **280**, 37481-37488, doi:M506412200 [pii]
10.1074/jbc.M506412200 (2005).

44 Weissenborn, K. *et al.* Hepatitis C virus infection and the brain. *Metab Brain Dis* **24**, 197-210, doi:10.1007/s11011-008-9130-5 (2009).

45 Forton, D. M. *et al.* Hepatitis C and cognitive impairment in a cohort of patients with mild liver disease. *Hepatology (Baltimore, Md* **35**, 433-439, doi:S0270913902540994 [pii]
10.1053/jhep.2002.30688 (2002).

46 Forton, D. M. *et al.* A review of cognitive impairment and cerebral metabolite abnormalities in patients with hepatitis C infection. *AIDS* **19 Suppl 3**, S53-63, doi:00002030-200510003-00010 [pii] (2005).

47 Pyrsopoulos, N. T. & Reddy, K. R. Extrahepatic manifestations of chronic viral hepatitis. *Curr Gastroenterol Rep* **3**, 71-78 (2001).

48 Kammer, A. R. *et al.* Molecular mimicry of human cytochrome P450 by hepatitis C virus at the level of cytotoxic T cell recognition. *J Exp Med* **190**, 169-176 (1999).

49 Bianchi, F. B. *et al.* Hepatitis C and autoreactivity. *Dig Liver Dis* **39 Suppl 1**, S22-24, doi:S1590-8658(07)80006-5 [pii] (2007).

50 Kim, W. R. The burden of hepatitis C in the United States. *Hepatology (Baltimore, Md* **36**, S30-34, doi:S0270913902001696 [pii]

10.1053/jhep.2002.36791 (2002).

51 Tanaka, T. *et al.* Molecular cloning of hepatitis C virus genome from a single Japanese carrier: sequence variation within the same individual and among infected individuals. *Virus research* **23**, 39-53 (1992).

52 Neville, J. A. *et al.* Antigenic variation of core, NS3, and NS5 proteins among genotypes of hepatitis C virus. *J Clin Microbiol* **35**, 3062-3070 (1997).

53 Cuevas, J. M. *et al.* Genetic variability of hepatitis C virus before and after combined therapy of interferon plus ribavirin. *PLoS One* **3**, e3058, doi:10.1371/journal.pone.0003058 (2008).

54 Zhang, Z. X., Sonnerborg, A. & Sallberg, M. Antigenic structure of the hepatitis C virus envelope 2 protein. *Clin Exp Immunol* **98**, 382-387 (1994).

55 Cooper, A. C., Banasiak, N. C. & Allen, P. J. Management and prevention strategies for respiratory syncytial virus (RSV) bronchiolitis in infants and young children: a review of evidence-based practice interventions. *Pediatr Nurs* **29**, 452-456 (2003).

56 Haas, W. H. *et al.* Imported Lassa fever in Germany: surveillance and management of contact persons. *Clin Infect Dis* **36**, 1254-1258, doi:CID30594 [pii]

10.1086/374853 (2003).

57 Pawlotsky, J. M. Mechanisms of antiviral treatment efficacy and failure in chronic hepatitis C. *Antiviral research* **59**, 1-11, doi:S0166354203000883 [pii] (2003).

58 Leyssen, P., Balzarini, J., De Clercq, E. & Neyts, J. The predominant mechanism by which ribavirin exerts its antiviral activity in vitro against flaviviruses and paramyxoviruses is mediated by inhibition of IMP dehydrogenase. *Journal of virology* **79**, 1943-1947, doi:79/3/1943 [pii]

10.1128/JVI.79.3.1943-1947.2005 (2005).

59 Chevaliez, S., Brillet, R., Lazaro, E., Hezode, C. & Pawlotsky, J. M. Analysis of ribavirin mutagenicity in human hepatitis C virus infection. *Journal of virology* **81**, 7732-7741, doi:JVI.00382-07 [pii]

10.1128/JVI.00382-07 (2007).

60 Moreno-Otero, R. Therapeutic modalities in hepatitis C: challenges and development. *J Viral Hepat* **12**, 10-19, doi:JVH563 [pii]

10.1111/j.1365-2893.2005.00563.x (2005).

61 Marcellin, P. *et al.* Safety and efficacy of viramidine versus ribavirin in ViSER2: randomized, double-blind study in therapy-naive hepatitis C patients. *J Hepatol* **52**, 32-38, doi:S0168-8278(09)00661-8 [pii]
10.1016/j.jhep.2009.10.015 (2010).

62 Nelson, D. R. *et al.* Randomized Trial of Albinterferon Alfa-2b for the Treatment of Patients With Chronic Hepatitis C Virus Genotype 2 or 3. *Gastroenterology*, doi:S0016-5085(10)01005-X [pii]
10.1053/j.gastro.2010.06.062 (2010).

63 Zeuzem, S. *et al.* Randomized Trial of Albinterferon Alfa-2b for the Treatment of Patients With Chronic Hepatitis C Virus Genotype 1. *Gastroenterology*, doi:S0016-5085(10)01009-7 [pii]
10.1053/j.gastro.2010.06.066 (2010).

64 Lamarre, D. *et al.* An NS3 protease inhibitor with antiviral effects in humans infected with hepatitis C virus. *Nature* **426**, 186-189, doi:10.1038/nature02099
nature02099 [pii] (2003).

65 Hinrichsen, H. *et al.* Short-term antiviral efficacy of BILN 2061, a hepatitis C virus serine protease inhibitor, in hepatitis C genotype 1 patients. *Gastroenterology* **127**, 1347-1355, doi:S0016508504013915 [pii] (2004).

66 Lu, L. *et al.* Mutations conferring resistance to a potent hepatitis C virus serine protease inhibitor in vitro. *Antimicrobial agents and chemotherapy* **48**, 2260-2266, doi:10.1128/AAC.48.6.2260-2266.2004
48/6/2260 [pii] (2004).

67 Reiser, M. *et al.* Antiviral efficacy of NS3-serine protease inhibitor BILN-2061 in patients with chronic genotype 2 and 3 hepatitis C. *Hepatology (Baltimore, Md* **41**, 832-835, doi:10.1002/hep.20612 (2005).

68 Babine, R. E. *et al.* Peptidomimetic Protease Inhibitors. WO0218369 (2002).

69 Reesink, H. W. *et al.* Rapid decline of viral RNA in hepatitis C patients treated with VX-950: a phase Ib, placebo-controlled, randomized study. *Gastroenterology* **131**, 997-1002, doi:S0016-5085(06)01539-3 [pii]
10.1053/j.gastro.2006.07.013 (2006).

70 Sarrazin, C. *et al.* Dynamic hepatitis C virus genotypic and phenotypic changes in patients treated with the protease inhibitor telaprevir. *Gastroenterology* **132**, 1767-1777, doi:S0016-5085(07)00394-0 [pii]
10.1053/j.gastro.2007.02.037 (2007).

71 Mederacke, I., Wedemeyer, H. & Manns, M. P. Boceprevir, an NS3 serine protease inhibitor of hepatitis C virus, for the treatment of HCV infection. *Curr Opin Investig Drugs* **10**, 181-189 (2009).

72 Kwo, P. Y., Lawitz, E. & McCone, J. in *American Association for the Study of Liver Diseases (AASLD) Annual Meeting* (Boston, MA, USA, 2009).

73 Mathy, J. E., Ma, S., Compton, T. & Lin, K. Combinations of cyclophilin inhibitor NIM811 with hepatitis C Virus NS3-4A Protease or NS5B polymerase inhibitors enhance antiviral activity and suppress the emergence of resistance. *Antimicrobial agents and chemotherapy* **52**, 3267-3275, doi:10.1128/AAC.00498-08

AAC.00498-08 [pii] (2008).

74 Pierra, C. *et al.* Synthesis and pharmacokinetics of valopicitabine (NM283), an efficient prodrug of the potent anti-HCV agent 2'-C-methylcytidine. *J Med Chem* **49**, 6614-6620, doi:10.1021/jm0603623 (2006).

75 Masson, D. *et al.* Increased HDL cholesterol and apoA-I in humans and mice treated with a novel SR-BI inhibitor. *Arterioscler Thromb Vasc Biol* **29**, 2054-2060, doi:ATVBAHA.109.191320 [pii]

10.1161/ATVBAHA.109.191320 (2009).

76 Hopkins, S. *et al.* SCY-635, a novel nonimmunosuppressive analog of cyclosporine that exhibits potent inhibition of hepatitis C virus RNA replication in vitro. *Antimicrobial agents and chemotherapy* **54**, 660-672, doi:AAC.00660-09 [pii]

10.1128/AAC.00660-09 (2010).

77 Flisiak, R. *et al.* The cyclophilin inhibitor Debio 025 combined with PEG IFNalpha2a significantly reduces viral load in treatment-naive hepatitis C patients. *Hepatology (Baltimore, Md* **49**, 1460-1468, doi:10.1002/hep.22835 (2009).

78 Lindenbach, B. D. *et al.* Complete replication of hepatitis C virus in cell culture. *Science (New York, N.Y* **309**, 623-626 (2005).

79 Wakita, T. *et al.* Production of infectious hepatitis C virus in tissue culture from a cloned viral genome. *Nature medicine* **11**, 791-796 (2005).

80 Zhong, J. *et al.* Robust hepatitis C virus infection in vitro. *Proceedings of the National Academy of Sciences of the United States of America* **102**, 9294-9299, doi:0503596102 [pii]

10.1073/pnas.0503596102 (2005).

81 Nielsen, S. U. *et al.* Association between hepatitis C virus and very-low-density lipoprotein (VLDL)/LDL analyzed in iodixanol density gradients. *Journal of virology* **80**, 2418-2428, doi:80/5/2418 [pii]

10.1128/JVI.80.5.2418-2428.2006 (2006).

82 Agnello, V., Abel, G., Elfahal, M., Knight, G. B. & Zhang, Q. X. Hepatitis C virus and other flaviviridae viruses enter cells via low density lipoprotein receptor. *Proceedings of the National Academy of Sciences of the United States of America* **96**, 12766-12771 (1999).

83 Andre, P. *et al.* Characterization of low- and very-low-density hepatitis C virus RNA-containing particles. *Journal of virology* **76**, 6919-6928 (2002).

84 Thomssen, R., Bonk, S. & Thiele, A. Density heterogeneities of hepatitis C virus in human sera due to the binding of beta-lipoproteins and immunoglobulins. *Med Microbiol Immunol* **182**, 329-334 (1993).

85 Nahmias, Y., Casali, M., Barbe, L., Berthiaume, F. & Yarmush, M. L. Liver endothelial cells promote LDL-R expression and the uptake of HCV-like particles in primary rat and human hepatocytes. *Hepatology (Baltimore, Md* **43**, 257-265, doi:10.1002/hep.21016 (2006).

86 Bartenschlager, R. & Sparacio, S. Hepatitis C virus molecular clones and their replication capacity in vivo and in cell culture. *Virus research* **127**, 195-207 (2007).

87 Tan, S.-L. *Hepatitis C viruses : genomes and molecular biology*. (Horizon Bioscience, 2006).

88 Rijnbrand, R. C. & Lemon, S. M. Internal ribosome entry site-mediated translation in hepatitis C virus replication. *Curr Top Microbiol Immunol* **242**, 85-116 (2000).

89 Ito, T. & Lai, M. M. Determination of the secondary structure of and cellular protein binding to the 3'-untranslated region of the hepatitis C virus RNA genome. *Journal of virology* **71**, 8698-8706 (1997).

90 Fields, B. N., Knipe, D. M. & Howley, P. M. *Fields' virology*. 5th ed. / editors-in-chief, David M. Knipe, Peter M. Howley ; associate editors, Diane E. Griffin ... [et al.]. edn, (Wolters Kluwer/Lippincott Williams & Wilkins, 2007).

91 Pestova, T. V., Shatsky, I. N., Fletcher, S. P., Jackson, R. J. & Hellen, C. U. A prokaryotic-like mode of cytoplasmic eukaryotic ribosome binding to the initiation codon during internal translation initiation of hepatitis C and classical swine fever virus RNAs. *Genes & development* **12**, 67-83 (1998).

92 Jopling, C. L., Yi, M., Lancaster, A. M., Lemon, S. M. & Sarnow, P. Modulation of hepatitis C virus RNA abundance by a liver-specific MicroRNA. *Science (New York, N.Y* **309**, 1577-1581, doi:309/5740/1577 [pii]

10.1126/science.1113329 (2005).

93 Friebe, P. & Bartenschlager, R. Genetic analysis of sequences in the 3' nontranslated region of hepatitis C virus that are important for RNA replication. *Journal of virology* **76**, 5326-5338 (2002).

94 Kolykhalov, A. A., Feinstone, S. M. & Rice, C. M. Identification of a highly conserved sequence element at the 3' terminus of hepatitis C virus genome RNA. *Journal of virology* **70**, 3363-3371 (1996).

95 Kolykhalov, A. A., Mihalik, K., Feinstone, S. M. & Rice, C. M. Hepatitis C virus-encoded enzymatic activities and conserved RNA elements in the 3' nontranslated region are essential for virus replication in vivo. *Journal of virology* **74**, 2046-2051 (2000).

96 Yanagi, M., St Claire, M., Emerson, S. U., Purcell, R. H. & Bukh, J. In vivo analysis of the 3' untranslated region of the hepatitis C virus after in vitro mutagenesis of an infectious cDNA clone. *Proceedings of the National Academy of Sciences of the United States of America* **96**, 2291-2295 (1999).

97 Yi, M. & Lemon, S. M. Structure-function analysis of the 3' stem-loop of hepatitis C virus genomic RNA and its role in viral RNA replication. *RNA (New York, N.Y* **9**, 331-345 (2003).

98 Branch, A. D., Stump, D. D., Gutierrez, J. A., Eng, F. & Walewski, J. L. The hepatitis C virus alternate reading frame (ARF) and its family of novel products: the alternate reading frame protein/F-protein, the double-frameshift protein, and others. *Semin Liver Dis* **25**, 105-117, doi:10.1055/s-2005-864786 (2005).

99 Cohen, M. *et al.* Development of specific antibodies to an ARF protein in treated patients with chronic HCV infection. *Dig Dis Sci* **52**, 2427-2432, doi:10.1007/s10620-006-9630-2 (2007).

100 Walewski, J. L., Keller, T. R., Stump, D. D. & Branch, A. D. Evidence for a new hepatitis C virus antigen encoded in an overlapping reading frame. *RNA (New York, N.Y* **7**, 710-721 (2001).

101 Moradpour, D., Penin, F. & Rice, C. M. Replication of hepatitis C virus. *Nat Rev Microbiol* **5**, 453-463, doi:nrmicro1645 [pii]

10.1038/nrmicro1645 (2007).

102 Santolini, E., Migliaccio, G. & La Monica, N. Biosynthesis and biochemical properties of the hepatitis C virus core protein. *Journal of virology* **68**, 3631-3641 (1994).

103 McLauchlan, J., Lemberg, M. K., Hope, G. & Martoglio, B. Intramembrane proteolysis promotes trafficking of hepatitis C virus core protein to lipid droplets. *The EMBO journal* **21**, 3980-3988, doi:10.1093/emboj/cdf414 (2002).

104 Boulant, S., Vanbelle, C., Ebel, C., Penin, F. & Lavergne, J. P. Hepatitis C virus core protein is a dimeric alpha-helical protein exhibiting membrane protein features. *Journal of virology* **79**, 11353-11365, doi:79/17/11353 [pii]

10.1128/JVI.79.17.11353-11365.2005 (2005).

105 Boulant, S. *et al.* Structural determinants that target the hepatitis C virus core protein to lipid droplets. *The Journal of biological chemistry* **281**, 22236-22247, doi:M601031200 [pii]
10.1074/jbc.M601031200 (2006).

106 Dubuisson, J., Penin, F. & Moradpour, D. Interaction of hepatitis C virus proteins with host cell membranes and lipids. *Trends Cell Biol* **12**, 517-523, doi:S0962892402023838 [pii] (2002).

107 Schwer, B. *et al.* Targeting of hepatitis C virus core protein to mitochondria through a novel C-terminal localization motif. *Journal of virology* **78**, 7958-7968, doi:10.1128/JVI.78.15.7958-7968.2004
78/15/7958 [pii] (2004).

108 Rouille, Y. *et al.* Subcellular localization of hepatitis C virus structural proteins in a cell culture system that efficiently replicates the virus. *Journal of virology* **80**, 2832-2841, doi:80/6/2832 [pii]
10.1128/JVI.80.6.2832-2841.2006 (2006).

109 Shimoike, T., Mimori, S., Tani, H., Matsuura, Y. & Miyamura, T. Interaction of hepatitis C virus core protein with viral sense RNA and suppression of its translation. *Journal of virology* **73**, 9718-9725 (1999).

110 Baumert, T. F., Ito, S., Wong, D. T. & Liang, T. J. Hepatitis C virus structural proteins assemble into viruslike particles in insect cells. *Journal of virology* **72**, 3827-3836 (1998).

111 McLauchlan, J. Properties of the hepatitis C virus core protein: a structural protein that modulates cellular processes. *J Viral Hepat* **7**, 2-14, doi:jvh201 [pii] (2000).

112 Ray, R. B. & Ray, R. Hepatitis C virus core protein: intriguing properties and functional relevance. *FEMS Microbiol Lett* **202**, 149-156, doi:S0378109701002865 [pii] (2001).

113 Tellinghuisen, T. L. & Rice, C. M. Interaction between hepatitis C virus proteins and host cell factors. *Current opinion in microbiology* **5**, 419-427 (2002).

114 Deleersnyder, V. *et al.* Formation of native hepatitis C virus glycoprotein complexes. *Journal of virology* **71**, 697-704 (1997).

115 Goffard, A. & Dubuisson, J. Glycosylation of hepatitis C virus envelope proteins. *Biochimie* **85**, 295-301, doi:S030090840300004X [pii] (2003).

116 Zhang, M. *et al.* Tracking global patterns of N-linked glycosylation site variation in highly variable viral glycoproteins: HIV, SIV, and HCV envelopes and influenza hemagglutinin. *Glycobiology* **14**, 1229-1246, doi:10.1093/glycob/cwh106
cwh106 [pii] (2004).

117 Bartosch, B. & Cosset, F. L. Cell entry of hepatitis C virus. *Virology* **348**, 1-12, doi:S0042-6822(05)00841-X [pii]
10.1016/j.virol.2005.12.027 (2006).

118 Cocquerel, L., Voisset, C. & Dubuisson, J. Hepatitis C virus entry: potential receptors and their biological functions. *The Journal of general virology* **87**, 1075-1084, doi:87/5/1075 [pii]
10.1099/vir.0.81646-0 (2006).

119 Pileri, P. *et al.* Binding of hepatitis C virus to CD81. *Science (New York, N.Y* **282**, 938-941 (1998).

120 Scarselli, E. *et al.* The human scavenger receptor class B type I is a novel candidate receptor for the hepatitis C virus. *The EMBO journal* **21**, 5017-5025 (2002).

121 Weiner, A. J. *et al.* Variable and hypervariable domains are found in the regions of HCV corresponding to the flavivirus envelope and NS1 proteins and the pestivirus envelope glycoproteins. *Virology* **180**, 842-848 (1991).

122 Bartosch, B. *et al.* Cell entry of hepatitis C virus requires a set of co-receptors that include the CD81 tetraspanin and the SR-B1 scavenger receptor. *The Journal of biological chemistry* **278**, 41624-41630, doi:10.1074/jbc.M305289200
M305289200 [pii] (2003).

123 Callens, N. *et al.* Basic residues in hypervariable region 1 of hepatitis C virus envelope glycoprotein e2 contribute to virus entry. *Journal of virology* **79**, 15331-15341, doi:79/24/15331 [pii]
10.1128/JVI.79.24.15331-15341.2005 (2005).

124 Roccasecca, R. *et al.* Binding of the hepatitis C virus E2 glycoprotein to CD81 is strain specific and is modulated by a complex interplay between hypervariable regions 1 and 2. *Journal of virology* **77**, 1856-1867 (2003).

125 Schnell, J. R. & Chou, J. J. Structure and mechanism of the M2 proton channel of influenza A virus. *Nature* **451**, 591-595, doi:nature06531 [pii]
10.1038/nature06531 (2008).

126 Luik, P. *et al.* The 3-dimensional structure of a hepatitis C virus p7 ion channel by electron microscopy. *Proceedings of the National Academy of Sciences of the United States of America* **106**, 12712-12716, doi:0905966106 [pii]
10.1073/pnas.0905966106 (2009).

127 Pallaoro, M. *et al.* Characterization of the hepatitis C virus NS2/3 processing reaction by using a purified precursor protein. *Journal of virology* **75**, 9939-9946, doi:10.1128/JVI.75.20.9939-9946.2001 (2001).

128 Lorenz, I. C., Marcotrigiano, J., Dentzer, T. G. & Rice, C. M. Structure of the catalytic domain of the hepatitis C virus NS2-3 protease. *Nature* **442**, 831-835, doi:nature04975 [pii] 10.1038/nature04975 (2006).

129 Reed, K. E., Grakoui, A. & Rice, C. M. Hepatitis C virus-encoded NS2-3 protease: cleavage-site mutagenesis and requirements for bimolecular cleavage. *Journal of virology* **69**, 4127-4136 (1995).

130 Blight, K. J., Kolykhalov, A. A. & Rice, C. M. Efficient initiation of HCV RNA replication in cell culture. *Science (New York, N.Y* **290**, 1972-1974 (2000).

131 Lohmann, V. *et al.* Replication of subgenomic hepatitis C virus RNAs in a hepatoma cell line. *Science (New York, N.Y* **285**, 110-113, doi:7638 [pii] (1999).

132 Dumoulin, F. L. *et al.* Hepatitis C virus NS2 protein inhibits gene expression from different cellular and viral promoters in hepatic and nonhepatic cell lines. *Virology* **305**, 260-266, doi:S0042682202917010 [pii] (2003).

133 Erdtmann, L. *et al.* The hepatitis C virus NS2 protein is an inhibitor of CIDE-B-induced apoptosis. *The Journal of biological chemistry* **278**, 18256-18264, doi:10.1074/jbc.M209732200 M209732200 [pii] (2003).

134 Bazan, J. F. & Fletterick, R. J. Detection of a trypsin-like serine protease domain in flaviviruses and pestiviruses. *Virology* **171**, 637-639 (1989).

135 Bartenschlager, R., Ahlborn-Laake, L., Mous, J. & Jacobsen, H. Nonstructural protein 3 of the hepatitis C virus encodes a serine-type proteinase required for cleavage at the NS3/4 and NS4/5 junctions. *Journal of virology* **67**, 3835-3844 (1993).

136 Eckart, M. R. *et al.* The hepatitis C virus encodes a serine protease involved in processing of the putative nonstructural proteins from the viral polyprotein precursor. *Biochemical and biophysical research communications* **192**, 399-406, doi:S0006-291X(83)71429-4 [pii] 10.1006/bbrc.1993.1429 (1993).

137 Grakoui, A., McCourt, D. W., Wychowski, C., Feinstone, S. M. & Rice, C. M. Characterization of the hepatitis C virus-encoded serine proteinase: determination of proteinase-dependent polyprotein cleavage sites. *Journal of virology* **67**, 2832-2843 (1993).

138 Hijikata, M. *et al.* Two distinct proteinase activities required for the processing of a putative nonstructural precursor protein of hepatitis C virus. *Journal of virology* **67**, 4665-4675 (1993).

139 Manabe, S. *et al.* Production of nonstructural proteins of hepatitis C virus requires a putative viral protease encoded by NS3. *Virology* **198**, 636-644, doi:S0042-6822(84)71075-0 [pii]

10.1006/viro.1994.1075 (1994).

140 Tomei, L., Failla, C., Santolini, E., De Francesco, R. & La Monica, N. NS3 is a serine protease required for processing of hepatitis C virus polyprotein. *Journal of virology* **67**, 4017-4026 (1993).

141 Wang, W. *et al.* Conserved C-terminal threonine of hepatitis C virus NS3 regulates autoproteolysis and prevents product inhibition. *Journal of virology* **78**, 700-709 (2004).

142 Bartenschlager, R., Ahlborn-Laake, L., Mous, J. & Jacobsen, H. Kinetic and structural analyses of hepatitis C virus polyprotein processing. *Journal of virology* **68**, 5045-5055 (1994).

143 Bartenschlager, R., Lohmann, V., Wilkinson, T. & Koch, J. O. Complex formation between the NS3 serine-type proteinase of the hepatitis C virus and NS4A and its importance for polyprotein maturation. *Journal of virology* **69**, 7519-7528 (1995).

144 Failla, C., Tomei, L. & De Francesco, R. Both NS3 and NS4A are required for proteolytic processing of hepatitis C virus nonstructural proteins. *Journal of virology* **68**, 3753-3760 (1994).

145 Lin, C., Pragai, B. M., Grakoui, A., Xu, J. & Rice, C. M. Hepatitis C virus NS3 serine proteinase: trans-cleavage requirements and processing kinetics. *Journal of virology* **68**, 8147-8157 (1994).

146 Tanji, Y., Hijikata, M., Satoh, S., Kaneko, T. & Shimotohno, K. Hepatitis C virus-encoded nonstructural protein NS4A has versatile functions in viral protein processing. *Journal of virology* **69**, 1575-1581 (1995).

147 Li, K. *et al.* Immune evasion by hepatitis C virus NS3/4A protease-mediated cleavage of the Toll-like receptor 3 adaptor protein TRIF. *Proceedings of the National Academy of Sciences of the United States of America* **102**, 2992-2997 (2005).

148 Meylan, E., Tschopp, J. & Karin, M. Intracellular pattern recognition receptors in the host response. *Nature* **442**, 39-44, doi:Doi 10.1038/Nature04946 (2006).

149 Meylan, E. *et al.* Cardif is an adaptor protein in the RIG-I antiviral pathway and is targeted by hepatitis C virus. *Nature* **437**, 1167-1172, doi:nature04193 [pii]

10.1038/nature04193 (2005).

150 Seth, R. B., Sun, L., Ea, C. K. & Chen, Z. J. Identification and characterization of MAVS, a mitochondrial antiviral signaling protein that activates NF-kappaB and IRF 3. *Cell* **122**, 669-682, doi:S0092-8674(05)00816-0 [pii]

10.1016/j.cell.2005.08.012 (2005).

151 Xu, L. G. *et al.* VISA is an adapter protein required for virus-triggered IFN-beta signaling. *Mol Cell* **19**, 727-740, doi:S1097-2765(05)01556-X [pii]

10.1016/j.molcel.2005.08.014 (2005).

152 Hornung, V. *et al.* 5'-Triphosphate RNA is the ligand for RIG-I. *Science (New York, N.Y* **314**, 994-997, doi:1132505 [pii]

10.1126/science.1132505 (2006).

153 Pichlmair, A. *et al.* RIG-I-mediated antiviral responses to single-stranded RNA bearing 5 '-phosphates. *Science (New York, N.Y* **314**, 997-1001, doi:DOI 10.1126/science.1132998 (2006).

154 Cordin, O., Banroques, J., Tanner, N. K. & Linder, P. The DEAD-box protein family of RNA helicases. *Gene* **367**, 17-37 (2006).

155 Dumont, S. *et al.* RNA translocation and unwinding mechanism of HCV NS3 helicase and its coordination by ATP. *Nature* **439**, 105-108, doi:nature04331 [pii]

10.1038/nature04331 (2006).

156 Ma, Y., Yates, J., Liang, Y., Lemon, S. M. & Yi, M. NS3 helicase domains involved in infectious intracellular hepatitis C virus particle assembly. *Journal of virology* **82**, 7624-7639, doi:JVI.00724-08 [pii]

10.1128/JVI.00724-08 (2008).

157 Liu, W. J., Sedlak, P. L., Kondratieva, N. & Khromykh, A. A. Complementation analysis of the flavivirus Kunjin NS3 and NS5 proteins defines the minimal regions essential for formation of a replication complex and shows a requirement of NS3 in cis for virus assembly. *Journal of virology* **76**, 10766-10775 (2002).

158 Patkar, C. G. & Kuhn, R. J. Yellow Fever virus NS3 plays an essential role in virus assembly independent of its known enzymatic functions. *Journal of virology* **82**, 3342-3352, doi:JVI.02447-07 [pii]

10.1128/JVI.02447-07 (2008).

159 Cicero, D. O. *et al.* Structural characterization of the interactions of optimized product inhibitors with the N-terminal proteinase domain of the hepatitis C virus (HCV) NS3 protein by NMR and modelling studies. *Journal of molecular biology* **289**, 385-396, doi:10.1006/jmbi.1999.2746

S0022-2836(99)92746-8 [pii] (1999).

160 Egger, D. *et al.* Expression of hepatitis C virus proteins induces distinct membrane alterations including a candidate viral replication complex. *Journal of virology* **76**, 5974-5984 (2002).

161 Gosert, R. *et al.* Identification of the hepatitis C virus RNA replication complex in Huh-7 cells harboring subgenomic replicons. *Journal of virology* **77**, 5487-5492 (2003).

162 Elazar, M., Liu, P., Rice, C. M. & Glenn, J. S. An N-terminal amphipathic helix in hepatitis C virus (HCV) NS4B mediates membrane association, correct localization of replication complex proteins, and HCV RNA replication. *Journal of virology* **78**, 11393-11400, doi:10.1128/JVI.78.20.11393-11400.2004

78/20/11393 [pii] (2004).

163 Gao, L., Aizaki, H., He, J. W. & Lai, M. M. Interactions between viral nonstructural proteins and host protein hVAP-33 mediate the formation of hepatitis C virus RNA replication complex on lipid raft. *Journal of virology* **78**, 3480-3488 (2004).

164 Gouttenoire, J., Montserret, R., Kennel, A., Penin, F. & Moradpour, D. An amphipathic alpha-helix at the C terminus of hepatitis C virus nonstructural protein 4B mediates membrane association. *Journal of virology* **83**, 11378-11384, doi:JVI.01122-09 [pii]

10.1128/JVI.01122-09 (2009).

165 Einav, S., Elazar, M., Danieli, T. & Glenn, J. S. A nucleotide binding motif in hepatitis C virus (HCV) NS4B mediates HCV RNA replication. *Journal of virology* **78**, 11288-11295, doi:10.1128/JVI.78.20.11288-11295.2004

78/20/11288 [pii] (2004).

166 Neddermann, P. *et al.* Reduction of hepatitis C virus NS5A hyperphosphorylation by selective inhibition of cellular kinases activates viral RNA replication in cell culture. *Journal of virology* **78**, 13306-13314, doi:78/23/13306 [pii]

10.1128/JVI.78.23.13306-13314.2004 (2004).

167 Huang, L. *et al.* Hepatitis C virus nonstructural protein 5A (NS5A) is an RNA-binding protein. *The Journal of biological chemistry* **280**, 36417-36428 (2005).

168 Tan, S. L. *et al.* NS5A, a nonstructural protein of hepatitis C virus, binds growth factor receptor-bound protein 2 adaptor protein in a Src homology 3 domain/ligand-dependent manner and perturbs mitogenic signaling. *Proceedings of the National Academy of Sciences of the United States of America* **96**, 5533-5538 (1999).

169 Nanda, S. K., Herion, D. & Liang, T. J. The SH3 binding motif of HCV [corrected] NS5A protein interacts with Bin1 and is important for apoptosis and infectivity. *Gastroenterology* **130**, 794-809 (2006).

170 Lan, K. H. *et al.* HCV NS5A interacts with p53 and inhibits p53-mediated apoptosis. *Oncogene* **21**, 4801-4811, doi:10.1038/sj.onc.1205589 (2002).

171 Enomoto, N. *et al.* Comparison of full-length sequences of interferon-sensitive and resistant hepatitis C virus 1b. Sensitivity to interferon is conferred by amino acid substitutions in the NS5A region. *J Clin Invest* **96**, 224-230, doi:10.1172/JCI118025 (1995).

172 Gale, M. J., Jr. *et al.* Evidence that hepatitis C virus resistance to interferon is mediated through repression of the PKR protein kinase by the nonstructural 5A protein. *Virology* **230**, 217-227, doi:S0042-6822(97)98493-2 [pii]
10.1006/viro.1997.8493 (1997).

173 Pflugheber, J. *et al.* Regulation of PKR and IRF-1 during hepatitis C virus RNA replication. *Proceedings of the National Academy of Sciences of the United States of America* **99**, 4650-4655, doi:10.1073/pnas.062055699
062055699 [pii] (2002).

174 Taguchi, T. *et al.* Hepatitis C virus NS5A protein interacts with 2',5'-oligoadenylate synthetase and inhibits antiviral activity of IFN in an IFN sensitivity-determining region-independent manner. *The Journal of general virology* **85**, 959-969 (2004).

175 Hamamoto, I. *et al.* Human VAP-B is involved in hepatitis C virus replication through interaction with NS5A and NS5B. *Journal of virology* **79**, 13473-13482 (2005).

176 Wang, C. *et al.* Identification of FBL2 as a geranylgeranylated cellular protein required for hepatitis C virus RNA replication. *Mol Cell* **18**, 425-434, doi:S1097-2765(05)01248-7 [pii]
10.1016/j.molcel.2005.04.004 (2005).

177 Bressanelli, S., Tomei, L., Rey, F. A. & De Francesco, R. Structural analysis of the hepatitis C virus RNA polymerase in complex with ribonucleotides. *Journal of virology* **76**, 3482-3492 (2002).

178 Lesburg, C. A. *et al.* Crystal structure of the RNA-dependent RNA polymerase from hepatitis C virus reveals a fully encircled active site. *Nat Struct Biol* **6**, 937-943, doi:10.1038/13305 (1999).

179 Simister, P. *et al.* Structural and functional analysis of hepatitis C virus strain JFH1 polymerase. *Journal of virology* **83**, 11926-11939, doi:JVI.01008-09 [pii]
10.1128/JVI.01008-09 (2009).

180 Watashi, K. *et al.* Cyclophilin B is a functional regulator of hepatitis C virus RNA polymerase. *Mol Cell* **19**, 111-122, doi:S1097-2765(05)01320-1 [pii]
10.1016/j.molcel.2005.05.014 (2005).

181 McGivern, D. R., Villanueva, R. A., Chinnaswamy, S., Kao, C. C. & Lemon, S. M. Impaired replication of hepatitis C virus containing mutations in a conserved NS5B retinoblastoma protein-binding motif. *Journal of virology* **83**, 7422-7433, doi:JVI.00262-09 [pii]
10.1128/JVI.00262-09 (2009).

182 Munakata, T., Nakamura, M., Liang, Y., Li, K. & Lemon, S. M. Down-regulation of the retinoblastoma tumor suppressor by the hepatitis C virus NS5B RNA-dependent RNA

polymerase. *Proceedings of the National Academy of Sciences of the United States of America* **102**, 18159-18164, doi:0505605102 [pii]
10.1073/pnas.0505605102 (2005).

183 Koutsoudakis, G. *et al.* Characterization of the early steps of hepatitis C virus infection by using luciferase reporter viruses. *Journal of virology* **80**, 5308-5320 (2006).

184 Evans, M. J. *et al.* Claudin-1 is a hepatitis C virus co-receptor required for a late step in entry. *Nature* **446**, 801-805, doi:nature05654 [pii]
10.1038/nature05654 (2007).

185 Ploss, A. *et al.* Human occludin is a hepatitis C virus entry factor required for infection of mouse cells. *Nature* **457**, 882-886, doi:nature07684 [pii]
10.1038/nature07684 (2009).

186 Blanchard, E. *et al.* Hepatitis C virus entry depends on clathrin-mediated endocytosis. *Journal of virology* **80**, 6964-6972, doi:80/14/6964 [pii]
10.1128/JVI.00024-06 (2006).

187 Tscherne, D. M. *et al.* Time- and temperature-dependent activation of hepatitis C virus for low-pH-triggered entry. *Journal of virology* **80**, 1734-1741, doi:80/4/1734 [pii]
10.1128/JVI.80.4.1734-1741.2006 (2006).

188 Pfeifer, U. *et al.* Experimental non-A, non-B hepatitis: four types of cytoplasmic alteration in hepatocytes of infected chimpanzees. *Virchows Arch B Cell Pathol Incl Mol Pathol* **33**, 233-243 (1980).

189 Konan, K. V. *et al.* Nonstructural protein precursor NS4A/B from hepatitis C virus alters function and ultrastructure of host secretory apparatus. *Journal of virology* **77**, 7843-7855 (2003).

190 Hugle, T. *et al.* The hepatitis C virus nonstructural protein 4B is an integral endoplasmic reticulum membrane protein. *Virology* **284**, 70-81, doi:10.1006/viro.2001.0873
S0042-6822(01)90873-6 [pii] (2001).

191 Gouttenoire, J., Penin, F. & Moradpour, D. Hepatitis C virus nonstructural protein 4B: a journey into unexplored territory. *Reviews in medical virology* **20**, 117-129, doi:10.1002/rmv.640 (2010).

192 Lundin, M., Monne, M., Widell, A., Von Heijne, G. & Persson, M. A. Topology of the membrane-associated hepatitis C virus protein NS4B. *Journal of virology* **77**, 5428-5438 (2003).

193 Lundin, M., Lindstrom, H., Gronwall, C. & Persson, M. A. Dual topology of the processed hepatitis C virus protein NS4B is influenced by the NS5A protein. *The Journal of general virology* **87**, 3263-3272, doi:87/11/3263 [pii]

10.1099/vir.0.82211-0 (2006).

194 Gretton, S. N., Taylor, A. I. & McLauchlan, J. Mobility of the hepatitis C virus NS4B protein on the endoplasmic reticulum membrane and membrane-associated foci. *The Journal of general virology* **86**, 1415-1421 (2005).

195 Gouttenoire, J. *et al.* Identification of a novel determinant for membrane association in hepatitis C virus nonstructural protein 4B. *Journal of virology* **83**, 6257-6268, doi:JVI.02663-08 [pii]

10.1128/JVI.02663-08 (2009).

196 Miller, S. & Krijnse-Locker, J. Modification of intracellular membrane structures for virus replication. *Nat Rev Microbiol* **6**, 363-374, doi:nrmicro1890 [pii]

10.1038/nrmicro1890 (2008).

197 Mackenzie, J. Wrapping things up about virus RNA replication. *Traffic (Copenhagen, Denmark)* **6**, 967-977 (2005).

198 Ng, M. L. Ultrastructural studies of Kunjin virus-infected Aedes albopictus cells. *The Journal of general virology* **68 (Pt 2)**, 577-582 (1987).

199 Westaway, E. G., Mackenzie, J. M., Kenney, M. T., Jones, M. K. & Khromykh, A. A. Ultrastructure of Kunjin virus-infected cells: colocalization of NS1 and NS3 with double-stranded RNA, and of NS2B with NS3, in virus-induced membrane structures. *Journal of virology* **71**, 6650-6661 (1997).

200 Mackenzie, J. M., Jones, M. K. & Young, P. R. Immunolocalization of the dengue virus nonstructural glycoprotein NS1 suggests a role in viral RNA replication. *Virology* **220**, 232-240, doi:S0042-6822(96)90307-4 [pii]

10.1006/viro.1996.0307 (1996).

201 Bienz, K., Egger, D., Rasser, Y. & Bossart, W. Intracellular distribution of poliovirus proteins and the induction of virus-specific cytoplasmic structures. *Virology* **131**, 39-48 (1983).

202 Kujala, P. *et al.* Biogenesis of the Semliki Forest virus RNA replication complex. *Journal of virology* **75**, 3873-3884, doi:10.1128/JVI.75.8.3873-3884.2001 (2001).

203 Magliano, D. *et al.* Rubella virus replication complexes are virus-modified lysosomes. *Virology* **240**, 57-63, doi:S0042-6822(97)98906-6 [pii]

10.1006/viro.1997.8906 (1998).

204 Friebe, P., Lohmann, V., Krieger, N. & Bartenschlager, R. Sequences in the 5' nontranslated region of hepatitis C virus required for RNA replication. *Journal of virology* **75**, 12047-12057, doi:10.1128/JVI.75.24.12047-12057.2001 (2001).

205 Okamoto, T. *et al.* Hepatitis C virus RNA replication is regulated by FKBP8 and Hsp90. *The EMBO journal* **25**, 5015-5025 (2006).

206 Quinkert, D., Bartenschlager, R. & Lohmann, V. Quantitative analysis of the hepatitis C virus replication complex. *Journal of virology* **79**, 13594-13605 (2005).

207 Griffin, S. D. *et al.* The p7 protein of hepatitis C virus forms an ion channel that is blocked by the antiviral drug, Amantadine. *FEBS letters* **535**, 34-38, doi:S0014579302038516 [pii] (2003).

208 Jones, C. T., Murray, C. L., Eastman, D. K., Tassello, J. & Rice, C. M. Hepatitis C virus p7 and NS2 proteins are essential for production of infectious virus. *Journal of virology* **81**, 8374-8383, doi:JVI.00690-07 [pii]
10.1128/JVI.00690-07 (2007).

209 Steinmann, E. *et al.* Hepatitis C virus p7 protein is crucial for assembly and release of infectious virions. *PLoS pathogens* **3**, e103, doi:07-PLPA-RA-0033 [pii]
10.1371/journal.ppat.0030103 (2007).

210 Wozniak, A. L. *et al.* Intracellular proton conductance of the hepatitis C virus p7 protein and its contribution to infectious virus production. *PLoS pathogens* **6**, e1001087, doi:10.1371/journal.ppat.1001087 (2010).

211 Jirasko, V. *et al.* Structural and functional characterization of nonstructural protein 2 for its role in hepatitis C virus assembly. *The Journal of biological chemistry* **283**, 28546-28562, doi:M803981200 [pii]
10.1074/jbc.M803981200 (2008).

212 Jirasko, V. *et al.* Structural and functional studies of nonstructural protein 2 of the hepatitis C virus reveal its key role as organizer of virion assembly. *PLoS pathogens* **6**, e1001233, doi:10.1371/journal.ppat.1001233 (2010).

213 Yi, M., Ma, Y., Yates, J. & Lemon, S. M. Trans-complementation of an NS2 defect in a late step in hepatitis C virus (HCV) particle assembly and maturation. *PLoS pathogens* **5**, e1000403, doi:10.1371/journal.ppat.1000403 (2009).

214 Ma, Y. *et al.* Hepatitis C virus NS2 protein serves as a scaffold for virus assembly by interacting with both structural and nonstructural proteins. *Journal of virology* **85**, 86-97, doi:JVI.01070-10 [pii]
10.1128/JVI.01070-10 (2011).

215 Jones, D. M., Patel, A. H., Targett-Adams, P. & McLauchlan, J. The hepatitis C virus NS4B protein can trans-complement viral RNA replication and modulates production of infectious virus. *Journal of virology* **83**, 2163-2177, doi:JVI.01885-08 [pii]
10.1128/JVI.01885-08 (2009).

216 Tellinghuisen, T. L., Foss, K. L., Treadaway, J. C. & Rice, C. M. Identification of residues required for RNA replication in domains II and III of the hepatitis C virus NS5A protein. *Journal of virology* **82**, 1073-1083, doi:JVI.00328-07 [pii]
10.1128/JVI.00328-07 (2008).

217 Tellinghuisen, T. L., Foss, K. L. & Treadaway, J. Regulation of hepatitis C virion production via phosphorylation of the NS5A protein. *PLoS pathogens* **4**, e1000032, doi:10.1371/journal.ppat.1000032 (2008).

218 Appel, N. *et al.* Essential role of domain III of nonstructural protein 5A for hepatitis C virus infectious particle assembly. *PLoS pathogens* **4**, e1000035, doi:10.1371/journal.ppat.1000035 (2008).

219 Masaki, T. *et al.* Interaction of hepatitis C virus nonstructural protein 5A with core protein is critical for the production of infectious virus particles. *Journal of virology* **82**, 7964-7976, doi:JVI.00826-08 [pii]
10.1128/JVI.00826-08 (2008).

220 Targett-Adams, P., Hope, G., Boulant, S. & McLauchlan, J. Maturation of hepatitis C virus core protein by signal peptide peptidase is required for virus production. *The Journal of biological chemistry* **283**, 16850-16859, doi:M802273200 [pii]
10.1074/jbc.M802273200 (2008).

221 Miyanari, Y. *et al.* The lipid droplet is an important organelle for hepatitis C virus production. *Nature cell biology* **9**, 1089-1097 (2007).

222 Olofsson, S. O. *et al.* Lipid droplets as dynamic organelles connecting storage and efflux of lipids. *Biochimica et biophysica acta* **1791**, 448-458, doi:S1388-1981(08)00150-9 [pii]
10.1016/j.bbalip.2008.08.001 (2009).

223 Shelness, G. S. & Sellers, J. A. Very-low-density lipoprotein assembly and secretion. *Curr Opin Lipidol* **12**, 151-157 (2001).

224 Chang, K. S., Jiang, J., Cai, Z. & Luo, G. Human apolipoprotein e is required for infectivity and production of hepatitis C virus in cell culture. *Journal of virology* **81**, 13783-13793, doi:JVI.01091-07 [pii]
10.1128/JVI.01091-07 (2007).

225 Benga, W. J. *et al.* Apolipoprotein E interacts with hepatitis C virus nonstructural protein 5A and determines assembly of infectious particles. *Hepatology (Baltimore, Md* **51**, 43-53, doi:10.1002/hep.23278 (2010).

226 Jiang, J. & Luo, G. Apolipoprotein E but not B is required for the formation of infectious hepatitis C virus particles. *Journal of virology* **83**, 12680-12691, doi:JVI.01476-09 [pii]
10.1128/JVI.01476-09 (2009).

227 Merz, A. *et al.* Biochemical and morphological properties of hepatitis C virus particles and determination of their lipidome. *The Journal of biological chemistry* **286**, 3018-3032, doi:M110.175018 [pii]
10.1074/jbc.M110.175018 (2011).

228 Hatters, D. M., Peters-Libeu, C. A. & Weisgraber, K. H. Apolipoprotein E structure: insights into function. *Trends Biochem Sci* **31**, 445-454, doi:S0968-0004(06)00170-8 [pii]
10.1016/j.tibs.2006.06.008 (2006).

229 Segrest, J. P., Jones, M. K., De Loof, H. & Dashti, N. Structure of apolipoprotein B-100 in low density lipoproteins. *J Lipid Res* **42**, 1346-1367 (2001).

230 Gastaminza, P. *et al.* Cellular determinants of hepatitis C virus assembly, maturation, degradation, and secretion. *Journal of virology* **82**, 2120-2129, doi:JVI.02053-07 [pii]
10.1128/JVI.02053-07 (2008).

231 Huang, H. *et al.* Hepatitis C virus production by human hepatocytes dependent on assembly and secretion of very low-density lipoproteins. *Proceedings of the National Academy of Sciences of the United States of America* **104**, 5848-5853, doi:0700760104 [pii]
10.1073/pnas.0700760104 (2007).

232 Garrus, J. E. *et al.* Tsg101 and the vacuolar protein sorting pathway are essential for HIV-1 budding. *Cell* **107**, 55-65, doi:S0092-8674(01)00506-2 [pii] (2001).

233 Martin-Serrano, J., Zang, T. & Bieniasz, P. D. HIV-1 and Ebola virus encode small peptide motifs that recruit Tsg101 to sites of particle assembly to facilitate egress. *Nature medicine* **7**, 1313-1319, doi:10.1038/nm1201-1313
nm1201-1313 [pii] (2001).

234 Hurley, J. H. & Hanson, P. I. Membrane budding and scission by the ESCRT machinery: it's all in the neck. *Nature reviews* **11**, 556-566, doi:nrm2937 [pii]
10.1038/nrm2937 (2010).

235 Ariumi, Y. *et al.* The ESCRT system is required for hepatitis C virus production. *PLoS One* **6**, e14517, doi:10.1371/journal.pone.0014517 (2011).

236 Corless, L., Crump, C. M., Griffin, S. D. & Harris, M. Vps4 and the ESCRT-III complex are required for the release of infectious hepatitis C virus particles. *The Journal of general virology* **91**, 362-372, doi:vir.0.017285-0 [pii]

10.1099/vir.0.017285-0 (2010).

237 Parent, R., Qu, X., Petit, M. A. & Beretta, L. The heat shock cognate protein 70 is associated with hepatitis C virus particles and modulates virus infectivity. *Hepatology (Baltimore, Md* **49**, 1798-1809, doi:10.1002/hep.22852 (2009).

238 Backes, P. *et al.* Role of annexin A2 in the production of infectious hepatitis C virus particles. *Journal of virology* **84**, 5775-5789, doi:JVI.02343-09 [pii]

10.1128/JVI.02343-09 (2010).

239 Boulant, S. *et al.* Hepatitis C virus core protein induces lipid droplet redistribution in a microtubule- and dynein-dependent manner. *Traffic (Copenhagen, Denmark)* **9**, 1268-1282, doi:TRA767 [pii]

10.1111/j.1600-0854.2008.00767.x (2008).

240 Penin, F. *et al.* Structure and function of the membrane anchor domain of hepatitis C virus nonstructural protein 5A. *The Journal of biological chemistry* **279**, 40835-40843, doi:10.1074/jbc.M404761200

M404761200 [pii] (2004).

241 Hinson, E. R. & Cresswell, P. The antiviral protein, viperin, localizes to lipid droplets via its N-terminal amphipathic alpha-helix. *Proceedings of the National Academy of Sciences of the United States of America* **106**, 20452-20457, doi:0911679106 [pii]

10.1073/pnas.0911679106 (2009).

242 Matto, M., Rice, C. M., Aroeti, B. & Glenn, J. S. Hepatitis C virus core protein associates with detergent-resistant membranes distinct from classical plasma membrane rafts. *Journal of virology* **78**, 12047-12053, doi:78/21/12047 [pii]

10.1128/JVI.78.21.12047-12053.2004 (2004).

243 Aizaki, H. *et al.* Critical role of virion-associated cholesterol and sphingolipid in hepatitis C virus infection. *Journal of virology* **82**, 5715-5724, doi:JVI.02530-07 [pii]

10.1128/JVI.02530-07 (2008).

244 Phan, T., Beran, R. K., Peters, C., Lorenz, I. C. & Lindenbach, B. D. Hepatitis C virus NS2 protein contributes to virus particle assembly via opposing epistatic interactions with the E1-E2 glycoprotein and NS3-NS4A enzyme complexes. *Journal of virology* **83**, 8379-8395, doi:JVI.00891-09 [pii]

10.1128/JVI.00891-09 (2009).

245 Thomssen, R. *et al.* Association of hepatitis C virus in human sera with beta-lipoprotein. *Med Microbiol Immunol* **181**, 293-300 (1992).

246 Bradley, D. *et al.* Hepatitis C virus: buoyant density of the factor VIII-derived isolate in sucrose. *Journal of medical virology* **34**, 206-208 (1991).

247 Hijikata, M. *et al.* Equilibrium centrifugation studies of hepatitis C virus: evidence for circulating immune complexes. *Journal of virology* **67**, 1953-1958 (1993).

248 Lindenbach, B. D. *et al.* Cell culture-grown hepatitis C virus is infectious in vivo and can be recultured in vitro. *Proceedings of the National Academy of Sciences of the United States of America* **103**, 3805-3809 (2006).

249 Kanto, T. *et al.* Serial density analysis of hepatitis C virus particle populations in chronic hepatitis C patients treated with interferon-alpha. *Journal of medical virology* **46**, 230-237 (1995).

250 Kanto, T. *et al.* Density analysis of hepatitis C virus particle population in the circulation of infected hosts: implications for virus neutralization or persistence. *J Hepatol* **22**, 440-448, doi:0168827895801073 [pii] (1995).

251 Podevin, P. *et al.* Production of infectious hepatitis C virus in primary cultures of human adult hepatocytes. *Gastroenterology* **139**, 1355-1364, doi:S0016-5085(10)01001-2 [pii]
10.1053/j.gastro.2010.06.058 (2010).

252 Thimme, R. *et al.* Viral and immunological determinants of hepatitis C virus clearance, persistence, and disease. *Proceedings of the National Academy of Sciences of the United States of America* **99**, 15661-15668, doi:10.1073/pnas.202608299
202608299 [pii] (2002).

253 Farci, P. *et al.* Prevention of hepatitis C virus infection in chimpanzees after antibody-mediated in vitro neutralization. *Proceedings of the National Academy of Sciences of the United States of America* **91**, 7792-7796 (1994).

254 Farci, P. *et al.* Prevention of hepatitis C virus infection in chimpanzees by hyperimmune serum against the hypervariable region 1 of the envelope 2 protein. *Proceedings of the National Academy of Sciences of the United States of America* **93**, 15394-15399 (1996).

255 Yu, M. Y. *et al.* Neutralizing antibodies to hepatitis C virus (HCV) in immune globulins derived from anti-HCV-positive plasma. *Proceedings of the National Academy of Sciences of the United States of America* **101**, 7705-7710, doi:10.1073/pnas.0402458101
0402458101 [pii] (2004).

256 Shimizu, Y. K. *et al.* A hyperimmune serum against a synthetic peptide corresponding to the hypervariable region 1 of hepatitis C virus can prevent viral infection in cell cultures. *Virology* **223**, 409-412, doi:S0042-6822(96)90497-3 [pii]
10.1006/viro.1996.0497 (1996).

257 Shimizu, Y. K., Purcell, R. H. & Yoshikura, H. Correlation between the infectivity of hepatitis C virus in vivo and its infectivity in vitro. *Proceedings of the National Academy of Sciences of the United States of America* **90**, 6037-6041 (1993).

258 Allander, T. *et al.* Recombinant human monoclonal antibodies against different conformational epitopes of the E2 envelope glycoprotein of hepatitis C virus that inhibit its interaction with CD81. *The Journal of general virology* **81**, 2451-2459 (2000).

259 Lagging, L. M. *et al.* Neutralization of pseudotyped vesicular stomatitis virus expressing hepatitis C virus envelope glycoprotein 1 or 2 by serum from patients. *The Journal of infectious diseases* **185**, 1165-1169, doi:JID011041 [pii]
10.1086/339679 (2002).

260 Hsu, M. *et al.* Hepatitis C virus glycoproteins mediate pH-dependent cell entry of pseudotyped retroviral particles. *Proceedings of the National Academy of Sciences of the United States of America* **100**, 7271-7276, doi:10.1073/pnas.0832180100
0832180100 [pii] (2003).

261 Mondelli, M. U., Cerino, A., Meola, A. & Nicosia, A. Variability or conservation of hepatitis C virus hypervariable region 1? Implications for immune responses. *Journal of biosciences* **28**, 305-310 (2003).

262 Meunier, J. C. *et al.* Evidence for cross-genotype neutralization of hepatitis C virus pseudo-particles and enhancement of infectivity by apolipoprotein C1. *Proceedings of the National Academy of Sciences of the United States of America* **102**, 4560-4565, doi:0501275102 [pii]
10.1073/pnas.0501275102 (2005).

263 Logvinoff, C. *et al.* Neutralizing antibody response during acute and chronic hepatitis C virus infection. *Proceedings of the National Academy of Sciences of the United States of America* **101**, 10149-10154, doi:10.1073/pnas.0403519101
0403519101 [pii] (2004).

264 Cooper, S. *et al.* Analysis of a successful immune response against hepatitis C virus. *Immunity* **10**, 439-449, doi:S1074-7613(00)80044-8 [pii] (1999).

265 Lechner, F. *et al.* Analysis of successful immune responses in persons infected with hepatitis C virus. *J Exp Med* **191**, 1499-1512 (2000).

266 Shoukry, N. H. *et al.* Memory CD8+ T cells are required for protection from persistent hepatitis C virus infection. *J Exp Med* **197**, 1645-1655, doi:10.1084/jem.20030239 jem.20030239 [pii] (2003).

267 Urbani, S. *et al.* Virus-specific CD8+ lymphocytes share the same effector-memory phenotype but exhibit functional differences in acute hepatitis B and C. *Journal of virology* **76**, 12423-12434 (2002).

268 Diepolder, H. M. *et al.* Possible mechanism involving T-lymphocyte response to non-structural protein 3 in viral clearance in acute hepatitis C virus infection. *Lancet* **346**, 1006-1007, doi:S0140-6736(95)91691-1 [pii] (1995).

269 Gerlach, J. T. *et al.* Recurrence of hepatitis C virus after loss of virus-specific CD4(+) T-cell response in acute hepatitis C. *Gastroenterology* **117**, 933-941, doi:S0016508599003601 [pii] (1999).

270 Hoffmann, R. M. *et al.* Mapping of immunodominant CD4+ T lymphocyte epitopes of hepatitis C virus antigens and their relevance during the course of chronic infection. *Hepatology (Baltimore, Md* **21**, 632-638, doi:0270-9139(95)90510-3 [pii] (1995).

271 Missale, G. *et al.* Different clinical behaviors of acute hepatitis C virus infection are associated with different vigor of the anti-viral cell-mediated immune response. *J Clin Invest* **98**, 706-714, doi:10.1172/JCI118842 (1996).

272 Diepolder, H. M. *et al.* Immunodominant CD4+ T-cell epitope within nonstructural protein 3 in acute hepatitis C virus infection. *Journal of virology* **71**, 6011-6019 (1997).

273 Nascimbeni, M. *et al.* Kinetics of CD4+ and CD8+ memory T-cell responses during hepatitis C virus rechallenge of previously recovered chimpanzees. *Journal of virology* **77**, 4781-4793 (2003).

274 Neumann-Haefelin, C., Blum, H. E., Chisari, F. V. & Thimme, R. T cell response in hepatitis C virus infection. *J Clin Virol* **32**, 75-85, doi:S138665320400157X [pii] 10.1016/j.jcv.2004.05.008 (2005).

275 Ferrari, C. *et al.* T-cell response to structural and nonstructural hepatitis C virus antigens in persistent and self-limited hepatitis C virus infections. *Hepatology (Baltimore, Md* **19**, 286-295, doi:S0270913994000418 [pii] (1994).

276 Takaki, A. *et al.* Cellular immune responses persist and humoral responses decrease two decades after recovery from a single-source outbreak of hepatitis C. *Nature medicine* **6**, 578-582, doi:10.1038/75063 (2000).

277 Farci, P. *et al.* Lack of protective immunity against reinfection with hepatitis C virus. *Science (New York, N.Y* **258**, 135-140 (1992).

278 Farci, P. *et al.* The natural history of infection with hepatitis C virus (HCV) in chimpanzees: comparison of serologic responses measured with first- and second-generation assays and relationship to HCV viremia. *The Journal of infectious diseases* **165**, 1006-1011 (1992).

279 Kao, J. H. *et al.* Superinfection by homotypic virus in hepatitis C virus carriers: studies on patients with post-transfusion hepatitis. *Journal of medical virology* **50**, 303-308, doi:10.1002/(SICI)1096-9071(199612)50:4<303::AID-JMV4>3.0.CO;2-C [pii]
10.1002/(SICI)1096-9071(199612)50:4<303::AID-JMV4>3.0.CO;2-C (1996).

280 Lai, M. E. *et al.* Hepatitis C virus in multiple episodes of acute hepatitis in polytransfused thalassaemic children. *Lancet* **343**, 388-390, doi:S0140-6736(94)91224-6 [pii] (1994).

281 Prince, A. M. *et al.* Immunity in hepatitis C infection. *The Journal of infectious diseases* **165**, 438-443 (1992).

282 Proust, B. *et al.* Two successive hepatitis C virus infections in an intravenous drug user. *J Clin Microbiol* **38**, 3125-3127 (2000).

283 Mehta, S. H. *et al.* Protection against persistence of hepatitis C. *Lancet* **359**, 1478-1483, doi:S0140-6736(02)08435-0 [pii]
10.1016/S0140-6736(02)08435-0 (2002).

284 Grakoui, A. *et al.* HCV persistence and immune evasion in the absence of memory T cell help. *Science (New York, N.Y* **302**, 659-662, doi:10.1126/science.1088774
302/5645/659 [pii] (2003).

285 Thimme, R., Neumann-Haefelin, C., Boettler, T. & Blum, H. E. Adaptive immune responses to hepatitis C virus: from viral immunobiology to a vaccine. *Biol Chem* **389**, 457-467 (2008).

286 Thimme, R. *et al.* Determinants of viral clearance and persistence during acute hepatitis C virus infection. *J Exp Med* **194**, 1395-1406 (2001).

287 Kanto, T. *et al.* Impaired allostimulatory capacity of peripheral blood dendritic cells recovered from hepatitis C virus-infected individuals. *J Immunol* **162**, 5584-5591 (1999).

288 Della Bella, S. *et al.* Decrease and dysfunction of dendritic cells correlate with impaired hepatitis C virus-specific CD4+ T-cell proliferation in patients with hepatitis C virus infection. *Immunology* **121**, 283-292, doi:IMM2577 [pii]
10.1111/j.1365-2567.2007.02577.x (2007).

289 Larsson, M. *et al.* Lack of phenotypic and functional impairment in dendritic cells from chimpanzees chronically infected with hepatitis C virus. *Journal of virology* **78**, 6151-6161, doi:10.1128/JVI.78.12.6151-6161.2004
78/12/6151 [pii] (2004).

290 Piccioli, D. *et al.* Comparable functions of plasmacytoid and monocyte-derived dendritic cells in chronic hepatitis C patients and healthy donors. *J Hepatol* **42**, 61-67, doi:S0168-8278(04)00454-4 [pii]
10.1016/j.jhep.2004.09.014 (2005).

291 Kittlesen, D. J., Chianese-Bullock, K. A., Yao, Z. Q., Braciale, T. J. & Hahn, Y. S. Interaction between complement receptor gC1qR and hepatitis C virus core protein inhibits T-lymphocyte proliferation. *J Clin Invest* **106**, 1239-1249, doi:10.1172/JCI10323 (2000).

292 Yao, Z. Q. *et al.* gC1qR expression in chimpanzees with resolved and chronic infection: potential role of HCV core/gC1qR-mediated T cell suppression in the outcome of HCV infection. *Virology* **346**, 324-337, doi:S0042-6822(05)00768-3 [pii]
10.1016/j.virol.2005.11.020 (2006).

293 Day, C. L. *et al.* Ex vivo analysis of human memory CD4 T cells specific for hepatitis C virus using MHC class II tetramers. *J Clin Invest* **112**, 831-842, doi:10.1172/JCI18509
112/6/831 [pii] (2003).

294 Semmo, N. *et al.* Preferential loss of IL-2-secreting CD4+ T helper cells in chronic HCV infection. *Hepatology (Baltimore, Md* **41**, 1019-1028, doi:10.1002/hep.20669 (2005).

295 Barber, D. L. *et al.* Restoring function in exhausted CD8 T cells during chronic viral infection. *Nature* **439**, 682-687, doi:nature04444 [pii]
10.1038/nature04444 (2006).

296 Urbani, S. *et al.* PD-1 expression in acute hepatitis C virus (HCV) infection is associated with HCV-specific CD8 exhaustion. *Journal of virology* **80**, 11398-11403, doi:JVI.01177-06 [pii]
10.1128/JVI.01177-06 (2006).

297 Radziewicz, H. *et al.* Liver-infiltrating lymphocytes in chronic human hepatitis C virus infection display an exhausted phenotype with high levels of PD-1 and low levels of CD127 expression. *Journal of virology* **81**, 2545-2553, doi:JVI.02021-06 [pii]
10.1128/JVI.02021-06 (2007).

298 Rutebemberwa, A. *et al.* High-programmed death-1 levels on hepatitis C virus-specific T cells during acute infection are associated with viral persistence and require preservation of cognate antigen during chronic infection. *J Immunol* **181**, 8215-8225, doi:181/12/8215 [pii] (2008).

299 Cabrera, R. *et al.* An immunomodulatory role for CD4(+)CD25(+) regulatory T lymphocytes in hepatitis C virus infection. *Hepatology (Baltimore, Md* **40**, 1062-1071, doi:10.1002/hep.20454 (2004).

300 Boettler, T. *et al.* T cells with a CD4+CD25+ regulatory phenotype suppress in vitro proliferation of virus-specific CD8+ T cells during chronic hepatitis C virus infection. *Journal of virology* **79**, 7860-7867, doi:79/12/7860 [pii]
10.1128/JVI.79.12.7860-7867.2005 (2005).

301 Accapezzato, D. *et al.* Hepatic expansion of a virus-specific regulatory CD8(+) T cell population in chronic hepatitis C virus infection. *J Clin Invest* **113**, 963-972, doi:10.1172/JCI20515 (2004).

302 Eckels, D. D., Wang, H., Bian, T. H., Tabatabai, N. & Gill, J. C. Immunobiology of hepatitis C virus (HCV) infection: the role of CD4 T cells in HCV infection. *Immunol Rev* **174**, 90-97 (2000).

303 Cox, A. L. *et al.* Cellular immune selection with hepatitis C virus persistence in humans. *J Exp Med* **201**, 1741-1752, doi:jem.20050121 [pii]
10.1084/jem.20050121 (2005).

304 Burke, K. P. & Cox, A. L. Hepatitis C virus evasion of adaptive immune responses: a model for viral persistence. *Immunol Res* **47**, 216-227, doi:10.1007/s12026-009-8152-3 (2010).

305 Wolfl, M. *et al.* Hepatitis C virus immune escape via exploitation of a hole in the T cell repertoire. *J Immunol* **181**, 6435-6446, doi:181/9/6435 [pii] (2008).

306 Horner, S. M. & Gale, M., Jr. Intracellular innate immune cascades and interferon defenses that control hepatitis C virus. *J Interferon Cytokine Res* **29**, 489-498, doi:10.1089/jir.2009.0063 (2009).

307 Kanneganti, T. D. *et al.* Critical role for Cryopyrin/Nalp3 in activation of caspase-1 in response to viral infection and double-stranded RNA. *The Journal of biological chemistry* **281**, 36560-36568, doi:M607594200 [pii]
10.1074/jbc.M607594200 (2006).

308 Petrilli, V., Dostert, C., Muruve, D. A. & Tschopp, J. The inflammasome: a danger sensing complex triggering innate immunity. *Curr Opin Immunol* **19**, 615-622, doi:S0952-7915(07)00167-7 [pii]
10.1016/j.coi.2007.09.002 (2007).

309 Seki, E. & Brenner, D. A. Toll-like receptors and adaptor molecules in liver disease: update. *Hepatology (Baltimore, Md* **48**, 322-335, doi:10.1002/hep.22306 (2008).

310 Abe, T. *et al.* Hepatitis C virus nonstructural protein 5A modulates the toll-like receptor-MyD88-dependent signaling pathway in macrophage cell lines. *Journal of virology* **81**, 8953-8966, doi:JVI.00649-07 [pii]
10.1128/JVI.00649-07 (2007).

311 Kato, H. *et al.* Length-dependent recognition of double-stranded ribonucleic acids by retinoic acid-inducible gene-I and melanoma differentiation-associated gene 5. *J Exp Med* **205**, 1601-1610, doi:10.1084/jem.20080091

jem.20080091 [pii] (2008).

312 Saito, T., Owen, D. M., Jiang, F., Marcotrigiano, J. & Gale, M., Jr. Innate immunity induced by composition-dependent RIG-I recognition of hepatitis C virus RNA. *Nature* **454**, 523-527, doi:nature07106 [pii]

10.1038/nature07106 (2008).

313 Takahasi, K. *et al.* Nonself RNA-sensing mechanism of RIG-I helicase and activation of antiviral immune responses. *Mol Cell* **29**, 428-440, doi:S1097-2765(07)00859-3 [pii]

10.1016/j.molcel.2007.11.028 (2008).

314 Uzri, D. & Gehrke, L. Nucleotide Sequences and Modifications That Determine RIG-I/RNA Binding and Signaling Activities. *Journal of virology* **83**, 4174-4184, doi:Doi 10.1128/Jvi.02449-08 (2009).

315 Kawai, T. *et al.* IPS-1, an adaptor triggering RIG-I- and Mda5-mediated type I interferon induction. *Nature Immunology* **6**, 981-988, doi:Doi 10.1038/Ni1243 (2005).

316 Saito, T. *et al.* Regulation of innate antiviral defenses through a shared repressor domain in RIG-I and LGP2. *Proceedings of the National Academy of Sciences of the United States of America* **104**, 582-587 (2007).

317 Cui, S. *et al.* The C-terminal regulatory domain is the RNA 5'-triphosphate sensor of RIG-I. *Mol Cell* **29**, 169-179, doi:S1097-2765(07)00822-2 [pii]

10.1016/j.molcel.2007.10.032 (2008).

318 Sumpter, R., Jr. *et al.* Regulating intracellular antiviral defense and permissiveness to hepatitis C virus RNA replication through a cellular RNA helicase, RIG-I. *Journal of virology* **79**, 2689-2699 (2005).

319 Baril, M., Racine, M. E., Penin, F. & Lamarre, D. MAVS dimer is a crucial signaling component of innate immunity and the target of hepatitis C virus NS3/4A protease. *Journal of virology* **83**, 1299-1311, doi:JVI.01659-08 [pii]

10.1128/JVI.01659-08 (2009).

320 Tang, E. D. & Wang, C. Y. MAVS self-association mediates antiviral innate immune signaling. *Journal of virology* **83**, 3420-3428, doi:JVI.02623-08 [pii]

10.1128/JVI.02623-08 (2009).

321 Melen, K., Fagerlund, R., Nyqvist, M., Keskinen, P. & Julkunen, I. Expression of hepatitis C virus core protein inhibits interferon-induced nuclear import of STATs. *Journal of medical virology* **73**, 536-547, doi:10.1002/jmv.20123 (2004).

322 de Lucas, S., Bartolome, J. & Carreno, V. Hepatitis C virus core protein down-regulates transcription of interferon-induced antiviral genes. *The Journal of infectious diseases* **191**, 93-99, doi:JID32702 [pii]

10.1086/426509 (2005).

323 Lin, W. *et al.* Hepatitis C virus core protein blocks interferon signaling by interaction with the STAT1 SH2 domain. *Journal of virology* **80**, 9226-9235, doi:80/18/9226 [pii]

10.1128/JVI.00459-06 (2006).

324 Taylor, D. R., Shi, S. T., Romano, P. R., Barber, G. N. & Lai, M. M. Inhibition of the interferon-inducible protein kinase PKR by HCV E2 protein. *Science (New York, N.Y* **285**, 107-110 (1999).

325 Gale, M., Jr. *et al.* Control of PKR protein kinase by hepatitis C virus nonstructural 5A protein: molecular mechanisms of kinase regulation. *Molecular and cellular biology* **18**, 5208-5218 (1998).

326 Garson, J. A., Whitby, K., Watkins, P. & Morgan, A. J. Lack of susceptibility of the cottontop tamarin to hepatitis C infection. *Journal of medical virology* **52**, 286-288, doi:10.1002/(SICI)1096-9071(199707)52:3<286::AID-JMV9>3.0.CO;2-Z [pii] (1997).

327 Butkiewicz, N. *et al.* Virus-specific cofactor requirement and chimeric hepatitis C virus/GB virus B nonstructural protein 3. *Journal of virology* **74**, 4291-4301 (2000).

328 Bright, H., Carroll, A. R., Watts, P. A. & Fenton, R. J. Development of a GB virus B marmoset model and its validation with a novel series of hepatitis C virus NS3 protease inhibitors. *Journal of virology* **78**, 2062-2071 (2004).

329 Bigger, C. B. *et al.* Intrahepatic gene expression during chronic hepatitis C virus infection in chimpanzees. *Journal of virology* **78**, 13779-13792, doi:78/24/13779 [pii]

10.1128/JVI.78.24.13779-13792.2004 (2004).

330 Bassett, S. E., Brasky, K. M. & Lanford, R. E. Analysis of hepatitis C virus-inoculated chimpanzees reveals unexpected clinical profiles. *Journal of virology* **72**, 2589-2599 (1998).

331 Heckel, J. L., Sandgren, E. P., Degen, J. L., Palmiter, R. D. & Brinster, R. L. Neonatal bleeding in transgenic mice expressing urokinase-type plasminogen activator. *Cell* **62**, 447-456, doi:0092-8674(90)90010-C [pii] (1990).

332 Mercer, D. F. *et al.* Hepatitis C virus replication in mice with chimeric human livers. *Nature medicine* **7**, 927-933, doi:10.1038/90968

90968 [pii] (2001).

333 Ilan, E. *et al.* The hepatitis C virus (HCV)-Trimera mouse: a model for evaluation of agents against HCV. *The Journal of infectious diseases* **185**, 153-161, doi:JID010683 [pii] 10.1086/338266 (2002).

334 Blight, K. J., McKeating, J. A., Marcotrigiano, J. & Rice, C. M. Efficient replication of hepatitis C virus genotype 1a RNAs in cell culture. *Journal of virology* **77**, 3181-3190 (2003).

335 Kaplan, G. & Racaniello, V. R. Construction and characterization of poliovirus subgenomic replicons. *Journal of virology* **62**, 1687-1696 (1988).

336 Meyers, G., Tautz, N., Becher, P., Thiel, H. J. & Kummerer, B. M. Recovery of cytopathogenic and noncytopathogenic bovine viral diarrhea viruses from cDNA constructs. *Journal of virology* **70**, 8606-8613 (1996).

337 Khromykh, A. A. & Westaway, E. G. Subgenomic replicons of the flavivirus Kunjin: construction and applications. *Journal of virology* **71**, 1497-1505 (1997).

338 Yi, M. & Lemon, S. M. Adaptive mutations producing efficient replication of genotype 1a hepatitis C virus RNA in normal Huh7 cells. *Journal of virology* **78**, 7904-7915 (2004).

339 Kato, T. *et al.* Efficient replication of the genotype 2a hepatitis C virus subgenomic replicon. *Gastroenterology* **125**, 1808-1817, doi:S0016508503015142 [pii] (2003).

340 Kato, T. *et al.* Sequence analysis of hepatitis C virus isolated from a fulminant hepatitis patient. *Journal of medical virology* **64**, 334-339, doi:10.1002/jmv.1055 [pii] (2001).

341 Woerz, I., Lohmann, V. & Bartenschlager, R. Hepatitis C virus replicons: dinosaurs still in business? *J Viral Hepatitis* **16**, 1-9, doi:10.1111/j.1365-2893.2008.01066.x (2009).

342 Kanda, T. *et al.* Generation of infectious hepatitis C virus in immortalized human hepatocytes. *Journal of virology* **80**, 4633-4639, doi:80/9/4633 [pii] 10.1128/JVI.80.9.4633-4639.2006 (2006).

343 Liang, C. *et al.* Replication of a novel subgenomic HCV genotype 1a replicon expressing a puromycin resistance gene in Huh-7 cells. *Virology* **333**, 41-53, doi:S0042-6822(04)00872-4 [pii] 10.1016/j.virol.2004.12.031 (2005).

344 Yi, M., Villanueva, R. A., Thomas, D. L., Wakita, T. & Lemon, S. M. Production of infectious genotype 1a hepatitis C virus (Hutchinson strain) in cultured human hepatoma cells. *Proceedings of the National Academy of Sciences of the United States of America* **103**, 2310-2315, doi:0510727103 [pii] 10.1073/pnas.0510727103 (2006).

345 Guo, J. T., Bichko, V. V. & Seeger, C. Effect of alpha interferon on the hepatitis C virus replicon. *Journal of virology* **75**, 8516-8523 (2001).

346 Ikeda, M., Yi, M., Li, K. & Lemon, S. M. Selectable subgenomic and genome-length dicistronic RNAs derived from an infectious molecular clone of the HCV-N strain of hepatitis C virus replicate efficiently in cultured Huh7 cells. *Journal of virology* **76**, 2997-3006 (2002).

347 Yi, M., Bodola, F. & Lemon, S. M. Subgenomic hepatitis C virus replicons inducing expression of a secreted enzymatic reporter protein. *Virology* **304**, 197-210, doi:S0042682202916521 [pii] (2002).

348 Heller, T. *et al.* An in vitro model of hepatitis C virion production. *Proceedings of the National Academy of Sciences of the United States of America* **102**, 2579-2583, doi:0409666102 [pii]
10.1073/pnas.0409666102 (2005).

349 Krieger, N., Lohmann, V. & Bartenschlager, R. Enhancement of hepatitis C virus RNA replication by cell culture-adaptive mutations. *Journal of virology* **75**, 4614-4624, doi:10.1128/JVI.75.10.4614-4624.2001 (2001).

350 Lohmann, V., Hoffmann, S., Herian, U., Penin, F. & Bartenschlager, R. Viral and cellular determinants of hepatitis C virus RNA replication in cell culture. *Journal of virology* **77**, 3007-3019 (2003).

351 Grobler, J. A. *et al.* Identification of a key determinant of hepatitis C virus cell culture adaptation in domain II of NS3 helicase. *The Journal of biological chemistry* **278**, 16741-16746, doi:10.1074/jbc.M212602200
M212602200 [pii] (2003).

352 Maekawa, S. *et al.* Introduction of NS5A mutations enables subgenomic HCV replicon derived from chimpanzee-infectious HC-J4 isolate to replicate efficiently in Huh-7 cells. *J Viral Hepat* **11**, 394-403, doi:10.1111/j.1365-2893.2004.00525.x
JVH525 [pii] (2004).

353 Schaller, T. *et al.* Analysis of hepatitis C virus superinfection exclusion by using novel fluorochrome gene-tagged viral genomes. *Journal of virology* **81**, 4591-4603, doi:JVI.02144-06 [pii]
10.1128/JVI.02144-06 (2007).

354 Pietschmann, T. *et al.* Construction and characterization of infectious intragenotypic and intergenotypic hepatitis C virus chimeras. *Proceedings of the National Academy of Sciences of the United States of America* **103**, 7408-7413 (2006).

355 Murayama, A. *et al.* The NS3 helicase and NS5B-to-3'X regions are important for efficient hepatitis C virus strain JFH-1 replication in Huh7 cells. *Journal of virology* **81**, 8030-8040, doi:JVI.02088-06 [pii]
10.1128/JVI.02088-06 (2007).

356 Binder, M. *et al.* Identification of determinants involved in initiation of hepatitis C virus RNA synthesis by using intergenotypic replicase chimeras. *Journal of virology* **81**, 5270-5283 (2007).

357 Moreau, I. *et al.* Serendipitous identification of natural intergenotypic recombinants of hepatitis C in Ireland. *Virol J* **3**, 95, doi:1743-422X-3-95 [pii]
10.1186/1743-422X-3-95 (2006).

358 Kageyama, S. *et al.* A natural inter-genotypic (2b/1b) recombinant of hepatitis C virus in the Philippines. *Journal of medical virology* **78**, 1423-1428 (2006).

359 Legrand-Abravanel, F. *et al.* New natural intergenotypic (2/5) recombinant of hepatitis C virus. *Journal of virology* **81**, 4357-4362, doi:JVI.02639-06 [pii]
10.1128/JVI.02639-06 (2007).

360 Colina, R. *et al.* Evidence of intratypic recombination in natural populations of hepatitis C virus. *The Journal of general virology* **85**, 31-37 (2004).

361 Steinhauer, D. A., Domingo, E. & Holland, J. J. Lack of evidence for proofreading mechanisms associated with an RNA virus polymerase. *Gene* **122**, 281-288 (1992).

362 Ogata, N., Alter, H. J., Miller, R. H. & Purcell, R. H. Nucleotide sequence and mutation rate of the H strain of hepatitis C virus. *Proceedings of the National Academy of Sciences of the United States of America* **88**, 3392-3396 (1991).

363 Okamoto, H. *et al.* Genetic drift of hepatitis C virus during an 8.2-year infection in a chimpanzee: variability and stability. *Virology* **190**, 894-899 (1992).

364 Fernandez, J. *et al.* Long-term persistence of infection in chimpanzees inoculated with an infectious hepatitis C virus clone is associated with a decrease in the viral amino acid substitution rate and low levels of heterogeneity. *Journal of virology* **78**, 9782-9789, doi:10.1128/JVI.78.18.9782-9789.2004
78/18/9782 [pii] (2004).

365 Sheridan, I., Pybus, O. G., Holmes, E. C. & Klenerman, P. High-resolution phylogenetic analysis of hepatitis C virus adaptation and its relationship to disease progression. *Journal of virology* **78**, 3447-3454 (2004).

366 Enomoto, N. *et al.* Mutations in the nonstructural protein 5A gene and response to interferon in patients with chronic hepatitis C virus 1b infection. *N Engl J Med* **334**, 77-81 (1996).

367 Murakami, T. *et al.* Mutations in nonstructural protein 5A gene and response to interferon in hepatitis C virus genotype 2 infection. *Hepatology (Baltimore, Md* **30**, 1045-1053, doi:S0270913999004565 [pii]

10.1002/hep.510300405 (1999).

368 Kobayashi, M. *et al.* Amino acid substitutions in the nonstructural region 5A of hepatitis C virus genotypes 2a and 2b and its relation to viral load and response to interferon. *Am J Gastroenterol* **97**, 988-998, doi:10.1111/j.1572-0241.2002.05619.x (2002).

369 Bukh, J. *et al.* Mutations that permit efficient replication of hepatitis C virus RNA in Huh-7 cells prevent productive replication in chimpanzees. *Proceedings of the National Academy of Sciences of the United States of America* **99**, 14416-14421, doi:10.1073/pnas.212532699 212532699 [pii] (2002).

370 Windisch, M. P. *et al.* Dissecting the interferon-induced inhibition of hepatitis C virus replication by using a novel host cell line. *Journal of virology* **79**, 13778-13793, doi:79/21/13778 [pii] 10.1128/JVI.79.21.13778-13793.2005 (2005).

371 Date, T. *et al.* Genotype 2a hepatitis C virus subgenomic replicon can replicate in HepG2 and IMY-N9 cells. *The Journal of biological chemistry* **279**, 22371-22376, doi:10.1074/jbc.M311120200 M311120200 [pii] (2004).

372 Kato, T. *et al.* Nonhepatic cell lines HeLa and 293 support efficient replication of the hepatitis C virus genotype 2a subgenomic replicon. *Journal of virology* **79**, 592-596, doi:79/1/592 [pii] 10.1128/JVI.79.1.592-596.2005 (2005).

373 Zhu, Q., Guo, J. T. & Seeger, C. Replication of hepatitis C virus subgenomes in nonhepatic epithelial and mouse hepatoma cells. *Journal of virology* **77**, 9204-9210 (2003).

374 Chang, K. S. *et al.* Replication of hepatitis C virus (HCV) RNA in mouse embryonic fibroblasts: protein kinase R (PKR)-dependent and PKR-independent mechanisms for controlling HCV RNA replication and mediating interferon activities. *Journal of virology* **80**, 7364-7374, doi:80/15/7364 [pii] 10.1128/JVI.00586-06 (2006).

375 Blight, K. J., McKeating, J. A. & Rice, C. M. Highly permissive cell lines for subgenomic and genomic hepatitis C virus RNA replication. *Journal of virology* **76**, 13001-13014 (2002).

376 Li, K., Chen, Z. H., Kato, N., Gale, M. & Lemon, S. M. Distinct poly(I-C) and virus-activated signaling pathways leading to interferon-beta production in hepatocytes. *Journal of Biological Chemistry* **280**, 16739-16747, doi:DOI 10.1074/jbc.M414139200 (2005).

377 Sainz, B., Jr., Barretto, N. & Uprichard, S. L. Hepatitis C virus infection in phenotypically distinct Huh7 cell lines. *PLoS One* **4**, e6561, doi:10.1371/journal.pone.0006561 (2009).

378 Lanford, R. E., Bigger, C., Bassett, S. & Klimpel, G. The chimpanzee model of hepatitis C virus infections. *ILAR J* **42**, 117-126 (2001).

379 Bigger, C. B., Brasky, K. M. & Lanford, R. E. DNA microarray analysis of chimpanzee liver during acute resolving hepatitis C virus infection. *Journal of virology* **75**, 7059-7066, doi:10.1128/JVI.75.15.7059-7066.2001 (2001).

380 Su, A. I. *et al.* Genomic analysis of the host response to hepatitis C virus infection. *Proceedings of the National Academy of Sciences of the United States of America* **99**, 15669-15674 (2002).

381 Abe, K. *et al.* cDNA microarray analysis to compare HCV subgenomic replicon cells with their cured cells. *Virus research* **107**, 73-81 (2005).

382 Nishimura-Sakurai, Y. *et al.* Comparison of HCV-associated gene expression and cell signaling pathways in cells with or without HCV replicon and in replicon-cured cells. *Journal of gastroenterology*, doi:10.1007/s00535-009-0162-3 (2009).

383 Fillebeen, C. *et al.* Expression of the subgenomic hepatitis C virus replicon alters iron homeostasis in Huh7 cells. *J Hepatol* **47**, 12-22, doi:S0168-8278(07)00107-9 [pii]
10.1016/j.jhep.2007.01.035 (2007).

384 Fillebeen, C. *et al.* Iron inactivates the RNA polymerase NS5B and suppresses subgenomic replication of hepatitis C Virus. *The Journal of biological chemistry* **280**, 9049-9057, doi:M412687200 [pii]
10.1074/jbc.M412687200 (2005).

385 Itsui, Y. *et al.* Expressional screening of interferon-stimulated genes for antiviral activity against hepatitis C virus replication. *J Viral Hepat* **13**, 690-700, doi:JVH732 [pii]
10.1111/j.1365-2893.2006.00732.x (2006).

386 Ciccaglione, A. R. *et al.* Microarray analysis identifies a common set of cellular genes modulated by different HCV replicon clones. *BMC Genomics* **9**, 309, doi:1471-2164-9-309 [pii]
10.1186/1471-2164-9-309 (2008).

387 Scholle, F. *et al.* Virus-host cell interactions during hepatitis C virus RNA replication: impact of polyprotein expression on the cellular transcriptome and cell cycle association with viral RNA synthesis. *Journal of virology* **78**, 1513-1524 (2004).

388 Cao, W. *et al.* Hepatitis C virus targets over-expression of arginase I in hepatocarcinogenesis. *Int J Cancer* **124**, 2886-2892, doi:10.1002/ijc.24265 (2009).

389 Vandermeeren, A. M. *et al.* Subcellular forms and biochemical events triggered in human cells by HCV polyprotein expression from a viral vector. *Virol J* **5**, 102, doi:1743-422X-5-102 [pii]

10.1186/1743-422X-5-102 (2008).

390 Budhu, A. *et al.* Induction of a unique gene expression profile in primary human hepatocytes by hepatitis C virus core, NS3 and NS5A proteins. *Carcinogenesis* **28**, 1552-1560 (2007).

391 Dou, J., Liu, P., Wang, J. & Zhang, X. Preliminary analysis of gene expression profiles in HepG2 cell line induced by different genotype core proteins of HCV. *Cellular & molecular immunology* **3**, 227-233 (2006).

392 Dou, J., Liu, P., Wang, J. & Zhang, X. Effect of hepatitis C virus core shadow protein expressed in human hepatoma cell line on human gene expression profiles. *J Gastroenterol Hepatol* **21**, 1794-1800, doi:JGH4380 [pii]

10.1111/j.1440-1746.2006.04380.x (2006).

393 Aizaki, H. *et al.* Expression profiling of liver cell lines expressing entire or parts of hepatitis C virus open reading frame. *Hepatology (Baltimore, Md* **36**, 1431-1438 (2002).

394 Basu, A. *et al.* Microarray analyses and molecular profiling of Stat3 signaling pathway induced by hepatitis C virus core protein in human hepatocytes. *Virology* **349**, 347-358 (2006).

395 Hagist, S. *et al.* In vitro-targeted gene identification in patients with hepatitis C using a genome-wide microarray technology. *Hepatology (Baltimore, Md* **49**, 378-386, doi:10.1002/hep.22677 (2009).

396 Smith, M. W. *et al.* Hepatitis C virus and liver disease: global transcriptional profiling and identification of potential markers. *Hepatology (Baltimore, Md* **38**, 1458-1467 (2003).

397 Walters, K. A. *et al.* Identification of a specific gene expression pattern associated with HCV-induced pathogenesis in HCV- and HCV/HIV-infected individuals. *Virology* **350**, 453-464 (2006).

398 Helbig, K. J. *et al.* Differential expression of the CXCR3 ligands in chronic hepatitis C virus (HCV) infection and their modulation by HCV in vitro. *Journal of virology* **83**, 836-846, doi:JVI.01388-08 [pii]

10.1128/JVI.01388-08 (2009).

399 Thomas, P. D. *et al.* PANTHER: a library of protein families and subfamilies indexed by function. *Genome Res* **13**, 2129-2141, doi:10.1101/gr.772403

13/9/2129 [pii] (2003).

400 Thomas, P. D. *et al.* Applications for protein sequence-function evolution data: mRNA/protein expression analysis and coding SNP scoring tools. *Nucleic acids research* **34**, W645-650 (2006).

401 Saeed, A. I. *et al.* TM4 microarray software suite. *Methods Enzymol* **411**, 134-193, doi:S0076-6879(06)11009-5 [pii]
10.1016/S0076-6879(06)11009-5 (2006).

402 Hall, T. A. BioEdit: a user-friendly biological sequence alignment editor and analysis program for Windows 95/98/NT. *Nucleic Acids Symposium Series* **41**, 95-98 (1999).

403 Cobbold, J. F., Taylor-Robinson, S. D. & Cox, I. J. In vitro proton magnetic resonance spectroscopy of liver tissue informs in vivo hepatic proton magnetic resonance spectroscopy studies. *Hepatology (Baltimore, Md* **48**, 1016; author reply 1016-1017, doi:10.1002/hep.22453 (2008).

404 Cobbold, J. F. *et al.* Phenotyping murine models of non-alcoholic fatty liver disease through metabolic profiling of intact liver tissue. *Clin Sci (Lond)* **116**, 403-413, doi:CS20080159 [pii]
10.1042/CS20080159 (2009).

405 Wardell, A. D., Errington, W., Ciaramella, G., Merson, J. & McGarvey, M. J. Characterization and mutational analysis of the helicase and NTPase activities of hepatitis C virus full-length NS3 protein. *The Journal of general virology* **80 (Pt 3)**, 701-709 (1999).

406 Massariol, M. J., Zhao, S., Marquis, M., Thibeault, D. & White, P. W. Protease and helicase activities of hepatitis C virus genotype 4, 5, and 6 NS3-NS4A proteins. *Biochemical and biophysical research communications* **391**, 692-697, doi:S0006-291X(09)02318-3 [pii]
10.1016/j.bbrc.2009.11.122 (2010).

407 Imhof, I. & Simmonds, P. Development of an intergenotypic hepatitis C virus (HCV) cell culture method to assess antiviral susceptibilities and resistance development of HCV NS3 protease genes from HCV genotypes 1 to 6. *Journal of virology* **84**, 4597-4610, doi:JVI.02698-09 [pii]
10.1128/JVI.02698-09 (2010).

408 Kaul, A., Woerz, I., Meuleman, P., Leroux-Roels, G. & Bartenschlager, R. Cell culture adaptation of hepatitis C virus and in vivo viability of an adapted variant. *Journal of virology* **81**, 13168-13179, doi:JVI.01362-07 [pii]
10.1128/JVI.01362-07 (2007).

409 Delgrange, D. *et al.* Robust production of infectious viral particles in Huh-7 cells by introducing mutations in hepatitis C virus structural proteins. *The Journal of general virology* **88**, 2495-2503, doi:88/9/2495 [pii]

10.1099/vir.0.82872-0 (2007).

410 Morey, J. S., Ryan, J. C. & Van Dolah, F. M. Microarray validation: factors influencing correlation between oligonucleotide microarrays and real-time PCR. *Biol Proced Online* **8**, 175-193, doi:10.1251/bpo126 (2006).

411 Walters, K. A. *et al.* Genomic analysis reveals a potential role for cell cycle perturbation in HCV-mediated apoptosis of cultured hepatocytes. *PLoS pathogens* **5**, e1000269, doi:10.1371/journal.ppat.1000269 (2009).

412 Ren, X., Carpenter, A., Hogaboam, C. & Colletti, L. Mitogenic properties of endogenous and pharmacological doses of macrophage inflammatory protein-2 after 70% hepatectomy in the mouse. *Am J Pathol* **163**, 563-570 (2003).

413 Charo, I. F. & Ransohoff, R. M. The many roles of chemokines and chemokine receptors in inflammation. *N Engl J Med* **354**, 610-621, doi:354/6/610 [pii]

10.1056/NEJMra052723 (2006).

414 Yoshimura, A., Naka, T. & Kubo, M. SOCS proteins, cytokine signalling and immune regulation. *Nat Rev Immunol* **7**, 454-465, doi:nri2093 [pii]

10.1038/nri2093 (2007).

415 Chang, Y. Z. *et al.* [Study of the effect of hepatitis C virus core protein on interferon-induced antiviral genes expression and its mechanisms]. *Sheng Wu Gong Cheng Xue Bao* **23**, 1000-1004 (2007).

416 Persico, M. *et al.* Elevated expression and polymorphisms of SOCS3 influence patient response to antiviral therapy in chronic hepatitis C. *Gut* **57**, 507-515, doi:gut.2007.129478 [pii]

10.1136/gut.2007.129478 (2008).

417 Brown, K. S. *et al.* Severe fibrosis in hepatitis C virus-infected patients is associated with increased activity of the mannan-binding lectin (MBL)/MBL-associated serine protease 1 (MASP-1) complex. *Clin Exp Immunol* **147**, 90-98, doi:CEI3264 [pii]

10.1111/j.1365-2249.2006.03264.x (2007).

418 Farinati, F. *et al.* Hepatitis C virus: from oxygen free radicals to hepatocellular carcinoma. *J Viral Hepat* **14**, 821-829, doi:JVH878 [pii]

10.1111/j.1365-2893.2007.00878.x (2007).

419 Jozsi, M. & Zipfel, P. F. Factor H family proteins and human diseases. *Trends Immunol* **29**, 380-387, doi:S1471-4906(08)00159-2 [pii]

10.1016/j.it.2008.04.008 (2008).

420 Chung, K. M. *et al.* West Nile virus nonstructural protein NS1 inhibits complement activation by binding the regulatory protein factor H. *Proceedings of the National Academy of Sciences of the United States of America* **103**, 19111-19116, doi:0605668103 [pii]
10.1073/pnas.0605668103 (2006).

421 Avirutnan, P. *et al.* Antagonism of the complement component C4 by flavivirus nonstructural protein NS1. *J Exp Med* **207**, 793-806, doi:jem.20092545 [pii]
10.1084/jem.20092545 (2010).

422 Kim, K. H. *et al.* HCV core protein induces hepatic lipid accumulation by activating SREBP1 and PPARgamma. *Biochemical and biophysical research communications* **355**, 883-888 (2007).

423 Rakhshandehroo, M. *et al.* Comprehensive Analysis of PPARalpha-Dependent Regulation of Hepatic Lipid Metabolism by Expression Profiling. *PPAR Res* **2007**, 26839, doi:10.1155/2007/26839 (2007).

424 Oka, S. *et al.* Thioredoxin-binding protein-2-like inducible membrane protein is a novel vitamin D3 and peroxisome proliferator-activated receptor (PPAR)gamma ligand target protein that regulates PPARgamma signaling. *Endocrinology* **147**, 733-743, doi:en.2005-0679 [pii]
10.1210/en.2005-0679 (2006).

425 Li, Q. *et al.* A genome-wide genetic screen for host factors required for hepatitis C virus propagation. *Proceedings of the National Academy of Sciences of the United States of America* **106**, 16410-16415, doi:0907439106 [pii]
10.1073/pnas.0907439106 (2009).

426 Kawajiri, K. & Fujii-Kuriyama, Y. Cytochrome P450 gene regulation and physiological functions mediated by the aryl hydrocarbon receptor. *Archives of biochemistry and biophysics* **464**, 207-212, doi:S0003-9861(07)00165-8 [pii]
10.1016/j.abb.2007.03.038 (2007).

427 Sato, S. *et al.* Low-dose dioxins alter gene expression related to cholesterol biosynthesis, lipogenesis, and glucose metabolism through the aryl hydrocarbon receptor-mediated pathway in mouse liver. *Toxicol Appl Pharmacol* **229**, 10-19, doi:S0041-008X(08)00006-9 [pii]
10.1016/j.taap.2007.12.029 (2008).

428 Dai, C. Y. *et al.* Associations between hepatitis C viremia and low serum triglyceride and cholesterol levels: a community-based study. *J Hepatol* **49**, 9-16, doi:S0168-8278(08)00240-7 [pii]
10.1016/j.jhep.2008.03.016 (2008).

429 Robinzon, S. *et al.* Impaired cholesterol biosynthesis in a neuronal cell line persistently infected with measles virus. *Journal of virology* **83**, 5495-5504, doi:JVI.01880-08 [pii]
10.1128/JVI.01880-08 (2009).

430 Krutzfeldt, J. *et al.* Silencing of microRNAs in vivo with 'antagomirs'. *Nature* **438**, 685-689, doi:nature04303 [pii]
10.1038/nature04303 (2005).

431 Esau, C. *et al.* miR-122 regulation of lipid metabolism revealed by in vivo antisense targeting. *Cell Metab* **3**, 87-98, doi:S1550-4131(06)00029-5 [pii]
10.1016/j.cmet.2006.01.005 (2006).

432 Pedersen, I. M. *et al.* Interferon modulation of cellular microRNAs as an antiviral mechanism. *Nature* **449**, 919-922, doi:nature06205 [pii]
10.1038/nature06205 (2007).

433 Chang, J. *et al.* miR-122, a mammalian liver-specific microRNA, is processed from hcr mRNA and may downregulate the high affinity cationic amino acid transporter CAT-1. *RNA Biol* **1**, 106-113, doi:1066 [pii] (2004).

434 Elmen, J. *et al.* Antagonism of microRNA-122 in mice by systemically administered LNA-antimiR leads to up-regulation of a large set of predicted target mRNAs in the liver. *Nucleic acids research* **36**, 1153-1162, doi:gkm1113 [pii]
10.1093/nar/gkm1113 (2008).

435 Gramantieri, L. *et al.* Cyclin G1 is a target of miR-122a, a microRNA frequently down-regulated in human hepatocellular carcinoma. *Cancer Res* **67**, 6092-6099, doi:67/13/6092 [pii]
10.1158/0008-5472.CAN-06-4607 (2007).

436 Vidali, M. *et al.* Interplay between oxidative stress and hepatic steatosis in the progression of chronic hepatitis C. *J Hepatol* **48**, 399-406, doi:S0168-8278(07)00627-7 [pii]
10.1016/j.jhep.2007.10.011 (2008).

437 Chung-man Ho, J., Zheng, S., Comhair, S. A., Farver, C. & Erzurum, S. C. Differential expression of manganese superoxide dismutase and catalase in lung cancer. *Cancer Res* **61**, 8578-8585 (2001).

438 Girnun, G. D. *et al.* Synergy between PPARgamma ligands and platinum-based drugs in cancer. *Cancer Cell* **11**, 395-406, doi:S1535-6108(07)00066-9 [pii]
10.1016/j.ccr.2007.02.025 (2007).

439 Zilliox, M. J., Parmigiani, G. & Griffin, D. E. Gene expression patterns in dendritic cells infected with measles virus compared with other pathogens. *Proceedings of the National Academy of Sciences of the United States of America* **103**, 3363-3368, doi:0511345103 [pii]
10.1073/pnas.0511345103 (2006).

440 Wu, Y., Siadaty, M. S., Berens, M. E., Hampton, G. M. & Theodorescu, D. Overlapping gene expression profiles of cell migration and tumor invasion in human bladder cancer identify metallothionein 1E and nicotinamide N-methyltransferase as novel regulators of cell migration. *Oncogene* **27**, 6679-6689, doi:onc2008264 [pii]
10.1038/onc.2008.264 (2008).

441 Lu, D. D. *et al.* The relationship between metallothionein-1F (MT1F) gene and hepatocellular carcinoma. *Yale J Biol Med* **76**, 55-62 (2003).

442 Chan, K. Y. *et al.* Positional expression profiling indicates candidate genes in deletion hotspots of hepatocellular carcinoma. *Mod Pathol* **19**, 1546-1554, doi:3800674 [pii]
10.1038/modpathol.3800674 (2006).

443 Dalgin, G. S. *et al.* Identification of novel epigenetic markers for clear cell renal cell carcinoma. *J Urol* **180**, 1126-1130, doi:S0022-5347(08)01217-2 [pii]
10.1016/j.juro.2008.04.137 (2008).

444 Puca, R. *et al.* Restoring wtp53 activity in HIPK2 depleted MCF7 cells by modulating metallothionein and zinc. *Experimental cell research* **315**, 67-75, doi:S0014-4827(08)00427-8 [pii]
10.1016/j.yexcr.2008.10.018 (2009).

445 Carrera, G. *et al.* Hepatic metallothionein in patients with chronic hepatitis C: relationship with severity of liver disease and response to treatment. *Am J Gastroenterol* **98**, 1142-1149, doi:S0002927003001072 [pii]
10.1111/j.1572-0241.2003.07403.x (2003).

446 Nagamine, T. *et al.* Preliminary study of combination therapy with interferon-alpha and zinc in chronic hepatitis C patients with genotype 1b. *Biol Trace Elem Res* **75**, 53-63, doi:BTER:75:1-3:53 [pii]
10.1385/BTER:75:1-3:53 (2000).

447 Takagi, H. *et al.* Zinc supplementation enhances the response to interferon therapy in patients with chronic hepatitis C. *J Viral Hepat* **8**, 367-371, doi:jvh311 [pii] (2001).

448 Nagamine, T. *et al.* The possible role of zinc and metallothionein in the liver on the therapeutic effect of IFN-alpha to hepatitis C patients. *Biol Trace Elem Res* **58**, 65-76 (1997).

449 Bernstein, H. B. & Compans, R. W. Sulfation of the human immunodeficiency virus envelope glycoprotein. *Journal of virology* **66**, 6953-6959 (1992).

450 Chan, E. Y. *et al.* Dynamic host energetics and cytoskeletal proteomes in human immunodeficiency virus type 1-infected human primary CD4 cells: analysis by multiplexed label-free mass spectrometry. *Journal of virology* **83**, 9283-9295, doi:JVI.00814-09 [pii]
10.1128/JVI.00814-09 (2009).

451 Chapel, C. *et al.* Antiviral effect of alpha-glucosidase inhibitors on viral morphogenesis and binding properties of hepatitis C virus-like particles. *The Journal of general virology* **87**, 861-871, doi:87/4/861 [pii]
10.1099/vir.0.81503-0 (2006).

452 Durantel, D. Celgosivir, an alpha-glucosidase I inhibitor for the potential treatment of HCV infection. *Curr Opin Investig Drugs* **10**, 860-870 (2009).

453 Bost, A. G., Venable, D., Liu, L. & Heinz, B. A. Cytoskeletal requirements for hepatitis C virus (HCV) RNA synthesis in the HCV replicon cell culture system. *Journal of virology* **77**, 4401-4408 (2003).

454 Lai, C. K., Jeng, K. S., Machida, K. & Lai, M. M. Association of hepatitis C virus replication complexes with microtubules and actin filaments is dependent on the interaction of NS3 and NS5A. *Journal of virology* **82**, 8838-8848, doi:JVI.00398-08 [pii]
10.1128/JVI.00398-08 (2008).

455 Opdam, F. J. *et al.* The small GTPase Rab6B, a novel Rab6 subfamily member, is cell-type specifically expressed and localised to the Golgi apparatus. *Journal of cell science* **113 (Pt 15)**, 2725-2735 (2000).

456 Valsdottir, R. *et al.* Identification of rabaptin-5, rabex-5, and GM130 as putative effectors of rab33b, a regulator of retrograde traffic between the Golgi apparatus and ER. *FEBS letters* **508**, 201-209 (2001).

457 Itoh, T. *et al.* Golgi-resident small GTPase Rab33B interacts with Atg16L and modulates autophagosome formation. *Molecular biology of the cell* **19**, 2916-2925, doi:E07-12-1231 [pii]
10.1091/mbc.E07-12-1231 (2008).

458 Tanida, I. *et al.* Knockdown of autophagy-related gene decreases the production of infectious hepatitis C virus particles. *Autophagy* **5**, 937-945, doi:9243 [pii] (2009).

459 Masuda, E. S. *et al.* Rab37 is a novel mast cell specific GTPase localized to secretory granules. *FEBS letters* **470**, 61-64, doi:S0014-5793(00)01288-6 [pii] (2000).

460 Ostrowski, M. *et al.* Rab27a and Rab27b control different steps of the exosome secretion pathway. *Nature cell biology* **12**, 19-30; sup pp 11-13, doi:ncb2000 [pii]
10.1038/ncb2000 (2010).

461 Lan, L. *et al.* Hepatitis C virus infection sensitizes human hepatocytes to TRAIL-induced apoptosis in a caspase 9-dependent manner. *J Immunol* **181**, 4926-4935, doi:181/7/4926 [pii] (2008).

462 Ploner, C., Kofler, R. & Villunger, A. Noxa: at the tip of the balance between life and death. *Oncogene* **27 Suppl 1**, S84-92, doi:onc200946 [pii]
10.1038/onc.2009.46 (2008).

463 Krupp, M., Weinmann, A., Galle, P. R. & Teufel, A. Actin binding LIM protein 3 (abLIM3). *Int J Mol Med* **17**, 129-133 (2006).

464 Roof, D. J., Hayes, A., Adamian, M., Chishti, A. H. & Li, T. Molecular characterization of abLIM, a novel actin-binding and double zinc finger protein. *The Journal of cell biology* **138**, 575-588 (1997).

465 Barrientos, T. *et al.* Two novel members of the ABLIM protein family, ABLIM-2 and -3, associate with STARS and directly bind F-actin. *The Journal of biological chemistry* **282**, 8393-8403, doi:M607549200 [pii]
10.1074/jbc.M607549200 (2007).

466 Shakir, M. A. *et al.* The Arp2/3 activators WAVE and WASP have distinct genetic interactions with Rac GTPases in Caenorhabditis elegans axon guidance. *Genetics* **179**, 1957-1971, doi:genetics.108.088963 [pii]
10.1534/genetics.108.088963 (2008).

467 Garcia, M. C., Abbasi, M., Singh, S. & He, Q. Role of Drosophila gene dunc-115 in nervous system. *Invert Neurosci* **7**, 119-128, doi:10.1007/s10158-007-0047-1 (2007).

468 Matsuda, M., Yamashita, J. K., Tsukita, S. & Furuse, M. abLIM3 is a novel component of adherens junctions with actin-binding activity. *European journal of cell biology* **89**, 807-816, doi:S0171-9335(10)00157-3 [pii]
10.1016/j.ejcb.2010.07.009 (2010).

469 Timpe, J. M. *et al.* Hepatitis C virus cell-cell transmission in hepatoma cells in the presence of neutralizing antibodies. *Hepatology (Baltimore, Md* **47**, 17-24, doi:10.1002/hep.21959 (2008).

470 Harris, T. J. & Tepass, U. Adherens junctions: from molecules to morphogenesis. *Nature reviews* **11**, 502-514, doi:nrm2927 [pii]
10.1038/nrm2927 (2010).

471 Hankinson, O. The aryl hydrocarbon receptor complex. *Annu Rev Pharmacol Toxicol* **35**, 307-340, doi:10.1146/annurev.pa.35.040195.001515 (1995).

472 Gonzalez, F. J. Molecular genetics of the P-450 superfamily. *Pharmacol Ther* **45**, 1-38, doi:0163-7258(90)90006-N [pii] (1990).

473 Nebert, D. W. & McKinnon, R. A. Cytochrome P450: evolution and functional diversity. *Prog Liver Dis* **12**, 63-97 (1994).

474 Okey, A. B. Enzyme induction in the cytochrome P-450 system. *Pharmacol Ther* **45**, 241-298, doi:0163-7258(90)90030-6 [pii] (1990).

475 Hayes, C. L. *et al.* 17 beta-estradiol hydroxylation catalyzed by human cytochrome P450 1B1. *Proceedings of the National Academy of Sciences of the United States of America* **93**, 9776-9781 (1996).

476 Shimada, T. *et al.* Activation of chemically diverse procarcinogens by human cytochrome P-450 1B1. *Cancer Res* **56**, 2979-2984 (1996).

477 Morgan, J. E. & Whitlock, J. P., Jr. Transcription-dependent and transcription-independent nucleosome disruption induced by dioxin. *Proceedings of the National Academy of Sciences of the United States of America* **89**, 11622-11626 (1992).

478 Okino, S. T. & Whitlock, J. P., Jr. Dioxin induces localized, graded changes in chromatin structure: implications for Cyp1A1 gene transcription. *Molecular and cellular biology* **15**, 3714-3721 (1995).

479 Guengerich, F. P. Cytochrome P450 oxidations in the generation of reactive electrophiles: epoxidation and related reactions. *Archives of biochemistry and biophysics* **409**, 59-71, doi:S0003986102004150 [pii] (2003).

480 Ortiz de Montellano, P. R., Beilan, H. S., Kunze, K. L. & Mico, B. A. Destruction of cytochrome P-450 by ethylene. Structure of the resulting prosthetic heme adduct. *The Journal of biological chemistry* **256**, 4395-4399 (1981).

481 Osborne, C. K. Tamoxifen in the treatment of breast cancer. *N Engl J Med* **339**, 1609-1618 (1998).

482 Oyama, T. *et al.* Cytochrome P450 expression (CYP) in non-small cell lung cancer. *Front Biosci* **12**, 2299-2308, doi:2232 [pii] (2007).

483 Hsu, C. M. *et al.* Emodin inhibits the growth of hepatoma cells: finding the common anti-cancer pathway using Huh7, Hep3B, and HepG2 cells. *Biochemical and biophysical research communications* **392**, 473-478, doi:S0006-291X(09)02144-5 [pii]

10.1016/j.bbrc.2009.10.153 (2010).

484 Anderson, G. R., Hasan, A., Yin, H., Qadri, I. & Quattrochi, L. C. Regulation of the CYP1A1 gene by 2,3,7,8-tetrachlorodibenzo-p-dioxin but not by beta-naphthoflavone or 3-methylcholanthrene is altered in hepatitis C virus replicon-expressing cells. *Mol Pharmacol* **70**, 1062-1070, doi:mol.106.024125 [pii]
10.1124/mol.106.024125 (2006).

485 Shertzer, H. G. *et al.* Dioxin causes a sustained oxidative stress response in the mouse. *Biochemical and biophysical research communications* **253**, 44-48, doi:S0006-291X(98)99753-4 [pii]
10.1006/bbrc.1998.9753 (1998).

486 Schlezinger, J. J., White, R. D. & Stegeman, J. J. Oxidative inactivation of cytochrome P-450 1A (CYP1A) stimulated by 3,3',4,4'-tetrachlorobiphenyl: production of reactive oxygen by vertebrate CYP1As. *Mol Pharmacol* **56**, 588-597 (1999).

487 Hezode, C. *et al.* Impact of smoking on histological liver lesions in chronic hepatitis C. *Gut* **52**, 126-129 (2003).

488 Pessione, F. *et al.* Cigarette smoking and hepatic lesions in patients with chronic hepatitis C. *Hepatology (Baltimore, Md* **34**, 121-125, doi:S0270-9139(01)45382-1 [pii]
10.1053/jhep.2001.25385 (2001).

489 London, E. & Brown, D. A. Insolubility of lipids in triton X-100: physical origin and relationship to sphingolipid/cholesterol membrane domains (rafts). *Biochimica et biophysica acta* **1508**, 182-195, doi:S0304-4157(00)00007-1 [pii] (2000).

490 Hanada, K., Nishijima, M., Akamatsu, Y. & Pagano, R. E. Both sphingolipids and cholesterol participate in the detergent insolubility of alkaline phosphatase, a glycosylphosphatidylinositol-anchored protein, in mammalian membranes. *The Journal of biological chemistry* **270**, 6254-6260 (1995).

491 Fukasawa, M., Nishijima, M., Itabe, H., Takano, T. & Hanada, K. Reduction of sphingomyelin level without accumulation of ceramide in Chinese hamster ovary cells affects detergent-resistant membrane domains and enhances cellular cholesterol efflux to methyl-beta -cyclodextrin. *The Journal of biological chemistry* **275**, 34028-34034, doi:10.1074/jbc.M005151200
M005151200 [pii] (2000).

492 Simons, K. & Ikonen, E. Functional rafts in cell membranes. *Nature* **387**, 569-572, doi:10.1038/42408 (1997).

493 Hannun, Y. A. & Luberto, C. Ceramide in the eukaryotic stress response. *Trends Cell Biol* **10**, 73-80, doi:S0962-8924(99)01694-3 [pii] (2000).

494 Mathias, S., Pena, L. A. & Kolesnick, R. N. Signal transduction of stress via ceramide. *Biochem J* **335 (Pt 3)**, 465-480 (1998).

495 Spiegel, S. & Merrill, A. H., Jr. Sphingolipid metabolism and cell growth regulation. *Faseb J* **10**, 1388-1397 (1996).

496 Hornemann, T., Wei, Y. & von Eckardstein, A. Is the mammalian serine palmitoyltransferase a high-molecular-mass complex? *Biochem J* **405**, 157-164, doi:BJ20070025 [pii]
10.1042/BJ20070025 (2007).

497 Hornemann, T. *et al.* The SPTLC3 subunit of serine palmitoyltransferase generates short chain sphingoid bases. *The Journal of biological chemistry* **284**, 26322-26330, doi:M109.023192 [pii]
10.1074/jbc.M109.023192 (2009).

498 Hirata, Y., Sudoh, M. & Kohara, M. [Suppression of hepatitis C virus (HCV) replication with serine palmitoyltransferase inhibitor]. *Yakugaku Zasshi* **130**, 157-161, doi:JST.JSTAGE/yakushi/130.157 [pii] (2010).

499 Hirata, Y., Sudoh, M. & Kohara, M. [Suppression of hepatitis C virus with the reagent targetting host factors]. *Uirusu* **58**, 207-213 (2008).

500 Hanada, K. Serine palmitoyltransferase, a key enzyme of sphingolipid metabolism. *Biochimica et biophysica acta* **1632**, 16-30, doi:S1388198103000593 [pii] (2003).

501 Nishiyama, A. *et al.* Identification of thioredoxin-binding protein-2/vitamin D(3) up-regulated protein 1 as a negative regulator of thioredoxin function and expression. *The Journal of biological chemistry* **274**, 21645-21650 (1999).

502 Patwari, P., Higgins, L. J., Chutkow, W. A., Yoshioka, J. & Lee, R. T. The interaction of thioredoxin with Txnip. Evidence for formation of a mixed disulfide by disulfide exchange. *The Journal of biological chemistry* **281**, 21884-21891, doi:M600427200 [pii]
10.1074/jbc.M600427200 (2006).

503 Junn, E. *et al.* Vitamin D3 up-regulated protein 1 mediates oxidative stress via suppressing the thioredoxin function. *J Immunol* **164**, 6287-6295, doi:ji_v164n12p6287 [pii] (2000).

504 Yamanaka, H. *et al.* A possible interaction of thioredoxin with VDUP1 in HeLa cells detected in a yeast two-hybrid system. *Biochemical and biophysical research communications* **271**, 796-800, doi:10.1006/bbrc.2000.2699
S0006-291X(00)92699-8 [pii] (2000).

505 Sheth, S. S. *et al.* Hepatocellular carcinoma in Txnip-deficient mice. *Oncogene* **25**, 3528-3536, doi:1209394 [pii]
10.1038/sj.onc.1209394 (2006).

506 Jeon, J. H. *et al.* Tumor suppressor VDUP1 increases p27(kip1) stability by inhibiting JAB1. *Cancer Res* **65**, 4485-4489, doi:65/11/4485 [pii]
10.1158/0008-5472.CAN-04-2271 (2005).

507 Dutta, K. K. *et al.* Two distinct mechanisms for loss of thioredoxin-binding protein-2 in oxidative stress-induced renal carcinogenesis. *Lab Invest* **85**, 798-807, doi:3700280 [pii]
10.1038/labinvest.3700280 (2005).

508 Nishinaka, Y. *et al.* Loss of thioredoxin-binding protein-2/vitamin D3 up-regulated protein 1 in human T-cell leukemia virus type I-dependent T-cell transformation: implications for adult T-cell leukemia leukemogenesis. *Cancer Res* **64**, 1287-1292 (2004).

509 Han, S. H. *et al.* VDUP1 upregulated by TGF-beta1 and 1,25-dihydorxyvitamin D3 inhibits tumor cell growth by blocking cell-cycle progression. *Oncogene* **22**, 4035-4046, doi:10.1038/sj.onc.1206610
1206610 [pii] (2003).

510 Song, H. *et al.* Vitamin D(3) up-regulating protein 1 (VDUP1) antisense DNA regulates tumorigenicity and melanogenesis of murine melanoma cells via regulating the expression of fas ligand and reactive oxygen species. *Immunol Lett* **86**, 235-247, doi:S0165247803000245 [pii] (2003).

511 Butler, L. M. *et al.* The histone deacetylase inhibitor SAHA arrests cancer cell growth, up-regulates thioredoxin-binding protein-2, and down-regulates thioredoxin. *Proceedings of the National Academy of Sciences of the United States of America* **99**, 11700-11705, doi:10.1073/pnas.182372299
182372299 [pii] (2002).

512 Chen, C. L. *et al.* Ceramide induces p38 MAPK and JNK activation through a mechanism involving a thioredoxin-interacting protein-mediated pathway. *Blood* **111**, 4365-4374, doi:blood-2007-08-106336 [pii]
10.1182/blood-2007-08-106336 (2008).

513 Lee, K. N. *et al.* VDUP1 is required for the development of natural killer cells. *Immunity* **22**, 195-208, doi:S1074-7613(05)00035-X [pii]
10.1016/j.immuni.2004.12.012 (2005).

514 Buchanan, B. B., Schurmann, P., Decottignies, P. & Lozano, R. M. Thioredoxin: a multifunctional regulatory protein with a bright future in technology and medicine. *Archives of biochemistry and biophysics* **314**, 257-260, doi:S0003-9861(84)71439-1 [pii]
10.1006/abbi.1994.1439 (1994).

515 Holmgren, A. Thioredoxin structure and mechanism: conformational changes on oxidation of the active-site sulfhydryls to a disulfide. *Structure* **3**, 239-243 (1995).

516 Nakamura, H. *et al.* Adult T cell leukemia-derived factor/human thioredoxin protects endothelial F-2 cell injury caused by activated neutrophils or hydrogen peroxide. *Immunol Lett* **42**, 75-80, doi:0165-2478(94)90038-8 [pii] (1994).

517 Matsuda, M. *et al.* Protective activity of adult T cell leukemia-derived factor (ADF) against tumor necrosis factor-dependent cytotoxicity on U937 cells. *J Immunol* **147**, 3837-3841 (1991).

518 Nakamura, H., Nakamura, K. & Yodoi, J. Redox regulation of cellular activation. *Annual review of immunology* **15**, 351-369, doi:10.1146/annurev.immunol.15.1.351 (1997).

519 Ichijo, H. *et al.* Induction of apoptosis by ASK1, a mammalian MAPKKK that activates SAPK/JNK and p38 signaling pathways. *Science (New York, N.Y* **275**, 90-94 (1997).

520 Matthews, J. R., Wakasugi, N., Virelizier, J. L., Yodoi, J. & Hay, R. T. Thioredoxin regulates the DNA binding activity of NF-kappa B by reduction of a disulphide bond involving cysteine 62. *Nucleic acids research* **20**, 3821-3830 (1992).

521 Hirota, K. *et al.* AP-1 transcriptional activity is regulated by a direct association between thioredoxin and Ref-1. *Proceedings of the National Academy of Sciences of the United States of America* **94**, 3633-3638 (1997).

522 Blum, H., Rollinghoff, M. & Gessner, A. Expression and co-cytokine function of murine thioredoxin/adult T cell leukaemia-derived factor (ADF). *Cytokine* **8**, 6-13, doi:S1043-4666(96)90002-2 [pii]
10.1006/cyto.1996.0002 (1996).

523 Bhat, N. R. & Zhang, P. Hydrogen peroxide activation of multiple mitogen-activated protein kinases in an oligodendrocyte cell line: role of extracellular signal-regulated kinase in hydrogen peroxide-induced cell death. *J Neurochem* **72**, 112-119 (1999).

524 Biguet, C. *et al.* Thioredoxin increases the proliferation of human B-cell lines through a protein kinase C-dependent mechanism. *The Journal of biological chemistry* **269**, 28865-28870 (1994).

525 Yu, F. X. & Luo, Y. Tandem ChoRE and CCAAT motifs and associated factors regulate Txnip expression in response to glucose or adenosine-containing Molecules. *PLoS One* **4**, e8397, doi:10.1371/journal.pone.0008397 (2009).

526 Chen, K. S. & DeLuca, H. F. Isolation and characterization of a novel cDNA from HL-60 cells treated with 1,25-dihydroxyvitamin D-3. *Biochimica et biophysica acta* **1219**, 26-32, doi:0167-4781(94)90242-9 [pii] (1994).

527 Wang, Z. *et al.* Thioredoxin-interacting protein (txnip) is a glucocorticoid-regulated primary response gene involved in mediating glucocorticoid-induced apoptosis. *Oncogene* **25**, 1903-1913, doi:1209218 [pii]
10.1038/sj.onc.1209218 (2006).

528 Kolbus, A. *et al.* Cooperative signaling between cytokine receptors and the glucocorticoid receptor in the expansion of erythroid progenitors: molecular analysis by expression profiling. *Blood* **102**, 3136-3146, doi:10.1182/blood-2003-03-0923
2003-03-0923 [pii] (2003).

529 Billiet, L. *et al.* Enhanced VDUP-1 gene expression by PPARgamma agonist induces apoptosis in human macrophage. *J Cell Physiol* **214**, 183-191, doi:10.1002/jcp.21179 (2008).

530 Huang, L. & Pardee, A. B. Suberoylanilide hydroxamic acid as a potential therapeutic agent for human breast cancer treatment. *Molecular medicine (Cambridge, Mass* **6**, 849-866 (2000).

531 Yu, F. X., Goh, S. R., Dai, R. P. & Luo, Y. Adenosine-containing molecules amplify glucose signaling and enhance txnip expression. *Mol Endocrinol* **23**, 932-942, doi:me.2008-0383 [pii]
10.1210/me.2008-0383 (2009).

532 Kim, K. Y. *et al.* Heat shock factor regulates VDUP1 gene expression. *Biochemical and biophysical research communications* **315**, 369-375, doi:10.1016/j.bbrc.2004.01.047
S0006291X04000877 [pii] (2004).

533 Parikh, H. *et al.* TXNIP regulates peripheral glucose metabolism in humans. *PLoS Med* **4**, e158, doi:06-PLME-RA-0918R1 [pii]
10.1371/journal.pmed.0040158 (2007).

534 Minn, A. H., Hafele, C. & Shalev, A. Thioredoxin-interacting protein is stimulated by glucose through a carbohydrate response element and induces beta-cell apoptosis. *Endocrinology* **146**, 2397-2405, doi:en.2004-1378 [pii]
10.1210/en.2004-1378 (2005).

535 Schulze, P. C. *et al.* Hyperglycemia promotes oxidative stress through inhibition of thioredoxin function by thioredoxin-interacting protein. *The Journal of biological chemistry* **279**, 30369-30374, doi:10.1074/jbc.M400549200
M400549200 [pii] (2004).

536 Shalev, A. *et al.* Oligonucleotide microarray analysis of intact human pancreatic islets: identification of glucose-responsive genes and a highly regulated TGFbeta signaling pathway. *Endocrinology* **143**, 3695-3698 (2002).

537 Hui, J. M. *et al.* Insulin resistance is associated with chronic hepatitis C virus infection and fibrosis progression [corrected]. *Gastroenterology* **125**, 1695-1704, doi:S0016508503015166 [pii] (2003).

538 Moucari, R. *et al.* Insulin resistance in chronic hepatitis C: association with genotypes 1 and 4, serum HCV RNA level, and liver fibrosis. *Gastroenterology* **134**, 416-423, doi:S0016-5085(07)02023-9 [pii]

10.1053/j.gastro.2007.11.010 (2008).

539 Negro, F. Insulin resistance and HCV: will new knowledge modify clinical management? *J Hepatol* **45**, 514-519, doi:S0168-8278(06)00388-6 [pii]

10.1016/j.jhep.2006.07.011 (2006).

540 Romero-Gomez, M. *et al.* Insulin resistance impairs sustained response rate to peginterferon plus ribavirin in chronic hepatitis C patients. *Gastroenterology* **128**, 636-641, doi:S0016508504023522 [pii] (2005).

541 Conjeevaram, H. S. *et al.* Race, insulin resistance and hepatic steatosis in chronic hepatitis C. *Hepatology (Baltimore, Md* **45**, 80-87, doi:10.1002/hep.21455 (2007).

542 Camma, C. *et al.* Insulin resistance is associated with steatosis in nondiabetic patients with genotype 1 chronic hepatitis C. *Hepatology (Baltimore, Md* **43**, 64-71, doi:10.1002/hep.20983 (2006).

543 D'Souza, R., Sabin, C. A. & Foster, G. R. Insulin resistance plays a significant role in liver fibrosis in chronic hepatitis C and in the response to antiviral therapy. *Am J Gastroenterol* **100**, 1509-1515, doi:AJG41403 [pii]

10.1111/j.1572-0241.2005.41403.x (2005).

544 Poustchi, H. *et al.* Insulin resistance and response to therapy in patients infected with chronic hepatitis C virus genotypes 2 and 3. *J Hepatol* **48**, 28-34, doi:S0168-8278(07)00508-9 [pii]

10.1016/j.jhep.2007.07.026 (2008).

545 Kaadige, M. R., Looper, R. E., Kamalanaadhan, S. & Ayer, D. E. Glutamine-dependent anapleurosis dictates glucose uptake and cell growth by regulating MondoA transcriptional activity. *Proceedings of the National Academy of Sciences of the United States of America*, doi:0901221106 [pii]

10.1073/pnas.0901221106 (2009).

546 Chutkow, W. A., Patwari, P., Yoshioka, J. & Lee, R. T. Thioredoxin-interacting protein (Txnip) is a critical regulator of hepatic glucose production. *The Journal of biological chemistry* **283**, 2397-2406, doi:M708169200 [pii]

10.1074/jbc.M708169200 (2008).

547 Patwari, P. *et al.* Thioredoxin-independent Regulation of Metabolism by the alpha-Arrestin Proteins. *Journal of Biological Chemistry* **284**, 24996-25003, doi:DOI 10.1074/jbc.M109.018093 (2009).

548 Zhou, R., Tardivel, A., Thorens, B., Choi, I. & Tschopp, J. Thioredoxin-interacting protein links oxidative stress to inflammasome activation. *Nat Immunol* **11**, 136-140, doi:ni.1831 [pii]

10.1038/ni.1831 (2010).

549 Davis, B. K. & Ting, J. P. NLRP3 has a sweet tooth. *Nat Immunol* **11**, 105-106, doi:ni0210-105 [pii]

10.1038/ni0210-105 (2010).

550 Muruve, D. A. *et al.* The inflammasome recognizes cytosolic microbial and host DNA and triggers an innate immune response. *Nature* **452**, 103-107, doi:nature06664 [pii]

10.1038/nature06664 (2008).

551 Reichard, P. From RNA to DNA, why so many ribonucleotide reductases? *Science (New York, N.Y* **260**, 1773-1777 (1993).

552 Saitoh, T., Tanaka, S. & Koike, T. Rapid induction and Ca(2+) influx-mediated suppression of vitamin D3 up-regulated protein 1 (VDUP1) mRNA in cerebellar granule neurons undergoing apoptosis. *J Neurochem* **78**, 1267-1276 (2001).

553 Jeong, M. *et al.* Thioredoxin-interacting protein regulates hematopoietic stem cell quiescence and mobilization under stress conditions. *J Immunol* **183**, 2495-2505, doi:jimmunol.0804221 [pii]

10.4049/jimmunol.0804221 (2009).

554 Zhang, P. *et al.* The ubiquitin ligase itch regulates apoptosis by targeting thioredoxin-interacting protein for ubiquitin-dependent degradation. *The Journal of biological chemistry*, doi:M109.063321 [pii]

10.1074/jbc.M109.063321 (2010).

555 Bodnar, J. S. *et al.* Positional cloning of the combined hyperlipidemia gene Hyplip1. *Nat Genet* **30**, 110-116, doi:10.1038/ng811

ng811 [pii] (2002).

556 Hui, T. Y. *et al.* Mice lacking thioredoxin-interacting protein provide evidence linking cellular redox state to appropriate response to nutritional signals. *The Journal of biological chemistry* **279**, 24387-24393, doi:10.1074/jbc.M401280200

M401280200 [pii] (2004).

557 Oka, S. *et al.* Impaired fatty acid utilization in thioredoxin binding protein-2 (TBP-2)-deficient mice: a unique animal model of Reye syndrome. *Faseb J* **20**, 121-123, doi:05-4439fje [pii]
10.1096/fj.05-4439fje (2006).

558 Ahsan, M. K. *et al.* Thioredoxin-binding Protein-2 Deficiency Enhances Methionine-Choline Deficient Diet-induced Hepatic Steatosis but Inhibits Steatohepatitis in Mice. *Antioxid Redox Signal*, doi:10.1089/ARS.2008.2385 (2009).

559 Kato, T. *et al.* Marked increase of serum hepatitis C virus (HCV) RNA titer during treatment with high-dose prednisolone in a case of polymyositis. *Clin Rheumatol* **24**, 182-186, doi:10.1007/s10067-004-1020-6 (2005).

560 Cobbold, J. F. *et al.* Hepatic lipid profiling in chronic hepatitis C: an in vitro and in vivo proton magnetic resonance spectroscopy study. *J Hepatol* **52**, 16-24, doi:S0168-8278(09)00652-7 [pii]
10.1016/j.jhep.2009.10.006 (2010).

561 Puri, P. *et al.* A lipidomic analysis of nonalcoholic fatty liver disease. *Hepatology (Baltimore, Md* **46**, 1081-1090, doi:10.1002/hep.21763 (2007).

562 Noga, A. A., Zhao, Y. & Vance, D. E. An unexpected requirement for phosphatidylethanolamine N-methyltransferase in the secretion of very low density lipoproteins. *The Journal of biological chemistry* **277**, 42358-42365, doi:10.1074/jbc.M204542200
M204542200 [pii] (2002).

563 Yao, Z. M. & Vance, D. E. The active synthesis of phosphatidylcholine is required for very low density lipoprotein secretion from rat hepatocytes. *The Journal of biological chemistry* **263**, 2998-3004 (1988).

564 Walkey, C. J., Yu, L., Agellon, L. B. & Vance, D. E. Biochemical and evolutionary significance of phospholipid methylation. *The Journal of biological chemistry* **273**, 27043-27046 (1998).

565 Tai, A. W. *et al.* A functional genomic screen identifies cellular cofactors of hepatitis C virus replication. *Cell Host Microbe* **5**, 298-307, doi:S1931-3128(09)00061-4 [pii]
10.1016/j.chom.2009.02.001 (2009).

566 Berger, K. L. *et al.* Roles for endocytic trafficking and phosphatidylinositol 4-kinase III alpha in hepatitis C virus replication. *Proceedings of the National Academy of Sciences of the United States of America* **106**, 7577-7582, doi:0902693106 [pii]
10.1073/pnas.0902693106 (2009).

567 Yamaguchi, F. *et al.* Rare sugar D-allose induces specific up-regulation of TXNIP and subsequent G1 cell cycle arrest in hepatocellular carcinoma cells by stabilization of p27kip1. *Int J Oncol* **32**, 377-385 (2008).

568 Lin, S., Cullen, W. R. & Thomas, D. J. Methylarsenicals and arsinothiols are potent inhibitors of mouse liver thioredoxin reductase. *Chem Res Toxicol* **12**, 924-930, doi:tx9900775 [pii] (1999).

569 Krey, T. *et al.* The disulfide bonds in glycoprotein E2 of hepatitis C virus reveal the tertiary organization of the molecule. *PLoS pathogens* **6**, e1000762, doi:10.1371/journal.ppat.1000762 (2010).

570 Kato, T. *et al.* Cell culture and infection system for hepatitis C virus. *Nature protocols* **1**, 2334-2339 (2006).

Appendix

A1 Primer Sequences

These tables list all primers used in this thesis. Primers were purchased from Invitrogen or Sigma. The sequences of all primers are written in the standard 5'-3' order. All primers were designed using Primer3 (http://frodo.wi.mit.edu/primer3/) or Primer-Blast software (http://www.ncbi.nlm.nih.gov/tools/primer-blast/).

A1.1 Primers used in the construction of chimaeric JFH-1

Target of Primer Pair	Forward Primer		Reverse Primer	
	Name	Sequence	Name	Sequence
JFH-1 NS3 (AflII-NsiI)	AflII NS3ampF	TTGGGCCTGCTTACCTCTTA	NsiI NS3ampR	ACCTCAAGGTCAGCTTGCAT
S.D.M. to insert BlpI	QC NS32a BlpI F	CATCACTGCTTATGCTCAGCAAACACGAGG	QC NS32a BlpI R	CCTCGTGTTTGCTGAGCATAAGCAGTGATG
HCV 1a NS3	BlpI NS31a F	GCTCAGCAGACGAGAGGCCTCCTAGG	NsiI NS31a R	ATGCATGTCATGATGTATTTGG
HCV 1a NS3 Protease	BlpI NS31a F	GCTCAGCAGACGAGAGGCCTCCTAGG	ClaI NS31a Pro R	ATCGATTTTAGCCACTCCACGGG
HCV 1a NS3 Helicase	ClaI NS31a Hel F	ATCGATGACTTTATCCCTGTGGAG	NsiI NS31a R	ATGCATGTCATGATGTATTTGG
HCV 1b NS3	BlpI NS31b F	GCTCAGCAGACGCGAGGCCTACTTGG	NsiI NS31b R	ATGCATTCGAACTCCCGGTAAAGG
HCV 1b NS3 Protease	BlpI NS31b F	GCTCAGCAGACGCGAGGCCTACTTGG	ClaI NS31b Pro R	ATCGATTTTCGCAACCCCTCGGG
HCV 1b NS3 Helicase	ClaI NS31b Hel F	ATCGATGACTTTGTACCCGTCGAG	NsiI NS31b R	ATGCATTCGAACTCCCGGTAAAGG

A1.2Primer used for reverse transcription of JFH-1 RNA

Name	Sequence
HCV2a RT 9482	GGAACAGTTAGCTATGGAGTGTACC

A1.3 Primers used in the sequencing of JFH-1

Forward Primer		Reverse Primer	
Name	Sequence	Name	Sequence
JFH 64 F	CTGTGAGGAACTACTGTCTT	JFH 829 R	GGTAGGTTCCCTGTTGCATA
JFH 637 F	TGGGCAGGATGGCTCCTGTC	JFH 1303 R	GGCGACCAGTTCATCATCAT
JFH 1158 F	GATGTCCGCCACCTTCTGCT	JFH 2348 R	CCATTCCGTGGTAGAGTGCA
JFH 2305 F	AACTTCACTCGTGGGGATCG	JFH 3491 R	TGTCCTGTCACGCCCCGTCA
JFH 3489 F	CCTGGGCGCCATAGTGGTGA	JFH 4648 R	GCGTCGGTGGCGACGACCAC
JFH 4566 F	AAAGTGTGACGAGCTCGCGG	JFH 5951 R	CTTCTCGCCAGACATGATCT
JFH 5902 F	CTGGGTAAGGTGCTGGTGGA	JFH 6983 R	GGTGGTGCAGGTGGCCCGCA
JFH 6967 F	GCGAGCTCCTCAGTGAGCCA	JFH 8015 R	CCACACGGACTTGATGTGGT
JFH 7972 F	TCTGCAAGATCCAAGTATGG	JFH 8872 R	GCCATGAATTGATAGGGGAG
JFH 8700 F	CTTCACGGAGGCCATGACCA	JFH 9262 R	AATGGAGTGAGTTTGAGCTT

A1.4 Primers used in JFH-1 quantitative PCR

Forward Primer		Reverse Primer	
Name	Sequence	Name	Sequence
HCV2a RTqPCR F	TCTGCGGAACCGGTGAGTA	HCV2a RTqPCR R	TCAGGCAGTACCACAAGGC

A1.5 Primers used in qRT-PCR and qPCR of host genes

Gene	Forward Primer	Reverse Primer
Normalising Controls		
GAPDH	TCTCTGCTCCTCCTGTTCGAC	CGGATTTGGTCGTATTGGG
RPLPO	CGACCTGGAAGTCCAACTAC	ATCTGCTGCATCTGCTTG
Oxidative Stress	Forward Primer	Reverse Primer
AHR	CTGCCTTTCCCACAAGATGT	AGTTATCCTGGCCTCCGTTT
AOX1	TTGCTTTGTTGCCTCCTTCT	ATGGATAGCGAAAAACACGG
CAT	CGTGCTGAATGAGGAACAGA	AGTCAGGGTGGACCTCAGTG
CYP1A1	AACTAGCCAAACCAGGACCC	TAGGGTCAGATTGCTCAGCC
CYP1B1	CCCCAGTCTCAATCTCAACG	CTCCCACTCGAGTCTCTTGG
DNAJC8	GGAAAGTCGAGATGGTCGTG	GGTTCTGTGCCTGTGACCTT
GPX2	CCTTCACCCTTGTCCAAAAA	AAATGATGAGCTTGGGATCG
GPX3	ATCCTGTCCTACATGAGGCG	TGGAGACACGGATTTCTTCC
GPX8	CAGGAGGAGATTTGAAAGCG	GGTAGCAGCACATCAGCAAA
GSTM3	TCCTGGAGTTCACGGATACC	TCTTGTTCTTCCCATCCAGG
GSTM4	CGCCTATGATGTCCTTGACC	ATGCCACAGGAAACCTCAAA
HSPB8	GCTTCAAGCCAGAGGAGTTG	TGCAGGAAGCTGGATTTTCT
MT1E	GCAAGTGCAAAGAGTGCAAA	AGAGCTGTTCCCACATCAGG
MT1F	GCAAGTGCAAAGAGTGCAAA	AAAGGTTGTCCTGGCATCAG
MT1M	TGAGATCTCCAGCCTTACCG	AGGAGCAGCAGCTCTTCTTG
MT2A	GCCTCCTCCAAGTCCCAG	TGCATTTGCACTCTTTGCAT
NQO1	TATGACAAAGGACCCTTCCG	AATGACATTCATGTCCCCGT
SOD2	GGAACGGGGACACTTACAAA	GGTAGTAAGCGTGCTCCCAC
Interferon Signalling	Forward Primer	Reverse Primer
IRF1	ACCCTGGCTAGAGATGCAGA	AGGCATCCTTGTTGATGTCC
IRF9	ATGGATGTTGCTGAGCCCTA	ATGGCATCCTCTTCCTCCTT
MX1	CCACATCCCTTTGATCATCC	TTCAGGAGCCAGCTGTAGGT
SOCS2	AGGGACTCGTTTTGGGATTC	GGGTCATGAGAGAAGGGTCA
SOCS3	TGGTCAGCTGGTCTCCTTTT	AGGGAGCATTTAAGGCGAAT
Apoptosis and proliferation	Forward Primer	Reverse Primer
CCNB1	ATAAAGCTTGTGGCCCCTTT	TCAATTGGATCCCCAGGTAA
CDC25C	ATGCATCATCAGGACCACAA	GCCAGTGGCTGGAATGTTAT
GADD445B	ACAGTGGGGGTGTACGAGTC	GGATGAGCGTGAAGTGGATT
GADD45A	GGCCCGGAGATAGATGACTT	TTTTCCTTCCTGCATGGTTC
Inflammatory Chemokines	Forward Primer	Reverse Primer
CXCL1	GGAGGAGGAAGCTCACTGG	GCGATGCTCAAACACATTAGG
CXCL16	TTCCTGGAGCGTGTGTGG	GGGCTGGTAGGAAGTAAATGC
CXCL2	ACCAGAAGGAAGGAGGAAGC	TGATGCTCAAACACATTAGGC
CXCL3	GGGCTTTCCAGTCTCAACC	GGAAGCTGTGCGAGAAGC
CXCL5	ACCCAGGGAAGACAAGAAGG	GCTTAAGCGGCAAACATAGG

Cholesterol Metabolism	Forward Primer	Reverse Primer
EBP	AGACAGCCGATACATCCTGG	CTGTAGAATGAAGCGGAGGG
FDFT1	CTCAAGAGGTTTGGAGCAGG	TGATGACATCTGGGATGTGG
HMGCR	ATAATCCTGGGGAAAATGCC	TTGACAAGATGTCCTGCTGC
MVD	GATGAAGAGCTGGTTCTGCC	GTGAAGTCCTTGCTGATGACG
SQLE	AATCTTTAGGTTGGGGCTGC	TTCAGAGGCTTCTTTTTCCG
Sphingolipid Metabolism	Forward Primer	Reverse Primer
SGMS2	CAATTCCTTGCTGCTTCTCC	AGCTGATGCCTTTGTTTTGC
SGPL1	AAGATGGAGAAGCATGTGCC	TTGAAAAACACCATCTCCCC
SGPP1	CTTCTGGATCTGGAACCTGG	AGACCTCCAACTTGACCACG
SPTLC1	ACTGATTGAAGAGTGGCAACC	ACAGTTTTGTGGCTTGGAGG
Fatty acid Metabolism	Forward Primer	Reverse Primer
ACADSB	CACCATTGCAAAGCATATCG	GTGGAAGTTTATTCCCACGC
ACAT2	AGATGATCTGTGGGTCAGGC	ATATTTTCCATGCCTCCTGC
ACLY	CCACACTGCAAACTTCCTCC	GTGGTGCTCTTTCCTTGTGG
ACSL3	TGTTGTGCCAAATCAAAAGG	TTGCTGAAATAGCAGCTTCG
ELOVL4	CTGGTCCATCGCAGATAAGC	AGGTTCTCGGTCCTTCATCC
ELOVL7	CTATGGACTTTCTGCATTGGG	AACTGGCTTATGTGGATGGC
FABP3	AGTTCAGTCAGTGATGGGGC	GAACCTGAATTCTGGAAAGGG
PPARGC1A	TCAAGCCACTACAGACACCG	GCCTCTCGTGCTGATATTCC
SREBF1	GGAGAGCCTGTACAGCTTGG	TGGGTCACACAGTTCAGTGC
TXNIP	ATAAAAGCCCTTTGAACCCC	GCTCAGTGCTCTGACACAGG
Vesicle Trafficking/ Cytoskeleton	Forward Primer	Reverse Primer
ABLIM3	GACCCTTCCCTCTTTCAAGG	GCTCTGGTGGGAACATTAGC3
RAB21	AGTAGCATTTGCCTTTTGGG	AAATTCAACATGAGCCACCC
RAB27A	TGGTTGATTGAAGGGTCAGG	CTCATCGCAAATAACTCGGC
RAB27B	AATCTGACACCTGCTCTCCC	AGAAATGTTGTCTTCCCCACC
RAB33B	GAAACGTCTGCTAAAAACCCC	TAATTCCATTATCAGGGGGC
RAB37	GAGCAGCGAAAGAGTGATCC	CGGTATTTCAGTTCCTTGGC
RAB40B	CATCTCAGATCCCGGTTCC	CAAGAGCTTCATGCACATCC
RAB6B	CTACAGGCAGGAAAACCAGG	CATTTGTTCACACACAGGGC

A2 siRNA Sequences

All siRNAs were purchased from Ambion, except for the HCV, Non-Targeting 1 and Non-Targeting 2 siRNAs which were purchased from Sigma. All sequences are written in the standard 5'-3' order, with deoxyribonucleic acids indicated in brackets. DDX3X 1-4 were always used as a single combined pool of siRNAs.

siRNA	Sense Strand	Antisense Strand
HCV	CCCGGGAGGUCUCGUAGAC[dT][dT]	GUCUACGAGACCUCCCGGG[dT][dT]
Non-Targeting 1	GAUCAUACGUGCGAUCAGA[dT][dT]	UCUGAUCGCACGUAUGAUC[dT][dT]
Non-Targeting 2	CACUGGAUGUGGAUGACUA[dT][dT]	UAUAUUCGCGCUAUCGCGC[dT][dT]
CFH 1	GGACCAAUGAUAUUCCUAU[dT][dT]	AUAGGAAUAUCAUUGGUCC[dA][dT]
CFH 2	GGUUGCUCUUAAUCCAUUA[dT][dT]	UAAUGGAUUAAGAGCAACC[dC][dA]
CFI 1	CGACCUUAAACGUAUAGUA[dT][dT]	UACUAUACGUUUAAGGUCG[dG][dG]
CFI 2	GAACUAUGGGUUACCAGGA[dT][dT]	UCCUGGUAACCCAUAGUUC[dT][dT]
CYP1A1 1	CCCUCAUCAGUAAUGGUCA[dT][dT]	UGACCAUUACUGAUGAGGG[dT][dG]
CYP1A1 2	GUGUAUCGGUGAGACCAUU[dT][dT]	AAUGGUCUCACCGAUACAC[dT][dT]
DDX3X 1	GGUAUUAGCACCAACGAGA[dT][dT]	UCUCGUUGGUGCUAAUACC[dT][dT]
DDX3X 2	GCAAAUACUUGGUGUUAGA[dT][dT]	UCUAACACCAAGUAUUUGC[dT][dT]
DDX3X 3	ACAUUGAGCUUACUCGUUA[dT][dT]	UAACGAGUAAGCUCAAUGU[dT][dT]
DDX3X 4	CUAUAUUCCUCCUCAUUUA[dT][dT]	UAAAUGAGGAGGAAUAUAG[dT][dT]
MAT1A 1	AGGGUUUGAUGUUCGGCUA[dT][dT]	UAGCCGAACAUCAAACCCU[dG][dA]
MAT1A 2	GAUUAUUGUGGACACCUAU[dT][dT]	AUAGGUGUCCACAAUAAUC[dT][dT]
MT1F 1	AGACAUGUACAAACCUGGA[dT][dT]	UCCAGGUUUGUACAUGUCU[dC][dT]
MT1F 2	CCUUGACCCAUUUGCUACA[dT][dT]	UGUAGCAAAUGGGUCAAGG[dT][dG]
MT1G 1	GAGUGACCCGUAAAAUCUA[dT][dT]	UAGAUUUUACGGGUCACUC[dT][dA]
MT1G 2	CAAAUAGAGUGACCCGUAA[dT][dT]	UUACGGGUCACUCUAUUUG[dT][dA]
MT2A 1	ACCCUGACCGUGACCGUUU[dT][dT]	AAACGGUCACGGUCAGGGU[dT][dG]
MT2A 2	AGAACGCGACUUCCACAAA[dT][dT]	UUUGUGGAAGUCGCGUUCU[dT][dT]
RAB27B 1	GACUUAAUCAUGAAGCGAA[dT][dT]	UUCGCUUCAUGAUUAAGUC[dC][dA]
RAB27B 2	GGAAUAGACUUUCGGGAAA[dT][dT]	UUUCCCGAAAGUCUAUUCC[dT][dA]
RAB37 1	CCAGAUCCGAGACUAUGUA[dT][dT]	UACAUAGUCUCGGAUCUGG[dA][dA]
RAB37 2	CCAGCUUCCAGAUCCGAGA[dT][dT]	UCUCGGAUCUGGAAGCUGG[dG][dC]
RAB40B 1	CGCUGGUCUUUUGACGGCA[dT][dT]	UGCCGUCAAAAGACCAGCG[dG][dT]
RAB40B 2	UCACAGAGUCGUUCACGGA[dT][dT]	UCCGUGAACGACUCUGUGA[dT][dG]
SLC27A2 1	GUAUAUCGGUGAACUGCUU[dT][dT]	AAGCAGUUCACCGAUAUAC[dT][dG]
SLC27A2 2	GCACAUUGCUGAUUACCUA[dT][dT]	UAGGUAAUCAGCAAUGUGC[dT][dG]
SOCS3 1	UGAUUUGGUUUAAACCUGA[dT][dT]	UCAGGUUUAAACCAAAUCA[dA][dA]
SOCS3 2	AGAAGAGCCUAUUACAUCU[dT][dT]	AGAUGUAAUAGGCUCUUCU[dG][dG]
SPTLC3 1	CAAAUCAUCAGAUCACUAA[dT][dT]	UUAGUGAUCUGAUGAUUUG[dC][dT]
SPTLC3 2	GGAUGGGAUUCGCAACUAA[dT][dT]	UUAGUUGCGAAUCCCAUCC[dC][dA]
TXNIP 1	CAUCCUUCAAAGGAAAAUA[dT][dT]	UAUUUUCCUUUGAAGGAUG[dT][dT]
TXNIP 2	GAAUAUUCCUUACUGAUCU[dT][dT]	AGAUCAGUAAGGAAUAUUC[dA][dA]

A3 SDS-PAGE and Western Blotting Solutions

Resolving Gel (10ml at 10% acrylamide)	
Protogel (30% w/v acrylamide:bisacrylamide 37.5:1, National Diagnostics)	3.3ml
4x Protogel Resolving Buffer (National Diagnostics)	2.5ml
10% Ammonium Persulphate	100µl
N,N,N',N'-Tetramethylethylenediamine (TEMED)	10µl
Water	4.2ml
Stacking gel (10ml at 4% acrylamide)	
Protogel (30% w/v acrylamide:bisacrylamide 37.5:1, National Diagnostics)	1.3ml
4x Protogel Stacking Buffer (National Diagnostics)	2.5ml
10% Ammonium Persulphate	100µl
N,N,N',N'-Tetramethylethylenediamine (TEMED)	10µl
Water	6.2ml
Sample Loading Buffer	
125mM Tris-HCl pH6.8	
10% SDS	
10% β-mercaptoethanol	
10% Glycerol	
0.1% Bromophenol blue	
Western Transfer Buffer	
10x Tris-Glycine SDS-PAGE Running Buffer (National Diagnostics)	100ml
Methanol	200ml
Water	700ml
Coomassie Blue Stain	
0.1% Brilliant Blue R	
25% Isopropanol	
10% Acetic Acid	
Coomassie Blue Destain	
40% Methanol	
10% Acteic Acid	

A4 Immunofluorescence microscopy reagents

Mowiol mounting medium

2.4g Mowiol 4-88 (Sigma) was added to 6g glycerol and 6ml water and stirred for 2 hours. 12ml 0.2M Tris-HCl pH8.5 was added and the mixture stirred at 50°C until the Mowiol dissolved. The solution was clarified by centrifugation at 3000g for 20 minutes. 0.72g 1, 4-Diazabicyclo [2.2.2] octane (DABCO, Sigma) and 0.1% 4, 6-diamidino-2-phenylindole, dilactate (DAPI, Invitrogen) were added to the clarified Mowiol, and it was aliquoted for storage at -20°C.

A5 DNA Ladders

DNA ladders were purchased from Promega.

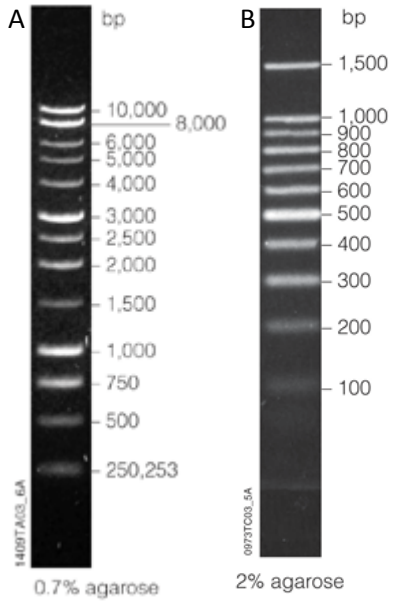


Figure 48: DNA Ladders.

These DNA ladders were used as reference markers for agarose gel electrophoresis. **A** 1kb DNA ladder. **B** 100bp DNA ladder.

A6 Characterisation of JFH-1 Cell Culture

It is now possible to study the full life cycle of HCV *in vitro* thanks to the discovery of the genotype 2a isolate called JFH-1[79]. This isolate formed the major model for these studies, so the system had to be set up and characterised. Initial preparation of *in vitro* transcribed RNA from plasmid DNA was performed by a method based on that described by Wakita *et al*[79,570]. Plasmid pJFH-1 provided the wild type sequence to produce infectious virus. Two controls were used during the characterisation of the system. JFH-1 GND (hereafter referred to as GND) contains an asparagine amino acid codon in place of the first aspartic acid codon in the GDD motif of NS5B. This mutation inhibits the viral polymerase activity, resulting in a viral genome which is unable to replicate. JFH-1 delE1E2 (hereafter referred to as delE1E2) has had the E1 and E2 regions of the genome deleted. This means that, although the viral genome can replicate, it cannot produce infectious virus particles.

The initial step in production of RNA transcripts is to digest plasmid DNA with restriction enzymes XbaI and Mung Bean Nuclease. Linearisation of DNA was confirmed by agarose gel electrophoresis (Figure 49A). RNA was produced by *in vitro* transcription and the presence of single transcripts of the desired size was confirmed by agarose gel electrophoresis (Figure 49B).

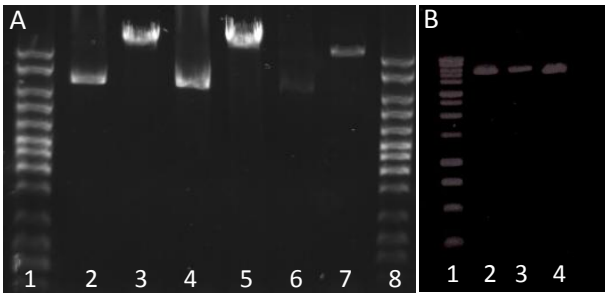


Figure 49: Preparation of RNA transcripts of JFH-1 and its derivatives.
A Agarose gel electrophoresis of JFH-1 constructs in supercoiled plasmid form and linearised form after digestion with XbaI and mung bean nuclease restriction enzymes. Each lane contains approximately 100ng DNA. Lanes 1 and 8: 1kb DNA ladder, Lane 2: Undigested pJFH-1, Lane 3: Digested pJFH-1, Lane 4: Undigested pJFH-1 GND, Lane 5: Digested pJFH-1 GND, Lane 6: Undigested pJFH-1 delE1E2, Lane 7: Digested pJFH-1 delE1E2. **B** Non-denaturing agarose gel electrophoresis of purified RNA transcripts. Each lane contains approximately 1µg RNA. Lane 1: 1kb DNA ladder, Lane 2: JFH-1, Lane 3: JFH-1 GND, Lane 4: JFH-1 delE1E2.

After the production of RNA, optimisation of the protocol for transfection of Huh7.5 cells was performed. Huh7.5 cells were chosen for production of JFH-1 as they have been shown to be permissible to JFH-1 replication after transfection with RNA. Several scales of transfection were

attempted. The 6-well format was chosen as the most practical scale. As shown in Table 13, transfection of 5 x 10^5 Huh7.5 cells with 5µg RNA and 10µg transfection reagent resulted in 20% of cells staining positive for HCV core protein four days post-transfection.

RNA (µg)	Lipofectamine 2000 (µl)	Lipofectamine:RNA ratio	Number of Cells	Scale	Cells transfected (%)
2	4	2	$5x10^5$	6-well	5
5	5	1	$5x10^5$	6-well	15
5	10	2	$5x10^5$	6-well	20
10	20	2	$5x10^5$	6-well	5

Table 13: Transfection optimisation of Huh7.5 cells with JFH-1.
In all cases, 5 x 10^5 Huh7.5 cells were seeded on coverslips in 6-well plates, and transfection was performed with Lipofectamine 2000 for 8 hours in 1ml of OptiMEM. At four days post-transfection, transfected cells were stained for HCV Core protein, and visualised by immunofluorescence microscopy. The number of HCV positive cells was estimated by counting the percentage of cells stained for HCV core in two microscope fields of view at 40x magnification.

After transfection of Huh7.5 cells with JFH-1 RNA, immunofluorescence staining for HCV core protein was performed. The staining pattern of cells expressing HCV core protein (Huh7.5 cells transfected with JFH-1, Figure 50A) is clear and distinct from cells which do not contain core protein and therefore do not stain red by this protocol (Huh7.5 cells, Figure 50B). A high magnification image of a single cell, exhibiting the expected pattern of staining, is shown in Figure 51.

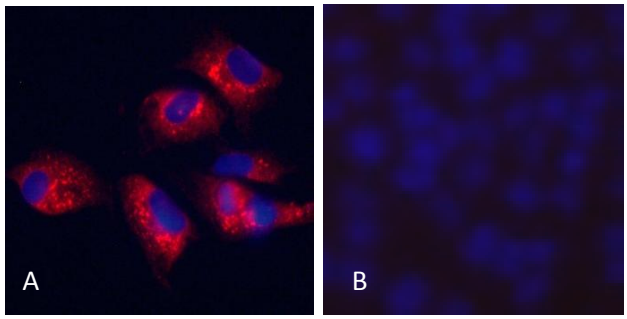


Figure 50: Immunofluorescent staining for HCV core protein.
A Huh7.5 cells transfected with JFH-1. Core protein can be observed as the red staining in the cytoplasm of the cells. Nuclei are stained blue with DAPI. **B** Mock transfected Huh7.5 cells do not stain red as there is no HCV core present.

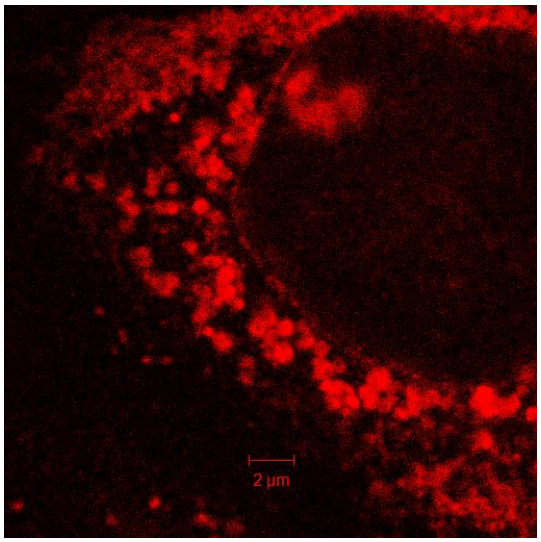


Figure 51: Image of a JFH-1 infected Huh7.5 cell stained for HCV core protein.
Huh7.5 cells transfected with JFH-1 RNA were stained for core protein (red) and imaged at 63x magnification by confocal microscopy. The nucleus, observed in the top right of the picture, is not stained as the virus localises to the cytoplasm. The general staining of the cytoplasm is typical of the localisation of the virus to the endoplasmic reticulum and Golgi apparatus. The nuclear envelope is also seen to be stained positive for HCV core. The round bodies, of various sizes up to 1µm, seen in the cytoplasm are likely to be lipid droplets coated in HCV core protein

Huh7.5 cells transfected with JFH-1 RNA were cultured in 75cm^2 flasks until all cells were infected with JFH-1, as observed by immunofluorescent staining. Cultures at this stage were characterised by measurement of RNA and infectious virus levels. Intracellular JFH-1 RNA was typically in the order of 10^8 copies per µg total cell RNA, extracellular RNA was typically in the order of 10^7 copies per ml culture medium, and infectious virus was typically in the order of 10^3 focus forming units per ml culture medium.

Once concentrated by centrifugal filtration, titres of infectious JFH-1 generated by the cell passage method were in the order of 10^5 infectious viruses per ml. In order to perform infection experiments where the majority of cells in culture were infected during the first round of infection, higher titre stocks needed to be generated. To obtain higher titres of infectious virus, the cell culture medium containing infectious virus was harvested from transfected Huh7.5 cells and used to infect naive Huh7.5 cells. Using this process, it was possible to obtain titres in the order of 10^6, as is shown in

Figure 52. Since performing this experiment, others have demonstrated use of media passage techniques to produce virus for infection studies[411].

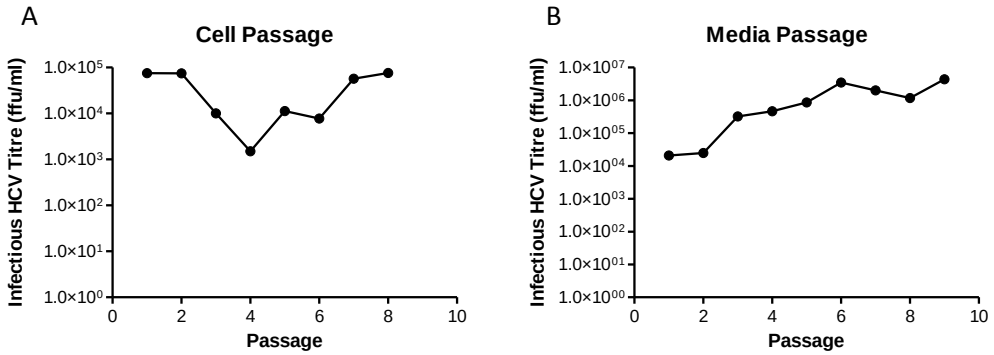


Figure 52: Production of infectious JFH-1 virus titres by cell culture.

A culture of Huh7.5 cells with all cells infected with JFH-1 was selected as the seed culture for this experiment. Culture media containing JFH-1 collected from each method were concentrated by the centrifugal method previously described (2.3.7), before titration of JFH-1. **A** Infected cells were continuously passaged as normal Huh7.5. This method shows the infectious titres initially at 7.5 x 10^4, before dropping to 1x10^4 (and even lower at passage 4) before recovering at passage 7 to the high 10^4 range. **B** Cell culture medium containing infectious JFH-1 was passaged onto naive cells. 10% of the medium from the previous passage was transferred onto the new passage. This method showed an increase in infectious titre at each passage from 2.5 x10^4 at passage 1, to the low 10^6 range at passage 5, which was then maintained to passage 8. Titres are initially low as a low percentage of cells were infected, but as media titres increased, so did the number of cells that could be initially infected with the virus from the medium. A constant volume of medium was passaged in these experiments, not a constant MOI of JFH-1, hence initial low levels of infection.

In order to establish the percentage of cells in culture that could be infected, Huh7.5 cells and Huh7 cells were infected with JFH-1 at a range of MOI. Figure 53 shows that for both Huh7.5 cells and Huh7 cells infection with an MOI of 3 resulted in the maximum possible intracellular JFH-1 RNA titre at 48 hours post-infection. Immunofluorescent staining for core protein revealed that greater than 95% of Huh7.5 cells and Huh7 cells were expressing HCV core at 48 hours post-infection with an MOI of 3.

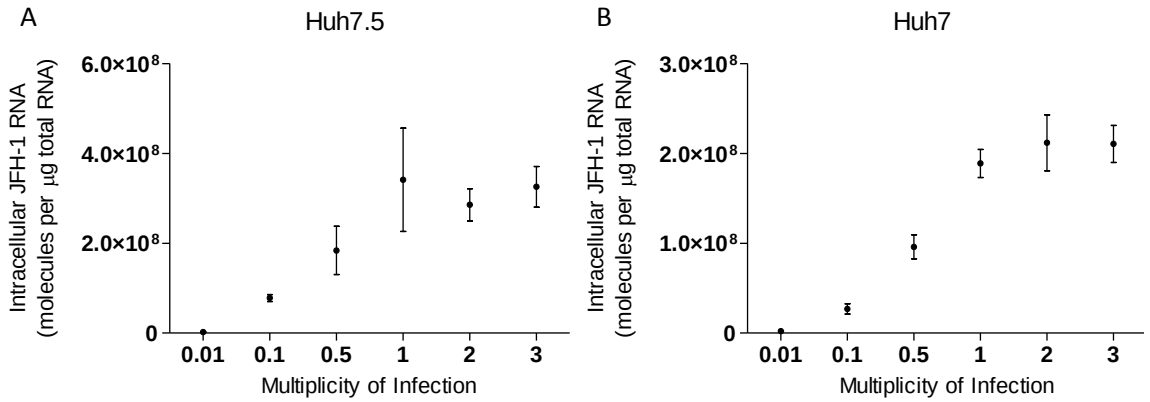


Figure 53: Intracellular JFH-1 RNA levels after infection with a range of MOI.
Huh7.5 cells (**A**) and Huh7 cells (**B**) were infected with JFH-1 at a range of MOI. $5x10^5$ cells in 4ml DMEM were seeded into T25 flasks. The next day, 1ml of JFH-1 was added to the flasks. 4 hours later the medium was removed, cells were washed with 5ml PBS and 5ml DMEM was added to the flasks. 48 hours post-infection intracellular RNA was harvested by the Trizol method, and JFH-1 RNA quantified by RT-qPCR.

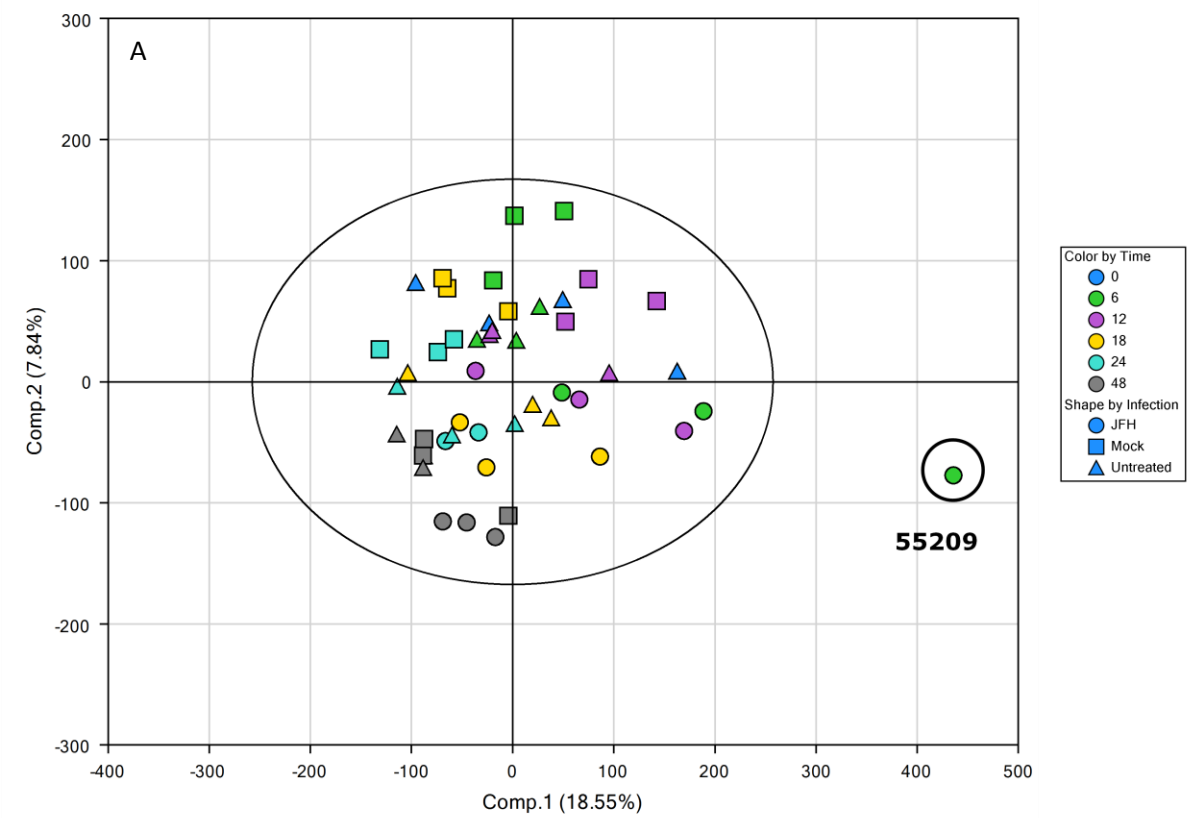
A7 Microarray Data Quality Control

Quality control (QC) was vital to obtain accurate results from the microarray experiments. The qualities of RNAs extracted from cells were tested by Expression Analysis using Agilent Bioanalyzer technology. All RNAs were determined to be of sufficient quality to be used for the microarray hybridisation protocol. Controls were also performed on the data obtained from the microarray hybridisation. Two forms of quality control were performed on data obtained using Array Studio software.

Principal component analysis (PCA) is used to reduce the high dimensionality of the relationships between the 55,000 probe sets down to (in this case) two dimensions, which can be easily and usefully represented visually. From this visual representation, arrays can be identified as outliers and excluded from the subsequent analyses of gene expression data.

Correlation based quality control in Array Studio calculated the MADScore for each array. In this case, arrays with a MADScore of less than -5 were considered outliers. Array Studio calculates MADScores based on these principles:
MADScore = (Correlation Difference Sample – Median Correlation Differences)/ (MAD * 1.46138189)
Median Absolute Deviation= median (|Yi-Median Correlation Differences|).

PCA and correlation based QC results are shown for the microarray experiment using Huh7.5 cells (Figure 54) and the experiment using Huh7 cells (Figure 55). In the experiment using Huh7.5 cells, one array was identified as an outlier by both QC methods. This was a sample in the group that was infected with JFH-1 virus for 6 hours. This array was excluded from the subsequent analyses of gene expression data. In the experiment using Huh7 cells, one array was identified as an outlier by PCA (Figure 55A), and two arrays were identified as outliers by correlation QC (Figure 55B). These were a sample in the group that was infected with JFH-1 virus for 6 hours, and a sample in the group which had RNA extracted at 0 hours. Both arrays were excluded from the subsequent analyses of gene expression data. Scatter plots providing another visual representation of the unsuitable variation observed in the probe sets of these two outlier arrays are given in Figure 55C and Figure 55D.


A
Comp.2 (7.84%)
Comp.1 (18.55%)
55209
Color by Time
0
6
12
18
24
48
Shape by Infection
JFH
Mock
Untreated

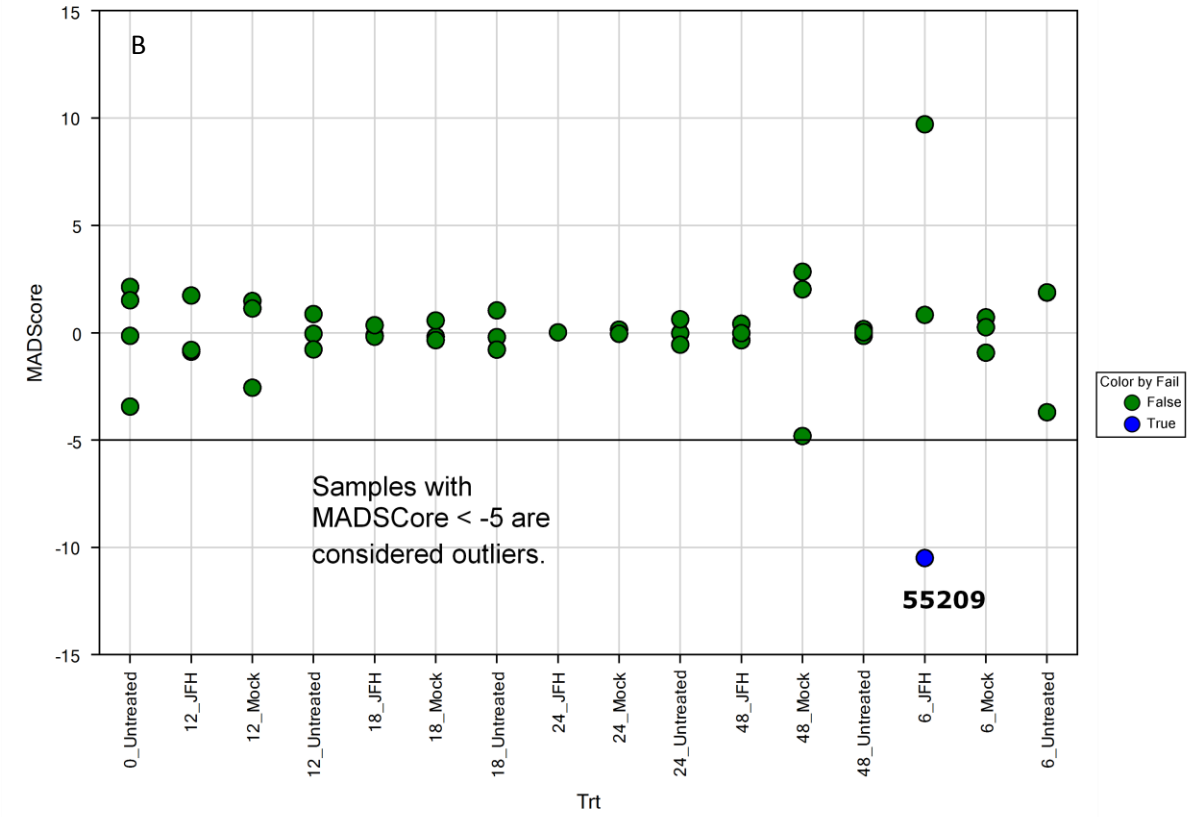
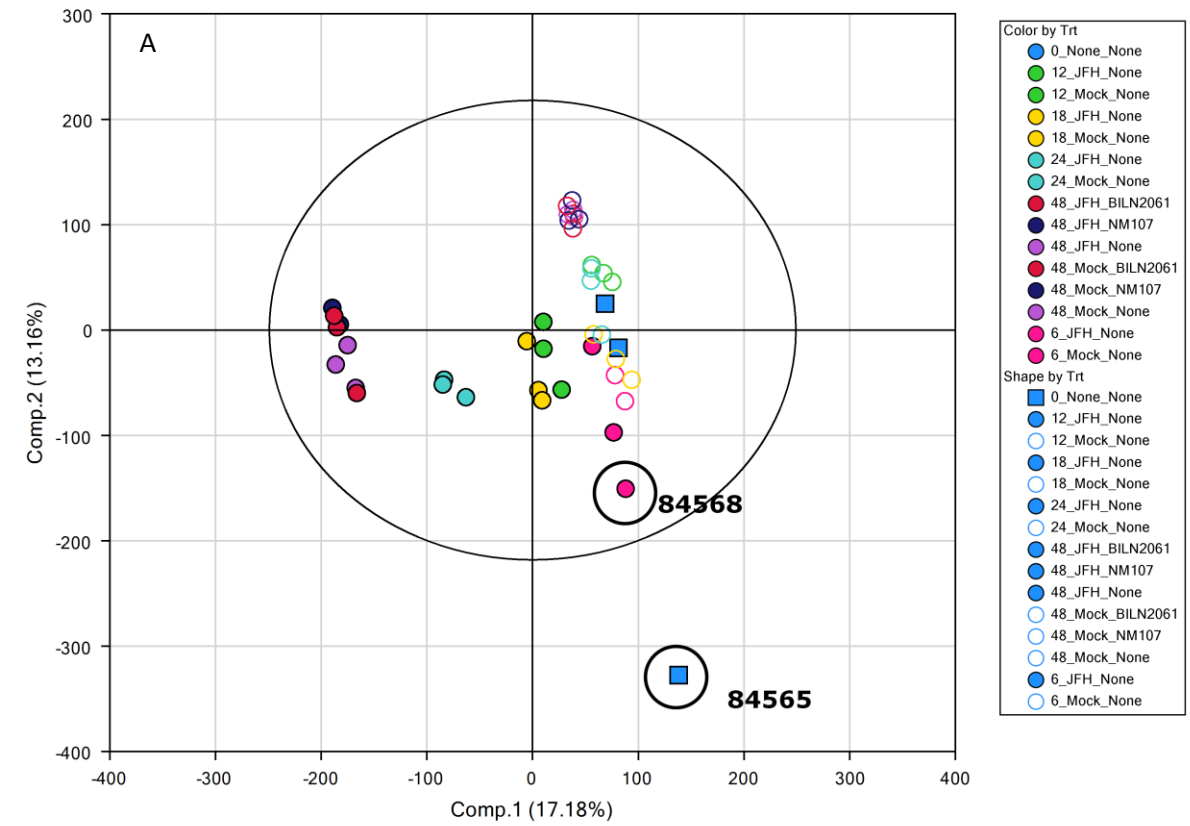
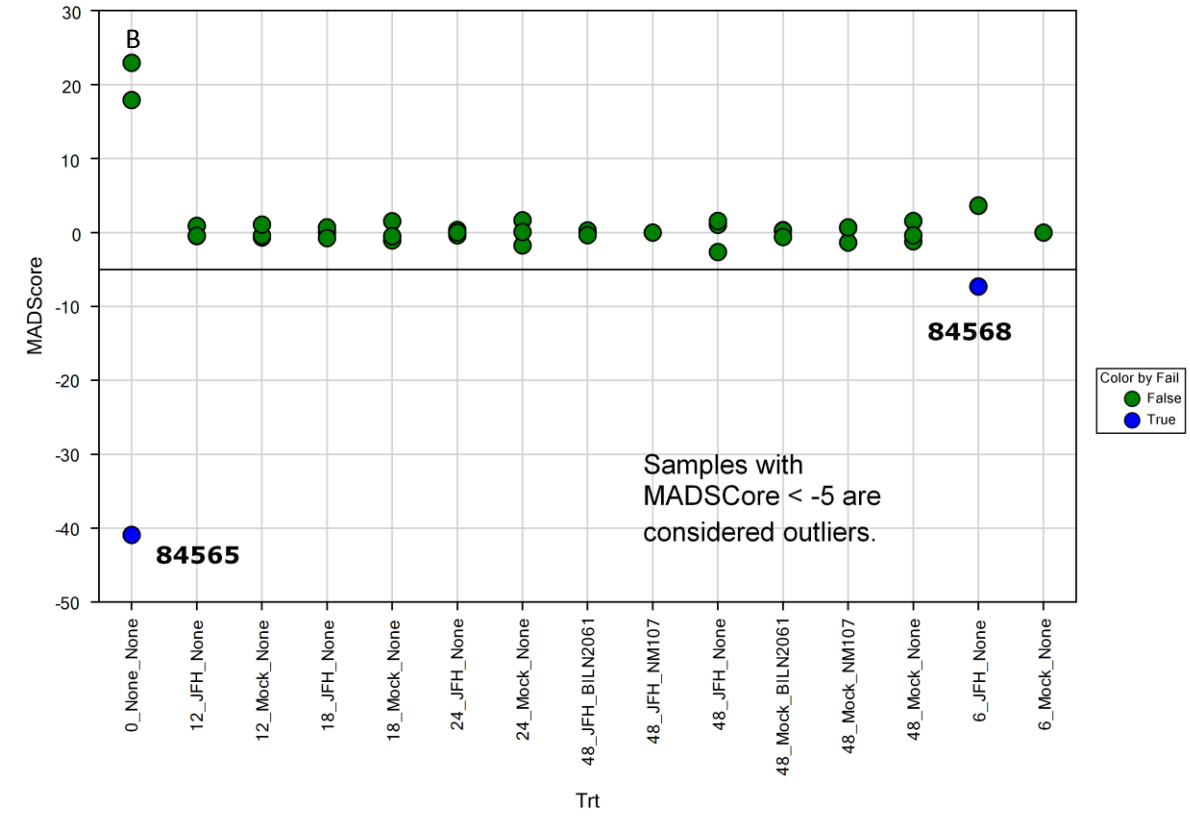
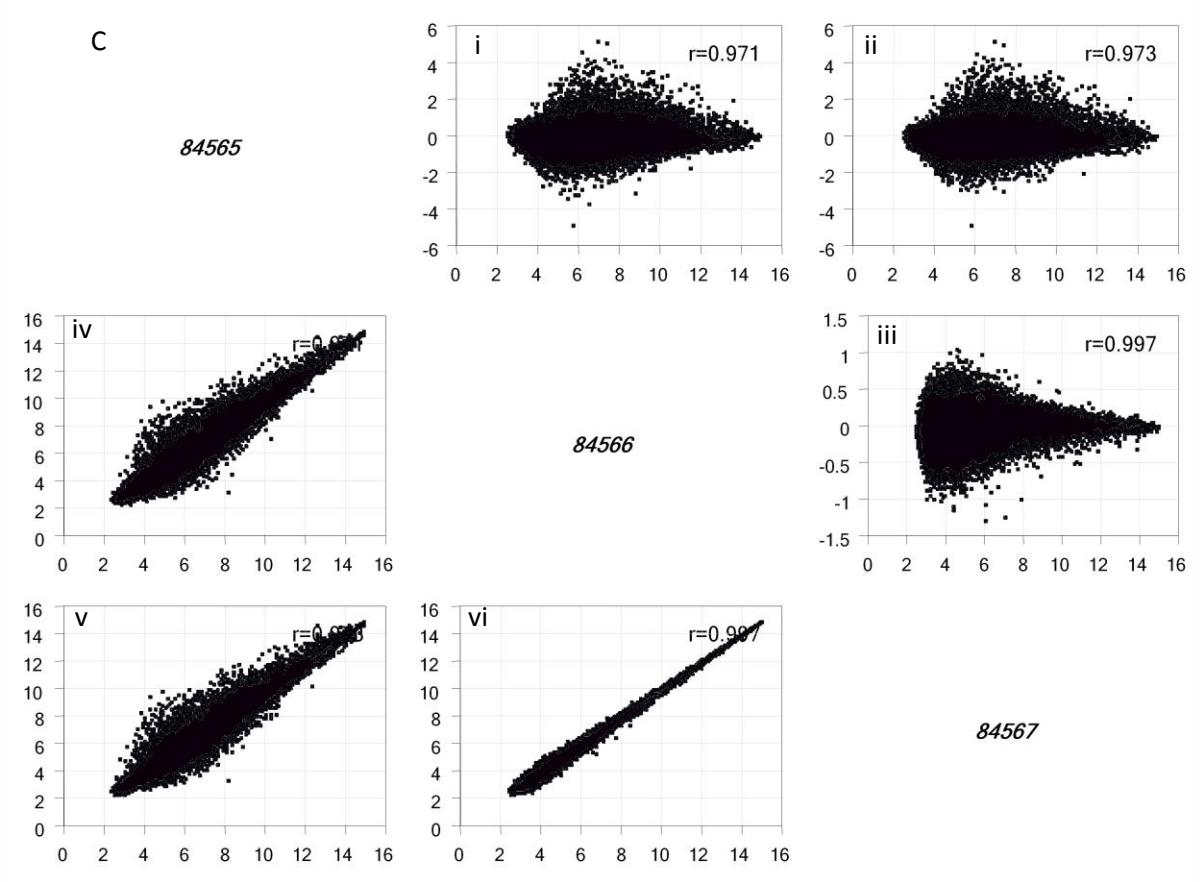

B
MADScore
Samples with
MADSCore < -5 are
considered outliers.
55209
0_Untreated
12_JFH
12_Mock
12_Untreated
18_JFH
18_Mock
18_Untreated
24_JFH
24_Mock
24_Untreated
48_JFH
48_Mock
48_Untreated
6_JFH
6_Mock
6_Untreated
Trt
Color by Fail
False
True

Figure 54: Quality control of arrays used in Huh7.5 microarray experiment, performed using Array Studio.

A Principal component analysis of arrays. Each array is colour coded by time, and shape coded by treatment. In this two dimensional representation, most arrays were observed to cluster together indicating good correlation. One outlier was identified, labelled with the array code 55209, which represented a sample infected with JFH-1 for 6 hours. **B** Correlation based QC of arrays. Arrays are grouped by time and treatment. One outlier, array 55209 was identified as having a MADScore of less than -5. This was also identified as an outlier by PCA, and consequently excluded from subsequent analyses.


A
Comp.2 (13.16%)
Comp.1 (17.18%)
84568
84565
Color by Trt
0_None_None
12_JFH_None
12_Mock_None
18_JFH_None
18_Mock_None
24_JFH_None
24_Mock_None
48_JFH_BILN2061
48_JFH_NM107
48_JFH_None
48_Mock_BILN2061
48_Mock_NM107
48_Mock_None
6_JFH_None
6_Mock_None
Shape by Trt
0_None_None
12_JFH_None
12_Mock_None
18_JFH_None
18_Mock_None
24_JFH_None
24_Mock_None
48_JFH_BILN2061
48_JFH_NM107
48_JFH_None
48_Mock_BILN2061
48_Mock_NM107
48_Mock_None
6_JFH_None
6_Mock_None


B
MADScore
84568
84565
Samples with
MADSCore < -5 are
considered outliers.
Color by Fail
False
True
0_None_None
12_JFH_None
12_Mock_None
18_JFH_None
18_Mock_None
24_JFH_None
24_Mock_None
48_JFH_BILN2061
48_JFH_NM107
48_JFH_None
48_Mock_BILN2061
48_Mock_NM107
48_Mock_None
6_JFH_None
6_Mock_None
Trt


C
84565
i
r=0.971
ii
r=0.973
iv
84566
iii
r=0.997
v
vi
84567

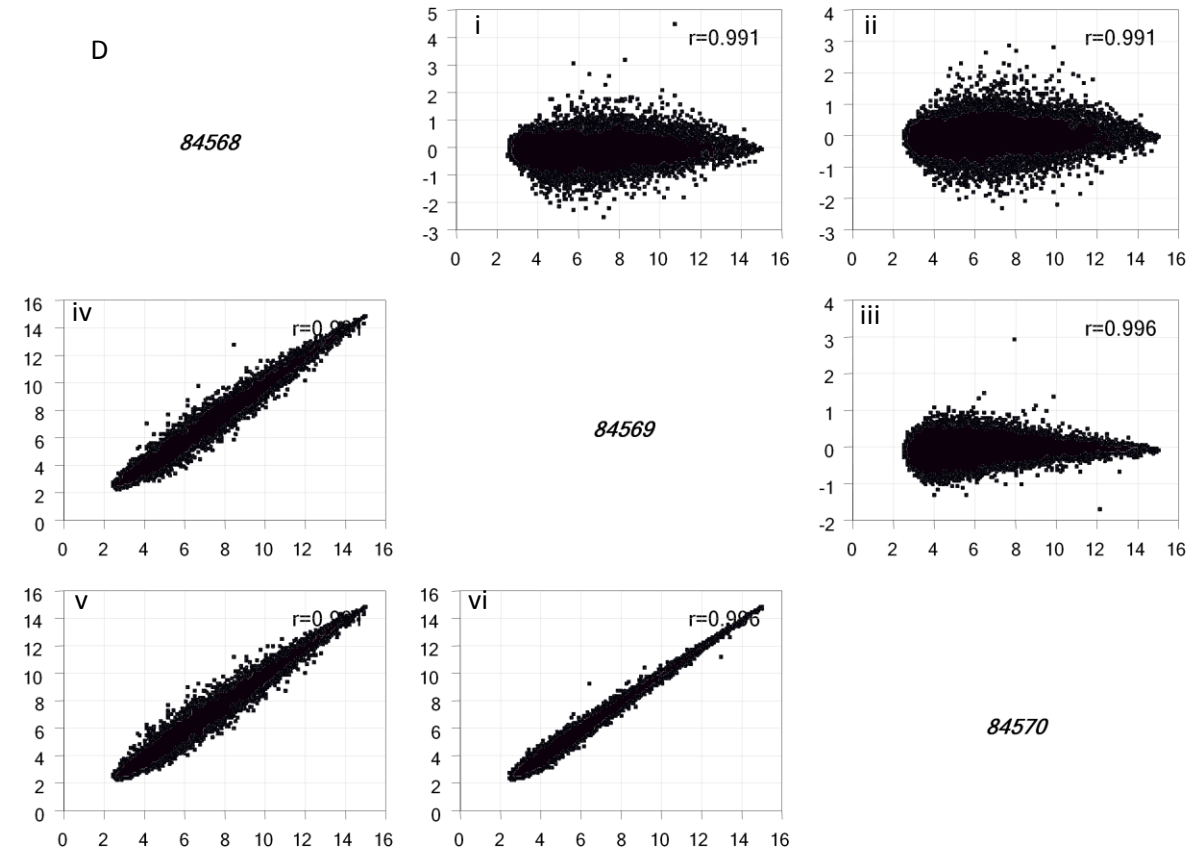

D
84568
i
r=0.991
ii
r=0.991
iv
84569
iii
r=0.996
v
vi
84570

Figure 55: Quality control of arrays used in Huh7 microarray experiment, performed using Array Studio.

A Principal component analysis of arrays. Each array is colour coded by time, and shape coded by treatment. In this two dimensional representation, most arrays were observed to cluster together indicating good correlation. One outlier was identified, labelled with the array code 84565, which represented a sample infected with JFH-1 for 6 hours. **B** Correlation based QC of arrays. Arrays are grouped by time and treatment. Two outliers, arrays 84565 and 84568 were identified as having a MADScore of less than -5. These were both consequently excluded from subsequent analyses. **C** Scatter matrix plots of arrays. The scatter matrices of pairwise comparisons of arrays are given to show the unacceptable variation in the outlier array 84565. The expected patterns can be seen in plots **iii** and **vi**, where arrays 84566 and 84567 are compared. The increased scatter observed in the comparisons involving array 84565 (**i**, **ii**, **iv** and **v**)show the unsuitability of this array for use in gene expression analysis. **D** Scatter matrix plots of arrays. The scatter matrices of pairwise comparisons of arrays are given to show the unacceptable variation in the outlier array 84568. The expected patterns can be seen in plots **iii** and **vi**, where arrays 84569 and 84570 are compared. The increased scatter observed in the comparisons involving array 84565 (**i**, **ii**, **iv** and **v**) show the unsuitability of this array for use in gene expression analysis.

A8 Metallothionein proteins levels

Gene expression analysis indicated that metallothioneins were downregulated during infection with JFH-1. To determine whether this downregulation of transcripts lead to a downregulation of protein, western blotting was performed. Huh7.5 cells were infected with JFH-1 at an MOI of three, or mock infected. Triplicates of each condition were performed. Three days post-infection, protein was harvested, 100µg put through SDS-PAGE, and western blotting performed. Figure 56 indicates that metallothionein protein levels in JFH-1 infected Huh7.5 cells may be lower than in mock infected cells. Repeat experiments are required before a conclusion can be drawn.

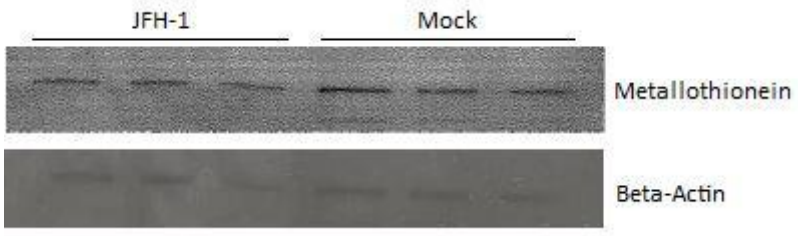


Figure 56: Metallothionein protein levels in JFH-1 infected and Mock infected Huh7.5 cells.